THE ROLE OF INHIBITORY RECEPTORS IN INFLAMMATION AND CANCER

EDITED BY: Ali A. Zarrin and Renato C. Monteiro
PUBLISHED IN: Frontiers in Immunology

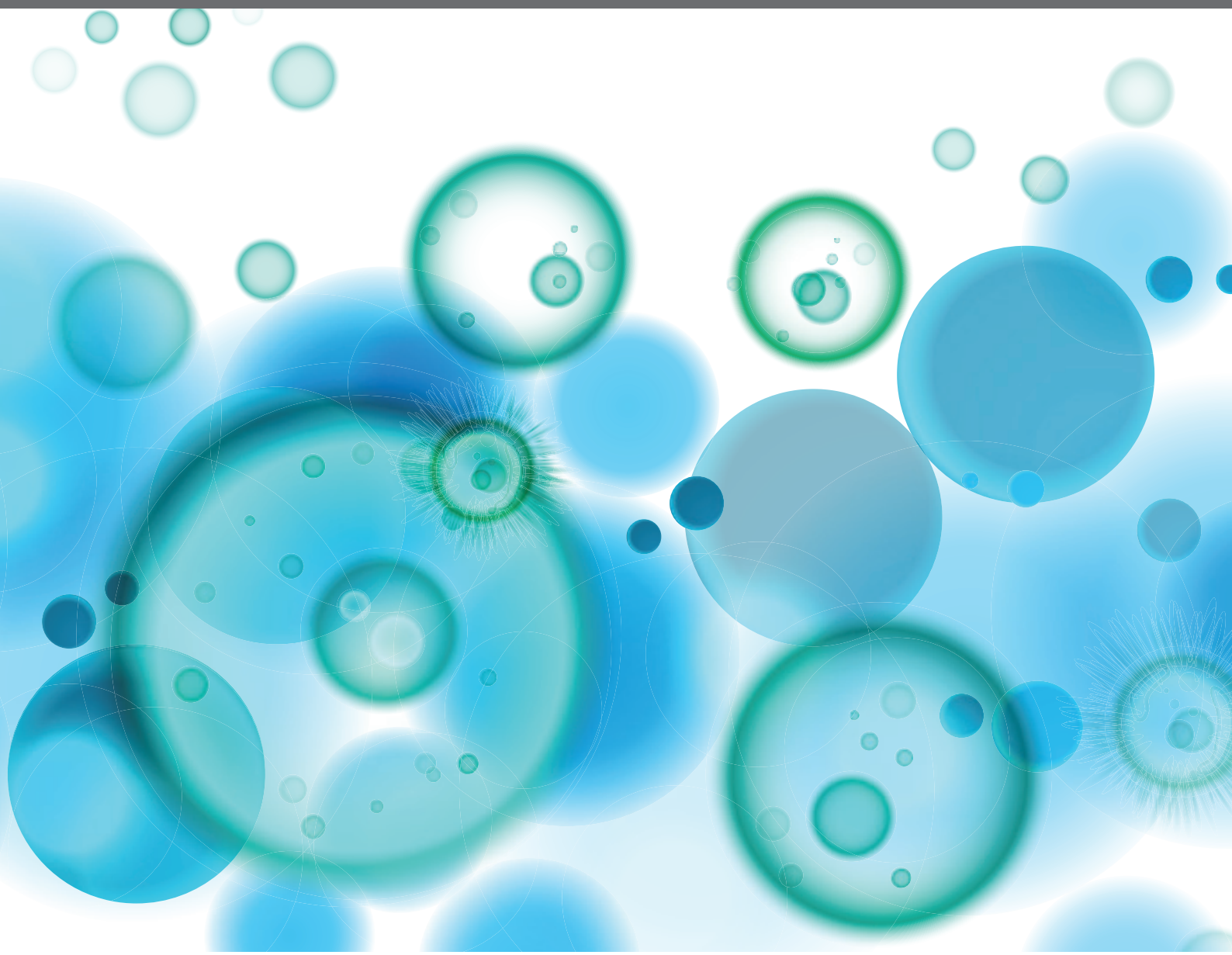

frontiers Research Topics

frontiers

ISSN 1664-8714
ISBN 978-2-88966-459-7
DOI 10.3389/978-2-88966-459-7

About Frontiers

Frontiers is more than just an open-access publisher of scholarly articles: it is a pioneering approach to the world of academia, radically improving the way scholarly research is managed. The grand vision of Frontiers is a world where all people have an equal opportunity to seek, share and generate knowledge. Frontiers provides immediate and permanent online open access to all its publications, but this alone is not enough to realize our grand goals.

Frontiers Journal Series

The Frontiers Journal Series is a multi-tier and interdisciplinary set of open-access, online journals, promising a paradigm shift from the current review, selection and dissemination processes in academic publishing. All Frontiers journals are driven by researchers for researchers; therefore, they constitute a service to the scholarly community. At the same time, the Frontiers Journal Series operates on a revolutionary invention, the tiered publishing system, initially addressing specific communities of scholars, and gradually climbing up to broader public understanding, thus serving the interests of the lay society, too.

Dedication to Quality

Each Frontiers article is a landmark of the highest quality, thanks to genuinely collaborative interactions between authors and review editors, who include some of the world's best academicians. Research must be certified by peers before entering a stream of knowledge that may eventually reach the public - and shape society; therefore, Frontiers only applies the most rigorous and unbiased reviews.
Frontiers revolutionizes research publishing by freely delivering the most outstanding research, evaluated with no bias from both the academic and social point of view. By applying the most advanced information technologies, Frontiers is catapulting scholarly publishing into a new generation.

What are Frontiers Research Topics?

Frontiers Research Topics are very popular trademarks of the Frontiers Journals Series: they are collections of at least ten articles, all centered on a particular subject. With their unique mix of varied contributions from Original Research to Review Articles, Frontiers Research Topics unify the most influential researchers, the latest key findings and historical advances in a hot research area! Find out more on how to host your own Frontiers Research Topic or contribute to one as an author by contacting the Frontiers Editorial Office: frontiersin.org/about/contact

THE ROLE OF INHIBITORY RECEPTORS IN INFLAMMATION AND CANCER

Topic Editors:
Ali A. Zarrin, TRex Bio, United States
Renato C. Monteiro, Université de Paris, France

Topic Editor Dr. Monteiro is the co-founder of Inatherys.
Topic Editor Dr. Zarrin declares no conflict of interest with regard to the Research Topic theme.

Citation: Zarrin, A. A., Monteiro, R. C., eds. (2021). The Role of Inhibitory Receptors in Inflammation and Cancer. Lausanne: Frontiers Media SA.
doi: 10.3389/978-2-88966-459-7

Table of Contents

frontiers in Immunology

EDITORIAL
published: 22 December 2020
doi: 10.3389/fimmu.2020.633686

Editorial: The Role of Inhibitory Receptors in Inflammation and Cancer

Ali A. Zarrin[1]* *and Renato C. Monteiro*[2]*

[1] TRexBio, South San Francisco, CA, United States, [2] Center for Research on Inflammation, Université de Paris, Paris, France

Keywords: inhibitory receptor, cancer, inflammatory disease, ITIM, immunoreceptor tyrosine-based inhibitory motif, ITAM

Editorial on the Research Topic

The Role of Inhibitory Receptors in Inflammation and Cancer

Inhibitory signals play an essential role in the control of immune responses allowing to preserve self while eliminating the insults. They are crucial to prevent tissue injury induced by overactivation of the immune system and to maintain homeostasis (1). They are delivered by receptors primarily expressed on lymphoid and myeloid cells that allow the pairing of activation and inhibition necessary to initiate, amplify, and then terminate immune responses. The importance of both type of receptors has been illustrated for example by paired Ig-like type receptors (PILR) in which inhibitory receptor and its counterpart activating receptor are coexpressed on single myeloid cells (2). Impairment of these signals increases the chance of developing chronic inflammation and autoimmunity and in contrast, tools activating such receptors could be beneficial to reduce inflammation (3). Genetic variants of certain immunoreceptors (IRs) validate their important role in the development of human disease (4).

The human genome contains more than 300 genes encoding potential inhibitory receptors, of which more than 60 have been functionally characterized over the past decades (1). Negative signaling in the immune system classically involves phosphatases and anti-inflammatory cytokines which prevent or abort kinase-dependent activating signaling (5). Inhibitory receptors containing immunoreceptor tyrosine-based inhibition motif (ITIM) in their cytoplasmic domain co-aggregate with immunoreceptor tyrosine-based activation motif (ITAM)-containing activating receptors during activation (5). Kinases associated with ITAMs induce the tyrosine phosphorylation of juxtaposed ITIMs, resulting in phosphatase recruitment to the phosphorylated ITIMs to abrogate the ITAM-dependent positive signal (6). ITAM motifs are present in essential receptors of the immune system such as T- and B-cell antigen receptors (TCR, BCR) and Fc receptors (FcR) as well as in an expanding family of ITAM-associated receptors with various functions in both innate and adaptative immunity. The main phosphatases implicated in inhibitory receptor signals are tyrosine phosphatases (e.g., SHP-1) or phosphatidylinositol phosphatases (e.g., SHIP-1). Once recruited they are ideally localized to find their respective substrates (e.g., kinases, adaptor proteins, signal effector molecules, or their membrane lipid anchors) to impede ITAM-initiated signaling.

Edited and reviewed by:
Francesca Granucci,
University of Milano-Bicocca, Italy

***Correspondence:**
Ali A. Zarrin
ali@trex.bio
Renato C. Monteiro
renato.monteiro@inserm.fr

Specialty section:
This article was submitted to Molecular Innate Immunity, a section of the journal Frontiers in Immunology

Received: *25 November 2020*
Accepted: *27 November 2020*
Published: *22 December 2020*

Citation:
Zarrin AA and Monteiro RC (2020) Editorial: The Role of Inhibitory Receptors in Inflammation and Cancer. Front. Immunol. 11:633686. doi: 10.3389/fimmu.2020.633686

Besides ITIM, ITAM motif can also propagate inhibitory signaling to heterologous activating receptors, being named, in this configuration, inhibitory ITAM (ITAMi) (6, 7). Some FcR (CD16A, CD32A, CD89) or TREM2, are associated with the ITAM-bearing adaptors FcRγ or DAP12 and act as bi-functional receptors that can trigger inhibitory signals toward a whole array of activating receptors (7). The ITAMi signals are initiated by targeting ITAM-containing FcR at low valency and is operative at distance independent of a co-aggregation mechanism, hence without requirement of signals initiated by the activating receptors. They recruit the tyrosine phosphatase SHP-1. Such dual receptor functions are controlled by Src kinases (8). They have been observed for other ITAM-bearing receptors including several innate immune receptors, suggesting that this could represent a widespread mechanism of immune regulation. Thus, a selective pressure during evolution may have generated single switch molecules capable of mediating either activation or inhibition depending on the type/valency of the ligand.

Yet, despite the clear protective role of inhibitory receptors, dysregulated inhibitory signals can be deleterious to the host as shown by the blockade of T lymphocyte responses to tumors. For example, tumor-specific T cells that exhibit an exhausted, unresponsive phenotype express high levels of inhibitory receptors such as CTLA4, PD1, and LAG3 (9, 10), and intra-tumoral regulatory T cells promote immunosuppression through expression of multiple inhibitory receptors. Overcoming this inhibitory receptor-mediated immune tolerance thus has been a major focus of recent cancer immunotherapeutic developments promoting enormous progress for patient treatment that have been rewarded by the Nobel prize in Physiology or Medicine in 2018.

Inhibitory signals are also exploited by microorganisms. For example, bacteria and parasites can evade the immune system by eliciting ITAMi signal through FcR (CD16) or C-type lectins (Mincle) on phagocytes leading to uncontrolled systemic infection, sepsis or parasite invasion (11, 12). In the case of CD16A, its direct targeting by *E. coli* on macrophages strongly inhibited phagocytosis through scavenger receptor MARCO. The ITAMi signal involved SHP-1 recruitment to CD16A-FcRγ and resulted in the reduced phosphorylation of phosphoinositide 3-kinase (PI3K), a key signal effector molecule in phagocytosis.

In this volume, Crute et al. present a new method for identification of inhibitory receptors that bind to specific SH2 domains, termed Inhibitory Receptor Trap (IRT). The authors use immunoblotting to show that IRT works to selectively isolate SH2 interacting partners and ultimately providing mass spectrometry as a read-out to identify unexpected interacting partners (Crute et al.). As an example, they have identified novel candidates following interaction between SHIP and PD-1. This new method should find broad use in many cell biology investigations.

Sivori et al. contribute with an overview on NK cell function that is finely regulated by HLA-specific inhibitory receptors such as killer Ig-like receptors (KIR) and non-HLA inhibitory receptors such as Siglecs which discriminate between HLA and non-HLA antigens in healthy cells and tumor or virus-infected cells. They discussed how ITIM-bearing receptors such as Siglec 7, LAIR-1, and IRp60, recognize ligands including sialic acids, extracellular matrix/collagen, or aminophospholipids. These ligands can be expressed at the surface of tumor cells, thus inhibiting NK cell function, which can further be blocked by expression of the PD-1 on NK cells induced by cytokines with cortisol, a combination which may occur in the microenvironment of various tumors (Sivori et al.). The authors provide new perspectives on how to block inhibitory receptor checkpoints on NK cells to restore their anti-tumor activity for tumor immunotherapy. The mechanisms responsible for immune checkpoint inhibitor resistance remain incompletely understood. Liu et al. utilize a computational approach to show that the immune inhibitors and immune stimulators were positively and concomitantly correlated with PD-1 expression. Authors suggest that there might be a regulatory interaction among these immune receptor hubs which may promote relapses.

Davis provides an example of such a scenario in the context of human cancer where expression of certain IRs are associated with PD1 and highlights the utility of Fc receptor-like (FCRL1–6) gene family as a therapeutic and/or biomarker target. FCRL1–6 genes encode type I transmembrane glycoproteins with cytoplasmic ITAM or ITIM motifs (Davis). FCRL1–5 are preferentially expressed by B cells and modulate B cell antigen-receptor-mediated signaling (Davis). In contrast, FCRL6 is expressed by mature T cell and NK subpopulations with cytotoxic potential (Davis). Its restricted expression and extracellular interactions with MHCII/HLA-DR, is emerging as an important regulatory axis in tolerance and cancer immunity (13). FCRL6 is upregulated in HLA-DR+ tumor samples from melanoma, breast, and lung cancer patients who relapsed following PD-1 blockade (13). Thus, FCRL6 may serve as a unique inhibitory receptor to counteract the productive immunity in cancer.

Leukocyte-associated immunoglobulin-like receptor 1 (LAIR-1) is an immune inhibitory receptor which *in vitro* binds to collagen and collagen domain containing proteins including surfactant protein D and C1q as well as epithelial cellular adhesion molecule (Ep-CAM) (1). LAIR-1 recruits SHP-1 and SHP-2 phosphatases upon activation, and cross-linking of the LAIR-1 on NK cells or T cells results in strong inhibition of NK or T cell–mediated cytotoxicity (1). Carvalheiro et al. report that LAIR1 is expressed in skin CD14+ cells, macrophages and CD1c + DCs. Authors show that LAIR1 ligation with anti-LAIR1 antibody in monocytes, inhibits toll-like receptor (TLR)4- and Interferon (IFN)-α-induced signals suggesting that LAIR1 could act as a negative regulator of inflammatory response under certain pathogenic cues (Carvalheiro et al.). The authors provide comprehensive kinetics and gene expression studies on how LAIR1 is regulated under different stimulatory conditions in monocyte-derived macrophages and monocyte-derived DCs (Carvalheiro et al.). LAIR1 is upregulated in wound healing preclinical models and its expression is correlated with increased macrophage markers (Carvalheiro et al.). Interestingly, soluble

LAIR-1 and/or LAIR-2 are increased in inflammatory diseases such as rheumatoid arthritis, Graves' disease and autoimmune thyroiditis (14, 15). In preclinical cancer models, LAIR1-collagen interactions promote CD8 T cell exhaustion and the combination of PD-1 blockade with LAIR2 over-expression reduces lung tumor growth and metastasis (16). Thus, LAIR1 may have an important function in different immune cells against broad inflammatory and cytotoxic pathways to control productive immunity.

Signal regulatory protein alpha (SIRPα) is another inhibitory immunoreceptor expressed on myeloid and neuronal cells. SIRPα interacts with CD47 which is expressed broadly in different tissues (17). Upon phosphorylation the SIRPα ITIM acts to recruit and activate the tyrosine phosphatases SHP-1 and/or SHP-2, which inhibit tyrosine phosphorylation-dependent signaling events and the resulting downstream cellular effector functions, including, e.g., phagocytosis (17). CD47-SIRPα axis forms an important innate immune checkpoint, with CD47 acting as so-called "don't-eat-me" signal, which prevents the engulfment of healthy cells by myeloid cells. Cancer cells may highjack this pathway by over-expressing CD47 thus escaping immune-mediated destruction (17). Franke et al. show that SIRPα on B1 cells negatively regulates their migration, B1 cell numbers in the spleen, and systemic natural antibody production, without directly affecting B1 cell activation. B1 cells are a subset of B cells that is the main source of natural low affinity antibodies. Authors utilize the mice lacking the cytoplasmic tail of SIRPα (SIRPαΔCYT mice) in their hematopoietic compartment and show that they are protected against atherosclerosis with increased natural antibody levels against oxidized lipids (Franke et al.). Additional studies with SIRPα B cell specific conditional knockout might help to better dissect the function of this inhibitory receptor in B cells trafficking. Thus, novel functions may emerge depending on cellular context for various IRs adding another level of complexity to understand their biology.

Alfarra et al. provide in-depth on clinical applications of IRs for multiple myeloma (MM) focusing on Natural killer (NK) cell. NK cells are an intriguing immune cell type in MM given promising results of elotuzumab (anti-SLAMF7) and daratumumab (anti-CD38) that enhance NK cell-mediated anti-tumor cell toxicity by activating the antibody-dependent cellular cytotoxicity (ADCC) mechanism (Alfarra et al.). Although these mAbs have improved the clinical outcomes of both newly diagnosed and relapsed or refractory MM (RRMM) patients, only a subgroup of patients responds to these mAbs, highlighting the complexity of the disease. CAR-NK cell therapies and combinations of existing treatments also work to restore the innate killing capacity of NK cells in MM. Authors provide a detailed review and their perspectives summarizing the advances made in this area and highlight the utility of several NK cell IRs including several molecules such as CD38, CD138, SLAMF7, SLAMF3, CD56, NKG2D, and BCMA (Alfarra et al.).

Immunoglobulin G4-related disease (IgG4-RD) is a systemic multiorgan autoimmune condition of unknown cause characterized by enhanced serum IgG4 antibodies and tissue expressing plasma cells accompanied by immunopathology associated with altered acquired immunity (18). During active IgG4-RD, the expansion of circulating plasmablasts, T cells, and eosinophils plus autoantibodies are detected. Recent transcriptome studies have revealed some insights into the molecules and pathways that might be involved in IgG4-RD (18). Several cytokines such as Th2-related, T follicular helper cell (Tfh)-related and Treg-related transcripts have been reported (18). In this issue, Cai et al. utilized an unbiased proteomic approach plus existing transcriptome data to study how different pathways/genes might be altered in IgG4-RD comparing both serum and tissue samples from naive IgG4-RD patients and healthy volunteers. The authors identify multiple signaling pathways that are dysregulated including MAPK, PI3K-Akt, Ras, TGF-β, NF-κB, and Rap1 modules (Cai et al.). They also report modulation of Fc gamma receptor (FcγR) and increased IgG3 levels which may potentiate phagocytosis, antigen presentation, as well as FcγR-mediated systemic pathology through inhibitory and activating receptors (5). This analysis plus availability of tool molecules against candidate pathways might help to model pathogenic pathways *in vitro* and ultimately to identify druggable targets that could be beneficial in IgG4-RD patients.

Complex interactions between immune inhibitors and immune stimulators in various cell types regulate productive immunity in inflammation and cancer. Given the success of checkpoint immunotherapies, we are beginning to better understand the function and dominant effect of each inhibitory receptor in humans. It has been more and more appreciated that understanding disease heterogeneity and underlying immune pathology is critical to enable effective therapeutics. Profiling tumor microenvironment or inflammatory disease tissues using high resolution gene expression, multi-omics, and multiparameter histological studies combined with functional studies should help to point to rationale therapeutic approaches in different disease areas. Functional characterization of various inhibitory receptors in different immune cell subsets should reveal novel therapeutics or essential biomarkers to track these important regulatory molecules in the immune system.

AUTHOR CONTRIBUTIONS

Both authors contributed equally to finalize the manuscript. All authors contributed to the article and approved the submitted version.

FUNDING

RCM laboratory is supported by ANR-11-IDEX-0005-02 Laboratory of Excellence INFLAMEX and Fondation pour la Recherche Médicale (EQU201903007816).

REFERENCES

1. Rumpret M, Drylewicz J, Ackermans LJE, Borghans JAM, Medzhitov R, Meyaard L. Functional categories of immune inhibitory receptors. *Nat Rev Immunol* (2020) 20:771–80. doi: 10.1038/s41577-020-0352-z
2. Sun Y, Senger K, Baginski TK, Mazloom A, Chinn Y, Pantua H, et al. Evolutionarily conserved paired immunoglobulin-like receptor alpha (PILRalpha) domain mediates its interaction with diverse sialylated ligands. *J Biol Chem* (2012) 287(19):15837–50. doi: 10.1074/jbc.M111.286633
3. Sun Y, Caplazi P, Zhang J, Mazloom A, Kummerfeld S, Quinones G, et al. PILRalpha negatively regulates mouse inflammatory arthritis. *J Immunol* (2014) 193(2):860–70. doi: 10.4049/jimmunol.1400045
4. Rathore N, Ramani SR, Pantua H, Pantua J, Bhangale T, Wuster A, et al. Paired Immunoglobulin-like Type 2 Receptor Alpha G78R variant alters ligand binding and confers protection to Alzheimer's disease. *PloS Genet* (2018) 14(11):e1007427. doi: 10.1371/journal.pgen.1007427
5. Ravetch JV, Lanier LL. Immune inhibitory receptors. *Science* (2000) 290 (5489):84–9. doi: 10.1126/science.290.5489.84
6. Pasquier B, Launay P, Kanamaru Y, Moura IC, Pfirsch S, Ruffié C, et al. Identification of FcalphaRI as an inhibitory receptor that controls inflammation: dual role of FcRgamma ITAM. *Immunity* (2005) 22(1):31–42. doi: 10.1016/j.immuni.2004.11.017
7. Getahun A, Cambier JC. Of ITIMs, ITAMs, and ITAMis: revisiting immunoglobulin Fc receptor signaling. *Immunol Rev* (2015) 268(1):66–73. doi: 10.1111/imr.12336
8. Mkaddem SB, Murua A, Flament H, Titeca-Beauport D, Bounaix C, Danelli L, et al. Lyn and Fyn function as molecular switches that control immunoreceptors to direct homeostasis or inflammation. *Nat Commun* (2017) 8(1):246. doi: 10.1038/s41467-017-00294-0
9. Okazaki T, Chikuma S, Iwai Y, Fagarasan S, Honjo T. A rheostat for immune responses: the unique properties of PD-1 and their advantages for clinical application. *Nat Immunol* (2013) 14(12):1212–8. doi: 10.1038/ni.2762
10. Pardoll DM. The blockade of immune checkpoints in cancer immunotherapy. *Nat Rev Cancer* (2012) 12(4):252–64. doi: 10.1038/nrc3239
11. Iborra S, Martínez-López M, Cueto FJ, Conde-Garrosa R, Del Fresno C, Izquierdo HM, et al. Leishmania Uses Mincle to Target an Inhibitory ITAM Signaling Pathway in Dendritic Cells that Dampens Adaptive Immunity to Infection. *Immunity* (2016) 45(4):788–801. doi: 10.1016/j.immuni.2016.09.012
12. Pinheiro da Silva F, et al. CD16 promotes Escherichia coli sepsis through an FcR gamma inhibitory pathway that prevents phagocytosis and facilitates inflammation. *Nat Med* (2007) 13(11):1368–74. doi: 10.1038/nm1665
13. Crute BW, et al. Inhibitory Receptor Trap: A Platform for Discovery of Inhibitory Receptors That Utilize Inositol Lipid and Phosphotyrosine Phosphatase Effectors. *Front Immunol* (2020) 11:592329. doi: 10.3389/fimmu.2020.592329
14. Olde Nordkamp MJ, et al. Enhanced secretion of leukocyte-associated immunoglobulin-like receptor 2 (LAIR-2) and soluble LAIR-1 in rheumatoid arthritis: LAIR-2 is a more efficient antagonist of the LAIR-1-collagen inhibitory interaction than is soluble LAIR-1. *Arthritis Rheum* (2011) 63(12):3749–57. doi: 10.1002/art.30612
15. Simone R, et al. Serum LAIR-2 is increased in autoimmune thyroid diseases. *PloS One* (2013) 8(5):e63282. doi: 10.1371/journal.pone.0063282
16. Peng DH, Rodriguez BL, Diao L, Chen L, Wang J, Byers LA, et al. Collagen promotes anti-PD-1/PD-L1 resistance in cancer through LAIR1-dependent CD8(+) T cell exhaustion. *Nat Commun* (2020) 11(1):4520. doi: 10.1038/s41467-020-18298-8
17. Weiskopf K. Cancer immunotherapy targeting the CD47/SIRPalpha axis. *Eur J Cancer* (2017) 76:100–9. doi: 10.1016/j.ejca.2017.02.013
18. Perugino CA, Stone JH. IgG4-related disease: an update on pathophysiology and implications for clinical care. *Nat Rev Rheumatol* (2020) 16(12):702–14. doi: 10.1038/s41584-020-0500-7

Conflict of Interest: AZ was employed by TRexBio.

The remaining authors declare that the research was conducted in the absence of any commercial or financial relationships that could be construed as a potential conflict of interest.

frontiers in Immunology

ORIGINAL RESEARCH
published: 19 August 2020
doi: 10.3389/fimmu.2020.01793

Leukocyte Associated Immunoglobulin Like Receptor 1 Regulation and Function on Monocytes and Dendritic Cells During Inflammation

Tiago Carvalheiro[1,2], *Samuel Garcia*[1,2,3,4], *M. Inês Pascoal Ramos*[1,5], *Barbara Giovannone*[1,6], *Timothy R. D. J. Radstake*[1,2], *Wioleta Marut*[1,2†] *and Linde Meyaard*[1,5*†]

[1] Center for Translational Immunology, University Medical Center Utrecht, University of Utrecht, Utrecht, Netherlands, [2] Department of Rheumatology & Clinical Immunology, University Medical Center Utrecht, University of Utrecht, Utrecht, Netherlands, [3] Rheumatology & Immuno-Mediated Diseases Research Group (IRIDIS), Galicia Sur Health Research Institute (IIS Galicia Sur), SERGAS-UVIGO, Vigo, Spain, [4] Rheumatology Department, University Hospital Complex of Vigo, Vigo, Spain, [5] Oncode Institute, Utrecht, Netherlands, [6] Department of Dermatology, University Medical Center Utrecht, Utrecht University, Utrecht, Netherlands

OPEN ACCESS

Edited by:
Ali A. Zarrin,
Independent Researcher,
San Francisco, United States

Reviewed by:
Attila Bacsi,
University of Debrecen, Hungary
Claudia Ida Brodskyn,
Gonçalo Moniz Institute (IGM), Brazil

***Correspondence:**
Linde Meyaard
l.meyaard@umcutrecht.nl

[†] *These authors have contributed equally to this work*

Specialty section:
This article was submitted to Molecular Innate Immunity, a section of the journal Frontiers in Immunology

Received: *11 May 2020*
Accepted: *06 July 2020*
Published: *19 August 2020*

Citation:
Carvalheiro T, Garcia S, Pascoal Ramos MI, Giovannone B, Radstake TRDJ, Marut W and Meyaard L (2020) Leukocyte Associated Immunoglobulin Like Receptor 1 Regulation and Function on Monocytes and Dendritic Cells During Inflammation. Front. Immunol. 11:1793. doi: 10.3389/fimmu.2020.01793

Inhibitory receptors are crucial immune regulators and are essential to prevent exacerbated responses, thus contributing to immune homeostasis. Leukocyte associated immunoglobulin like receptor 1 (LAIR-1) is an immune inhibitory receptor which has collagen and collagen domain containing proteins as ligands. LAIR-1 is broadly expressed on immune cells and has a large availability of ligands in both circulation and tissues, implicating a need for tight regulation of this interaction. In the current study, we sought to examine the regulation and function of LAIR-1 on monocyte, dendritic cell (DC) and macrophage subtypes, using different *in vitro* models. We found that LAIR-1 is highly expressed on intermediate monocytes as well as on plasmacytoid DCs. LAIR-1 is also expressed on skin immune cells, mainly on tissue $CD14^+$ cells, macrophages and $CD1c^+$ DCs. *In vitro*, monocyte and type-2 conventional DC stimulation leads to LAIR-1 upregulation, which may reflect the importance of LAIR-1 as negative regulator under inflammatory conditions. Indeed, we demonstrate that LAIR-1 ligation on monocytes inhibits toll like receptor (TLR)4 and Interferon (IFN)-α- induced signals. Furthermore, LAIR-1 is downregulated on GM-CSF and IFN-γ monocyte-derived macrophages and monocyte-derived DCs. In addition, LAIR-1 triggering during monocyte derived-DC differentiation results in significant phenotypic changes, as well as a different response to TLR4 and IFN-α stimulation. This indicates a role for LAIR-1 in skewing DC function, which impacts the cytokine expression profile of these cells. In conclusion, we demonstrate that LAIR-1 is consistently upregulated on monocytes and DC during the inflammatory phase of the immune response and tends to restore its expression during the resolution phase. Under inflammatory conditions, LAIR-1 has an inhibitory function, pointing toward to a potential intervention opportunity targeting LAIR-1 in inflammatory conditions.

Keywords: LAIR-1, CD305, monocytes, macrophages, dendritic cells, inflammation

INTRODUCTION

Inflammation is a normal physiological response of the immune system to a variety of factors, including pathogens, damaged tissue, malignant cells, and toxic compounds. Under normal circumstances, inflammation rapidly ends to prevent adverse events. However, an exacerbated inflammatory response may result in autoimmunity and unwanted collateral damage or immune pathology (1, 2). Uncontrolled inflammation is a key player in the pathogenesis of many chronic conditions and a persistent inflammatory response can lead to significant tissue and organ damage (3, 4). Inhibitory immune receptors are essential for immunological homeostasis; during health, immune responses are balanced to prevent damage to self, while being aggressive enough to eliminate pathogens and tumors (5).

Leukocyte associated immunoglobulin-like receptor-1 (LAIR-1), also known as CD305, is a transmembrane glycoprotein inhibitory receptor with a cytoplasmic tail containing two immunoreceptor tyrosine-based inhibitory motifs (ITIMs) (6, 7). LAIR-1 has previously been shown to be expressed on almost all immune cells, including NK cells, T cells, B cells and monocytes, monocyte derived dendritic cells (moDCs), eosinophils, basophils and mast cells, as well as on $CD34^+$ hematopoietic progenitor cells, the majority of thymocytes, but also neutrophils upon activation (7, 8).

Collagens are functional LAIR-1 ligands and directly inhibit immune cell activation *in vitro* (9). In addition, LAIR-1 also recognizes proteins that have collagen domains, such as surfactant protein D (10) and C1q, a component of the classical complement pathway (11). Activation of LAIR-1 *in vitro* potently inhibits diverse immune functions. Crosslinking of LAIR-1 results in inhibition of T cell receptor-mediated signaling (12–14), immunoglobulin (Ig)G and IgE production by B cells (15) and lysis of target cells by NK cells (6). Moreover, LAIR-1 crosslinking and C1q stimulation suppresses interferon alpha (IFN-α) release in plasmacytoid dendritic cells (pDC) (11, 16) and toll-like receptor (TLR)9-stimulated cytokine production by monocytes (17).

Aberrant LAIR-1 expression has been associated with autoimmune diseases, leukemia and viral infections. For example, pDCs and B cells from SLE patients express lower levels of LAIR-1, resulting in increased IFN-α and antibody secretion upon stimulation (16, 18). Moreover, soluble LAIR-1, a shed form of LAIR-1, and the soluble family member LAIR-2 are increased in urine and synovial fluid of rheumatoid arthritis patients (19). Additionally, LAIR-1 is absent in high–risk B cell chronic lymphocytic leukemia cells and LAIR-1 is downregulated on NK cells isolated from patients enduring a chronic active Epstein-Barr virus infection (20, 21). More recently, it was shown that LAIR-1 is expressed on *in vivo* activated human neutrophils and that LAIR-1 suppresses neutrophil extracellular trap formation by airway-infiltrated neutrophils obtained from patients with respiratory syncytial virus (RSV) bronchiolitis (22). In mice, LAIR-1 limits neutrophilic airway inflammation (23).

LAIR-1 is a distinctive receptor in the immune inhibitory receptor family because of the broad expression pattern of both the receptor and the ligands. The regulation of LAIR-1-mediated inhibition might be dependent on different factors such as the strength of the activation signals, the levels of expression of the receptor, but also on soluble LAIR-1 and LAIR-2 molecules (7). Potentially, the interaction of LAIR-1 with collagen could play a role in controlling immune cells in various phases of the inflammatory response. To better understand the role of LAIR-1 during inflammation, we investigated the expression and function of LAIR-1 under *in vitro* inflammatory conditions on monocyte, DC and macrophage subtypes.

MATERIALS AND METHODS

Peripheral Blood Mononuclear Cells Isolation and Monocyte Isolation

Blood from healthy controls (HC) was obtained following institutional ethical approval. Peripheral blood mononuclear cells (PBMCs) from heparinized blood were isolated by density centrifugation using Ficoll-Paque Plus (GE Healthcare). Fresh monocytes were isolated using anti-CD14 magnetic microbeads (Miltenyi Biotec) based on positive separation on auto-MACS assisted cell sorting (Miltenyi Biotec) according to the manufacturer's protocol.

PBMC Stimulation

A total of 1×10^6 isolated PBMCs were seeded in a 48 well plate (Corning Costar) in a final volume of 0.5 mL and cultured in complete medium: RPMI 1640 GlutaMAX (Life Technologies-Thermo Fisher Scientific), supplemented with 10% heat-inactivated fetal calf serum (FCS) (Biowest Riverside) and 1% penicillin/streptomycin (Thermo Fisher Scientific). Cells were left unstimulated or stimulated overnight at 37°C in a 5% CO_2 incubator with Pam3CSK4(P3C)-TLR2/1 ligand (5 μg/mL), LPS-TLR4 ligand (100 ng/mL), R848-TLR7/8 ligand (1 μg/mL), CpG-C-TLR9 ligand (1 μM), all from Invivogen, recombinant CXCL4 (5 μg/mL; PeproTech), recombinant IFN-α2a (1,000 U/mL, Cell Sciences), recombinant TNF-α (10 ng/mL; R&D Systems), recombinant TGF-β1 (10 ng/mL; Biolegend), and recombinant TGF-β2 (10 ng/mL; R&D Systems). Cells were then harvested and LAIR-1 expression was determined using flow cytometry. As $CD141^+$ cDC1 are a very rare population in circulation and no LAIR-1 expression was detected on steady-state, no further functional experiments were performed on this cell subset.

Skin Cells Isolation

Healthy human skin samples were collected as discarded tissue after cosmetic surgery from anonymous donors who gave prior informed consent for the use of material in research. A single-cell suspension was obtained using the whole skin dissociation kit (Miltenyi Biotech), following the manufacturer's protocol. Briefly, 3 × 4 mm biopsies were digested overnight at 37°C and processed with the gentle MACS dissociator (Miltenyi Biotech) to obtain a single cell suspension. LAIR-1 expression was determined in the single cell suspension using flow cytometry.

Monocyte Derived Macrophage and Dendritic Cell Differentiation

Purified monocytes were cultured at a density of 1×10^6 cells per mL in complete medium in the presence of recombinant GM-CSF (5 ng/mL), M-CSF (25 ng/mL), IFN-γ (10 ng/mL), IL-10 (10 ng/mL), and IL-4 (800 U/mL); all from R&D Systems, to generate macrophages. For dendritic cell differentiation, monocytes were cultured in the presence of GM-CSF (800 U/mL) in combination with IL-4 (500 U/mL), or GM-CSF (800 U/mL) in combination with IFN-α2a (1,000 U/mL, Cell Sciences). Monocytes were differentiated for 7 days at 37°C in a 5% CO_2 incubator. At day 3, medium was refreshed with the same concentration of recombinant proteins. Cells were harvested at day 7, after 5 min incubation with accutase (Sigma-Aldrich). Next, LAIR-1 expression was determined using flow cytometry, together with the expression of CD14, CD11c, CD163, CD64, CD1a, and CD80, to assess the markers for macrophage and DC differentiation (**Supplementary Figure 1**).

Flow Cytometry

Cell suspensions were first incubated with a fixable viability dye (eBioscience) to allow exclusion of dead cells and blocked either with normal mouse serum (Fitzgerald) or with Fc receptor blocking reagent (Miltenyi Biotech) and then stained for 20 min at 4°C with fluorochome-conjugated monoclonal antibodies according to the panels on **Supplementary Table 1**. Samples were acquired on a BD LSR Fortessa (BD Biosciences), or on a BD FACSCanto (BD Biosciences) using the BD FACSDiva software (BD Biosciences). FlowJo software (Tree Star) was used for data analyses.

Immunofluorescence

Frozen sections (6 μm) from healthy human skin samples, collected as described above, were fixed in 4% formaldehyde for 10 min at room temperature (RT). After washing step, specimens were blocked with 5% bovine serum albumin (BSA) diluted in PBS. Next, mouse anti-human LAIR-1 biotin labeled (clone NKTA255; Abcam) or mouse isotype control IgG1 biotin labeled (eBioscience) diluted in PBS + 1% BSA buffer were incubated overnight at 4°C. Samples were then washed and incubated for 45 min with streptavidin conjugate with Alexa Fluor 594 (Life Technologies- Thermo Fisher Scientific) diluted in PBS + 1% BSA buffer. Slides were finally washed and mounted with DAPI VectaShield hardset (Vector Lab) and allow to settle before image acquisition on a Zeiss fluorescence microscopy (Zeiss) using the Axiovision software (Zeiss). Images were further processed with ImageJ software.

Analysis of LAIR-1 Function

24 well Nunc culture plates (Thermo Fisher Scientific) were coated with 10 μg/mL of anti-LAIR-1 agonist (clone Dx26) (6) or 10 μg/mL of mouse isotype control IgG1 (eBioscience-Thermo Fisher Scientific) diluted in PBS overnight at 4°C. A total of 1×10^6 PBMCs or 0.5×10^6 purified monocytes were seeded in the pre-coated plates with complete medium after incubation with Fc receptor blocking reagent (Miltenyi Biotech). Cells were pre-incubated for 2 h at 37°C in a 5% CO_2 incubator and then either left unstimulated or stimulated with LPS-TLR4 ligand (100 ng/mL, Invivogen) or IFN-α2a (1,000 U/mL, Cell Sciences). PBMCs were stimulated overnight at 37°C in a 5% CO_2 incubator and then harvested for flow cytometry staining. Monocytes were stimulated for 5 h at 37°C in a 5% CO_2 incubator and afterwards supernatants were collected and stored at −80°C and cells were lysed with RLT buffer (Qiagen) and stored at −20°C until further analysis.

Crosslink of LAIR-1 During Monocyte Derived Dendritic Cell Differentiation

Purified monocytes were cultured in pre-coated 24 well plates, as described above, at a density of 1×10^6 cells per mL in complete medium. To generate moDCs, recombinant human IL-4 (500 U/mL) and GM-CSF (800 U/mL); both from R&D Systems were added to the medium. moDCs were differentiated for 6 days at 37°C in a 5% CO_2 incubator and at day 3 medium was supplemented with the same concentrations of IL-4 and GM-CSF. At day 6, cells were either harvest for flow cytometry staining or 100.000 cells were re-seeded in a 48 well culture plate (Corning, Costar) and rested overnight. On the day after, cells were left unstimulated or stimulated with LPS-TLR4 ligand (100 ng/mL, Invivogen) or IFN-α2a (1,000 U/mL, Cell Sciences) for 5 h. Finally, cells were lysed with RLT buffer (Qiagen) and stored at −20°C for further analysis.

Measurement of Cytokine Production

Cytokines in cell-free supernatant were measured using enzyme-linked immunosorbent assay (ELISA) for IL-6 (Sanquin), IL-8 (Sanquin), TNF-α (Diaclone), CXCL10 (R&D Systems), following the manufacturer's instructions.

RNA Isolation and Quantitative PCR

Total RNA was isolated from cell lysates using the RNeasy micro kit (Qiagen) with RNase-Free DNase Set (Qiagen), followed by retrotranscription with iScript reverse transcriptase kit (Biorad), or superscript IV (Life Technologies-Thermo Fisher Scientific) according to the manufacturer's instructions. Gene expression was determined by quantitative real-time PCR (RT-qPCR) on the QuantStudio 12 k flex (Life Technologies-Thermo Fisher Scientific) using SybrSelect mastermix (Life Technologies-Thermo Fisher Scientific) with specific primer sets listed in **Supplementary Table 2**. Relative gene expression levels on monocytes and moDCs were normalized using the *RPL13A* and *B2M* housekeeping genes, respectively. The relative fold change (FC) of each sample was calculated in relation to the ΔCt of the unstimulated sample treated with isotype control (reference) according to the formula $FC = 2^{-\Delta\Delta Ct}$.

LAIR-1 Expression From Profiling Data

LAIR-1 gene expression was retrieved from array profiling data available on the Gene Expression Omnibus (GEO–NCBI) using GEO2R (NCBI).

Statistical Analysis

Statistical analysis was performed using GraphPad Prism 8 software (GraphPad Software Inc.). Differences between

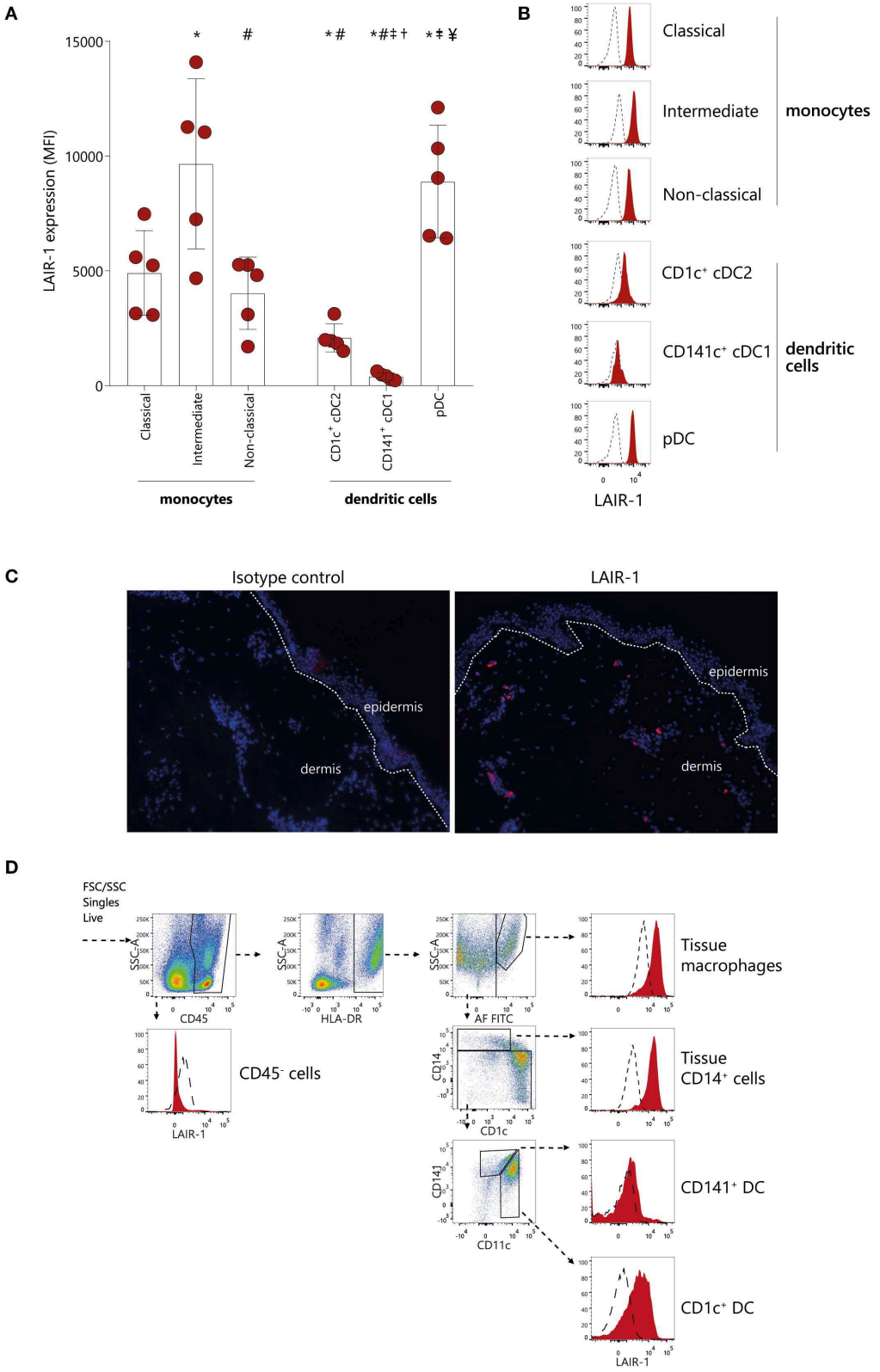

FIGURE 1 | LAIR-1 is differentially expressed on circulating monocytes subsets and dendritic cells subpopulations and on skin immune cells. **(A)** Quantification and **(B)** representative histograms of LAIR-1 expression, represented as median fluorescence intensity (MFI), on classical, intermediate and non-classical monocytes as

(Continued)

FIGURE 1 | well as on CD1c$^+$cDC1s, CD141$^+$cDC2s, and pDCs, determined on peripheral blood mononuclear cells (PBMC) by flow cytometry. Results are represented as mean with SD. Differences were considered statistically significant when $p < 0.05$: *vs. classical monocytes, #vs. intermediate monocytes, †vs. non-classical monocytes, ‡vs. CD1c$^+$cDC1s, $^{¥}$vs. CD141$^+$cDC2s (one-way ANOVA test). **(C)** Immunofluorescence analysis of LAIR-1 (red staining), in normal skin section and isotype control is shown as negative control. DAPI nuclear counterstain is shown in blue. Representative images out of three independent stainings were acquired in 20× magnification. **(D)** Flow cytometry of enzymatically digested skin. Gating strategy used to identify tissue macrophages, tissue CD14$^+$ cells, CD141$^+$, and CD1c$^+$ DCs is shown. LAIR-1 expression (filled) on these cells is shown compared to isotype control (dashed). Representative data from three donors are shown.

experimental groups were analyzed using parametric unpaired *t*-test, paired *t*-tests, one-way ANOVA test or non-parametric, Wilcoxon's test and Friedman test, when appropriate and corrected for multiple comparison. Pearson's correlation coefficient test was applied to detect the association between different parameters. Two-sided testing was performed for all analyses. Differences were considered to be statistically significant at $p < 0.05$.

RESULTS

LAIR-1 Is Differentially Expressed on Circulating Monocytes Subsets and Dendritic Cell Subpopulations and on Skin Immune Cells

LAIR-1 expression was evaluated on different monocytes subsets (classical, intermediate and non-classical) as well as on different subpopulations of classical dendritic cells (cDCs) (CD1c$^+$ cDC2 and CD141$^+$ cDC1) and on pDC in peripheral blood of HC (**Supplementary Figure 2**). LAIR-1 was expressed on all different monocyte subsets, with highest expression on intermediate monocytes, and comparable levels of expression between classical and non-classical monocytes (**Figures 1A,B**). Among DC subpopulations in circulation, pDC had highest levels of LAIR-1, cDC2 (CD1c$^+$ DC) had intermediate levels, while cDC1 (CD141$^+$ DC) did not express LAIR-1 at all (**Figure 1B**).

Since LAIR-1 is a collagen receptor, we next investigated whether LAIR-1 was expressed on immune cells present in collagen rich tissue. Collagen is highly present in skin, and we found that LAIR-1-expressing cells were present scattered through the dermis but not in the epidermis (**Figure 1C**). We next determined which cell populations expressed LAIR-1 in skin by flow cytometry, based on the populations defined by McGovern et al. (24). LAIR-1 was not expressed on non-immune cells (CD45$^-$) but was highly expressed on tissue macrophages as well as on tissue CD14$^+$ cells. Skin CD1c$^+$ DC also expressed LAIR-1, but to lesser extent than tissue macrophages and tissue CD14$^+$ cells. Similar to circulating CD141$^+$ cDC1s, tissue CD141$^+$ DC did not express LAIR-1 (**Figure 1D**). Thus, LAIR-1 is broadly expressed on blood monocytes, and it is particularly highly expressed on intermediate monocytes, and it is also expressed in skin myeloid cells.

LAIR-1 Is Upregulated Upon Inflammatory Triggers

The actual dynamic of LAIR-1 expression on monocytes under an inflammatory response remains unclear. Therefore, we made use of available array profiling data from Italiani et al. [GSE47122] (25) to determine LAIR-1 expression (RNA) kinetics in monocytes on the recruitment, inflammatory and resolution phase of the immune response mimicked *in vitro*. In this model, *LAIR1* was rapidly upregulated 2 h after CCL2 chemoattractant treatment, and these expression levels were maintained under inflammation triggered by LPS and TNF-α (inflammatory phase). *LAIR1* expression was further increased upon treatment with IFN-γ (time point 14 h). Furthermore, during the initial step of the resolution phase, the addition of IL-10 led to the highest *LAIR1* expression. In the final stage of resolution, TGF-β addition resulted on downregulation of *LAIR1* expression to the levels found during the inflammatory phase (**Figure 2A**). Since SLE is a known chronic inflammatory disease and the soluble mediators present in SLE patients' serum are able to induce and perpetuate an inflammatory response (26–28), we next made use of the model from Rodriguez-Pla et al. [GSE46920] (29), in which HC monocytes cultured in the presence of SLE serum, exhibited higher *LAIR1* levels when compared to HC serum-treated monocytes (**Figure 2B**).

In order to further investigate the regulation of LAIR-1 expression on the different monocytes subsets and DCs subpopulations, we isolated PBMCs and stimulated them with different TLR agonists, chemokine and cytokines. Monocytes were identified based on HLA-DR and CD11c expression and even though CD16 is upregulated on monocytes in culture [**Supplementary Figure 3A** and as observed by others (30)], it was possible to identify two different subsets of monocytes (CD14$^+$CD16$^+$ and CD14$^-$CD16$^+$ monocytes). On both monocyte populations, LAIR-1 expression increased upon TLR2/1, TLR4, TLR7/8, TLR9, or IFN-α stimulation, compared to medium alone. Remarkably, TNF-α stimulation induced LAIR-1 expression only on the CD14$^-$CD16$^+$ monocyte population (**Figure 2C**, **Supplementary Figure 3B**). On CD1c$^+$ cDC2, LAIR-1 expression only increased after TLR4 and TLR7/8 stimulation (**Figure 2C**, **Supplementary Figure 3B**). On pDC, LAIR-1 expression was stable regardless of stimulation (**Figure 2C**, **Supplementary Figure 3B**). Furthermore, stimulation with CXCL4 or TGF-β did not modulate LAIR-1 expression on any cell type (**Figure 2C**, **Supplementary Figure 3B**). Thus, *in vitro*, inflammatory mediators lead to LAIR-1 upregulation on monocytes and cDC2s.

Monocyte Function Is Modulated *in vitro* via LAIR-1

In order to understand the role of LAIR-1 in the regulation of monocyte function, LAIR-1 was crosslinked with a specific anti-LAIR-1 agonistic antibody (clone Dx26) prior to LPS

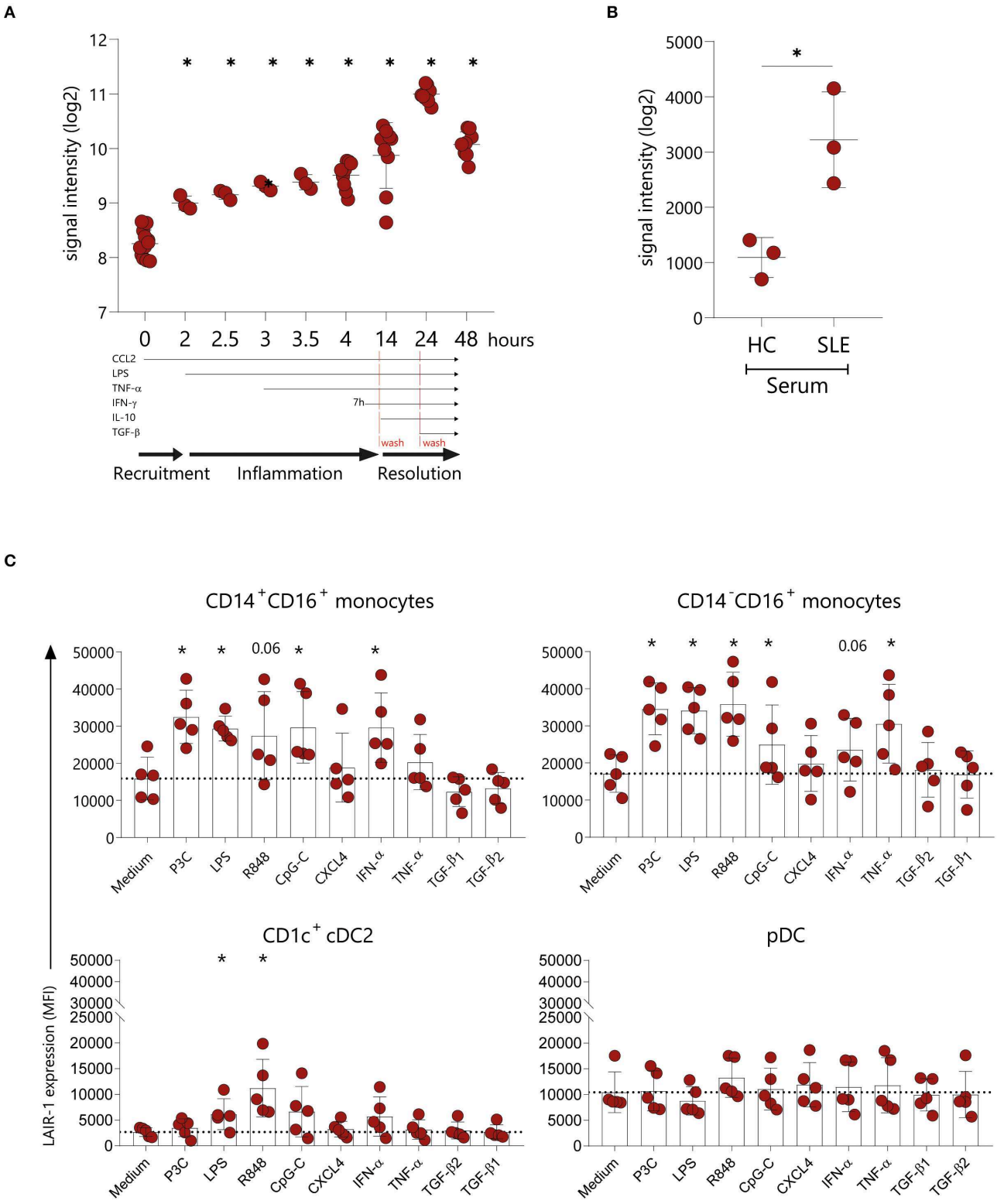

FIGURE 2 | LAIR-1 is upregulated upon inflammatory triggers. LAIR-1 gene expression was determined by array profiling and retrieved from publicly available datasets. **(A)** Kinetics of the *LAIR1* expression in human monocytes from an *in vitro* model of inflammation (GSE47122). Results are represented as mean with SD. Differences were considered statistically significant when $*p < 0.05$ vs. time-point 0 condition (one-way ANOVA test). **(B)** *LAIR1* expression in healthy blood monocytes exposed during 6 h to 20% serum from healthy controls (HC) or newly diagnosed, untreated systemic lupus erythematosus (SLE) patients (GSE46920).

(Continued)

FIGURE 2 | Results are represented as mean with SD. Differences were considered statistically significant when $p < 0.05$ (Unpaired *t*-test) **(C)** LAIR-1 expression [represented as median fluorescence intensity (MFI)] on PBMCs stimulated overnight with different TLR agonists, cytokines and chemokines was assessed by flow cytometry on $CD14^+CD16^+$and $CD14^-CD16^+$ monocytes subpopulations as well as on $CD1c^+$ DCs and pDCs. Results are represented as mean with SD. Statistically significant differences were considered when $^*p < 0.05$ vs. medium condition (Friedman's test).

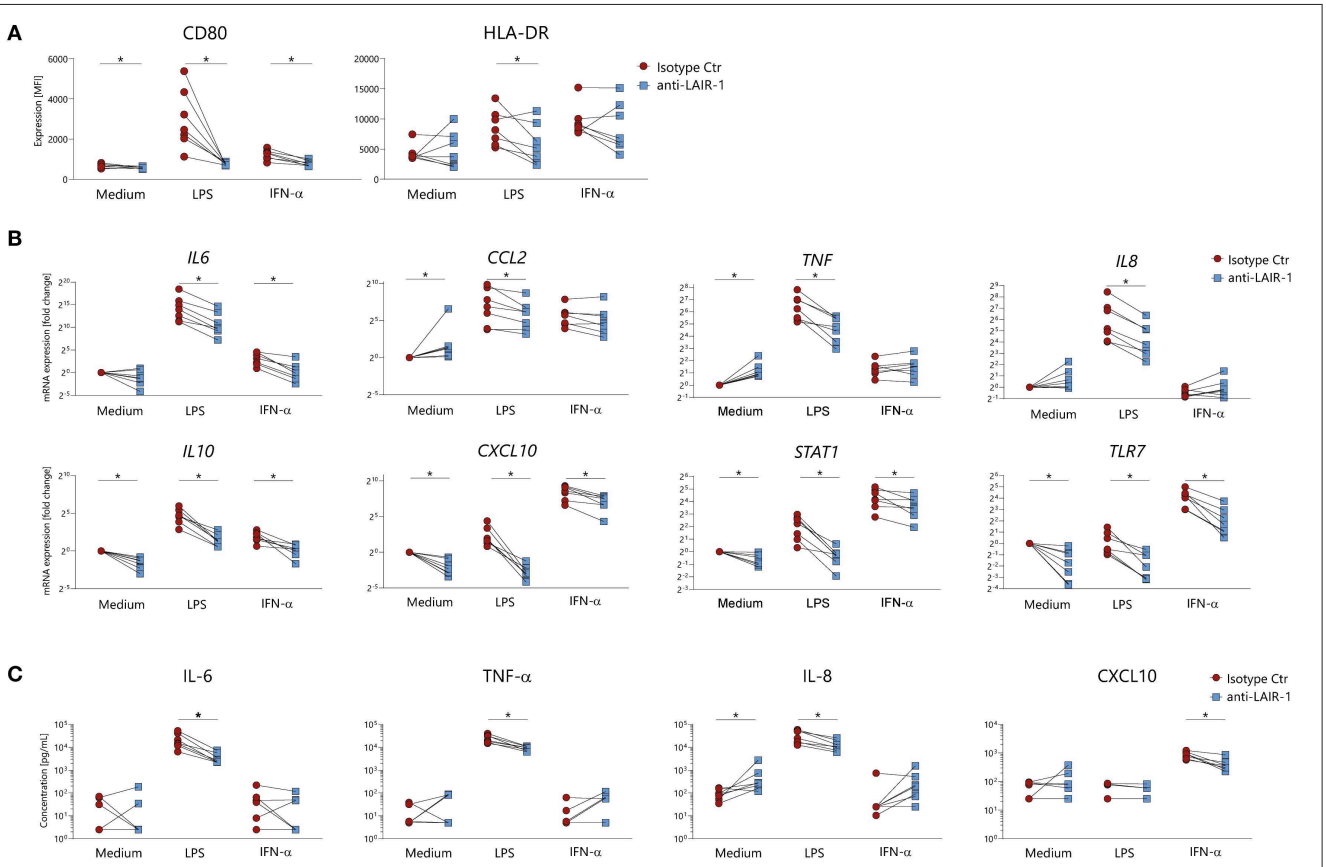

FIGURE 3 | LAIR-1 triggering modulates monocytes activation upon *in vitro* stimulation. **(A)** PBMCs were pre-treated with anti-LAIR-1 agonist (Dx26) or isotype control (2 h) and stimulated overnight with TLR4 agonist- LPS or IFN-α and the expression of CD80 and HLA-DR was determined on gated monocytes, using flow cytometry. **(B,C)** MACS purified monocytes were pre-treated (2 h) with anti-LAIR-1 agonist (Dx26) or isotype control and stimulated 5 h with TLR4 agonist- LPS or IFN-α. **(B)** *IL6*, *CXCL10*, *TNF*, *TLR7*, *IL8*, *IL10*, *CCL2,* and *STAT1* gene expression was evaluated by qRT-PCR and **(C)** protein production of IL-6, TNF-α, IL-8, and CXCL10 was measured by ELISA. Results are represented as paired samples. Statistically significant differences were considered when $^*p < 0.05$ (Wilcoxon's test).

(TLR4 ligand) or IFN-α stimulation. In cultured PBMCs, LAIR-1 signaling prevented LPS or IFN-α induced upregulation of the co-stimulator molecule CD80 and LPS induced HLA-DR expression on monocytes (**Figure 3A**). The expression of other markers, such as CD86, HLA class I (HLA-ABC) and activating collagen receptor osteoclast-associated immunoglobulin-like receptor (OSCAR) was not modulated upon stimulation. Of note, LAIR-1 expression was downregulated upon LAIR-1 engagement, most likely due to receptor internalization (**Supplementary Figure 4**).

In purified monocytes, LAIR-1 ligation inhibited LPS induced *IL-6, TNF, IL8, CCL2, CXCL10, TLR7, IL10,* and *STAT1* mRNA expression (**Figure 3B**). In line with mRNA expression, LPS induced IL-6, TNF-α, and IL-8 protein production was also inhibited by LAIR-1 triggering (**Figure 3C**). Additionally, LAIR-1 signaling inhibited IFN-α induced *IL6, CXCL10, TLR7, IL10,* and *STAT1* mRNA expression (**Figure 3B**). For CXCL10 this was confirmed at protein level (**Figure 3C**). In unstimulated cells, LAIR-1 activation led to decreased *CXCL10, TLR7, IL10,* and *STAT1* gene expression while *TNF* and *CCL2* gene expression was increased. Furthermore, LAIR-1 ligation resulted in increased IL-8 protein production (**Figures 3B,C**). Taken together, LAIR-1 ligation inhibits both TLR4 activating signals and IFN mediated responses *in vitro*.

LAIR-1 Is Downregulated on GM-CSF and IFN-γ Monocyte-Derived Macrophages and Monocyte Derived-Dendritic Cells

Under inflammatory conditions, monocytes are attracted from the circulation to injured tissues and once arrived,

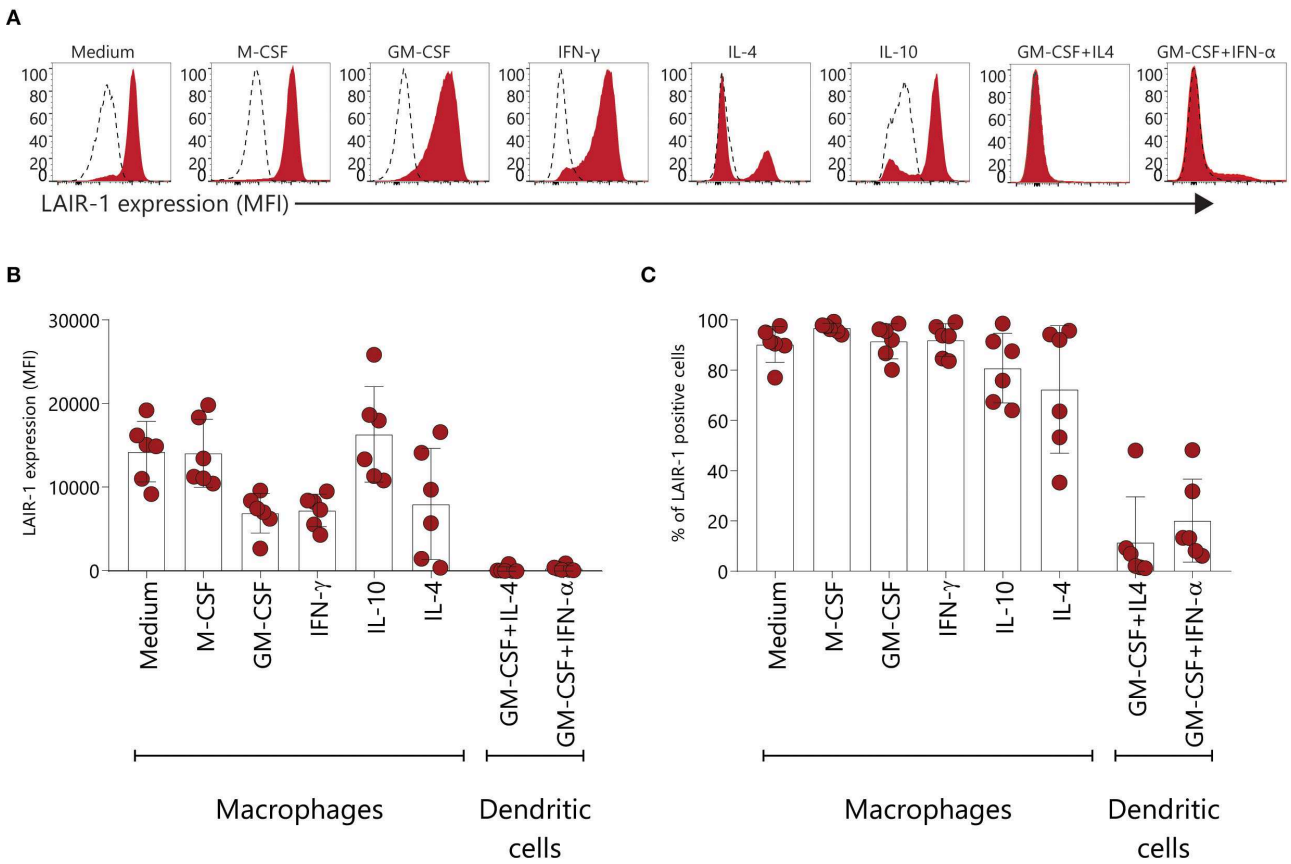

FIGURE 4 | LAIR-1 is downregulated on GM-CSF and IFN-γ monocyte-derived macrophages and monocyte derived-dendritic cells. **(A)** Representative histogram of LAIR-1 expression assessed on different types of *in vitro* monocyte-derived macrophages and dendritic cells using flow cytometry. **(B)** Quantification of LAIR-1 expression represented as median fluorescence intensity (MFI). **(C)** The percentage (%) of cells expressing LAIR-1 is displayed. Results are represented as mean with SD.

monocytes can enter macrophage or dendritic cell reprograming, depending on the micro-environment (31). Here we assessed LAIR-1 expression on monocyte-derived macrophages and dendritic cells differentiated *in vitro*. LAIR-1 expression was downregulated on GM-CSF and IFN-γ derived macrophages, while on M-CSF and IL-10 derived macrophages LAIR-1 expression was maintained (**Figures 4A,B**). Moreover, on IL-4 and IL-10 derived macrophages LAIR-1 expression was downregulated on a subset of cells (**Figures 4A,B**). LAIR-1 was profoundly downregulated on monocyte-derived dendritic cells differentiated in the presence of GM-CSF combined with IL-4 or combined with IFN-α, with only an average of 11.5 and 21.1% of LAIR-1- expressing cells, respectively (**Figures 4B,C**). Thereby, these results demonstrate that monocyte reprogramming toward macrophages or DCs critically regulates LAIR-1 expression; while GM-CSF and IFN-γ differentiated macrophages (M1) and moDCs downregulate LAIR-1 expression, M-CSF, IL-10 and IL-4 differentiated macrophages (M2) maintain in great part LAIR-1 expression.

LAIR-1 Impacts Monocyte-Derived Dendritic Cell Differentiation

To examine the contribution of LAIR-1 activation on monocyte derived dendritic cells differentiation, we generated dendritic cells from monocytes (moDCs) with GM-CSF and IL-4 in the presence of plate bound anti-LAIR1 antibody (clone Dx26). LAIR-1 ligation during moDCs differentiation resulted in a lower percentage $CD1a^+$ or CD1c expressing cells when compared to the isotype control condition. On the other hand, LAIR-1 ligation resulted in a higher percentage of $CD86^+$ cells and increased CD14, CD141, HLA-ABC, and HLA-DR expression. LAIR-1 ligation did not affect CD11c and CD80 expression (**Figures 5A,B**). Thus, LAIR-1 ligation during moDC differentiation, clearly alters their phenotype with potential impact on their function.

We next sought to understand whether moDC differentiated in the presence of LAIR-1 ligation responded differently to subsequent TLR4- ligand (LPS) or IFN-α stimulation. After 6 days of differentiation, moDCs were harvested and further stimulated with LPS or IFN-α. moDCs differentiated in the

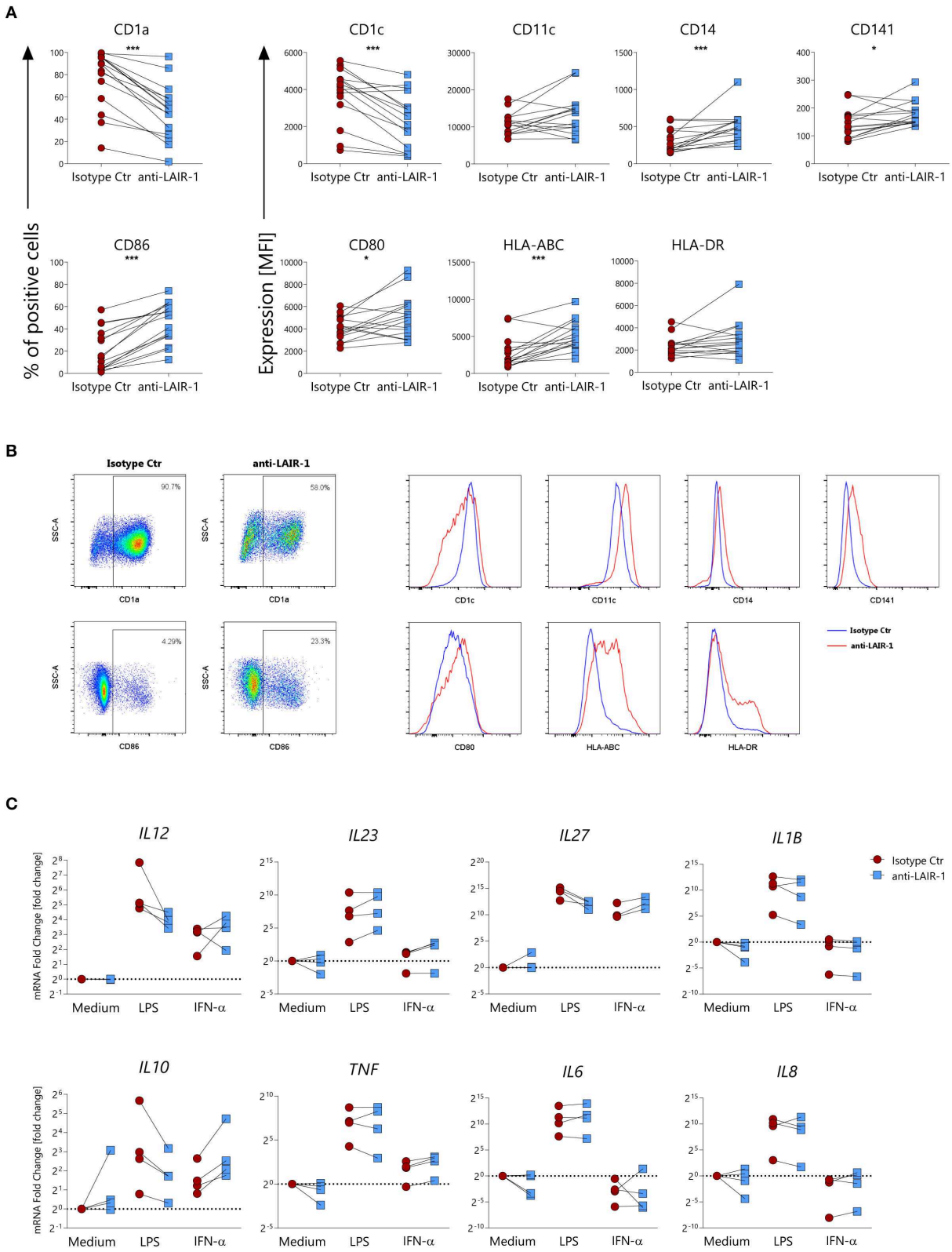

FIGURE 5 | LAIR-1 activation during differentiation of monocyte-derived dendritic cells results in phenotypic and cytokine profile alterations. **(A)** Purified monocytes were differentiated for 6 days into monocyte-derived dendritic cells using GM-CSF and IL-4 in the presence of anti-LAIR-1 agonist (Dx26) or isotype control and the

(Continued)

FIGURE 5 | expression of CD1a, CD1c, CD11c, CD14, CD141, CD86, CD80, HLA-ABC, and HLA-DR was assessed by flow cytometry. Quantification is shown as percentage (%) of positive cells or median fluorescence intensity (MFI). **(B)** Representative plots or histograms are shown. **(C)** Monocyte derived dendritic cells differentiated in the presence of anti-LAIR-1 agonist (Dx26) or isotype control were stimulated during 4 h with TLR4 agonist- LPS or IFN-α and the *IL12A, IL23A, IL27A, IL1B, IL10, TNF, IL6, IL8* gene expression was evaluated by qRT-PCR. Results are represented as paired samples. Statistically significant differences were considered when $*p < 0.05$, $***p < 0.001$ (Wilcoxon's test).

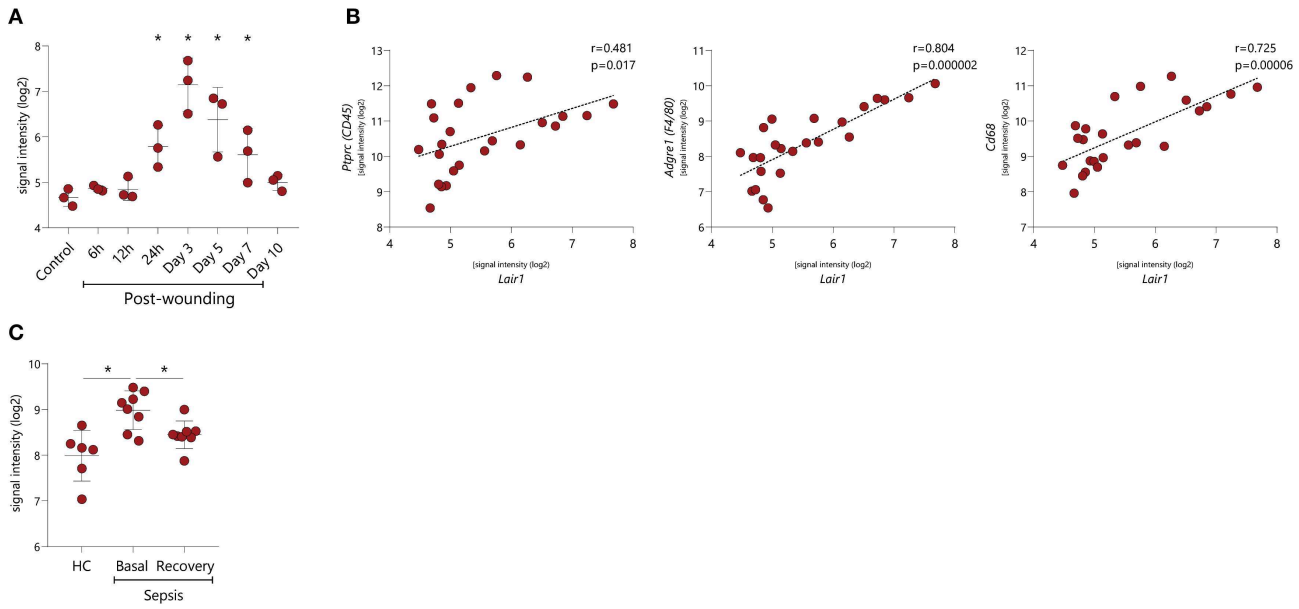

FIGURE 6 | LAIR-1 *in vivo* dynamics during inflammation. LAIR-1 gene expression was determined by array profiling and retrieved from publicly available datasets. **(A)** *Lair1* expression in mouse skin samples recovered from injury up to 10 days following wounding inflicted via punch biopsy (GSE23006). Results are represented as mean with SD. Differences were considered statistically significant when $*p < 0.05$ vs. control sample (one-way ANOVA test). **(B)** Correlation between *Lair1* expression and *Ptprc* (CD45), *Adgre1* (F4/80), and *Cd68* expression in mouse skin samples recovered from injury up to 10 days following wounding inflicted via punch biopsy (GSE23006). Correlations were assessed by the Pearson's correlation coefficient test. **(C)** LAIR-1 expression on peripheral blood monocytes from gram-negative sepsis patients during sepsis and following their recovery (GSE46955). Results are represented as mean with SD. Differences were considered statistically significant when $*p < 0.05$ (HC vs. sepsis basal and HC vs. sepsis recovery Unpaired *t*-test, sepsis basal vs. sepsis recovery Paired *t*-test).

presence of LAIR-1 agonist and stimulated with LPS expressed lower mRNA levels of *IL12A*, *IL27A*, *IL1B*, *IL8,* and *IL10* but showed higher expression levels of *IL23* (**Figure 5C**). On the other hand, IFN-α stimulation of moDCs differentiated in the presence of LAIR-1 agonist resulted in increased gene expression levels of *IL27A, IL10,* and *TNF* (**Figure 5C**). Hence, LAIR-1 ligation during moDC differentiation changes the response to TLR4 and IFN-α stimulation.

LAIR-1 Dynamics During Inflammation *in vivo*

Our *in vitro* data points toward an upregulation of LAIR-1 upon stimulation with several inflammatory mediators, however, the actual *in vivo* LAIR-1 regulation remains to unveil. Wound healing in mice is a conventional *in vivo* model to explore dynamics of inflammation during tissue repair. In the array profiling performed by Chen L et al. in this model [GSE23006] (32), we found that *Lair1* expression was unaltered during the first 12 h after the wound was induced, but after 24 h, *Lair1* expression was upregulated, with the highest *Lair1* expression being detected 3 days after injury. *Lair1* expression decreased at day 5 and normalized to the level of unwounded tissue at day 10 (**Figure 6A**). We next investigated a potential relation between the LAIR-1 dynamics of expression in this model with immune infiltration. Indeed, we observed a minor correlation between *Lair1* and *Ptprc* (CD45 gene) but a strong correlation between *Lair1* and macrophage markers like *Adgre1* (F4/80 gene) and *Cd68* (**Figure 6B**). Therefore, *Lair1* expression during wound-healing in this model may be related with macrophage infiltration.

Human sepsis is an example of a dysregulated inflammatory response to infection (33) and represents an interesting model to comprehend LAIR-1 dynamics *in vivo*. Array profiling data, on *ex vivo* isolated blood monocytes from HC and gram-negative sepsis patients during sepsis (basal) and following their recovery (recovery) were published by Shalova et al. [GSE46955] (34). *LAIR1* expression was higher in patient monocytes during sepsis compared to HC and was restored to HC levels after the recovery process (**Figure 6C**). These data indicate that the expression of LAIR-1 is dynamic and varies during the different phases of inflammation and resolution of the immune response.

DISCUSSION

It has been proposed that the interaction between LAIR-1 and its ligands should be critically regulated to ensure a balanced immune response. Differential expression of LAIR-1 on B cells, T cells, DCs and neutrophils was previously reported (7), pointing toward the importance of the expression levels for the regulation of LAIR-1-mediated inhibition.

Monocytes and DCs have a high complexity and heterogeneity (35, 36). In line with this, LAIR-1 is differently expressed among the different circulating monocytes subsets. Intermediate monocytes highly express LAIR-1 when compared to classical and non-classical monocytes. This differential expression could be related with the actual role of each monocyte subset in inflammation. For instance, the intermediate monocytes subset expresses the highest levels of antigen presentation-related molecules and was shown to produce higher amounts of TNF-α, IL-1β, IL-6, and CCL3 upon TLR stimulation. In addition, this cell subset is often increased in many inflammatory conditions (36–39). Thus, high levels of LAIR-1 expressed by this cell subset may reflect the importance of regulation of inflammation to return to homeostasis. In line, *in vitro* we demonstrate that stimulation with inflammatory cues, such as serum of SLE patients, TLR ligands, IFN-α or TNF-α, leads to LAIR-1 upregulation on monocytes and $CD1c^+$ cDC2s. This indicates, that in inflammatory conditions there might be a need for LAIR-1 upregulation to interact with its ligands in order to readily tune down the immune response. Of note, LAIR-1 upregulation mediated by IL-10 in the initial phase of the resolution phase can be important to inhibit the ongoing inflammatory process, however maintaining high levels of LAIR-1 could lead to an exacerbated inhibitory response, with detrimental effects. In this context, TGF-β seems to be important to return LAIR-1 expression back to homeostatic levels. Interestingly, stimulation with TGF-β1 and TGF-β2 alone did not impact LAIR-1 expression in monocytes or DCs.

In pDCs, we confirmed the high levels of LAIR-1, reported before (16), while the expression on $CD1c^+$ cDC2 is comparably lower. Whether LAIR-1 is maintained in tissue resident cells is yet unclear. Here we show that LAIR-1 is highly expressed on tissue macrophages and tissue $CD14^+$ cells present in skin, indicating that LAIR-1 might be an important mediator maintaining immune tolerance in peripheral tissues, especially in the presence of a high abundance of collagen. Interestingly, we found that circulating $CD141^+$ cDC1 do not express LAIR-1. Likewise, it has already been shown that cDC1s also lack the expression of other inhibitory receptors such as ILT2 and that PD-L1 is low expressed (40). This demonstrates that $CD141^+$ cDC1 display a different profile of inhibitory receptors compared with cDC2, and are not regulated via LAIR-1 in circulation or skin.

In monocytes, we also show that LAIR-1 regulates the expression of CD80 and HLA-DR, which indicates a potential importance for LAIR-1 in balancing antigen-presenting cell—T cell interaction. Furthermore, LAIR-1 triggering in monocytes modulates LPS-TLR4 and IFN-α mediated responses. All together, these findings implicate that LAIR-1 is expressed under inflammatory conditions and it is able to modulate immune responses to multiple activating cues. As a remark, we observed induction of CCL2 and IL-8 upon LAIR-1 antibody stimulation in unstimulated cells, which could be due to FC receptor mediated signals, which cannot be completely excluded in these experiments.

Macrophages are very plastic cell types that can be found in all tissues, displaying an enormous functional diversity as they play diverse roles in the development, homeostasis, tissue repair and immunity (41). We show that LAIR-1 expression on *in vitro* GM-CSF and IFN-γ differentiated macrophages (M1 macrophages) is low in line with similar observations in IFN-γ or IFN-γ+LPS stimulated THP-1-derived macrophages by Jin et al. (42). The low LAIR-1 levels on this macrophage type may contribute to their inflammatory profile. In line with this, LAIR-1 expression is maintained on M-CSF and IL-10 differentiated macrophages, associated with wound healing/immunoregulatory M2 macrophages (43, 44), which have an anti-inflammatory role. Consequently, retaining LAIR-1 expression might be beneficial for their immunosuppressive function.

MoDCs differentiated in the presence of LAIR-1 ligation have low CD1a and CD1c expression, but higher levels of CD86 (co-stimulatory molecule), CD14, HLA-ABC and HLA-DR molecules. These results are in line with previous reports indicating that LAIR-1 engagement can regulate the differentiation of monocytes into DCs with GM-CSF (45) and that LAIR-1 ligand C1q and C1 complexes are able to inhibit the differentiation of monocytes into DCs (11). Of note, the CD1a negative moDCs were previously shown to produce lower amounts of IL-12 upon stimulation and have less capacity to polarize T cells to a Th1 phenotype (46). The heterogeneity within moDC cultures is elegantly discussed by Sander et al. (47). Additionally, we also showed that LAIR-1 activation during moDC differentiation alters the response to TLR4 and IFN-α stimulation, whereas DCs differentiated in the presence of LAIR-1 ligation, have a lower inflammatory response to TLR4 activation, IFN-α stimulation results in an increased inflammatory response. On one hand, these cells can actively participate on the host defense against viruses (48), but on the other hand may play a potential role in the perpetuation of type I interferon-mediated autoimmune diseases (49).

Since an exacerbated inflammatory response might be potentially harmful, the control of the pro-inflammatory mechanisms by an anti-inflammatory counterbalance is an important protective process against further enhancement of inflammation (50, 51). Our different *in vitro* and *in vivo* models indicate that inflammation leads to an upregulation of LAIR-1, as observed here in monocytes from sepsis patients, but also on circulating monocytes in acute myocardial infarction, rheumatoid arthritis and liver cirrhosis (52–54). The upregulation of LAIR-1 during inflammation, for instance mediated by TLR or IFN signals, will facilitate its inhibitory signals. As shown here, this ranges from controlling the production of classical inflammatory cytokines (i.e., IL-6, TNF-α, or IL-8), but also IL-10 or IFN inducible proteins as CXCL10.

In conclusion, we show that LAIR-1 is broadly expressed on different monocyte subsets and macrophages, not only in circulation but also in tissue. Under inflammatory conditions LAIR-1 is upregulated and upon ligation its intrinsic inhibitory capacity is functional, and is able to reprogram monocyte derived

DC function. Thereby, our data indicate that LAIR-1 is a potentially targetable receptor to damp the immune responses in inflammatory conditions.

DATA AVAILABILITY STATEMENT

The raw data supporting the conclusions of this article will be made available by the authors, without undue reservation, to any qualified researcher.

ETHICS STATEMENT

This study was reviewed and approved by the Medical Ethical Committee of the University Medical Centre Utrecht. All the participants provided their written informed consent to participate in this study in accordance with the Declaration of Helsinki.

AUTHOR CONTRIBUTIONS

TC, SG, MP, TR, WM, and LM were involved in study conception and design of the experiments. TC and BG carried out the experiments. Analysis and interpretation of data was performed by TC, SG, MP, TR, WM, and LM. All authors were involved in drafting the manuscript or revising it critically, and all authors approved the final version.

FUNDING

TC was supported by a grant from the Portuguese national funding agency for science, research, and technology: Fundação para a Ciência e a Tecnologia [SFRH/BD/93526/2013]. SG is supported by the Miguel Servet program from the Instituto de Salud Carlos III (ISCIII) and the European Social Fund (CP19/00005). LM is supported by the Netherlands Organization for Scientific Research (NWO) (Vici 918.15.608).

SUPPLEMENTARY MATERIAL

The Supplementary Material for this article can be found online at: https://www.frontiersin.org/articles/10.3389/fimmu.2020.01793/full#supplementary-material

REFERENCES

1. Chen L, Deng H, Cui H, Fang J, Zuo Z, Deng J, et al. Inflammatory responses and inflammation-associated diseases in organs. *Oncotarget.* (2018) 9:7204–18. doi: 10.18632/oncotarget.23208
2. Medzhitov R, Schneider DS, Soares MP. Disease tolerance as a defense strategy. *Science.* (2012) 335:936–41. doi: 10.1126/science.1214935
3. Duan L, Rao X, Sigdel KR. Regulation of inflammation in autoimmune disease. *J Immunol Res.* (2019) 2019:7403796. doi: 10.1155/2019/7403796
4. Feehan KT, Gilroy DW. Is resolution the end of inflammation? *Trends Mol Med.* (2019) 25:198–214. doi: 10.1016/j.molmed.2019.01.006
5. van der Vlist M, Kuball J, Radstake TR, Meyaard L. Immune checkpoints and rheumatic diseases: what can cancer immunotherapy teach us? *Nat Rev Rheumatol.* (2016) 12:593–604. doi: 10.1038/nrrheum.2016.131
6. Meyaard L, Adema GJ, Chang C, Woollatt E, Sutherland GR, Lanier LL, et al. LAIR-1, a novel inhibitory receptor expressed on human mononuclear leukocytes. *Immunity.* (1997) 7:283–90. doi: 10.1016/S1074-7613(00)80530-0
7. Meyaard L. The inhibitory collagen receptor LAIR-1 (CD305). *J Leukoc Biol.* (2008) 83:799–803. doi: 10.1189/jlb.0907609
8. Verbrugge A, de Ruiter T, Geest C, Coffer PJ, Meyaard L. Differential expression of leukocyte-associated Ig-like receptor-1 during neutrophil differentiation and activation. *J Leukoc Biol.* (2006) 79:828–36. doi: 10.1189/jlb.0705370
9. Lebbink RJ, de Ruiter T, Adelmeijer J, Brenkman AB, van Helvoort JM, Koch M, et al. Collagens are functional, high affinity ligands for the inhibitory immune receptor LAIR-1. *J Exp Med.* (2006) 203:1419–25. doi: 10.1084/jem.20052554
10. Olde Nordkamp MJ, van Eijk M, Urbanus RT, Bont L, Haagsman HP, Meyaard L. Leukocyte-associated Ig-like receptor-1 is a novel inhibitory receptor for surfactant protein D. *J Leukoc Biol.* (2014) 96:105–11. doi: 10.1189/jlb.3AB0213-092RR
11. Son M, Santiago-Schwarz F, Al-Abed Y, Diamond B. C1q limits dendritic cell differentiation and activation by engaging LAIR-1. *Proc Natl Acad Sci USA.* (2012) 109:E3160–7. doi: 10.1073/pnas.1212753109
12. Maasho K, Masilamani M, Valas R, Basu S, Coligan JE, Borrego F. The inhibitory leukocyte-associated Ig-like receptor-1 (LAIR-1) is expressed at high levels by human naive T cells and inhibits TCR mediated activation. *Mol Immunol.* (2005) 42:1521–30. doi: 10.1016/j.molimm.2005.01.004
13. Park JE, Brand DD, Rosloniec EF, Yi AK, Stuart JM, Kang AH, et al. Leukocyte-associated immunoglobulin-like receptor 1 inhibits T-cell signaling by decreasing protein phosphorylation in the T-cell signaling pathway. *J Biol Chem.* (2020) 295:2239–47. doi: 10.1074/jbc.RA119.011150
14. Jansen CA, Cruijsen CW, de Ruiter T, Nanlohy N, Willems N, Janssens-Korpela PL, et al. Regulated expression of the inhibitory receptor LAIR-1 on human peripheral T cells during T cell activation and differentiation. *Eur J Immunol.* (2007) 37:914–24. doi: 10.1002/eji.200636678
15. Merlo A, Tenca C, Fais F, Battini L, Ciccone E, Grossi CE, et al. Inhibitory receptors CD85j, LAIR-1, and CD152 down-regulate immunoglobulin and cytokine production by human B lymphocytes. *Clin Diagn Lab Immunol.* (2005) 12:705–12. doi: 10.1128/CDLI.12.6.705-712.2005
16. Bonaccorsi I, Cantoni C, Carrega P, Oliveri D, Lui G, Conte R, et al. The immune inhibitory receptor LAIR-1 is highly expressed by plasmacytoid dendritic cells and acts complementary with NKp44 to control IFNalpha production. *PLoS ONE.* (2010) 5:e15080. doi: 10.1371/journal.pone.0015080
17. Son M, Diamond B. C1q-mediated repression of human monocytes is regulated by leukocyte-associated Ig-like receptor 1 (LAIR-1). *Mol Med.* (2015) 20:559–68. doi: 10.2119/molmed.2014.00185
18. Colombo BM, Canevali P, Magnani O, Rossi E, Puppo F, Zocchi MR, et al. Defective expression and function of the leukocyte associated Ig-like receptor 1 in B lymphocytes from systemic lupus erythematosus patients. *PLoS ONE.* (2012) 7:e31903. doi: 10.1371/journal.pone.0031903
19. Olde Nordkamp MJ, van Roon JA, Douwes M, de Ruiter T, Urbanus RT, Meyaard L. Enhanced secretion of leukocyte-associated immunoglobulin-like receptor 2 (LAIR-2) and soluble LAIR-1 in rheumatoid arthritis: LAIR-2 is a more efficient antagonist of the LAIR-1-collagen inhibitory interaction than is soluble LAIR-1. *Arthritis Rheum.* (2011) 63:3749–57. doi: 10.1002/art.30612
20. Poggi A, Catellani S, Bruzzone A, Caligaris-Cappio F, Gobbi M, Zocchi MR. Lack of the leukocyte-associated Ig-like receptor-1 expression in high-risk chronic lymphocytic leukaemia results in the absence of a negative signal regulating kinase activation and cell division. *Leukemia.* (2008) 22:980–8. doi: 10.1038/leu.2008.21
21. Aoukaty A, Lee IF, Wu J, Tan R. Chronic active epstein-barr virus infection associated with low expression of leukocyte-associated immunoglobulin-like receptor-1 (LAIR-1) on natural killer cells. *J Clin Immunol.* (2003) 23:141–5. doi: 10.1023/A:1022580929226

22. Geerdink RJ, Hennus MP, Westerlaken GHA, Abrahams AC, Albers KI, Walk J, et al. LAIR-1 limits neutrophil extracellular trap formation in viral bronchiolitis. *J Allergy Clin Immunol.* (2018) 141:811–4. doi: 10.1016/j.jaci.2017.08.031
23. Kumawat K, Geerdink RJ, Hennus MP, Roda MA, van Ark I, Leusink-Muis T, et al. LAIR-1 limits neutrophilic airway inflammation. *Front Immunol.* (2019) 10:842. doi: 10.3389/fimmu.2019.00842
24. McGovern N, Schlitzer A, Gunawan M, Jardine L, Shin A, Poyner E, et al. Human dermal $CD14^+$ cells are a transient population of monocyte-derived macrophages. *Immunity.* (2014) 41:465–77. doi: 10.1016/j.immuni.2014.08.006
25. Italiani P, Mazza EM, Lucchesi D, Cifola I, Gemelli C, Grande A, et al. Transcriptomic profiling of the development of the inflammatory response in human monocytes in vitro. *PLoS ONE.* (2014) 9:e87680. doi: 10.1371/journal.pone.0087680
26. Ohl K, Tenbrock K. Inflammatory cytokines in systemic lupus erythematosus. *J Biomed Biotechnol.* (2011) 2011:432595. doi: 10.1155/2011/432595
27. Joo H, Coquery C, Xue Y, Gayet I, Dillon SR, Punaro M, et al. Serum from patients with SLE instructs monocytes to promote IgG and IgA plasmablast differentiation. *J Exp Med.* (2012) 209:1335–48. doi: 10.1084/jem.20111644
28. Carvalheiro T, Gomes D, Pinto LA, Ines L, Lopes A, Henriques A, et al. Sera from patients with active systemic lupus erythematosus patients enhance the toll-like receptor 4 response in monocyte subsets. *J Inflamm (Lond).* (2015) 12:38. doi: 10.1186/s12950-015-0083-2
29. Rodriguez-Pla A, Patel P, Maecker HT, Rossello-Urgell J, Baldwin N, Bennett L, et al. IFN priming is necessary but not sufficient to turn on a migratory dendritic cell program in lupus monocytes. *J Immunol.* (2014) 192:5586–98. doi: 10.4049/jimmunol.1301319
30. Lee YS, Kim MH, Yi HS, Kim SY, Kim HH, Kim JH, et al. CX3CR1 differentiates F4/80(low) monocytes into pro-inflammatory F4/80(high) macrophages in the liver. *Sci Rep.* (2018) 8:15076. doi: 10.1038/s41598-018-33440-9
31. Jakubzick CV, Randolph GJ, Henson PM. Monocyte differentiation and antigen-presenting functions. *Nat Rev Immunol.* (2017) 17:349–62. doi: 10.1038/nri.2017.28
32. Chen L, Arbieva ZH, Guo S, Marucha PT, Mustoe TA, DiPietro LA. Positional differences in the wound transcriptome of skin and oral mucosa. *BMC Genomics.* (2010) 11:471. doi: 10.1186/1471-2164-11-471
33. Jain S. Sepsis: an update on current practices in diagnosis and management. *Am J Med Sci.* (2018) 356:277–86. doi: 10.1016/j.amjms.2018.06.012
34. Shalova IN, Lim JY, Chittezhath M, Zinkernagel AS, Beasley F, Hernandez-Jimenez E, et al. Human monocytes undergo functional re-programming during sepsis mediated by hypoxia-inducible factor-1alpha. *Immunity.* (2015) 42:484–98. doi: 10.1016/j.immuni.2015.02.001
35. Guilliams M, Ginhoux F, Jakubzick C, Naik SH, Onai N, Schraml BU, et al. Dendritic cells, monocytes and macrophages: a unified nomenclature based on ontogeny. *Nat Rev Immunol.* (2014) 14:571–8. doi: 10.1038/nri3712
36. Ziegler-Heitbrock L, Ancuta P, Crowe S, Dalod M, Grau V, Hart DN, et al. Nomenclature of monocytes and dendritic cells in blood. *Blood.* (2010) 116:e74–80. doi: 10.1182/blood-2010-02-258558
37. Wong KL, Yeap WH, Tai JJ, Ong SM, Dang TM, Wong SC. The three human monocyte subsets: implications for health and disease. *Immunol Res.* (2012) 53:41–57. doi: 10.1007/s12026-012-8297-3
38. Kapellos TS, Bonaguro L, Gemund I, Reusch N, Saglam A, Hinkley ER, et al. Human monocyte subsets and phenotypes in major chronic inflammatory diseases. *Front Immunol.* (2019) 10:2035. doi: 10.3389/fimmu.2019.02035
39. Boyette LB, Macedo C, Hadi K, Elinoff BD, Walters JT, Ramaswami B, et al. Phenotype, function, and differentiation potential of human monocyte subsets. *PLoS ONE.* (2017) 12:e0176460. doi: 10.1371/journal.pone.0176460
40. Carenza C, Calcaterra F, Oriolo F, Di Vito C, Ubezio M, Della Porta MG, et al. Costimulatory molecules and immune checkpoints are differentially expressed on different subsets of dendritic cells. *Front Immunol.* (2019) 10:1325. doi: 10.3389/fimmu.2019.01325
41. Wynn TA, Chawla A, Pollard JW. Macrophage biology in development, homeostasis and disease. *Nature.* (2013) 496:445–55. doi: 10.1038/nature12034
42. Jin J, Wang Y, Ma Q, Wang N, Guo W, Jin B, et al. LAIR-1 activation inhibits inflammatory macrophage phenotype *in vitro*. *Cell Immunol.* (2018) 331:78–84. doi: 10.1016/j.cellimm.2018.05.011
43. Mosser DM, Edwards JP. Exploring the full spectrum of macrophage activation. *Nat Rev Immunol.* (2008) 8:958–69. doi: 10.1038/nri2448
44. Martinez FO, Sica A, Mantovani A, Locati M. Macrophage activation and polarization. *Front Biosci.* (2008) 13:453–61. doi: 10.2741/2692
45. Poggi A, Tomasello E, Ferrero E, Zocchi MR, Moretta L. p40/LAIR-1 regulates the differentiation of peripheral blood precursors to dendritic cells induced by granulocyte-monocyte colony-stimulating factor. *Eur J Immunol.* (1998) 28:2086–91. doi: 10.1002/(SICI)1521-4141(199807)28:07<2086::AID-IMMU2086>3.0.CO;2-T
46. Cernadas M, Lu J, Watts G, Brenner MB. CD1a expression defines an interleukin-12 producing population of human dendritic cells. *Clin Exp Immunol.* (2009) 155:523–33. doi: 10.1111/j.1365-2249.2008.03853.x
47. Sander J, Schmidt SV, Cirovic B, McGovern N, Papantonopoulou O, Hardt AL, et al. Cellular differentiation of human monocytes is regulated by time-dependent interleukin-4 signaling and the transcriptional regulator NCOR2. *Immunity.* (2017) 47:1051–66.e12. doi: 10.1016/j.immuni.2017.11.024
48. McNab F, Mayer-Barber K, Sher A, Wack A, O'Garra A. Type I interferons in infectious disease. *Nat Rev Immunol.* (2015) 15:87–103. doi: 10.1038/nri3787
49. Psarras A, Emery P, Vital EM. Type I interferon-mediated autoimmune diseases: pathogenesis, diagnosis and targeted therapy. *Rheumatology (Oxford).* (2017) 56:1662–75. doi: 10.1093/rheumatology/kew431
50. Gerlach H. Agents to reduce cytokine storm. *F1000Res.* (2016) 5:2909. doi: 10.12688/f1000research.9092.1
51. van der Poll T, Opal SM. Host-pathogen interactions in sepsis. *Lancet Infect Dis.* (2008) 8:32–43. doi: 10.1016/S1473-3099(07)70265-7
52. Ellenbroek G, de Haan JJ, van Klarenbosch BR, Brans MAD, van de Weg SM, Smeets MB, et al. Leukocyte-associated immunoglobulin-like receptor-1 is regulated in human myocardial infarction but its absence does not affect infarct size in mice. *Sci Rep.* (2017) 7:18039. doi: 10.1038/s41598-017-13678-5
53. Zhang Y, Lv K, Zhang CM, Jin BQ, Zhuang R, Ding Y. The role of LAIR-1 (CD305) in T cells and monocytes/macrophages in patients with rheumatoid arthritis. *Cell Immunol.* (2014) 287:46–52. doi: 10.1016/j.cellimm.2013.12.005
54. Martinez-Esparza M, Ruiz-Alcaraz AJ, Carmona-Martinez V, Fernandez-Fernandez MD, Anton G, Munoz-Tornero M, et al. Expression of LAIR-1 (CD305) on human blood monocytes as a marker of hepatic cirrhosis progression. *J Immunol Res.* (2019) 2019:2974753. doi: 10.1155/2019/2974753

Conflict of Interest: LM has regular interaction with pharmaceutical and other industrial partners. She has not received personal fees or other personal benefits. LM's institute has received funding for investigator-initiated studies from Nextcure, Boehringer Ingelheim, Ono Pharmaceuticals, Ablynx and Janssen. LM received minor funding for consultation from Novo Nordisk, Biogen and Boehringer Ingelheim.

The remaining authors declare that the research was conducted in the absence of any commercial or financial relationships that could be construed as a potential conflict of interest.

frontiers in Immunology

ORIGINAL RESEARCH
published: 20 August 2020
doi: 10.3389/fimmu.2020.01795

Multiple Processes May Involve in the IgG4-RD Pathogenesis: An Integrative Study via Proteomic and Transcriptomic Analysis

Shaozhe Cai[1†], *Yu Chen*[1†], *ShengYan Lin*[1], *Cong Ye*[1], *Fang Zheng*[2,3*] *and Lingli Dong*[1*]

[1] Department of Rheumatology and Immunology, Tongji Hospital, Tongji Medical College, Huazhong University of Science and Technology, Wuhan, China, [2] Department of Immunology, School of Basic Medicine, Tongji Medical College, Huazhong University of Science and Technology, Wuhan, China, [3] NHC Key Laboratory of Organ Transplantation, Ministry of Education, Chinese Academy of Medical Sciences, Wuhan, China

Immunoglobulin G4-related disease (IgG4-RD) is a newly defined disease entity, while the exact pathogenesis is still not clear. Identifying the characters of IgG4-RD in proteomic and transcriptomic aspects will be critical to investigate the potential pathogenic mechanisms of IgG4-RD. We performed proteomic analysis realized with iTRAQ technique for serum samples from eight treatment-naive IgG4-RD patients and eight healthy volunteers, and tissue samples from two IgG4-RD patients and two non-IgG4-RD patients. Transcriptomic data (GSE40568 and GSE66465) was obtained from the GEO Dataset for validation. The weighted correlation network analysis (WGCNA) was applied to detect the gene modules correlated with IgG4-RD. KEGG pathway analysis was used to investigate pathways enriched in IgG4-RD samples. As a result, a total of 980 differentially expressed proteins (DEPs) in tissue and 94 DEPs in serum were identified between IgG4-RD and control groups. Three hundred fifty-four and two hundred forty-seven genes that most correlated with IgG4-RD were detected by WGCNA analysis in tissue and PBMC, respectively. We also found that DEPs in IgG4-RD samples were enriched in several immune-related activities including bacterial/viral infections and platelet activation as well as some immune related signaling pathways. In conclusion, we identified multiple processes/factors and several signaling pathways that may involve in the IgG4-RD pathogenesis, and found out some potential therapeutic targets for IgG4-RD.

Keywords: IgG4-related disease (IgG4-RD), proteomic analysis, WGCNA (Weighted Gene Co-expression Network Analyses), enrichment analysis, IgG4-RD pathogenesis

OPEN ACCESS

Edited by:
Ali A. Zarrin,
TRexBio, United States

Reviewed by:
Chunfu Zheng,
Fujian Medical University, China
Yi Zhao,
West China Hospital, Sichuan University, China

***Correspondence:**
Fang Zheng
zhengfangtj@hust.edu.cn
Lingli Dong
tjhdongll@163.com

[†] *These authors have contributed equally to this work*

Specialty section:
This article was submitted to Molecular Innate Immunity, a section of the journal Frontiers in Immunology

Received: *08 May 2020*
Accepted: *06 July 2020*
Published: *20 August 2020*

Citation:
Cai S, Chen Y, Lin S, Ye C, Zheng F and Dong L (2020) Multiple Processes May Involve in the IgG4-RD Pathogenesis: An Integrative Study via Proteomic and Transcriptomic Analysis. Front. Immunol. 11:1795. doi: 10.3389/fimmu.2020.01795

INTRODUCTION

Immunoglobulin G4-related disease (IgG4-RD) is a newly defined immune-mediated disease with common clinical, serological, and pathological features (1). Common features of IgG4-RD include serum IgG4 level elevation, multiple organ involvements, dense infiltration of IgG4+ plasma cells, and significant tissue infiltrates (2). This disease affects men more often than women and age at diagnosis ranges from 50 to 70 years (3). Although most patients do respond to steroids well, the relapse rate can be nearly 50% (4).

IgG4-RD is also characterized by alterations in acquired immune system, in which aberrant expansion of plasmablasts, CD4+ cytotoxic T cells, and follicular T helper cells have been observed (5–7). In addition, several inflammatory factors such as TGF-β, IL-4, and IL-10 have also been identified to play a role in the pathogenesis of IgG4-RD (8). The increase of these cytokines promotes eosinophilia in serum or certain tissues, high levels of IgG4-producing plasma cells, elevated production of IgE, and fibrosis, with inflammatory cell infiltrates ultimately causing organ damage (9). Furthermore, several autoantibodies, including anti-carbonic anhydrase II and anti-lactoferrin, are often present in patients with IgG4-RD, especially those with IgG4-related autoimmune pancreatitis (AIP) (10). At present, however, the exact pathogenic mechanism remains unclear, which is an important issue in IgG4-RD studies.

Due to the lack of ideal animal models, and limited sample origin, high throughput, and bioinformatics techniques may help understand the underlying pathogenesis of IgG4-RD more deeply. Transcriptome-wide profiling, as a downstream level of genome-scale mapping, can reveal a systemic dynamics of molecular interaction (11). Recently, studies have utilized transcript profiling in labial salivary glands (LSGs) to distinguish molecular features between IgG4-RD and Sjögren's syndrome (SS), a disease with common phenotypic elements (12, 13). Among other findings, active involvement of Th2- (IL-4, IL-5, and IL-21), T follicular helper cell (Tfh)—(BCL-6 and CXCR5) and Treg-related transcripts (IL-10, FOXP3, CCL18, and TGF-β1) in patients with IgG4-RD were observed. These data showed how elevated levels of such cytokines and chemokines can induce IgG4 plasma cell infiltration, high IgG4 levels in the periphery, and impact tissue fibrosis in the LSG of IgG4-RD patients (13). Further, researchers using high-throughput RNA sequencing technology revealed the molecular differences and effects from prednisone treatment among IgG4-related disease with salivary gland lesions (RD-SG), without SG lesions (RD-nonSG), and IgG4-related retroperitoneal fibrosis (RF) (14). However, the molecular mechanisms and appropriate therapeutic strategies underlying the pathogenesis of IgG4-RD are still unclear.

Proteins are effectors of biological function, and exert critical important roles in the pathogenesis of diseases. Investigation into proteins is crucial for the development of methods to realize early disease diagnosis, prognosis assessment and to monitor the disease development (15). Proteomics involves the applications of technologies for the identification and quantification of overall proteins present content of a cell, tissue or an organism. However, the proteomic study in the field of IgG4-RD is still blank. Thus, we detected both the serologic and tissue proteasome of IgG4-RD patients, and sought for the potential pathogenic information underlying the changes of expression level of proteins in IgG4-RD. Besides analysis at protein level, we also applied Weighted correlation network analysis (WGCNA) methods, a powerful analysis tool that can be utilized for constructing a weighted correlation network and finding modules comprised of highly correlated genes (16), to analyze two public datasets at transcriptomic levels in involved tissue and PBMC, respectively, of IgG4-RD patients.

In conclusion, based on proteomic and transcriptomic analyses, we have not only identified several differently expressed proteins in serum and tissue samples from IgG4-RD patients compared with healthy people, but also illustrated some features of immuno-inflammatory reactions in IgG4-RD, which also helped provide information of its potential therapeutic targets. These results may provide clues to the elucidation of the pathogenesis of, and the development of therapeutic agents for IgG4-RD.

Abbreviations: IgG4, Immunoglobulin G4; iTRAQ, Isobaric tags for relative and absolute quantitation; CV, coefficient of variation; WGCNA, weighted gene co-expression network analysis; KEGG, Kyoto Encyclopedia of Genes and Genomes; DEP, differentially expressed protein; FDR, false discovery rate; LSG, labial salivary glands; PBMC, peripheral blood mononuclear cell. BCR, B cell receptor; PAMP, pathogen associated molecular patterns; DAMP, danger associated molecular patterns. PRR, pattern recognition receptor; MMP, matrix metalloproteinase.

MATERIALS AND METHODS

Proteomic Analysis

Patients and Treatment

We studied eight diagnostic serum samples from eight treatment-naive IgG4-RD patients (25–70 years old) at Department of Rheumatology and Immunology, Wuhan Tongji Hospital (**Table 1**). The diagnosis of IgG4-RD has been made according to diagnostic criteria for IgG4-related disease (IgG4-RD) (17). Meanwhile, eight serum samples from healthy controls (HC) were collected and stored at −80°C for further analysis. Tissue samples of submandibular glands were obtained from two IgG4-RD patients and two non-IgG4-RD patients (adjacent normal edge of the surgical specimens), and stored in liquid nitrogen. All patients gave informed consent to the use of data records for research and to additional laboratory analysis on serum and tissue samples.

Sample Preparation

In this study, the Isobaric tags for relative and absolute quantitation (iTRAQ) technology was applied to investigate the proteasome of serum and tissue samples. First, the ProteoMiner Protein Enrichment Kit (Bio-rad laboratories, Hercules, CA, USA) was applied to deplete the high abundance proteins. Then, the protein solution (100 ug) with 8 M urea was diluted 4 times with 100 mM TEAB buffer. Trypsin Gold (Promega, Madison, WI, USA) was used to digest the proteins with the ratio of protein: trypsin = 40: 1 at 37°C overnight. After trypsin digestion, peptides were desalted with Strata X C (Phenomenex), and vacuum-dried according to the manufacturer's protocol. Peptide labeling was performed by iTRAQ Reagent. Peptide Fractionation were realized with a HPLC Pump system (Shimadzu LC-20AB) coupled with a high pH RP column. Supernatants of fractions were loaded on UHPLC system (Thermo Scientific™ UltiMate™ 3000) equipped with a trap and an analytical column, and peptides separated from nanoHPLC were subjected into the tandem mass spectrometry QEXACTIVE HF X (Thermo Fisher Scientific, San Jose, CA) for data-dependent acquisition (DDA) detection by nano-electrospray ionization. The parameters for MS analysis are listed as following: electrospray voltage: 2.0 kV; precursor

TABLE 1 | Basic clinical information of IgG4-RD patients in this study.

ID	Age	Involved organ	Sample type
1	40–50	Retroperitoneum, pancreas, biliary tract, submandibular glands	Serum, tissue
2	40–50	Submandibular glands, retroperitoneum	Serum
3	50–60	Pancreas, biliary tract, submandibular glands, lymph nodes	Serum
4	50–60	Pancreas, biliary tract, submandibular glands	Serum, tissue
5	70–80	Pancreas, submandibular glands, salivary glands, lymph nodes	Serum
6	40–50	Pancreas, biliary tracts, lymph nodes	Serum
7	20–30	Endocranium, lymph nodes	Serum
8	50–60	Submandibular glands, lymph nodes	Serum

scan range: 350–1,500 m/z at a resolution of 60,000 in Orbitrap; MS/MS fragment scan range: >100 m/z at a resolution of 15,000 in HCD mode; normalized collision energy setting: 30%; dynamic Exclusion time: 30 s; automatic gain control (AGC) for full MS target and MS2 target: 3e6 and 1e5, respectively; the number of MS/MS scans following one MS scan: 20 most abundant precursor ions above a threshold ion count of 10,000.

Protein Identification and Quantification

Protein identification and quantification were realized by software IQuant (18). The propensity score matchings (PSMs) were pre-filtered with false discovery rate (FDR) $\leq$ 1% to assess the confidence of peptides. Then, the identified peptide sequences were assembled into proteins. After protein inference, the protein will be estimated with FDR $\leq$ 0.01.

Transcriptomic Analysis

Microarray Data Collection

We downloaded DNA microarray dataset GSE40568 and GSE66465 from Gene Expression Omnibus (GEO). Specifically, LSG samples in GSE40568 were obtained from Japanese patients with IgG4-RD ($n = 5$) as well as from Japanese patients with SS ($n = 5$) and HCs ($n = 3$) who had been followed up at the University of Tsukuba Hospital (Ibaraki, Japan), Tokyo Women's Medical University Hospital (Tokyo, Japan), and Kyushu University Hospital (Fukuoka, Japan) (13). PBMC samples from peripheral blood mononuclear cell (PBMC) of IgG4-RD were obtained from patients with IgG4-RD before ($n = 2$) and after steroid ($n = 2$) therapy who registered in the research project of the Research Program for Intractable Disease of the Ministry of Health, Labor, and Welfare (MHLW) of Japan and HCs ($n = 4$) (19).

WGCNA Analysis

The coefficient of variation (CV) of each gene were calculated after expression matrix were imported and normalized. Genes with CV >5% were log2 transformed, and the corresponding expression data was applied as input for WGCNA analysis. Then weighted co-expression networks were constructed by employing blockwiseModules function in the WGCNA package (https://horvath.genetics.ucla.edu/html/CoexpressionNetwork/Rpackages/WGCNA/). In this study, we construct a scale-free network ($R^2 = 0.9$) based on the criteria that soft-thresholding power β were set as 20 (IgG4-RD LSG samples in GSE40568 dataset, **Figure S1**) and 12 (IgG4-RD PBMC sample in GSE66465 dataset, **Figure S2**) correspondingly. Genes, that possess edges with adjacency value of >0.2 in the module most correlated to IgG4-RD, were extracted for enrichment analysis.

Statistical Analysis

Log2 transformed data were used to calculate the difference of proteins between IgG4-RD and HC samples with "*t*-test" function in R package (version 3.5.1). Expression matrix from GEO datasets were extracted and normalized by using R package "GEOquery". WGCNA analysis was realized with R package "WGCNA" (version 1.68) (16). KEGG/GO analyses and network construction were realized and visualized with Cytoscape (version 3.4.0) and ClueGO plugin or R package "clusterprofiler" (version 3.12.0) (20, 21). Information of targeted drugs of hub proteins were obtaind via Therapeutic Target Database (22). Without specific indication in the manuscript, all DEPs or genes in gene-module were input to make enrichment analyses.

RESULTS

Identification of Differentially Expressed Proteins With Proteomic Data

A total of 980 (542 up-regulated and 438 down-regulated) differentially expressed proteins (DEPs) in tissue (**Figure 1A**, **Table S1**), while 94 (86 up-regulated, 8 down-regulated) differentially expressed proteins in serum (**Figure 1B**, **Table S2**) were identified between IgG4-RD and control samples based on our criteria (mean ratio of IgG4-RD vs. Control $\geq$1.2, $p < 0.05$). Among them, we found there were 12 DEPs (IGHG4, ITA2B, URP2, HV118, APOC2, GP1BA, CAP1, TBB1, APOE, DSC2, TSP1, and SODE) overlapped in the comparisons of tissue and serum and all those DEPs upregulated in IgG4-RD patients, suggesting their importance to IgG4-RD.

To understand the function of these DEPs which may involve in IgG4-RD, functional enrichment analysis of these DEPs identified in tissue/serum between IgG4-RD and control samples were carried out. Results indicated that most tissue upregulated DEPs were involved in terms including immune related cells activation (e.g., immune response-activating cell surface receptor signaling pathway) and cell adhesion (e.g., leukocyte cell-cell adhesion), and infection related processes

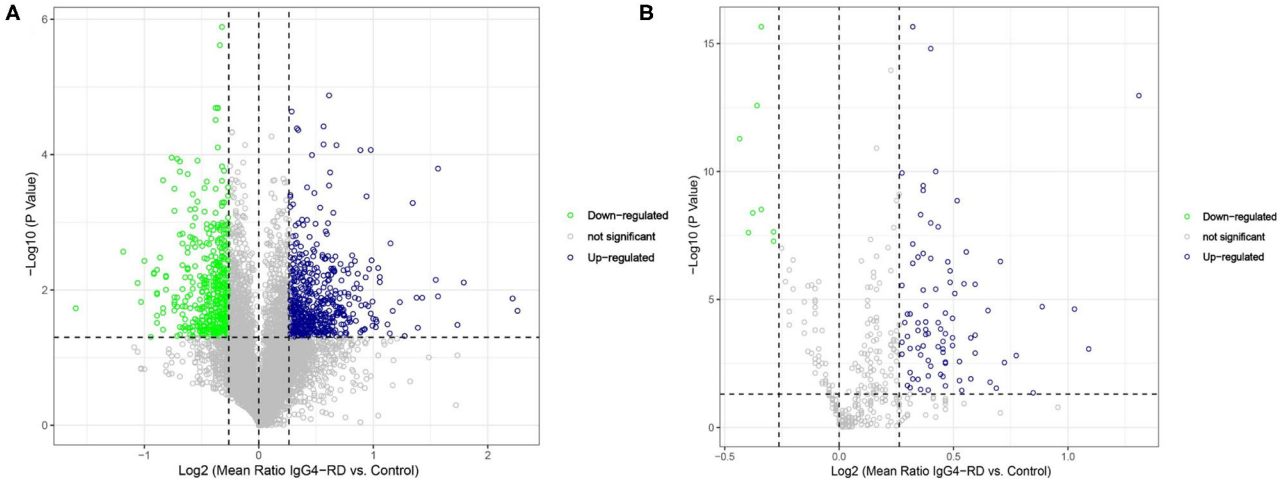

FIGURE 1 | Volcano plot of differentially expressed proteins between IgG4-RD patients and control. **(A)** 980 (542 up-regulated, 438 down-regulated) differentially expressed proteins were identified in tissue between IgG4-RD and control samples. **(B)** 94 (86 up-regulated, 8 down-regulated) proteins in serum were identified as differentially expressed between IgG4-RD and control samples. Proteins with mean ratio >1.2 and $p < 0.05$ were regarded as differentially expressed.

such as human immunodeficiency virus 1 infection, Epstein-Barr virus infection, and Salmonella infection etc. (**Figure 2A**). However, down-regulated DEPs in tissue were mainly involved in processed related to cell junction (e.g., cell junction assembly) (**Figure 2B**). Given the number of downregulated DEPs in serum is small, we focus on upregulated DEPs for further analysis and terms such as protein activation cascade, platelet activation, and extracellular structure organization were outstood in both GO biological process (BP) and KEGG pathway (**Figure 3**).

Weighted Gene Co-expression Network Analysis of Transcriptomic Data

A total of 4,364 genes with coefficient of variation (CV) >5% as input for the construction of WGCNA using GSE40568 dataset from LSC samples. Combined with the topological overlap matrix with the hierarchical average linkage clustering method, we detected the 13 modules in IgG4-RD ($n = 5$), pSS ($n = 5$), and HC samples ($n = 3$) (**Figure 4A**). Among them, module "turquoise" with 934 genes showed strongest correlation with IgG4-RD phenotype (correlation = 0.81, $p = 7e\text{-}5$) (**Figure 4A**, **Figures S3A,B**). Then, a total of 354 genes with edge-adjacency-value more than 0.2 in module "turquoise" were exported for further functional enrichment analysis (**Tables S3**, **S4**).

Based on GSE66456 dataset from PBMC samples, we identified 2,306 genes with coefficient of variation (CV) >5% as input for WGCNA. In this study, 14 modules were detected by WGCNA in IgG4-RD before treatment (IgG4-RD_BT, $n = 2$), IgG4-RD after treatment (IgG4-RD_AT, $n = 2$) and HC samples (HC, $n = 4$) based on the criteria referred in method section (**Figure 4B**). Among them, module "yellow" with 360 genes showed strongest correlation with IgG4-RD_BT phenotype (**Figure 2B**, **Figures S4A,B**). Further, 247 genes with edge-adjacency-value more than 0.2 in module "yellow" were exported for functional enrichment (**Tables S5**, **S6**). In general, we discovered three major biological processes and several signaling pathways that may involve in IgG4-RD.

Antibody Mediated Autoimmune Responses Are the Character of IgG4-RD

Antigen-receptor mediated signaling pathway was significantly enriched in IgG4-RD tissues. Besides T cell-related signaling pathways, using proteomic data by KEGG analysis, we found several KEGG pathways related to B cell-related immune processes, such as "Fc gamma R-mediated phagocytosis," "B cell receptor signaling pathway," "Antigen processing and presentation," and "Leukocyte transendothelial migration" were significantly enriched in IgG4-RD tissue (**Figure 2A**). Meanwhile, we also found term like "Fc gamma R-mediated phagocytosis" was enriched in genes from "turquoise" module in WGCNA analysis of the transcriptomic data of IgG4-RD LSG (**Table S7**). In addition, KEGG term "Systemic lupus erythematosus" was enriched in transcriptomic data of IgG4-RD derived PBMC ($p < 0.0001$, **Table S8**). These results indicated autoimmune characters of IgG4-RD, and also revealed an important role of antibodies in the autoimmune responses of IgG4-RD (23).

Potential Infection and Infection-Related Responses May Be the Trigger in IgG4-RD

Infectious agents are the main origin of pathogen associated molecular patterns (PAMPs), and can mediate the release of danger associated molecular patterns (DAMPs). Both PAMPs and DAMPs are ligands of pattern recognition receptors (PRRs), which can be found in many cellular components involved in immune reactions. Activation of PRRs can modulate the functional states of immune-related cells, which further influence the process of immune responses. Based on our proteomic data, many infection related terms such as "Human

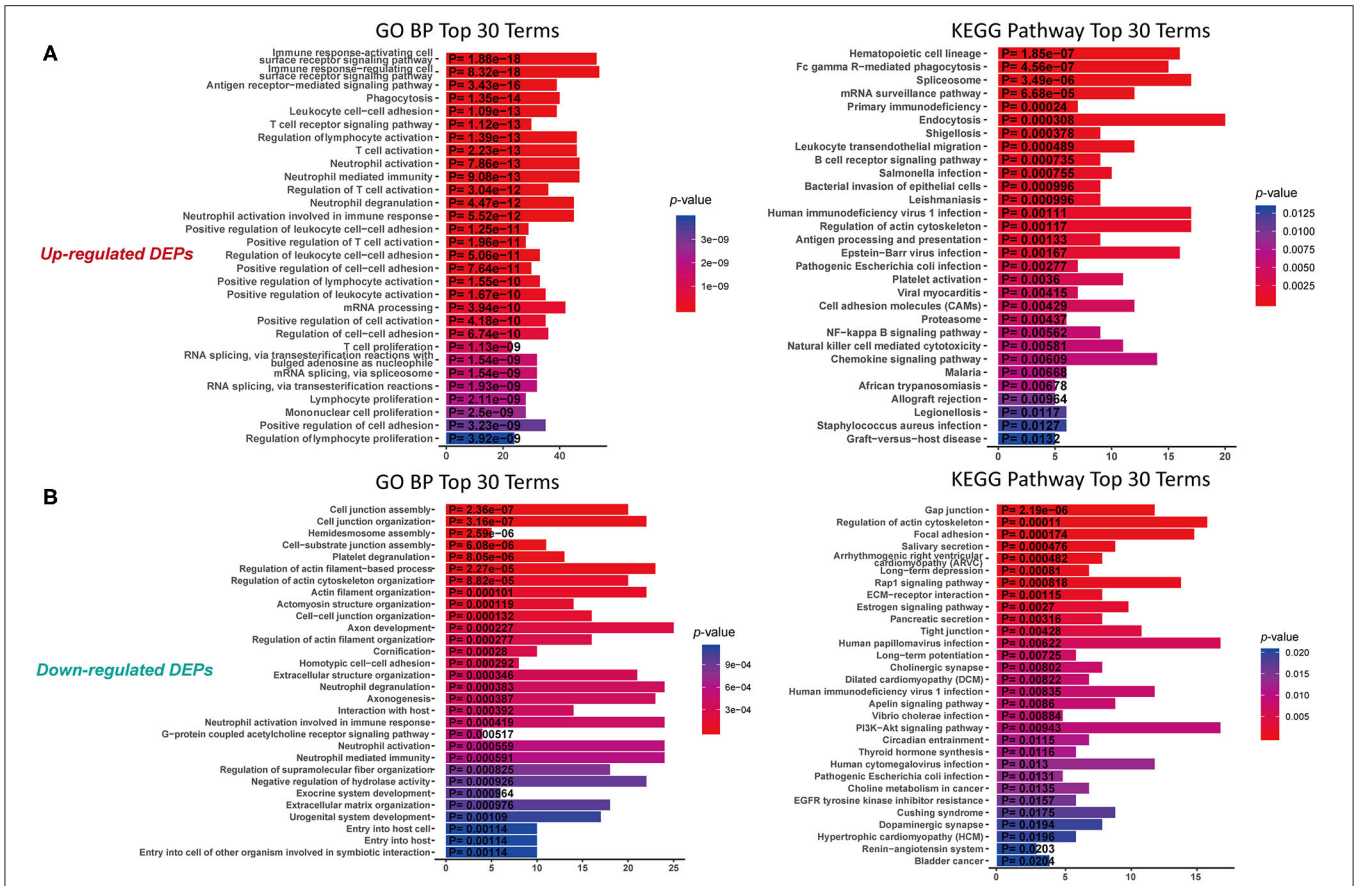

FIGURE 2 | Functional enrichment of DEPs in tissue with proteomic data. **(A)** KEGG analysis and GO Biological process (GO BP) enrichment of up-regulated DEPs in tissue. **(B)** KEGG analysis and GO enrichment of down-regulated DEPs in tissue. X-axis: the number of DEPs of the proteomic data involved in the corresponding enriched terms.

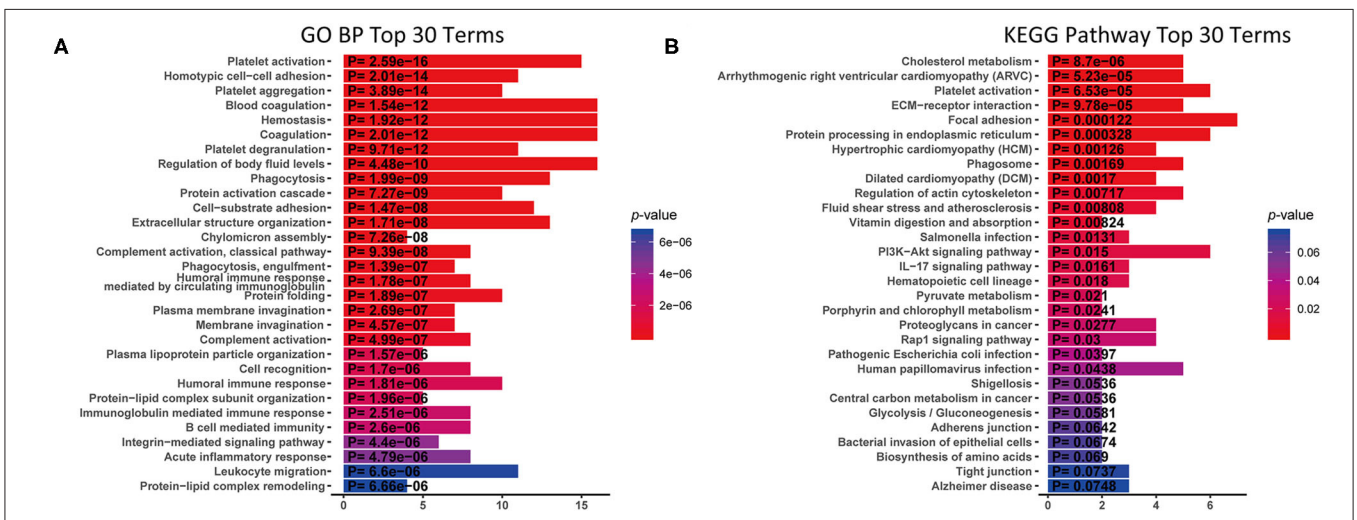

FIGURE 3 | KEGG analysis and GO Biological process (GO BP) enrichment of up-regulated DEPs in serum with proteomic data. X-axis: the number of DEPs of the proteomic data involved in the corresponding enriched terms. **(A)** GO BP enrichment analysis. **(B)** KEGG pathway analysis.

immunodeficiency virus 1 infection," "Epstein-Barr virus infection" and "Bacterial invasion of epithelial cells" were enriched in IgG4-RD tissue (**Figure 2A**, **Table 2**). Meanwhile, we also found genes from module "turquoise" in transcriptomic data also showed correlation with infection terms such as "Human papillomavirus infection," "Epithelial cell signaling in

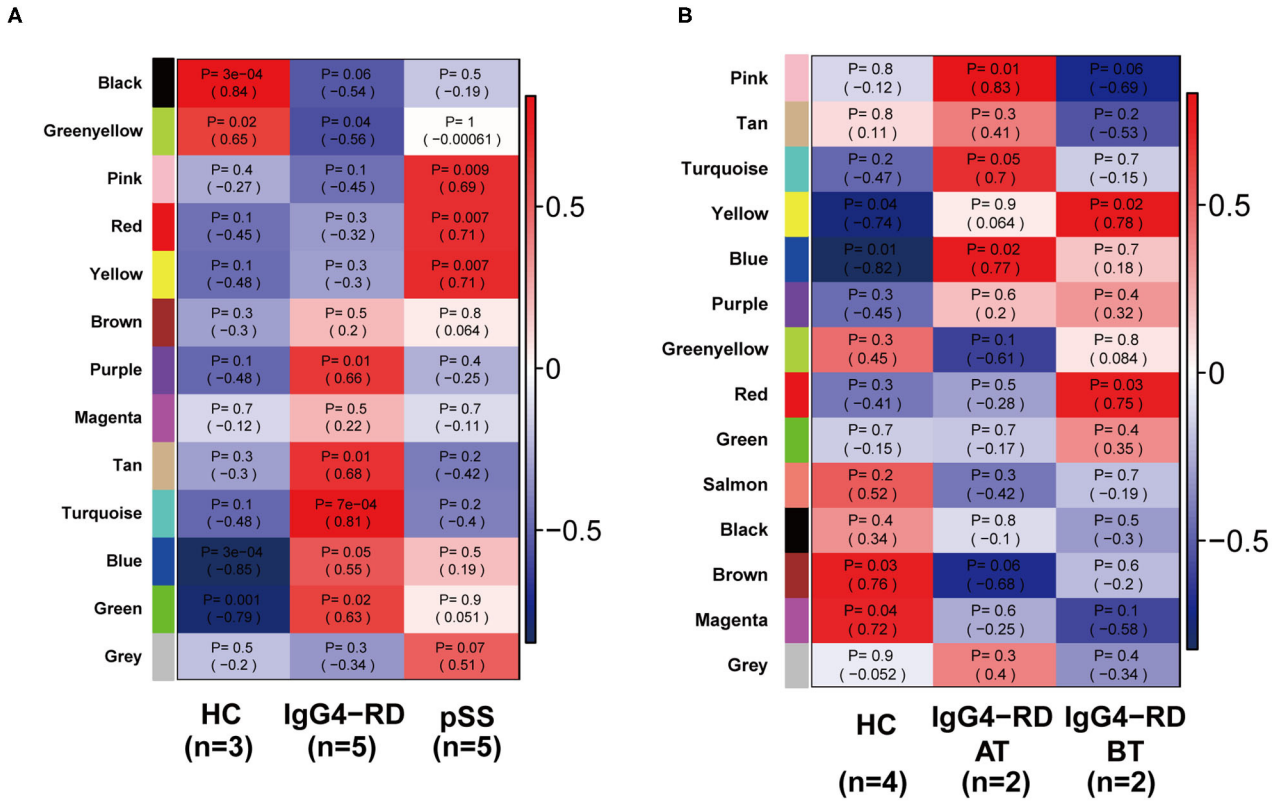

FIGURE 4 | Heatmap of module-trait relationships revealed by WGCNA analysis. **(A)** 13 modules were detected by WGCNA in all samples from GSE40568. Among all these 13 modules, module "turquoise" showed strongest correlation with IgG4-RD phenotype. **(B)** 14 modules were detected by WGCNA in all samples from GSE66465, and module "yellow" showed strongest correlation with IgG4-RD (before treatment) phenotype.

Helicobacter pylori infection," "Bacterial invasion of epithelial cells," etc (**Table 3**, **Table S7**). Most of these terms showed relationship with bacterial infection, which may echo the fact that most involved organs in IgG4-RD are exocrine organs, like pancreas, and submandibular glands (24). Thus, we may infer that infectious agents and infection related processes may play important roles in the development and progress of IgG4-RD.

Platelet Activation Were Observed in IgG4-RD Samples

In proteomic data, up-regulated DEPs from both serum and tissue samples of IgG4-RD patients were enriched in "Platelet activation" pathway (**Figures 2A**, **3**). Meanwhile, Enrichment of term "Platelet activation" was also observed in genes derived from "turquoise" module from tissue transcriptomic dataset (**Figure 5**). This result is consistent with the research on platelets that may serve as the immune components to possess modulate functions (25).

Multiple Signaling Pathways May Participate the Pathogenesis of IgG4-RD

Understanding the significantly enriched signaling pathways in IgG4-RD may help to search the potential therapeutic targets. In proteomic data, "Rap1 signaling pathway" and "NF-κB signaling pathway" were enriched in IgG4-RD tissue (**Figure 2B**), while terms such as "MAPK signaling pathway," "PI3K-Akt signaling pathway," "TGF-β signaling pathway," "Ras signaling pathway," and "Rap1 signaling pathway" were enriched in tissue transcriptomic data (**Table 4**, **Table S7**). Term "TGF-β signaling pathway" was also enriched in transcriptomic data from IgG4-RD PBMC (**Table S8**). In this study, only "Rap1 signaling pathway" was observed enriched in both tissue proteomic data and IgG4-RD LSG samples in GSE40568 dataset (**Figures 2B**, **6**). Activation of Rap1 signaling pathway can lead to the production of proinflammatory cytokines and modulate the expression level of MMPs, which are critical in the modulation of extracellular matrix, and influence the fibrogenic process (26). Beside terms illustrated above, there were also many other terms, like "Autophagy," "Necroptosis," etc., that were enriched in different datasets (**Tables S7**, **S8**).

Potential Therapeutic Target Identified by Tissue DEPs Related Biological Processes

In order to find out the potential therapeutic targets for IgG4-RD, we extracted all proteins (not only DEPs) involved in top 30 KEGG/GO BP terms enriched from all DEPs in our tissue proteomic data (**Figure 7**). One thousand six hundred seventy-four proteins in KEGG top 30 terms and, 2,291 proteins in GO BP top 30 terms were identified. Based on the involvements of these proteins in these different biological processes, we constructed networks and calculated the degree (number of connections, number of pathways in which the

TABLE 2 | KEGG terms related to infectious process enriched in IgG4-RD tissue proteomic data.

Pathway ID	KEGG term	Associated proteins	*P*-value
KEGG:05143	African trypanosomiasis	FAS, GNAQ, IL18, LAMA4, PLCB1, PLCB2, PRKCB, VCAM1	0.0010
KEGG:05146	Amoebiasis	CASP3, GNA11, GNAQ, LAMA4, LAMB3, PLCB1, PLCB2, PRKACB, PRKCB, RAB5C, SERPINB9, TLR2	0.0159
KEGG:05100	Bacterial invasion of epithelial cells	ARPC1B, ARPC2, ARPC3, ARPC5, CDH1, DNM3, ELMO1, ELMO3, RHOG, SEPT1, WAS	0.0050
KEGG:05142	Chagas disease American trypanosomiasis	C1QB, CD3E, CD3G, FAS, GNA11, GNAO1, GNAQ, PLCB1, PLCB2, PPP2CB, PPP2R1B, TLR2	0.0331
KEGG:05120	Epithelial cell signaling in Helicobacter pylori infection	ADAM17, ATP6V0C, ATP6V1G2, CASP3, CSK, F11R, LYN, NOD1, PLCG2, TJP1	0.0079
KEGG:05170	Human immunodeficiency virus 1 infection	AP1G2, AP1S3, APOBEC3C, APOBEC3F, ATM, CASP3, CD3E, CD3G, CD4, CFL1, CFL2, FAS, GNA11, GNAO1, GNAQ, GNG2, GNG7, HLA-E, LIMK1, MAP2K1, PLCG2, PRKCB, RAC2, RPS6KB2, SAMHD1, TLR2, TRADD, TRIM5	0.0001
KEGG:05134	Legionellosis	CASP3, CR1, HSF1, HSPA6, IL18, PYCARD, RAB1A, TLR2	0.0177
KEGG:05140	Leishmaniasis	CR1, CYBB, HLA-DQA2, HLA-DQB1, HLA-DRA, ITGA4, PRKCB, PTPN6, TLR2	0.0447
KEGG:05144	Malaria	CR1, IL18, ITGAL, SDC2, THBS1, TLR2, VCAM1	0.0282
KEGG:05130	Pathogenic *Escherichia coli* infection	ARPC1B, ARPC2, ARPC3, ARPC5, CDH1, EZR, KRT18, TUBA4A, TUBAL3, TUBB1, TUBB4B, WAS	0.0001
KEGG:05132	Salmonella infection	ARPC1B, ARPC2, ARPC3, ARPC5, IL18, KLC3, KLC4, PFN1, PKN1, PYCARD, RHOG, TJP1, WAS	0.0020
KEGG:05131	Shigellosis	ARPC1B, ARPC2, ARPC3, ARPC5, ELMO1, ELMO3, NOD1, PFN1, RHOG, UBE2D2, WAS	0.0018
KEGG:05110	Vibrio cholerae infection	ATP6V0C, ATP6V1G2, PLCG2, PRKACB, SLC12A2, TJP1, TJP2	0.0311
KEGG:05416	Viral myocarditis	CASP3, CXADR, DAG1, DMD, HLA-DQA2, HLA-DQB1, HLA-DRA, HLA-E, ITGAL, RAC2	0.0028

TABLE 3 | KEGG terms related to infectious process enriched in "turquoise" module in IgG4-RD tissue transcriptomic data.

Pathway ID	KEGG term	Associated proteins	*P*-value
KEGG:05165	Human papillomavirus infection	AKT3, COL1A1, COL1A2, COL6A1, COL6A3, EGFR, FN1, FZD7, ITGA9, JAG1, LAMA2, LAMA4, LAMC1, THBS2	0.0052
KEGG:05100	Bacterial invasion of epithelial cells	CAV1, CAV2, FN1, MET, WASF2	0.0112
KEGG:05146	Amoebiasis	COL1A1, COL1A2, COL3A1, FN1, GNAL, LAMA2, LAMA4, LAMC1	0.0004
KEGG:05144	Malaria	CD36, HGF, MET, SDC2, THBS2	0.0019

protein participates) of each protein. We identified proteins with top 15 degrees as hub proteins. Most of these hub proteins, for example, protein kinase C alpha/beta/delta/gamma type (PRCKA/B/D/G), mitogen-activated protein kinase 1/3 (MAPK1/3), and phosphatidylinositol 4,5-bisphosphate 3-kinase catalytic subunit alpha/beta/delta isoform (PIK3CA/B/D), are important components in immune related signaling pathways in various types of immune cells (27–29). Medication targeting these proteins may help the treatment to IgG4-RD. Therefore, we also obtained the information of targeted drugs to the hub proteins from Therapeutic Target Database (**Table 5**) (22).

DISCUSSION

To our knowledge, the pathogenesis of IgG4-RD is still not clear and this is the first report providing new insights to help the illustration of potential pathogenic mechanisms underlying IgG4-RD based on proteomic and transcriptomic data.

Existence of strong immune responses in IgG4-RD is well-known. Different T cell subsets may interact with B cell subsets in involved tissue, and further lead to the down-streaming fibrogenesis, which can also be partly reflected by our study (**Figure 2**) (30–34). In addition, this study indicated that other subclasses of immunoglobulin G could also be pathogenic in IgG4-RD (35). The membrane form of IgG4 is exactly the B cell receptor on IgG4+ plasmablasts/plasma cells, which can mediate the antigen capture and further lead to the antigen presentation from plasmablasts/plasma cells.

Our study detected significant enrichment of "Fc gamma R-mediated phagocytosis" process in IgG4-RD tissue (**Figure 2A**, **Table S7**), which may point out the potential role in the pathogenesis of IgG4-RD. Activation of Fcγ receptors

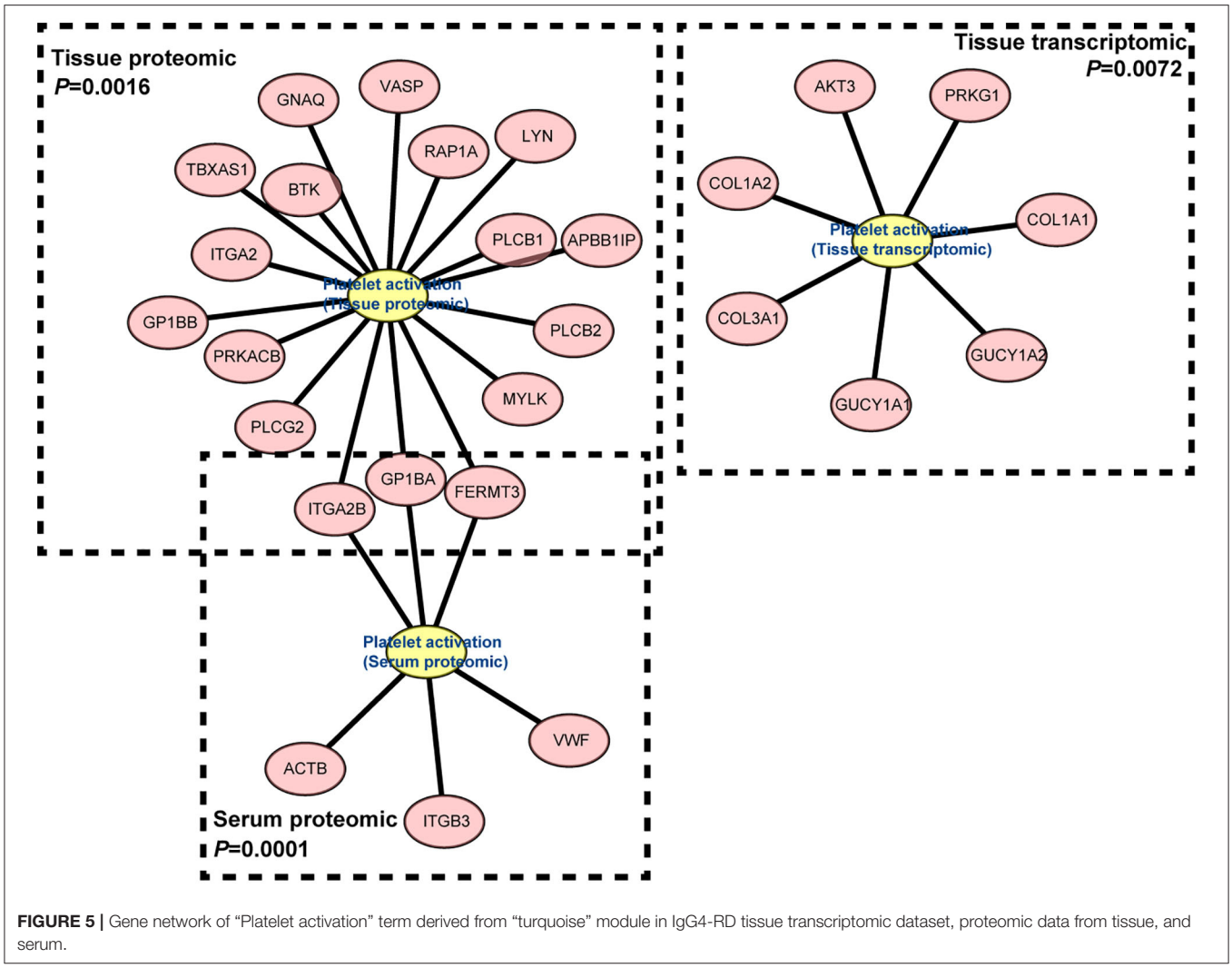

FIGURE 5 | Gene network of "Platelet activation" term derived from "turquoise" module in IgG4-RD tissue transcriptomic dataset, proteomic data from tissue, and serum.

(FcγR) on phagocytes can promote phagocytosis and the following antigen presentation process (36). Compared with high binding affinity of IgG1 and IgG3 to FcγR, the binding affinity of IgG4 to FcγR seems to be much milder. In IgG4-RD tissue, our proteomic study showed significant elevated IgG3 level, while IgG1 showed only the tendency of elevation. These clues indicate the potential role of IgG3 in IgG4-RD, at least, partly by Fc gamma receptor mediated phagocytosis, which can be another origin of antigen presentation, together with that mediated by IgG4+ plasmablasts/plama cells.

In this study, besides immunoglobulins produced by plasmablasts/plama cells, we found level of several cytokines, including CXCL13, IL-27, and IL-18, elevated significantly in IgG4-RD tissue. Cytokines exert essential effects on the immunoinflammatory process. IL-27 can act as antagonists to suppress Th1, Th2, Th9, and Th17 responses, while promote the proliferation and the expression of T-bet, EOMES, and IL-12Rβ2 associated with increased production of IFN-γ and cytotoxic activity (37). IL-18 is a member of IL-1 family, and involved not only in Th1 and NK cell activation, but also in Th2, IL-17-producing γδ T cells and macrophage activation (38). CXCL13 is critical for the recruitment of follicular Tfhs, and plasma CXCL13 can be a biomarker for germinal center activity (39, 40). Thus, all these three cytokines may exert important regulatory effects on the immune responses in IgG4-RD. However, these three cytokines were not detected in our serum proteomic analysis, and these might result from their low concentration in serum, and the detection threshold for iTRAQ methods. Thus, more validations should be applied to detect the existence and levels of these cytokines in serum, and examine the availability as biomarkers in IgG4-RD.

Infectious agents can modulate the status of immune responses, and even be the triggers of systemic lupus erythematosus (SLE) and Sjögren's syndrome (41). Our analyses enriched a large amount of processes related to infectious agents in both proteomic (**Figure 2A**) and transcriptomic data (**Tables S7**, **S8**). We may infer that the most frequently involved organs in IgG4-RD including pancreas, salivary glands

TABLE 4 | Signaling pathways and other potential pathogenic processes detected in IgG4-RD tissue transcriptomic data.

Pathway ID	KEGG term	Associated proteins/genes	*P*-value	Data origin
KEGG:04350	TGF-beta signaling pathway	BMP6, LTBP1, SMAD1, THBS1	0.0409	PBMC transcriptomic
KEGG:04217	Necroptosis	HIST1H2AB, HIST1H2AE, HIST1H2AH, HIST1H2AI, HIST1H2AJ, HIST1H2AK, HIST1H2AL, HIST1H2AM, TNFAIP3	0.0009	PBMC transcriptomic
KEGG:05203	Viral carcinogenesis	HIST1H2BB, HIST1H2BC, HIST1H2BG, HIST1H2BH, HIST1H2BI, HIST1H2BJ, HIST1H2BM, HIST1H2BN, HIST1H2BO, HIST1H4D, HIST2H2BE, HIST2H4A	0.0001	PBMC transcriptomic
KEGG:05202	Transcriptional misregulation in cancer	CD14, HIST1H3A, HIST1H3B, HIST1H3F, HIST1H3H, HIST1H3J, MEIS1, SMAD1	0.0081	PBMC transcriptomic
KEGG:04064	NF-kappa B signaling pathway	ATM, BTK, LYN, PARP1, PLCG2, PRKCB, TNFRSF11A, TRADD, UBE2I, VCAM1, ZAP70	0.0471	Tissue proteomic
KEGG:04015	Rap1 signaling pathway	APBB1IP, CDH1, CSF1R, FLT1, FYB1, GNAO1, GNAQ, ITGA2B, ITGAL, MAP2K1, NGFR, PARD3, PDGFA, PDGFC, PDGFRA, PFN1, PLCB1, PLCB2, PRKCB, RAC2, RAP1A, SIPA1, SIPA1L3, THBS1, VASP	0.0009	Tissue proteomic
KEGG:04140	Autophagy	DAPK1, GABARAPL1, HMGB1, MAP2K1, MTMR14, PIK3R4, PPP2CB, PRKACB, RPS6KB2, RRAGA, RRAGC, STX17, ULK2, WIPI1	0.0371	Tissue proteomic
KEGG:04217	Necroptosis	CHMP1B, CHMP4C, CYBB, FAS, FTH1, FTL, H2AFX, H2AFY, H2AFY2, HIST2H2AB, HMGB1, PARP1, PYCARD, PYGM, TRADD, TYK2, ZBP1	0.0289	Tissue proteomic
KEGG:05219	Bladder cancer	CDH1, DAPK1, MAP2K1, RPS6KA5, THBS1, TYMP	0.0368	Tissue proteomic
KEGG:04010	MAPK signaling pathway	AKT3, EGFR, FGF2, FGF7, HGF, KITLG, MAP3K20, MET, NTRK2, PDGFD, PDGFRA, TGFBR2	0.0115	Tissue transcriptomic
KEGG:04015	Rap1 signaling pathway	AKT3, DOCK4, EGFR, FGF2, FGF7, HGF, KITLG, MET, PDGFD, PDGFRA, SIPA1L2	0.0013	Tissue transcriptomic
KEGG:04151	PI3K-Akt signaling pathway	AKT3, COL1A1, COL1A2, COL6A1, COL6A3, EGFR, FGF2, FGF7, FN1, GHR, GNG11, HGF, ITGA9, KITLG, LAMA2, LAMA4, LAMC1, MET, NTRK2, PDGFD, PDGFRA, THBS2	<0.0001	Tissue transcriptomic
KEGG:05226	Gastric cancer	AKT3, EGFR, FGF2, FGF7, FZD7, HGF, MET, TGFBR2	0.0059	Tissue transcriptomic
KEGG:05222	Small cell lung cancer	AKT3, FN1, LAMA2, LAMA4, LAMC1	0.0276	Tissue transcriptomic
KEGG:05215	Prostate cancer	AKT3, EGFR, PDGFD, PDGFRA, PLAT	0.0323	Tissue transcriptomic
KEGG:05205	Proteoglycans in cancer	AKT3, ANK2, CAV1, CAV2, COL21A1, DCN, EGFR, FGF2, FN1, FZD7, GPC3, HGF, LUM, MET, SDC2, TIMP3	<0.0001	Tissue transcriptomic
KEGG:05218	Melanoma	AKT3, EGFR, FGF2, FGF7, HGF, MET, PDGFD, PDGFRA	<0.0001	Tissue transcriptomic

are mainly exocrine organs, which have more opportunity to contact infectious agents. Activation of toll-like receptors (TLRs) can involve in autoimmune responses indirectly via modulating innate immunity, and directly via modulating B cell signaling, and TLRs can even be the therapeutic targets for autoimmune connective tissue diseases (42, 43). In our proteomic data, the elevation of TLR2 was detected in IgG4-RD samples (**Table S1**), which indicated the possibility, that TLR2 may have the potential to exert modulatory effects in IgG4-RD *in vivo*.

Enrichment of platelet activation related processes in IgG4-RD patients was also observed in our study (**Figures 2**, **3**, **5**). As illustrated above, majority of the recent investigations focus on the pathogenetic roles of traditional immune cells like lymphocytes and macrophages (44). However, immune response is a complex process, and can be modulated by multiple factors. Recently, immunomodulatory effects of platelets have been observed in several immunoinflammatory conditions. Zhu et al. showed platelets first promoted the activation of Th1, Th17, and Treg cells, while only suppressed the immune response of Th1 and Th17 cells secondarily (45). Platelets can also express receptors including FcγRIIA, TLR4, and TLR9, which equips platelets the capacity to receive the stimuli, like immune complexes, PAMPs, and DAMPs, from microenvironments and response to them (46). Granules in platelets contain various growth factors, chemokines, and proinflammatory factors including TGF-β, EGF, CXCL12, HMGB1, and sCD40L etc., which

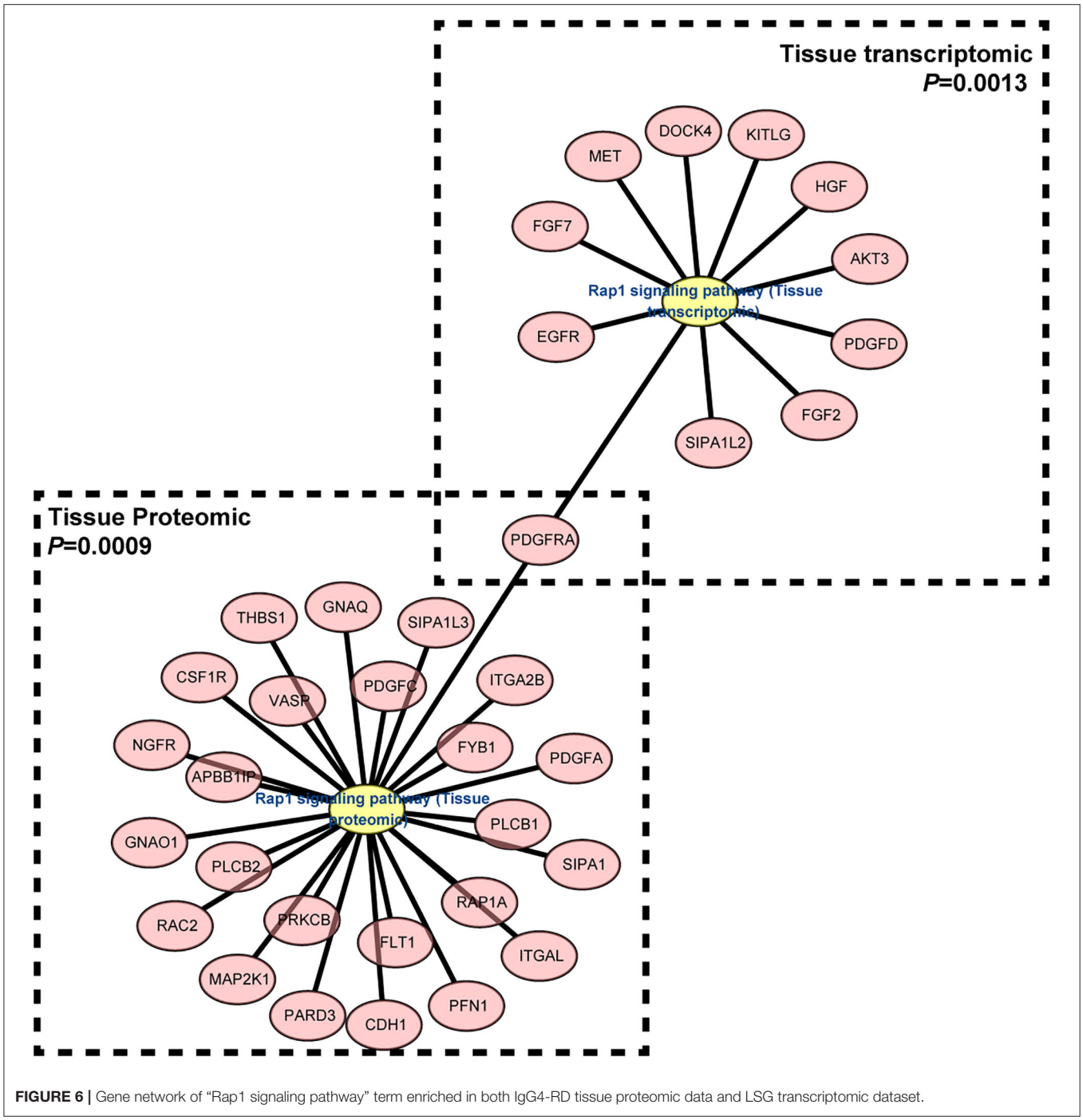

FIGURE 6 | Gene network of "Rap1 signaling pathway" term enriched in both IgG4-RD tissue proteomic data and LSG transcriptomic dataset.

can function in the modulation of immunoinflammatory processes (46, 47).

Genes (or proteins) related to several signaling pathways were also detected in IgG4-RD samples (tissue or PBMC), including MAPK signaling pathway, PI3K-Akt signaling pathway, Ras signaling pathway, TGF-β signaling pathway, NF-κB signaling pathway and Rap1 signaling pathway (**Figures 2A**, **3**, **Table 4**, **Table S7**). All these signaling pathway can regulate variety of biological process. Beside biological process described above, genes related to autophagy, necroptosis and adhesion molecules (e.g., "Focal adhesion," "Cell adhesion molecules (CAMs)," etc.) were also detected in IgG4-RD samples. Interestingly, several terms related to malignancy (e.g., "Choline metabolism in cancer," "Small cell lung cancer," "Bladder cancer," "Viral carcinogenesis," and "Proteoglycans in cancer") were also enriched in IgG4-RD samples. All these clues can reflect some parts of the characteristics of IgG4-RD, and indicate the potential similarities of the pathogenesis mechanisms underlying

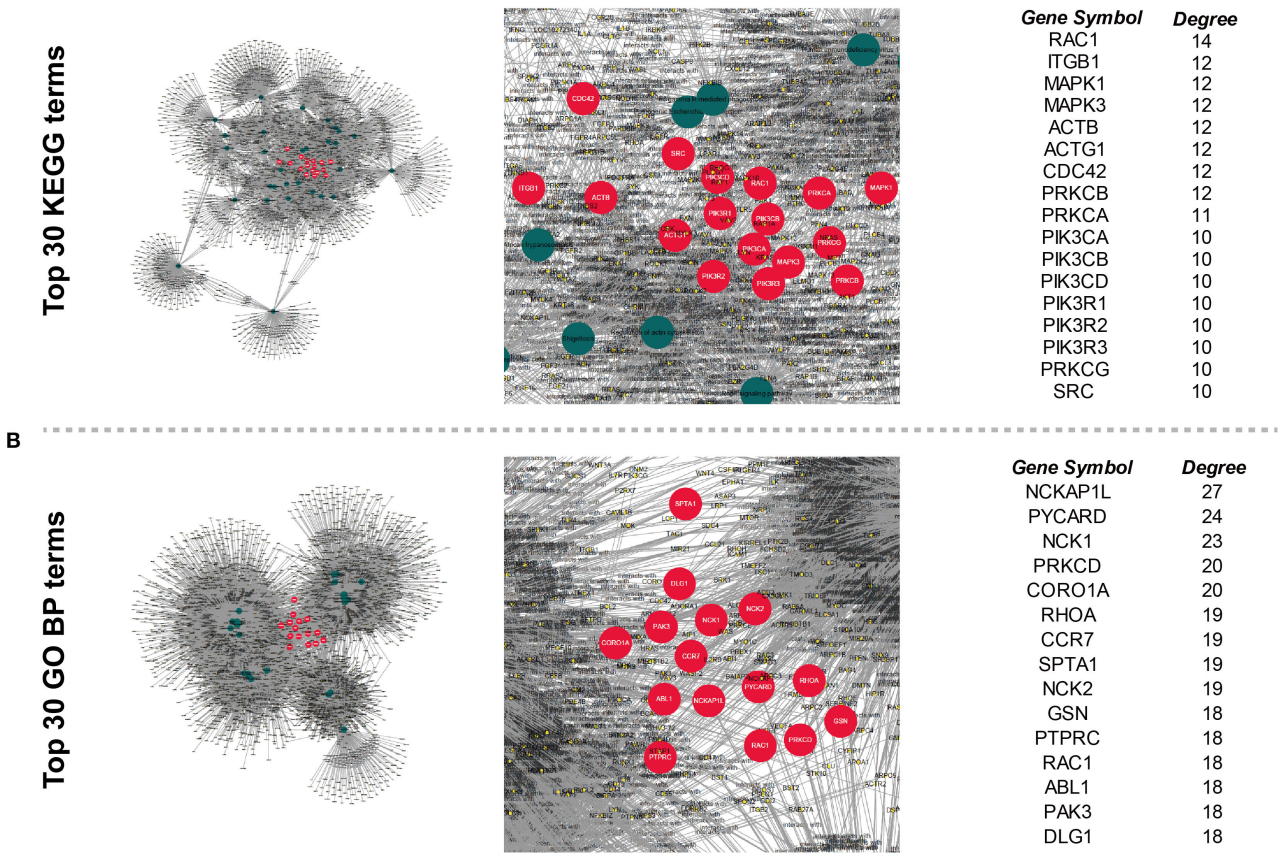

FIGURE 7 | Networks constructed by all proteins involved in the top 30 **(A)** KEGG and **(B)** GO Biological process (GO BP) terms enriched from all tissue DEPs. Circles (nodes) in the network represents proteins or KEGG/GO terms. Degree (number of connection) of each node was calculated, and nodes (except that represent KEGG/GO terms) with top 15 degree were regarded as hub nodes, and their corresponding proteins were identified as hub proteins. Hub nodes (proteins): red, large size; Term nodes: dark green, large size; other nodes (proteins): yellow, small size; Protein's involvement into biological process: line, dark gray.

IgG4-RD to the known mechanisms of the biological processes illustrated above.

How to treat IgG4-RD is another task we are facing. Despite glucocorticoids and rituximab are effective in the induction therapy, and application of conventional steroid sparing medication (e.g., azathioprine, mycophenolate mofetil, and methotrexate) can help control the disease, the problem of relapse and side effects after long-term usage of these medications are still remarkable (48–50). Based on the characteristics of IgG4-RD tissue proteomic data, we identified several hub proteins, which might be involved and play important roles in the pathogenesis of IgG4-RD. Most of these proteins are important signaling components in immune reactions, and some of these agents have been even applied into the clinical treatment of other diseases. Therefore, after the validation of the pathogenic roles of these proteins in IgG4-RD via laboratory experiments, these drugs have the potential to be therapeutic agents targeting IgG4-RD.

In summary, we provided the first integrative analysis of IgG4-RD via both proteomic and transcriptomic data, and described a landscape of biological processes of this mysterious disease, which indicated some potential pathogenic molecules and immunoinflammatory responses, and provided several potential therapeutic targets for the treatment of IgG4-RD. There are also limitations in our study. Firstly, despite the aim of our study is to provide the landscape at the level of mRNA and protein of IgG4-RD, the sample size of our analysis was relatively small, and we didn't enroll more IgG4-RD-like samples (e.g., tumors, and other rheumatic diseases), in our analyses; secondly, the transcriptomic data were originated from the published data of other centers, although analyses to them showed overlaps with our proteomic data, which may reflect the reliability of our analyses indirectly; thirdly, our analyses were based on the data of bulk samples, which cannot provide the information of specific cell types. Therefore, further studies with large sample size, and at single cell level are needed. Besides, other types of omics (e.g., lipidomics, metabolomics, and glycomics) and validation with laboratory experiments are also important to help us understand this mysterious disease more deeply.

TABLE 5 | Potential therapeutic targets and targeted drugs for IgG4-RD.

Gene symbol	Name	Drugs (target type)	Disease application
Targets identified from KEGG terms			
RAC1	Ras-related C3 botulinum toxin substrate 1	EHT-1864 (Literature-reported target)	Alzheimer disease
ITGB1	Integrin beta-1	131I-radretumab (Clinical trial target)	Non-small-cell lung cancer; Macular degeneration
		ATN-161(Clinical trial Target) *Target: Integrin alpha-5/beta-1	Non-small-cell lung cancer; Renal cell carcinoma
MAPK1	Extracellular signal-regulated kinase 2	CI-1040 (Clinical trial target)	Artery stenosis; Pancreatic cancer
MAPK3	Extracellular signal-regulated kinase 1	BVD-523 (Clinical trial Target)	Solid tumor/cancer; Artery stenosis
PRKCB	Protein kinase C beta	Enzastaurin (Clinical trial target)	Diffuse large B-cell lymphoma; Lymphoma
PRKCA	Protein kinase C alpha	Sodium phenylbutyrate (Successful target)	Spinal muscular atrophy; Renal transplantation;
PIK3CA	Phosphatidylinositol 3-kinase catalytic subunit alpha	BAY 80-6946 (Successful target)	Follicular lymphoma; Non-hodgkin lymphoma
PIK3CB	Phosphatidylinositol 3-kinase catalytic subunit beta	Buparlisib (Clinical trial target)	Breast cancer; Pain
PIK3CD	Phosphatidylinositol 3-kinase catalytic subunit delta	Idelalisib (Successful target)	Follicular lymphoma; Small lymphocytic lymphoma
PRKCG	Protein kinase C gamma	Midostaurin (Successful target)	Acute myeloid leukemia; Systemic mastocytosis
SRC	Proto-oncogene tyrosine-protein kinase Src	Herbimycin A (Successful target)	Breast cancer; Ischemia
Targets identified from GO Biological process terms			
NCK1	NCK adaptor protein	AX-024 (Clinical trial target)	Multiple sclerosis
PRKCD	Protein kinase C delta	KAI-9803 (Clinical trial target)	Acute myocardial infarction; Human immunodeficiency virus infection
PTPRC	Receptor-type tyrosine-protein phosphatase C	Iomab-B (Clinical trial target)	Bone marrow transplantation; Acute myeloid leukemia
RAC1	Ras-related C3 botulinum toxin substrate 1	EHT-1864(Literature-reported target)	Alzheimer disease
ABL1	Tyrosine-protein kinase ABL1	Adenosine triphosphate (Successful target)	Breast cancer; Ischemia

Only available targets were showed.

DATA AVAILABILITY STATEMENT

Data of GSE40568 and GSE66465 can be downloaded from Gene Expression Omnibus Dataset (GEO Dataset: http://www.ncbi.nlm.nih.gov/geo/). The proteomic data is available from the corresponding author on reasonable request.

ETHICS STATEMENT

The studies involving human participants were reviewed and approved by Tongji Hospital, Tongji Medical College, Huazhong University of Science, and Technology Institutional Review Board Approval. The ethics IRB ID is: TJ-C20151109. The patients/participants provided their written informed consent to participate in this study.

AUTHOR CONTRIBUTIONS

SC and YC made the sample collection, data analyses, and wrote this manuscript. SL and CY revised the manuscript and provided important advice. LD and FZ designed this program, and are the corresponding authors of this paper. All authors contributed to the article and approved the submitted version.

FUNDING

This study was supported by grants from the National Natural Science Foundation of China (NSFC Nos. 81771754 and 31670876), and Tongji Hospital Clinical Research Flagship Program (2019CR206).

SUPPLEMENTARY MATERIAL

The Supplementary Material for this article can be found online at: https://www.frontiersin.org/articles/10.3389/fimmu.2020.01795/full#supplementary-material

Figure S1 | Scale-free topological network of IgG4-RD LSG samples in GSE40568 dataset by WGCNA. Scale independence (Left) and mean connectivity (Right) were plotted, respectively.

Figure S2 | Scale-free topological network of IgG4-RD PBMC samples in GSE66465 dataset by WGCNA. Scale independence (Left) and mean connectivity (Right) were plotted, respectively.

Figure S3 | Module membership plots of "turquoise" **(A)** module and **(B)** eigengenenetwork plots in GSE40568.

Figure S4 | Module membership plots of "yellow" **(A)** module and **(B)** eigengenenetwork plots in GSE66465.

Table S1 | Differentially expressed proteins between IgG4-RD patients and controls in tissue.

Table S2 | Differentially expressed proteins between IgG4-RD patients and controls in serum.

Table S3 | Cytoscape Input nodes in turquoise.

Table S4 | Cytoscape Input edges in turquoise.

Table S5 | Cytoscape Input nodes in yellow.

Table S6 | Cytoscape Input edges in yellow.

Table S7 | KEGG analysis with genes (adjacency value > 0.2) in turquoise module in tissue transcriptomic data.

Table S8 | KEGG analysis with genes (adjacency value > 0.2) in yellow module in PBMC transcriptomic data.

REFERENCES

1. Stone JH, Khosroshahi A, Deshpande V, Chan JKC, Heathcote JG, Aalberse R, et al. Recommendations for the nomenclature of IgG4-related disease and its individual organ system manifestations. *Arthritis Rheum.* (2012) 64:3061–7. doi: 10.1002/art.34593
2. Al-Mujaini A, Al-Khabori M, Shenoy K, Wali U. Immunoglobulin G4-related disease: an update. *Oman Med J.* (2018) 33:97–103. doi: 10.5001/omj.2018.20
3. Beyer G, Schwaiger T, Lerch MM, Mayerle J. IgG4-related disease: a new kid on the block or an old aquaintance? *United Eur Gastroenterol J.* (2014) 2:165–72. doi: 10.1177/2050640614532457
4. Hart PA, Kamisawa T, Brugge WR, Chung JB, Culver EL, Czako L, et al. Long-term outcomes of autoimmune pancreatitis: a multicentre, international analysis. *Gut.* (2013) 62:1771–6. doi: 10.1136/gutjnl-2012-303617
5. Mattoo H, Stone JH, Pillai S. Clonally expanded cytotoxic CD4+ T cells and the pathogenesis of IgG4-related disease. *Autoimmunity.* (2017) 50:19–24. doi: 10.1080/08916934.2017.1280029
6. Moriyama M, Nakamura S. Th1/Th2 immune balance and other T helper subsets in IgG4-related disease. In: Okazaki K editor. *IgG4-Related Disease*. Osaka: Department of Gastroenterology and Hepatology; Kansai Medical University; Springer. (2016). p. 75–83. doi: 10.1007/82_2016_40
7. Chen Y, Lin W, Yang H, Wang M, Zhang P, Feng R, et al. Aberrant expansion and function of follicular helper T cell subsets in IgG4-related disease. *Arthritis Rheumatol.* (2018) 70:1853–65. doi: 10.1002/art.40556
8. Tsuboi H, Matsuo N, Iizuka M, Tsuzuki S, Kondo Y, Tanaka A, et al. Analysis of IgG4 class switch-related molecules in IgG4-related disease. *Arthritis Res Ther.* (2012) 14:R171. doi: 10.1186/ar3924
9. Stone JH, Zen Y, Deshpande V. IgG4-related disease. *N Engl J Med.* (2012) 366:539–51. doi: 10.1056/NEJMra1104650
10. Asada M, Nishio A, Akamatsu T, Tanaka J, Saga K, Kido M, et al. Analysis of humoral immune response in experimental autoimmune pancreatitis in mice. *Pancreas.* (2010) 39:224–31. doi: 10.1097/MPA.0b013e3181bab5e2
11. Lebedeva S, Jens M, Theil K, Schwanhäusser B, Selbach M, Landthaler M, et al. Transcriptome-wide analysis of regulatory interactions of the RNA-binding protein HuR. *Mol Cell.* (2011) 43:340–52. doi: 10.1016/j.molcel.2011.06.008
12. Maehara T, Moriyama M, Nakashima H, Miyake K, Hayashida J-N, Tanaka A, et al. Interleukin-21 contributes to germinal centre formation and immunoglobulin G4 production in IgG4-related dacryoadenitis and sialoadenitis, so-called mikulicz's disease. *Ann Rheum Dis.* (2012) 71:2011–9. doi: 10.1136/annrheumdis-2012-201477
13. Tsuboi H, Nakai Y, Iizuka M, Asashima H, Hagiya C, Tsuzuki S, et al. DNA microarray analysis of labial salivary glands in IgG4-related disease: comparison with Sjögren's syndrome. *Arthritis Rheum.* (2014) 66:2892–9. doi: 10.1002/art.38748
14. Higgs BW, Liu Y, Guo J, Sebastian Y, Morehouse C, Zhu W, et al. High-throughput RNA sequencing reveals distinct gene signatures in active IgG4-related disease. *Sci Rep.* (2017) 7:17567. doi: 10.1038/s41598-017-17602-9
15. Aslam B, Basit M, Nisar MA, Khurshid M, Rasool MH. Proteomics: technologies and their applications. *J Chromatogr Sci.* (2017) 55:182–96. doi: 10.1093/chromsci/bmw167
16. Langfelder P, Horvath S. WGCNA: an R package for weighted correlation network analysis. *BMC Bioinformatics.* (2008) 9:559. doi: 10.1186/1471-2105-9-559
17. Umehara H, Okazaki K, Masaki Y, Kawano M, Yamamoto M, Saeki T, et al. Comprehensive diagnostic criteria for IgG4-related disease (IgG4-RD), 2011. *Mod Rheumatol.* (2012) 22:21–30. doi: 10.3109/s10165-011-0571-z
18. Wen B, Zhou R, Feng Q, Wang Q, Wang J, Liu S. IQuant: an automated pipeline for quantitative proteomics based upon isobaric tags. *Proteomics.* (2014) 14:2280–5. doi: 10.1002/pmic.201300361
19. Nakajima A, Masaki Y, Nakamura T, Kawanami T, Ishigaki Y, Takegami T, et al. Decreased expression of innate immunity-related genes in peripheral blood mononuclear cells from patients with IgG4-related disease. *PLoS ONE.* (2015) 10:e0126582. doi: 10.1371/journal.pone.0126582
20. Bindea G, Mlecnik B, Hackl H, Charoentong P, Tosolini M, Kirilovsky A, et al. ClueGO: a cytoscape plug-in to decipher functionally grouped gene ontology and pathway annotation networks. *Bioinformatics.* (2009) 25:1091–3. doi: 10.1093/bioinformatics/btp101
21. Yu G, Wang LG, Han Y, He QY. clusterProfiler: an R package for comparing biological themes among gene clusters. *OMICS.* (2012) 16:284–7. doi: 10.1089/omi.2011.0118
22. Wang Y, Zhang S, Li F, Zhou Y, Zhang Y, Wang Z, et al. Therapeutic target database 2020: enriched resource for facilitating research and early development of targeted therapeutics. *Nucleic Acids Res.* (2020) 48:D1031–41. doi: 10.1093/nar/gkz981
23. Mahajan VS, Mattoo H, Deshpande V, Pillai SS, Stone JH. IgG4-related disease. *Annu Rev Pathol Mech Dis.* (2014) 9:315–47. doi: 10.1146/annurev-pathol-012513-104708
24. Kiyama K, Yoshifuji H, Kandou T, Hosono Y, Kitagori K, Nakashima R, et al. Screening for IgG4-type anti-nuclear antibodies in IgG4-related disease. *BMC Musculoskelet Disord.* (2015) 16:129. doi: 10.1186/s12891-015-0584-4
25. Semple JW, Italiano JE, Freedman J. Platelets and the immune continuum. *Nat Rev Immunol.* (2011) 11:264–74. doi: 10.1038/nri2956
26. Zhang YL, Wang RC, Cheng K, Ring BZ, Su L. Roles of Rap1 signaling in tumor cell migration and invasion. *Cancer Biol Med.* (2017) 14:90–9. doi: 10.20892/j.issn.2095-3941.2016.0086
27. Chuang HC, Wang X, Tan TH. MAP4K family kinases in immunity and inflammation. *Adv Immunol.* (2016) 129:277–314. doi: 10.1016/bs.ai.2015.09.006
28. Fruman DA, Chiu H, Hopkins BD, Bagrodia S, Cantley LC, Abraham RT. The PI3K pathway in human disease. *Cell.* (2017) 170:605–35. doi: 10.1016/j.cell.2017.07.029
29. Lim PS, Sutton CR, Rao S. Protein kinase C in the immune system: from signalling to chromatin regulation. *Immunology.* (2015) 146:508–22. doi: 10.1111/imm.12510
30. Wallace ZS, Mattoo H, Carruthers M, Mahajan VS, Della Torre E, Lee H, et al. Plasmablasts as a biomarker for IgG4-related disease, independent of serum IgG4 concentrations. *Ann Rheum Dis.* (2015) 74:190–5. doi: 10.1136/annrheumdis-2014-205233
31. Mattoo H, Mahajan VS, Maehara T, Deshpande V, Della-Torre E, Wallace ZS, et al. Clonal expansion of $CD4^+$ cytotoxic T lymphocytes in patients with IgG4-related disease. *J Allergy Clin Immunol.* (2016) 138:825–38. doi: 10.1016/j.jaci.2015.12.1330
32. Lin W, Zhang P, Chen H, Chen Y, Yang H, Zheng W, et al. Circulating plasmablasts/plasma cells: a potential biomarker for IgG4-related disease. *Arthritis Res Ther.* (2017) 19:25. doi: 10.1186/s13075-017-1231-2

33. Heeringa JJ, Karim AF, van Laar JAM, Verdijk RM, Paridaens D, van Hagen PM, et al. Expansion of blood IgG4$^+$ B, TH2, and regulatory T cells in patients with IgG4-related disease. *J Allergy Clin Immunol.* (2017) 141:1831–43.e10. doi: 10.1016/j.jaci.2017.07.024
34. Della-Torre E, Feeney E, Deshpande V, Mattoo H, Mahajan V, Kulikova M, et al. B-cell depletion attenuates serological biomarkers of fibrosis and myofibroblast activation in IgG4-related disease. *Ann Rheum Dis.* (2015) 74:2236–43. doi: 10.1136/annrheumdis-2014-205799
35. Shiokawa M, Kodama Y, Kuriyama K, Yoshimura K, Tomono T, Morita T, et al. Pathogenicity of IgG in patients with IgG4-related disease. *Gut.* (2016) 65:1322–32. doi: 10.1136/gutjnl-2015-310336
36. Flannagan RS, Jaumouillé V, Grinstein S. The cell biology of phagocytosis. *Annu Rev Pathol Mech Dis.* (2012) 7:61–98. doi: 10.1146/annurev-pathol-011811-132445
37. Yoshida H, Hunter CA. The immunobiology of interleukin-27. *Annu Rev Immunol.* (2015) 33:417–43. doi: 10.1146/annurev-immunol-032414-112134
38. Kaplanski G. Interleukin-18: biological properties and role in disease pathogenesis. *Immunol Rev.* (2018) 281:138–53. doi: 10.1111/imr.12616
39. Jones GW, Jones SA. Ectopic lymphoid follicles: inducible centres for generating antigen-specific immune responses within tissues. *Immunology.* (2016) 147:141–51. doi: 10.1111/imm.12554
40. Havenar-Daughton C, Lindqvist M, Heit A, Wu JE, Reiss SM, Kendric K, et al. CXCL13 is a plasma biomarker of germinal center activity. *Proc Natl Acad Sci USA.* (2016) 113:2702–7. doi: 10.1073/pnas.1520112113
41. Pasoto SG, Ribeiro AC, Bonfa E. Update on infections and vaccinations in systemic lupus erythematosus and sjogren's syndrome. *Curr Opin Rheumatol.* (2014) 26:528–37. doi: 10.1097/BOR.0000000000000084
42. Li J, Wang X, Zhang F, Yin H. Toll-like receptors as therapeutic targets for autoimmune connective tissue diseases. *Pharmacol Ther.* (2013) 138:441–51. doi: 10.1016/j.pharmthera.2013.03.003
43. Rawlings DJ, Metzler G, Wray-Dutra M, Jackson SW. Altered B cell signalling in autoimmunity. *Nat Rev Immunol.* (2017) 17:421–36. doi: 10.1038/nri.2017.24
44. Habets KL, Huizinga TW, Toes RE. Platelets and autoimmunity. *Eur J Clin Invest.* (2013) 43:746–57. doi: 10.1111/eci.12101
45. Zhu L, Huang Z, Stalesen R, Hansson GK, Li N. Platelets provoke distinct dynamics of immune responses by differentially regulating CD4+ T-cell proliferation. *J Thromb Haemost.* (2014) 12:1156–65. doi: 10.1111/jth.12612
46. Lam FW, Vijayan KV, Rumbaut RE. Platelets and their interactions with other immune cells. *Compr Physiol.* (2015) 5:1265–80. doi: 10.1002/cphy.c140074
47. Herter JM, Rossaint J, Zarbock A. Platelets in inflammation and immunity. *J Thromb Haemost.* (2014) 12:1764–75. doi: 10.1111/jth.12730
48. Khosroshahi A, Wallace ZS, Crowe JL, Akamizu T, Azumi A, Carruthers MN, et al. International consensus guidance statement on the management and treatment of IgG4-related disease. *Arthritis Rheumatol.* (2015) 67:1688–99. doi: 10.1002/art.39132
49. Ebbo M, Grados A, Samson M, Groh M, Loundou A, Rigolet A, et al. Long-term efficacy and safety of rituximab in IgG4-related disease: data from a French nationwide study of thirty-three patients. *PLoS ONE.* (2017) 12:e0183844. doi: 10.1371/journal.pone.0183844
50. Shirakashi M, Yoshifuji H, Kodama Y, Chiba T, Yamamoto M, Takahashi H, et al. Factors in glucocorticoid regimens associated with treatment response and relapses of IgG4-related disease: a multicentre study. *Sci Rep.* (2018) 8:10262. doi: 10.1038/s41598-018-28405-x

Conflict of Interest: The authors declare that the research was conducted in the absence of any commercial or financial relationships that could be construed as a potential conflict of interest.

frontiers in Immunology

MINI REVIEW
published: 03 September 2020
doi: 10.3389/fimmu.2020.02156

Inhibitory Receptors and Checkpoints in Human NK Cells, Implications for the Immunotherapy of Cancer

Simona Sivori[1†], Mariella Della Chiesa[1†], Simona Carlomagno[2], Linda Quatrini[3], Enrico Munari[4], Paola Vacca[3], Nicola Tumino[3], Francesca Romana Mariotti[3], Maria Cristina Mingari[1,5], Daniela Pende[5‡] and Lorenzo Moretta[3‡]*

[1] Department of Experimental Medicine (DIMES) and Center of Excellence for Biomedical Research, University of Genoa, Genoa, Italy, [2] Department of Experimental Medicine, University of Genoa, Genoa, Italy, [3] Department of Immunology, IRCCS Ospedale Pediatrico Bambino Gesù, Rome, Italy, [4] Department of Pathology, IRCCS Sacro Cuore Don Calabria, Negrar, Italy, [5] UOC Immunology, IRCCS Ospedale Policlinico San Martino, Genoa, Italy

OPEN ACCESS

Edited by:
Renato C. Monteiro, Université de Paris, France

Reviewed by:
Stephan von Gunten, University of Bern, Switzerland
Ana Stojanovic, Heidelberg University, Germany

***Correspondence:**
Lorenzo Moretta
lorenzo.moretta@opbg.net

[†] *These authors have contributed equally to this work*

[‡] *These authors share senior authorship*

Specialty section:
This article was submitted to Molecular Innate Immunity, a section of the journal Frontiers in Immunology

Received: *26 June 2020*
Accepted: *07 August 2020*
Published: *03 September 2020*

Citation:
Sivori S, Della Chiesa M, Carlomagno S, Quatrini L, Munari E, Vacca P, Tumino N, Mariotti FR, Mingari MC, Pende D and Moretta L (2020) Inhibitory Receptors and Checkpoints in Human NK Cells, Implications for the Immunotherapy of Cancer. Front. Immunol. 11:2156. doi: 10.3389/fimmu.2020.02156

The highly destructive mechanisms by which the immune system faces microbial infections is under the control of a series of inhibitory receptors. While most of these receptors prevent unwanted/excessive responses of individual effector cells, others play a more general role in immunity, acting as true inhibitory checkpoints controlling both innate and adaptive immunity. Regarding human NK cells, their function is finely regulated by HLA-class I-specific inhibitory receptors which allow discrimination between HLA-I$^+$, healthy cells and tumor or virus-infected cells displaying loss or substantial alterations of HLA-I molecules, including allelic losses that are sensed by KIRs. A number of non-HLA-specific receptors have been identified which recognize cell surface or extracellular matrix ligands and may contribute to the physiologic control of immune responses and tolerance. Among these receptors, Siglec 7 (p75/AIRM-1), LAIR-1 and IRp60, recognize ligands including sialic acids, extracellular matrix/collagen or aminophospholipids, respectively. These ligands may be expressed at the surface of tumor cells, thus inhibiting NK cell function. Expression of the PD-1 checkpoint by NK cells requires particular cytokines (IL-15, IL-12, IL-18) together with cortisol, a combination that may occur in the microenvironment of different tumors. Blocking of single or combinations of inhibitory receptors unleashes NK cells and restore their anti-tumor activity, with obvious implications for tumor immunotherapy.

Keywords: natural killer cells, inhibitory NK receptors, immune checkpoints, tumor immunotherapy, tumor escape

INTRODUCTION

To combat infections, the immune system exploits highly destructive mechanisms. These mechanisms are triggered by an array of receptors that evolved during phylogenesis from structures ensuring phagocytosis and killing of invading pathogens toward highly sophisticated, clonally distributed, receptors encoded by rearranging genes. Remarkably, most of the "primitive" receptors did not disappear during evolution but rather co-evolved with adaptive immunity and are playing, in contemporary vertebrates, a synergistic role, contributing to improved anti-microbial responses.

A good example is provided by the Fc-gamma receptors, evolved from a primitive surface protein into receptors recognizing IgG antibodies (Abs), allowing greater killing or phagocytosis of Ab-coated bacteria or target cells (1). In particular, NK cells, expressing the FcγRIIIa (also known as CD16), are considered the most important effectors of antibody-dependent cell-mediated cytotoxicity (ADCC) in humans.

The exploitation of highly destructive mechanisms to control infections would require means to avoid damages to healthy cells and, in general, to the whole organism. Thus, efficient mechanisms have been acquired to prevent damages to self by downmodulating immune responses and inflammation at the termination of infection. A major role in ensuring this crucial activity is played by an array of inhibitory receptors which may control the function of individual cells of both innate and adaptive immunity and, in some instances, may function as true checkpoints, ensuring a wide control of immune response and inflammation.

Focusing on human NK cells, they express different HLA class I–specific receptors that allow discrimination between healthy and virus-infected or tumor cells (2), while other receptors such as TIGIT and CD96, although controlling NK cell function, play a role also in the regulation of cell adhesion and migration/homing (3). In this context, studies of tissue distribution of their ligands, such as PVR (CD155) and Nectin-2 (CD112), may provide useful information on the possible migration/homing of cells expressing the corresponding receptor. Other receptors, such as CD69 and CD103, represent tissue retention receptors and may provide important markers to identify NK and T cells capable of infiltrating and staying in normal peripheral tissues or tumors (4).

In this contribution, we will delineate some of the main inhibitory receptors expressed by human NK cells. Remarkably, Killer Ig-like Receptors (KIR), discovered by Moretta et al. in 1990 (5, 6) are the prototype of the inhibitory receptors controlling cells of the immune system. These and other HLA class I-specific receptors provided the molecular basis of the "missing-self hypothesis" and explained how NK cells may discriminate between healthy and tumor or virus-infected cells (7). Moreover, NK cells can express several non-HLA-specific inhibitory receptors that contribute in regulating immune responses. Some inhibitory receptors are constitutively expressed by NK cells (such as KIR and NKG2A) and are involved in the regulation of NK cell tolerance against healthy tissues, while others (such as PD-1) are expressed at very low level in NK cells from healthy donors, but increase in pathological conditions. All these inhibitory receptors act as immune checkpoints regulating anti-tumor NK cell function by the recognition of specific ligands on tumor cells thus favoring tumor escape from NK cell cytotoxicity.

HLA-SPECIFIC INHIBITORY NK RECEPTORS

In humans, the molecular basis for NK cell tolerance toward healthy autologous cells is provided by HLA-specific inhibitory receptors (iNKR), that are mainly represented by KIR, CD94:NKG2A, and LILRB1 (2, 6, 8–10). Inhibitory KIRs (iKIR), characterized by 2 or 3 Ig-like extracellular domains and a long cytoplasmic tail (KIR2DL, KIR3DL), recognize allotypic determinants shared by distinct groups of HLA class I molecules (KIR-ligands, KIR-L), as recently reviewed (11). CD94:NKG2A heterodimer, composed by C-type lectin-like proteins, is specific for the non-classical HLA-E molecules, that are stabilized by peptides mainly derived from the leader sequences of HLA-A, -B, or –C (12, 13). LILRB1 displays a broad specificity for HLA (14, 15). Upon receptor engagement, the immunoreceptor tyrosine-based inhibitory motifs (ITIM) become phosphorylated and recruit tyrosine phosphatases, thus delivering an inhibitory signaling cascade (16–18). **Table 1** and **Figure 1** summarize these receptor/ligand interactions.

During NK cell development, immature stages primarily express CD94:NKG2A, while KIRs are acquired upon maturation. NK cells go through a process termed "education," involving the iNKR/self-HLA interaction, whose strength positively influences the functional potential of NK cells (19). Extremely diversified self-tolerant iNKR phenotypic repertoires can be observed on peripheral blood NK cell pool among the various individuals (17). This heterogeneity is primarily determined by the high polymorphism of the independently co-inherited *KIR* and *HLA* class I genotypes, and by the stochastic KIR expression pattern on NK cells (20). NK cells can be efficient even when expressing single-iKIR, provided that it strongly interacts with self-HLA. This NK cell can kill the pathological cell that has lost even a single-HLA allotype through the mechanism of "missing-self recognition." Regarding CD94:NKG2A/HLA-E interaction, a dimorphism in *HLA-B* leader sequence at residue − 21 encoding either a good binding methionine (− 21 M) or a low binding threonine (− 21 T) determines the variability in HLA-E expression; $NKG2A^+$ cells from individuals carrying at least one − 21 M *HLA-B* alleles are more educated (21). Consistent with this finding, in acute myeloid leukemia (AML) patients treated with immunotherapy, a better leukemia-free survival (LFS) was observed in patients with − 21 M/x than − 21 T/T *HLA-B* alleles (22).

In addition to genetics, environmental factors can impact on the receptor repertoire. The most remarkable example is represented by cytomegalovirus (CMV) infection, that promotes the expansion of functionally and phenotypically skewed NK cells with adaptive features through epigenetic alterations (23, 24). These cells are characterized by the expression of the activating CD94:NKG2C, mainly co-expressing KIR2DL specific for self-HLA-C allotypes, CD57 (a marker of terminally differentiation stage), and by the lack of NKG2A (25–27). Notably, in view of their long term persistence (28–30), expansion capabilities (31) and high ADCC abilities (32, 33), CMV-driven adaptive NK cells also represent a suitable target for anti-leukemia immunotherapeutic strategies (e.g., CD16-based immune engagers, adoptive cell transfer, CAR-engineering) (34).

KIRs have been shown to be clinically relevant in allogeneic hematopoietic stem cell transplantation (HSCT) to cure acute leukemia, in particular from HLA-haploidentical donors whose repertoire presents educated iKIR(s) that do not recognize the cognate KIR-L(s) in the recipient. When KIR/KIR-L mismatches

TABLE 1 | HLA-I specific and non-HLA-I specific inhibitory receptors, their distribution and ligands.

	Molecule	CD	Cell distribution	Ligand
HLA specific inhibitory receptors	KIR2DL1	CD158a	NK cells, T cells	HLA-C^{K80} allotypes (HLA-C2 epitope)
	KIR2DL2/3	CD158b1/b2	NK cells, T cells	HLA-C^{N80} allotypes (HLA-C1 epitope) HLA-B*46:01 and -B*73:01
	KIR2DL5	CD158f	NK cells, T cells	?
	KIR3DL1	CD158e1	NK cells, T cells	HLA-A Bw4, HLA-B Bw4
	KIR3DL2	CD158k	NK cells, T cells	HLA-A*03 and -A*11, HLA-F
	KIR3DL3	CD158z	NK cells, T cells	?
	LILRB1/LIR-1/ILT2	CD85j	NK cells, T cells, B cells, monocytes, DCs	HLA-G, various HLA-I allotypes
	NKG2A	CD159a	NK and T cells	HLA-E
	LAG-3	CD223	Activated NK cells, activated T cells, B cells, pDCs	HLA-II
Non-HLA specific inhibitory receptors	PD-1	CD279	NK cells, T cells, B cells, myeloid cells	PD-L1, PD-L2
	TIM-3	CD366	NK cells, T cells, DCs, monocytes, macrophages, mast cells	Gal-9, PS, HMGB1, CEACAM1
	TIGIT	NA	NK cells, T cells	CD155, CD112, CD113
	Tactile	CD96	NK cells, T cells	CD155, CD111
	Siglec-7/p75/AIRM-1	CD328	NK cells, T cells, granulocytes, monocytes,	Sialic acid
	Siglec-9	CD329	NK cells, T cells, B cells, granulocytes, monocytes	Sialic acid
	KLRG1	NA	NK cells, T cells	cadherins
	IRp60	CD300a	NK cells, T cells, B cells, neutrophils, eosinophils, mast cells, pDC	phosphatidylserine (PS), phoshatidylethanolamine (PE)
	LAIR-1/p40	CD305	NK cells, T cells, B cells, monocytes, granulocytes, DCs, mast cells, macrophages, $CD34^+$ hematopoietic progenitor cells, thymocytes	Collagen, C1q, surfactant protein D
	CEACAM-1	CD66a	epithelial cells, various leukocytes	CEACAM-1, CEACAM-5
	NKRP1A	CD161	NK cells, T cells	LLT1
	IAP	CD47	NK cells, T cells, B cells, monocytes, macrophages, DCs, neutrophils	SIRP1a, TSP-1

in graft-versus-host (GvH) direction occur, alloreactive NK cells can be generated in the transplanted patient, with efficient anti-leukemia activity (35). This has been proven especially beneficial in acute myeloid leukemia (AML) adult patients (36), and in acute lymphoblastic leukemia (ALL) pediatric patients (37). Algorithms for donor selection criteria have been created, considering NK alloreactivity and KIR gene profiles, to improve the clinical outcome in HSCT (38–41).

A great improvement in cancer immunotherapy has been achieved with immune checkpoint inhibitors (ICI), by the use of therapeutic antibodies blocking inhibitory checkpoints. With the aim to potentiate/unleash the anti-tumor NK cell function, clinical grade monoclonal antibodies (mAbs) targeting KIR and NKG2A have been produced. Lirilumab (1-7F9, IPH2101), a first-in-class fully human IgG4 mAb targeting KIR2D, has been employed in phase I trials to treat hematological malignancies or solid tumors, also in association with Lenalidomide (as NK cell stimulant) in multiple myeloma, resulting to be safe but with low anti-tumor efficacy (42–44). More promising clinical results have been obtained with IPH4102 targeting KIR3DL2 on cutaneous T cell lymphoma, particularly in Sèzary syndrome (45). Of extreme interest for the clinical potential is monalizumab, a humanized IgG4-blocking anti-NKG2A mAb, that can unleash both NK and T-cell responses (46). Indeed, NKG2A/HLA-E interaction can downregulate anti-tumor immune responses. Clinical trials using monalizumab in combination with durvalumab (anti-PD-L1) for the treatment of solid tumors, and, especially, in combination with cetuximab (anti-EGFR) for the treatment of head and neck cancers, show clear signs of efficacy (46).

NON-HLA-SPECIFIC INHIBITORY NK RECEPTORS

In addition to the HLA class I-specific receptors, NK cells express several other ITIM-containing receptors importantly contributing to regulate immune responses (**Table 1**) (47–60). We focus here on the critical immune checkpoint PD-1 and on Siglec-7/p75/AIRM1/CD328, LAIR-1/p40/CD305, and IRp60/CD300a, originally identified in our labs, representing additional immune checkpoints possibly dampening anti-tumor NK cell responses in given pathological settings (**Figure 1**). Siglec-7, IRp60 and LAIR-1 are rarely discussed in most reviews on immune checkpoints in NK cell context, however, they represent relevant receptors to target in anti-tumor immunotherapies. Indeed, their ligands are expressed or even upregulated on several tumors.

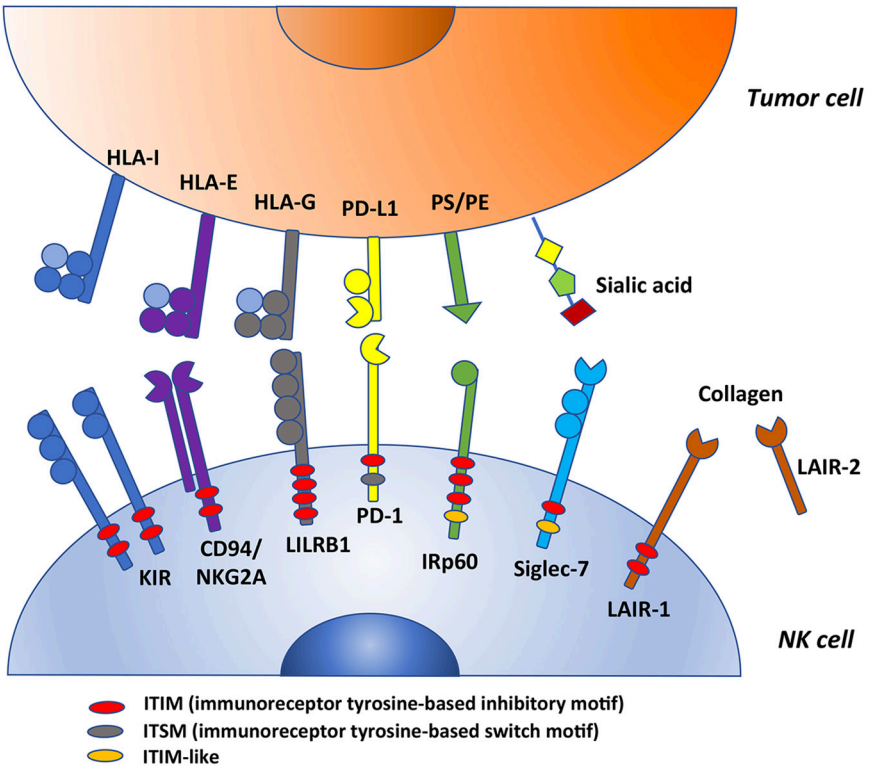

FIGURE 1 | This figure summarizes some ITIM-bearing molecules expressed by human NK cells that could act as checkpoints in cancer immunotherapy. KIRs, CD94/NKG2A and LILRB1 are HLA-specific inhibitory receptors whereas PD-1, IRp60, Siglec-7 and LAIR-1 are non-HLA-specific inhibitory receptors (their ligands are indicated in the figure). All these molecules possess variable numbers and different types of ITIMs. In particular, PD-1 express one ITIM; KIRs, CD94/NKG2A and LAIR-1 have two ITIMs (among KIRs, only KIR3DL3 and KIR2DL4 express one ITIM); IRp60 has three ITIMs; LILRB1 has four ITIMs (indicated in red in the figure). In addition, PD-1 carries also an ITSM motif (gray) whereas IRp60 and LAIR-1 an ITIM-like motif (orange). PS, phosphatidylserine; PE, phoshatidylethanolamine.

PD-1

PD-1 is a type I transmembrane glycoprotein belonging to the CD28/CTLA4 subfamily of the Ig superfamily, containing an IgV-type extracellular domain (61). Its cytoplasmic domain contains an ITIM and an immunoreceptor tyrosine-based switch motif (ITSM) and, interestingly, the tyrosine residue in the ITSM, but not in the ITIM, is required for the inhibitory cascade (62). PD-1 expression was initially described on T, B, myeloid cells and, more recently, on NK cells (47). PD-1 ligands (PD-Ls, namely PD-L1 and PD-L2) are expressed by hematopoietic and non-hematopoietic cells and, importantly, they are often expressed by tumor cells. Indeed, while in normal conditions PD-1/PD-L axis regulates peripheral tolerance, in the context of cancer it represents a mechanism of "escape" from immune system and in particular from PD-1-expressing cytotoxic lymphocytes (63). In addition to PD-1-expressing $CD8^+$ T cells, also PD-1^+ NK cells have been identified in several tumors, including multiple myeloma, Kaposi sarcoma, ovarian carcinoma, digestive and lung cancer (31, 47, 64–66). Differently from T cells, which are induced to upregulate PD-1 expression upon activation, NK cells from the peripheral blood of healthy donors do not express PD-1 on their surface, with the exception of a minor fraction of CMV seropositive individuals (47). Human NK cells have been shown to display an intra-cytoplasmatic pool of PD-1 mRNA and protein localized in the Golgi (67). An analysis of pleural effusion contents from primary and metastatic tumors identified glucocorticoids as key components of the tumor microenvironment indispensable for PD-1 induction on NK cells surface, in combination with the signals from the cytokines IL-12, IL-15 and IL-18 (68). Glucocorticoids were shown to increase PD-1 expression at the transcriptional level in both human and murine NK cells (68, 69). In addition, in human $CD56^{bright}$ NK cells, these hormones activate a transcriptional program responsible for enhanced translation and translocation of proteins to the plasma membrane, which indirectly contributes to increase PD-1 surface expression. Notably, PD-1^+ NK cells are not exhausted, but show an impaired response specifically against PD-L1-expressing target cells (68).

Blockade of the PD-1/PD-L1 axis through monoclonal antibodies represents a major breakthrough in oncology, showing significant clinical success in the treatment of several types of cancers (70, 71). This blockade allows unleashing not only T cell-, but also NK cell-mediated anti-tumor response. This is relevant especially in the treatment of tumors that have lost HLA-I expression and are thus "invisible" to T cells. Despite its success, only one third of patients is responsive to anti-PD-1 immunotherapy (72). One important factor that may

be responsible for this lack of response is represented by the misclassification of tumors in terms of PD-L1 expression. The immunohistochemical detection of this biomarker in tumor samples usually guides the decision of the appropriate therapeutic strategy, together with other parameters. PD-L1 expression heterogeneity, interclone differences among antibodies used for immunohistochemistry and inter/intra observer variability may explain why the rates of clinical response to treatment with PD-1/PD-L1 inhibitors do not always correlate with PD-L1 detected expression (73–76). Moreover, the recent identification of the molecular mechanisms driving PD-1 expression on NK cells suggests that including synthetic corticosteroids in the therapeutic regimen for cancer patients may be counterproductive in combination with the blockade of this checkpoint.

SIGLEC-7/p75/AIRM1/CD328

Siglec-7 is a surface inhibitory receptor belonging to a family of Sialic acid recognizing Immunoglobulin-like Lectins (Siglecs) that is mostly confined to NK cells, but is expressed also on monocytes, a minor fraction of $CD8^+$ T cells and granulocytes (48, 77). Siglec-7 was originally identified as a 75-kD glycoprotein, encoded by a gene located on chromosome 19 where most inhibitory receptors regulating NK-mediated cytotoxicity are found (i.e., KIRs, LILRB1, and LAIR-1) (48). In line with most inhibitory receptors, Siglec-7 is characterized by Ig-like domains in the extracellular portion and a classical ITIM, together with an ITIM-like domain, in its cytoplasmic tail, capable of switching off activating signals on NK cells (48). Siglec-7 preferentially binds to α2-6-linked sialic acids and to α2,8-disialic acid that is found on GD3 ganglioside (78).

Siglec-7, along with other Siglecs, can regulate immune responses contributing to immune tolerance, however, it can also decrease anti-tumor immunity on account of the aberrant expression of sialylated glycans on the surface of malignant cells of different histotypes [e.g., AML, CLL, melanoma, renal cell carcinoma, colon adenocarcinoma (79, 80)]. Indeed, hypersialylation represents a relevant tumor escape mechanism that can directly affect NK cell-mediated tumor killing, as demonstrated by reduced NK cell-cytotoxicity against tumors expressing Siglec-7 ligands. Remarkably, the employ of antibodies blocking Siglec-7 engagement could restore tumor lysis (80–82). Interestingly, Siglec-7 reduced expression represents a hallmark of CMV-driven adaptive NK cell subsets (32, 33) and could favor their cytotoxicity against HLA-$I^{low/neg}$ tumors.

Based on the above observations, Siglec-7 represents an attractive immune checkpoint that can be targeted to enhance anti-tumor responses (83). In this context, besides anti-Siglec-7 blocking antibodies, different approaches have been proposed, including the employ of small soluble Siglec-7 ligands, designed to display high avidity for the receptor based on its crystal structure (84, 85). These molecules can increase NK-cell mediated tumor lysis although less efficiently than specific anti-Siglec-7 antibodies (86). Interestingly, a recent study showed that cells engineered with a Siglec-7-based CAR construct can display efficient anti-tumor activity both *in vitro* against several tumor cell lines expressing Siglec-7 ligands and *in vivo* in xenograft murine models (87).

LAIR-1/p40/CD305

Another non-HLA-specific inhibitory NK receptor is represented by the Leukocyte-Associated Immunoglobulin-like Receptor-1 (LAIR-1) (88, 89), which is a type I transmembrane glycoprotein characterized by an extracellular C2-type Ig-like domain and two ITIMs in the cytoplasmic tail (90, 91).

LAIR-1 is one of the most widely distributed inhibitory receptors and could play a role in controlling various phases of the immune response. Indeed, it is expressed not only on NK cells but also on other cells of innate immunity (such as monocytes, granulocytes, dendritic cells, mast cells, macrophages) (90, 92–94), on T and B lymphocytes (49, 95, 96), on $CD34^+$ hematopoietic progenitor cells (97) and on the majority of thymocytes (90). Interestingly, during the process of cell maturation and activation LAIR-1 expression is decreased on various immune cells (i.e., $CD4^+$ T cells, neutrophils, B cells) (93, 96, 98).

The interaction between LAIR-1 and its several ligands, such as extracellular matrix collagens (99), the C1q complement component (100), and the surfactant protein D (101), induces phosphorylation of both ITIMs and inhibition of the immune cell activation or differentiation. In particular, the LAIR-1 cross-linking with monoclonal antibodies, or with its ligands, inhibits the NK and CTL cytotoxicity (102). LAIR-1-mediated inhibition occurs through SHP-1 and SHP-2, but also through the recruitment of Csk (103) that inactivates Src family kinases.

Remarkably, the upregulation of collagen expression by tumor cells and/or tumor stroma could lead to the downregulation of anti-tumor responses mediated by the inhibitory collagen receptor LAIR-1 expressed on NK cells and other effector immune cells.

LAIR-1 can be also detected in the supernatant of stimulated human lymphocytes, suggesting its shedding upon cellular activation (104). In the soluble form, LAIR-1 could interfere with the interaction between the transmembrane receptor and its ligands, thus restoring functions of immune cells.

A similar result could also occur with the LAIR-2 protein that is 84% homologous to LAIR-1 but lacks the transmembrane and intracellular domain. Indeed, the binding of LAIR-2 to collagens could efficiently block LAIR-1–collagen interaction (105). On this basis, an interesting approach has been developed to block immune suppression mediated by LAIR-1. It is based on the use of NC410, a novel reagent capable of mimicking the natural decoy effects of LAIR-2. The blockade of the LAIR-1-mediated inhibition by NC410 can restore the normal functionality of T and dendritic cells as well as the anti-tumor response[1]. In this context, it could be interesting to evaluate whether the increment of anti-tumor response mediated by NC410 can depend also on restoring of the NK cell function.

[1] www.nextcure.com/pipeline

IRp60/CD300a

IRp60/CD300a is an inhibitory receptor belonging to CD300 family, a set of genes clustered on chromosome 17 coding for receptors, predominantly expressed on leukocytes, able to generate inhibitory and activating signals regulating different immune processes, such as phagocytosis, cytokine release, proliferation and diseases (80, 106–112). In addition to NK cells, IRp60 is broadly expressed in cells of myeloid or lymphoid origin such as neutrophils (113), eosinophils (106), mast cells (114), pDC (113), B and T cells (115). IRp60 is expressed by the majority of blood NK cells but at higher level in $CD56^{bright}$ subset (50). Curiously it has been observed an age-dependent increase of IRp60 expression on NK cells that, in CMV seropositive donors, is associated with increase of $CD56^{dim}$ NK cells co-expressing CD57 (116).

IRp60 is a type I transmembrane protein with a single extracellular Ig V-like domain and a long cytoplasmic tail with three canonical ITIMs whose phosphorylation is required for the transmission of the inhibitory signal (50, 117). This inhibitory signal is able to strongly reduce NK cell cytotoxicity induced via different non-HLA-specific or HLA-specific activating receptors (50). IRp60 recognizes phosphatidylserine (PS) and phosphatidylethanolamine (PE), two aminophospholipids exposed on plasma membrane of activated, infected, transformed or apoptotic cells (107, 118–121). Expression of PS on tumor cells has been demonstrated to protect different tumor cell lines from NK cell mediated cytotoxicity (119). Moreover, IRp60 also binds non-lipid molecules such as the human adenovirus-D47 E3/49K protein (122).

To date, a clear role in the control of NK functions in hematological or solid tumors has not been described. However, IRp60 mRNA is highly expressed and associated with poor prognosis in AML (123) and in diffuse large B-cell lymphoma (124), it is hypoxia-inducible in primary human monocytes and macrophages (125) and is up-regulated in tumor-associated macrophages in ovarian carcinoma (126).

CONCLUDING REMARKS

The groundbreaking discoveries of an array of inhibitory receptors controlling the function of individual cells or even of the entire immune response provided tools for unprecedented progress in the therapy of cancer. Thus, KIRs recognizing allotypic determinants on cells offered the means to successfully treat patients with high-risk leukemias by the haplo-HSCT, mostly exploiting alloreactivity of donor-derived NK cells. Perhaps more importantly, the use of checkpoint inhibitors revolutioned the clinical outcome of different lethal-cancers, by reactivating "dormant" effectors potentially capable of destroying tumor cells. Other important receptors controlling cell adhesion/migration, tissue retention or blocking effector cell function at the tumor site, are being investigated in preclinical and clinical settings. It is conceivable that a deeper knowledge of inhibitory receptors useful in the control of excessive immune responses or inflammation, but playing a detrimental role in tumors, will offer important clues for identifying the prevalent mechanism of immunosuppression in a given tumor and to apply specific, evidence-based, approaches for cancer immunotherapy. This is particularly relevant if we consider that some inhibitory receptors are characterized by a broad expression, non-restricted only to NK cells. Thus, immunotherapeutic approaches blocking these inhibitory pathways could act on different types of immune cells, allowing to re-establish a correct cross-talk between the cells of the immune system, an event which is the basis of an optimal antitumor response.

AUTHOR CONTRIBUTIONS

All authors have provided intellectual contribution to the work and approved it for publication.

FUNDING

Supported by the following grants: AIRC 5 × 1000 2018 id. 21147 (LM and SS); AIRC IG 2017 id. 19920 (LM); AIRC IG 2017 id. 20312 (SS); AIRC IG 2015 id. 16764 (DP); PRIN 2017WC8499_004 (SS); H2020-MSCA-ITN-2017-765104-"MATURE-NK" (DP); RC-2019 IRCCS Ospedale Policlinico San Martino (DP); RC-2020 OPBG (LM). AIRC and European Union's Horizon 2020 Research and Innovation Program under the Marie Skłodowska-Curie grant agreement No 800924 (LQ); AIRC fellowship (NT); Fondazione Veronesi fellowship (FM).

REFERENCES

1. Janeway CA Jr. Approaching the asymptote? Evolution and revolution in immunology. *Cold Spring Harb Symp Quant Biol.* (1989) 54(Pt 1):1–13. doi: 10.1101/sqb.1989.054.01.003
2. Moretta A, Bottino C, Vitale M, Pende D, Biassoni R, Mingari MC, et al. Receptors for HLA class-I molecules in human natural killer cells. *Annu Rev Immunol.* (1996) 14:619–48. doi: 10.1146/annurev.immunol.14.1.619
3. Castriconi R, Carrega P, Dondero A, Bellora F, Casu B, Regis S, et al. Molecular mechanisms directing migration and retention of natural killer cells in human tissues. *Front Immunol.* (2018) 9:2324. doi: 10.3389/fimmu.2018.02324
4. Freud AG, Mundy-Bosse BL, Yu J, Caligiuri MA. The broad spectrum of human natural killer cell diversity. *Immunity.* (2017) 47:820–33. doi: 10.1016/j.immuni.2017.10.008
5. Moretta A, Tambussi G, Bottino C, Tripodi G, Merli A, Ciccone E, et al. A novel surface antigen expressed by a subset of human CD3- CD16+ natural killer cells. Role in cell activation and regulation of cytolytic function. *J Exp Med.* (1990) 171:695–714. doi: 10.1084/jem.171.3.695
6. Moretta A, Vitale M, Bottino C, Orengo AM, Morelli L, Augugliaro R, et al. P58 molecules as putative receptors for major histocompatibility complex (MHC) class I molecules in human natural killer (NK) cells. Anti-p58 antibodies reconstitute lysis of MHC class I-protected cells in NK clones displaying different specificities. *J Exp Med.* (1993) 178:597–604. doi: 10.1084/jem.178.2.597

7. Ljunggren HG, Karre K. In search of the 'missing self': MHC molecules and NK cell recognition. *Immunol Today.* (1990) 11:237–44. doi: 10.1016/0167-5699(90)90097-s
8. Moretta A, Vitale M, Sivori S, Bottino C, Morelli L, Augugliaro R, et al. Human natural killer cell receptors for HLA-class I molecules. Evidence that the Kp43 (CD94) molecule functions as receptor for HLA-B alleles. *J Exp Med.* (1994) 180:545–55. doi: 10.1084/jem.180.2.545
9. Colonna M. Specificity and function of immunoglobulin superfamily NK cell inhibitory and stimulatory receptors. *Immunol Rev.* (1997) 155:127–33. doi: 10.1111/j.1600-065x.1997.tb00945.x
10. Lanier LL. NK cell receptors. *Ann Rev Immunol.* (1998) 16:359–93. doi: 10.1146/annurev.immunol.16.1.359
11. Pende D, Falco M, Vitale M, Cantoni C, Vitale C, Munari E, et al. Killer Ig-like receptors (KIRs): their role in NK cell modulation and developments leading to their clinical exploitation. *Front Immunol.* (2019) 10:1179. doi: 10.3389/fimmu.2019.01179
12. Lee N, Llano M, Carretero M, Ishitani A, Navarro F, Lopez-Botet M, et al. HLA-E is a major ligand for the natural killer inhibitory receptor CD94/NKG2A. *Proc Natl Acad Sci USA.* (1998) 95:5199–204. doi: 10.1073/pnas.95.9.5199
13. Braud VM, Allan DS, O'Callaghan CA, Soderstrom K, D'Andrea A, Ogg GS, et al. HLA-E binds to natural killer cell receptors CD94/NKG2A, B and C. *Nature.* (1998) 391:795–9. doi: 10.1038/35869
14. Colonna M, Navarro F, Bellon T, Llano M, Garcia P, Samaridis J, et al. A common inhibitory receptor for major histocompatibility complex class I molecules on human lymphoid and myelomonocytic cells. *J Exp Med.* (1997) 186:1809–18. doi: 10.1084/jem.186.11.1809
15. Shiroishi M, Tsumoto K, Amano K, Shirakihara Y, Colonna M, Braud VM, et al. Human inhibitory receptors Ig-like transcript 2 (ILT2) and ILT4 compete with CD8 for MHC class I binding and bind preferentially to HLA-G. *Proc Natl Acad Sci USA.* (2003) 100:8856–61. doi: 10.1073/pnas.1431057100
16. Marsh SG, Parham P, Dupont B, Geraghty DE, Trowsdale J, Middleton D, et al. Killer-cell immunoglobulin-like receptor (KIR) nomenclature report, 2002. *Hum Immunol.* (2003) 64:648–54. doi: 10.1016/s0198-8859(03)00067-3
17. Parham P. MHC class I molecules and KIRs in human history, health and survival. *Nat Rev Immunol.* (2005) 5:201–14. doi: 10.1038/nri1570
18. Long EO. Negative signaling by inhibitory receptors: the NK cell paradigm. *Immunol Rev.* (2008) 224:70–84. doi: 10.1111/j.1600-065X.2008.00660.x
19. Elliott JM, Yokoyama WM. Unifying concepts of MHC-dependent natural killer cell education. *Trends Immunol.* (2011) 32:364–72. doi: 10.1016/j.it.2011.06.001
20. Boudreau JE, Hsu KC. Natural killer cell education and the response to infection and cancer therapy: stay tuned. *Trends Immunol.* (2018) 39:222–39. doi: 10.1016/j.it.2017.12.001
21. Horowitz A, Djaoud Z, Nemat-Gorgani N, Blokhuis J, Hilton HG, Beziat V, et al. Class I HLA haplotypes form two schools that educate NK cells in different ways. *Sci Immunol.* (2016) 1:eaag1672. doi: 10.1126/sciimmunol.aag1672 .
22. Hallner A, Bernson E, Hussein BA, Ewald Sander F, Brune M, Aurelius J, et al. The HLA-B -21 dimorphism impacts on NK cell education and clinical outcome of immunotherapy in acute myeloid leukemia. *Blood.* (2019) 133:1479–88. doi: 10.1182/blood-2018-09-874990
23. Sun JC, Lopez-Verges S, Kim CC, DeRisi JL, Lanier LLNK. cells and immune "memory". *J Immunol.* (2011) 186:1891–7. doi: 186/4/1891 [pii]10.4049/jimmunol.1003035 .
24. Rolle A, Brodin P. Immune adaptation to environmental influence: the case of NK Cells and HCMV. *Trends Immunol.* (2016) 37:233–43. doi: 10.1016/j.it.2016.01.005
25. Guma M, Angulo A, Vilches C, Gomez-Lozano N, Malats N, Lopez-Botet M. Imprint of human cytomegalovirus infection on the NK cell receptor repertoire. *Blood.* (2004) 104:3664–71. doi: 10.1182/blood-2004-05-2058 2004-05-2058 [pii].
26. Schlums H, Cichocki F, Tesi B, Theorell J, Beziat V, Holmes TD, et al. Cytomegalovirus infection drives adaptive epigenetic diversification of NK cells with altered signaling and effector function. *Immunity.* (2015) 42:443–56. doi: 10.1016/j.immuni.2015.02.008
27. Lee J, Zhang T, Hwang I, Kim A, Nitschke L, Kim M, et al. Epigenetic modification and antibody-dependent expansion of memory-like NK cells in human cytomegalovirus-infected individuals. *Immunity.* (2015) 42:431–42. doi: 10.1016/j.immuni.2015.02.013
28. Foley B, Cooley S, Verneris MR, Pitt M, Curtsinger J, Luo X, et al. Cytomegalovirus reactivation after allogeneic transplantation promotes a lasting increase in educated NKG2C+ natural killer cells with potent function. *Blood.* (2011) 119:2665–74. doi: 10.1182/blood-2011-10-386995
29. Della Chiesa M, Falco M, Podesta M, Locatelli F, Moretta L, Frassoni F, et al. Phenotypic and functional heterogeneity of human NK cells developing after umbilical cord blood transplantation: a role for human cytomegalovirus? *Blood.* (2012) 119:399–410. doi: 10.1182/blood-2011-08-372003
30. Muccio L, Falco M, Bertaina A, Locatelli F, Frassoni F, Sivori S, et al. Late development of fcepsilonrgamma(neg) adaptive natural killer cells upon human cytomegalovirus reactivation in umbilical cord blood transplantation recipients. *Front Immunol.* (2018) 9:1050. doi: 10.3389/fimmu.2018.01050
31. Liu Y, Cheng Y, Xu Y, Wang Z, Du X, Li C, et al. Increased expression of programmed cell death protein 1 on NK cells inhibits NK-cell-mediated anti-tumor function and indicates poor prognosis in digestive cancers. *Oncogene.* (2017) 36:6143–53. doi: 10.1038/onc.2017.209
32. Cichocki F, Cooley S, Davis Z, DeFor TE, Schlums H, Zhang B, et al. CD56dimCD57+NKG2C+ NK cell expansion is associated with reduced leukemia relapse after reduced intensity HCT. *Leukemia.* (2016) 30:456–63. doi: 10.1038/leu.2015.260
33. Muccio L, Bertaina A, Falco M, Pende D, Meazza R, Lopez-Botet M, et al. Analysis of memory-like natural killer cells in human cytomegalovirus-infected children undergoing alphabeta+T and B cell-depleted hematopoietic stem cell transplantation for hematological malignancies. *Haematologica.* (2016) 101:371–81. doi: 10.3324/haematol.2015.134155
34. Sivori S, Meazza R, Quintarelli C, Carlomagno S, Della Chiesa M, Falco M, et al. NK cell-based immunotherapy for hematological malignancies. *J Clin Med.* (2019) 8:1702. doi: 10.3390/jcm8101702
35. Locatelli F, Pende D, Falco M, Della Chiesa M, Moretta A, Moretta L. NK cells mediate a crucial graft-versus-leukemia effect in haploidentical-HSCT to cure high-risk acute leukemia. *Trends Immunol.* (2018) 39:577–90. doi: 10.1016/j.it.2018.04.009
36. Ruggeri L, Capanni M, Urbani E, Perruccio K, Shlomchik WD, Tosti A, et al. Effectiveness of donor natural killer cell alloreactivity in mismatched hematopoietic transplants. *Science.* (2002) 295:2097–100. doi: 10.1126/science.1068440
37. Pende D, Marcenaro S, Falco M, Martini S, Bernardo ME, Montagna D, et al. Anti-leukemia activity of alloreactive NK cells in KIR ligand-mismatched haploidentical HSCT for pediatric patients: evaluation of the functional role of activating KIR and redefinition of inhibitory KIR specificity. *Blood.* (2009) 113:3119–29. doi: 10.1182/blood-2008-06-164103
38. Cooley S, Weisdorf DJ, Guethlein LA, Klein JP, Wang T, Le CT, et al. Donor selection for natural killer cell receptor genes leads to superior survival after unrelated transplantation for acute myelogenous leukemia. *Blood.* (2010) 116:2411–9. doi: 10.1182/blood-2010-05-283051
39. Locatelli F, Merli P, Pagliara D, Li Pira G, Falco M, Pende D, et al. Outcome of children with acute leukemia given HLA-haploidentical HSCT after alphabeta T-cell and B-cell depletion. *Blood.* (2017) 130:677–85. doi: 10.1182/blood-2017-04-779769
40. Babor F, Peters C, Manser AR, Glogova E, Sauer M, Pötschger U, et al. Presence of centromeric but absence of telomeric group B KIR haplotypes in stem cell donors improve leukaemia control after HSCT for childhood ALL. *Bone Marrow Transplant.* (2019) 54:1847–58. doi: 10.1038/s41409-019-0543-z
41. Weisdorf D, Cooley S, Wang T, Trachtenberg E, Vierra-Green C, Spellman S, et al. KIR B donors improve the outcome for AML patients given reduced intensity conditioning and unrelated donor transplantation. *Blood Adv.* (2020) 4:740–54. doi: 10.1182/bloodadvances.2019001053
42. Benson DM Jr., Cohen AD, Jagannath S, Munshi NC, Spitzer G, Hofmeister CC, et al. A phase I trial of the anti-KIR antibody IPH2101 and lenalidomide in patients with relapsed/refractory multiple myeloma. *Clin Cancer Res.* (2015) 21:4055–61. doi: 10.1158/1078-0432.CCR-15-0304
43. Carlsten M, Korde N, Kotecha R, Reger R, Bor S, Kazandjian D, et al. Checkpoint inhibition of KIR2D with the monoclonal antibody IPH2101

induces contraction and hyporesponsiveness of NK cells in patients with myeloma. *Clin Cancer Res.* (2016) 22:5211–22. doi: 10.1158/1078-0432.CCR-16-1108
44. Vey N, Karlin L, Sadot-Lebouvier S, Broussais F, Berton-Rigaud D, Rey J, et al. A phase 1 study of lirilumab (antibody against killer immunoglobulin-like receptor antibody KIR2D; IPH2102) in patients with solid tumors and hematologic malignancies. *Oncotarget.* (2018) 9:17675–88. doi: 10.18632/oncotarget.24832
45. Bagot M, Porcu P, Marie-Cardine A, Battistella M, William BM, Vermeer M, et al. IPH4102, a first-in-class anti-KIR3DL2 monoclonal antibody, in patients with relapsed or refractory cutaneous T-cell lymphoma: an international, first-in-human, open-label, phase 1 trial. *Lancet Oncol.* (2019) 20:1160–70. doi: 10.1016/S1470-2045(19)30320-1
46. Andre P, Denis C, Soulas C, Bourbon-Caillet C, Lopez J, Arnoux T, et al. Anti-NKG2A mAb is a checkpoint inhibitor that promotes anti-tumor immunity by unleashing both T and NK cells. *Cell.* (2018) 175:1731–43.e13. doi: 10.1016/j.cell.2018.10.014
47. Pesce S, Greppi M, Tabellini G, Rampinelli F, Parolini S, Olive D, et al. Identification of a subset of human natural killer cells expressing high levels of programmed death 1: a phenotypic and functional characterization. *J Allergy Clin Immunol.* (2017) 139:335–46.e3. doi: 10.1016/j.jaci.2016.04.025
48. Falco M, Biassoni R, Bottino C, Vitale M, Sivori S, Augugliaro R, et al. Identification and molecular cloning of p75/AIRM1, a novel member of the sialoadhesin family that functions as an inhibitory receptor in human natural killer cells. *J Exp Med.* (1999) 190:793–802. doi: 10.1084/jem.190.6.793
49. Poggi A, Tomasello E, Revello V, Nanni L, Costa P, Moretta L. p40 molecule regulates NK cell activation mediated by NK receptors for HLA class I antigens and TCR-mediated triggering of T lymphocytes. *Int Immunol.* (1997) 9:1271–9. doi: 10.1093/intimm/9.9.1271
50. Cantoni C, Bottino C, Augugliaro R, Morelli L, Marcenaro E, Castriconi R, et al. Molecular and functional characterization of IRp60, a member of the immunoglobulin superfamily that functions as an inhibitory receptor in human NK cells. *Eur J Immunol.* (1999) 29:3148–59. doi: 10.1002/(SICI)1521-4141(199910)29:103.0.CO;2-L
51. Triebel F, Jitsukawa S, Baixeras E, Roman-Roman S, Genevee C, Viegas-Pequignot E, et al. LAG-3, a novel lymphocyte activation gene closely related to CD4. *J Exp Med.* (1990) 171:1393–405. doi: 10.1084/jem.171.5.1393
52. Ndhlovu LC, Lopez-Verges S, Barbour JD, Jones RB, Jha AR, Long BR, et al. Tim-3 marks human natural killer cell maturation and suppresses cell-mediated cytotoxicity. *Blood.* (2012) 119:3734–43. doi: 10.1182/blood-2011-11-392951
53. Stanietsky N, Simic H, Arapovic J, Toporik A, Levy O, Novik A, et al. The interaction of TIGIT with PVR and PVRL2 inhibits human NK cell cytotoxicity. *Proc Natl Acad Sci USA.* (2009) 106:17858–63. doi: 10.1073/pnas.0903474106
54. Fuchs A, Cella M, Giurisato E, Shaw AS, Colonna M. Cutting edge: CD96 (tactile) promotes NK cell-target cell adhesion by interacting with the poliovirus receptor (CD155). *J Immunol.* (2004) 172:3994–8. doi: 10.4049/jimmunol.172.7.3994
55. Zhang JQ, Nicoll G, Jones C, Crocker PR. Siglec-9, a novel sialic acid binding member of the immunoglobulin superfamily expressed broadly on human blood leukocytes. *J Biol Chem.* (2000) 275:22121–6. doi: 10.1074/jbc.M002788200
56. Lopez-Verges S, Milush JM, Pandey S, York VA, Arakawa-Hoyt J, Pircher H, et al. CD57 defines a functionally distinct population of mature NK cells in the human CD56dimCD16+ NK-cell subset. *Blood.* (2010) 116:3865–74. doi: 10.1182/blood-2010-04-282301
57. Markel G, Lieberman N, Katz G, Arnon TI, Lotem M, Drize O, et al. CD66a interactions between human melanoma and NK cells: a novel class I MHC-independent inhibitory mechanism of cytotoxicity. *J Immunol.* (2002) 168:2803–10. doi: 10.4049/jimmunol.168.6.2803
58. Aldemir H, Prod'homme V, Dumaurier MJ, Retiere C, Poupon G, Cazareth J, et al. Cutting edge: lectin-like transcript 1 is a ligand for the CD161 receptor. *J Immunol.* (2005) 175:7791–5. doi: 10.4049/jimmunol.175.12.7791
59. Nath PR, Pal-Nath D, Mandal A, Cam MC, Schwartz AL, Roberts DD. Natural killer cell recruitment and activation are regulated by CD47 expression in the tumor microenvironment. *Cancer Immunol Res.* (2019) 7:1547–61. doi: 10.1158/2326-6066.CIR-18-0367
60. Khan M, Arooj S, Wang HNK. Cell-based immune checkpoint inhibition. *Front Immunol.* (2020) 11:167. doi: 10.3389/fimmu.2020.00167
61. Chamoto K, Al-Habsi M, Honjo T. Role of PD-1 in immunity and diseases. *Curr Top Microbiol Immunol.* (2017) 410:75–97. doi: 10.1007/82_2017_67
62. Okazaki T, Maeda A, Nishimura H, Kurosaki T, Honjo TPD-. 1 immunoreceptor inhibits B cell receptor-mediated signaling by recruiting src homology 2-domain-containing tyrosine phosphatase 2 to phosphotyrosine. *Proc Natl Acad Sci USA.* (2001) 98:13866–71. doi: 10.1073/pnas.231486598
63. Mariotti FR, Quatrini L, Munari E, Vacca P, Moretta L. Innate lymphoid cells: expression of PD-1 and other checkpoints in normal and pathological conditions. *Front Immunol.* (2019) 10:910. doi: 10.3389/fimmu.2019.00910
64. Benson DM Jr., Bakan CE, Mishra A, Hofmeister CC, Efebera Y, Becknell B, et al. The PD-1/PD-L1 axis modulates the natural killer cell versus multiple myeloma effect: a therapeutic target for CT-011, a novel monoclonal anti-PD-1 antibody. *Blood.* (2010) 116:2286–94. doi: 10.1182/blood-2010-02-271874
65. Beldi-Ferchiou A, Lambert M, Dogniaux S, Vely F, Vivier E, Olive D, et al. PD-1 mediates functional exhaustion of activated NK cells in patients with Kaposi sarcoma. *Oncotarget.* (2016) 7:72961–77. doi: 10.18632/oncotarget.12150
66. Tumino N, Martini S, Munari E, Scordamaglia F, Besi F, Mariotti FR, et al. Presence of innate lymphoid cells in pleural effusions of primary and metastatic tumors: functional analysis and expression of PD-1 receptor. *Int J Cancer.* (2019) 145:1660–8. doi: 10.1002/ijc.32262
67. Mariotti FR, Petrini S, Ingegnere T, Tumino N, Besi F, Scordamaglia F, et al. PD-1 in human NK cells: evidence of cytoplasmic mRNA and protein expression. *Oncoimmunology.* (2019) 8:1557030. doi: 10.1080/2162402X.2018.1557030
68. Quatrini L, Vacca P, Tumino N, Besi F, Di Pace AL, Scordamaglia F, et al. Glucocorticoids and the cytokines IL-12, IL-15 and IL-18 present in the tumor microenvironment induce PD-1 expression on human Natural Killer cells. *J Allergy Clin Immunol.* (2020). (in press). doi: 10.1016/j.jaci.2020.04.044
69. Quatrini L, Wieduwild E, Escaliere B, Filtjens J, Chasson L, Laprie C, et al. Endogenous glucocorticoids control host resistance to viral infection through the tissue-specific regulation of PD-1 expression on NK cells. *Nat Immunol.* (2018) 19:954–62. doi: 10.1038/s41590-018-0185-0
70. Mariotti FR, Quatrini L, Munari E, Vacca P, Tumino N, Pietra G, et al. Inhibitory checkpoints in human natural killer cells: IUPHAR Review 28. *Br J Pharmacol.* (2020) 177:2889–903. doi: 10.1111/bph.15081
71. Pardoll DM. The blockade of immune checkpoints in cancer immunotherapy. *Nat Rev Cancer.* (2012) 12:252–64. doi: 10.1038/nrc3239
72. Sholl LM, Aisner DL, Allen TC, Beasley MB, Borczuk AC, Cagle PT, et al. Programmed death ligand-1 immunohistochemistry–a new challenge for pathologists: a perspective from members of the pulmonary pathology society. *Arch Pathol Lab Med.* (2016) 140:341–4. doi: 10.5858/arpa.2015-0506-SA
73. Munari E, Zamboni G, Marconi M, Sommaggio M, Brunelli M, Martignoni G, et al. PD-L1 expression heterogeneity in non-small cell lung cancer: evaluation of small biopsies reliability. *Oncotarget.* (2017) 8:90123–31. doi: 10.18632/oncotarget.21485
74. Munari E, Zamboni G, Lunardi G, Marchionni L, Marconi M, Sommaggio M, et al. PD-L1 expression heterogeneity in non-small cell lung cancer: defining criteria for harmonization between biopsy specimens and whole sections. *J Thorac Oncol.* (2018) 13:1113–20. doi: 10.1016/j.jtho.2018.04.017
75. Munari E, Rossi G, Zamboni G, Lunardi G, Marconi M, Sommaggio M, et al. PD-L1 Assays 22C3 and SP263 are Not interchangeable in non-small cell lung cancer when considering clinically relevant cutoffs: an interclone evaluation by differently trained pathologists. *Am J Surg Pathol.* (2018) 42:1384–9. doi: 10.1097/PAS.0000000000001105
76. Munari E, Zamboni G, Lunardi G, Marconi M, Sommaggio M, Brunelli M, et al. PD-L1 expression comparison between primary and relapsed non-small cell lung carcinoma using whole sections and clone SP263. *Oncotarget.* (2018) 9:30465–71. doi: 10.18632/oncotarget.25770
77. Nicoll G, Ni J, Liu D, Klenerman P, Munday J, Dubock S, et al. Identification and characterization of a novel siglec, siglec-7, expressed by human natural

killer cells and monocytes. *J Biol Chem.* (1999) 274:34089–95. doi: 10.1074/jbc.274.48.34089
78. Yamaji T, Teranishi T, Alphey MS, Crocker PR, Hashimoto YA. small region of the natural killer cell receptor, Siglec-7, is responsible for its preferred binding to alpha 2,8-disialyl and branched alpha 2,6-sialyl residues. A comparison with Siglec-9. *J Biol Chem.* (2002) 277:6324–32. doi: 10.1074/jbc.M110146200
79. Santegoets KCM, Gielen PR, Bull C, Schulte BM, Kers-Rebel, Kusters B, et al. Expression profiling of immune inhibitory Siglecs and their ligands in patients with glioma. *Cancer Immunol Immunother.* (2019) 68:937–49. doi: 10.1007/s00262-019-02332-w
80. Jandus C, Boligan KF, Chijioke O, Liu H, Dahlhaus M, Demoulins T, et al. Interactions between Siglec-7/9 receptors and ligands influence NK cell-dependent tumor immunosurveillance. *J Clin Investigat.* (2014) 124:1810–20. doi: 10.1172/JCI65899
81. Kawasaki Y, Ito A, Withers DA, Taima T, Kakoi N, Saito S, et al. Ganglioside DSGb5, preferred ligand for Siglec-7, inhibits NK cell cytotoxicity against renal cell carcinoma cells. *Glycobiology.* (2010) 20:1373–9. doi: 10.1093/glycob/cwq116
82. Nicoll G, Avril T, Lock K, Furukawa K, Bovin N, Crocker PR. Ganglioside GD3 expression on target cells can modulate NK cell cytotoxicity via siglec-7-dependent and -independent mechanisms. *Eur J Immunol.* (2003) 33:1642–8. doi: 10.1002/eji.200323693
83. Daly J, Carlsten M, O'Dwyer M. Sugar free: novel immunotherapeutic approaches targeting siglecs and sialic acids to enhance natural killer cell cytotoxicity against cancer. *Front Immunol.* (2019) 10:1047. doi: 10.3389/fimmu.2019.01047
84. Alphey MS, Attrill H, Crocker PR, van Aalten DM. High resolution crystal structures of Siglec-7. Insights into ligand specificity in the Siglec family. *J Biolo Chem.* (2003) 278:3372–7. doi: 10.1074/jbc.M210602200
85. Dimasi N, Moretta A, Moretta L, Biassoni R, Mariuzza RA. Structure of the saccharide-binding domain of the human natural killer cell inhibitory receptor p75/AIRM1. *Acta Crystallogr Sect D Biol Crystallogr.* (2004) 60(Pt 2):401–3. doi: 10.1107/S0907444903028439
86. Prescher H, Frank M, Gutgemann S, Kuhfeldt E, Schweizer A, Nitschke L, et al. Design, synthesis, and biological evaluation of small, high-affinity siglec-7 ligands: toward novel inhibitors of cancer immune evasion. *J Med Chem.* (2017) 60:941–56. doi: 10.1021/acs.jmedchem.6b01111
87. Meril S, Harush O, Reboh Y, Matikhina T, Barliya T, Cohen CJ. Targeting glycosylated antigens on cancer cells using siglec-7/9-based CAR T-cells. *Mol Carcinogenes.* (2020) 59:713–23. doi: 10.1002/mc.23213
88. Poggi A, Pella N, Morelli L, Spada F, Revello V, Sivori S, et al. p40, a novel surface molecule involved in the regulation of the non-major histocompatibility complex-restricted cytolytic activity in humans. *Eur J Immunol.* (1995) 25:369–76. doi: 10.1002/eji.1830250210
89. Kannourakis G, Johnson GR, Begley CG, Werkmeister JA, Burns GF. Enhancement of in vitro beta-thalassemic and normal hematopoiesis by a noncytotoxic monoclonal antibody, 9.1C3: evidence for negative regulation of hematopoiesis by monocytes and natural killer cells. *Blood.* (1988) 72:1124–33. doi: 10.1182/blood.v72.4.1124.1124
90. Meyaard L, Adema GJ, Chang C, Woollatt E, Sutherland GR, Lanier LL, et al. LAIR-1, a novel inhibitory receptor expressed on human mononuclear leukocytes. *Immunity.* (1997) 7:283–90. doi: 10.1016/s1074-7613(00)80530-0
91. Meyaard L. The inhibitory collagen receptor LAIR-1 (CD305). *J Leukoc Biol.* (2008) 83:799–803. doi: 10.1189/jlb.0907609
92. Poggi A, Tomasello E, Ferrero E, Zocchi MR, Moretta L. p40/LAIR-1 regulates the differentiation of peripheral blood precursors to dendritic cells induced by granulocyte-monocyte colony-stimulating factor. *Eur J Immunol.* (1998) 28:2086–91. doi: 10.1002/(SICI)1521-4141(199807)28:073.0.CO;2-T
93. Verbrugge A, de Ruiter T, Geest C, Coffer PJ, Meyaard L. Differential expression of leukocyte-associated Ig-like receptor-1 during neutrophil differentiation and activation. *J Leukoc Biol.* (2006) 79:828–36. doi: 10.1189/jlb.0705370
94. Florian S, Sonneck K, Czerny M, Hennersdorf F, Hauswirth AW, Buhring HJ, et al. Detection of novel leukocyte differentiation antigens on basophils and mast cells by HLDA8 antibodies. *Allergy.* (2006) 61:1054–62. doi: 10.1111/j.1398-9995.2006.01171.x
95. Maasho K, Masilamani M, Valas R, Basu S, Coligan JE, Borrego F. The inhibitory leukocyte-associated Ig-like receptor-1 (LAIR-1) is expressed at high levels by human naive T cells and inhibits TCR mediated activation. *Mol Immunol.* (2005) 42:1521–30. doi: 10.1016/j.molimm.2005.01.004
96. Van Der Vuurst de Vries AR, Clevers H, Logtenberg T, Meyaard L. Leukocyte-associated immunoglobulin-like receptor-1 (LAIR-1) is differentially expressed during human B cell differentiation and inhibits B cell receptor-mediated signaling. *Eur J Immunol.* (1999) 29:3160–7. doi: 10.1002/(SICI)1521-4141(199910)29:103.0.CO;2-S
97. Ouyang W, Ma D, Lin D, Sun Y, Liu X, Li Q, et al. 9.1C3 is identical to LAIR-1, which is expressed on hematopoietic progenitors. *Biochem Biophys Res Commun.* (2003) 310:1236–40. doi: 10.1016/j.bbrc.2003.09.152
98. Jansen CA, Cruijsen CW, de Ruiter T, Nanlohy N, Willems N, Janssens-Korpela PL, et al. Regulated expression of the inhibitory receptor LAIR-1 on human peripheral T cells during T cell activation and differentiation. *Eur J Immunol.* (2007) 37:914–24. doi: 10.1002/eji.200636678
99. Lebbink RJ, de Ruiter T, Adelmeijer J, Brenkman AB, van Helvoort JM, Koch M, et al. Collagens are functional, high affinity ligands for the inhibitory immune receptor LAIR-1. *J Exp Med.* (2006) 203:1419–25. doi: 10.1084/jem.20052554
100. Son M, Santiago-Schwarz F, Al-Abed Y, Diamond B. C1q limits dendritic cell differentiation and activation by engaging LAIR-1. *Proc Natl Acad Sci USA.* (2012) 109:E3160–7. doi: 10.1073/pnas.1212753109
101. Olde Nordkamp MJ, van Eijk M, Urbanus RT, Bont L, Haagsman HP, Meyaard L. Leukocyte-associated Ig-like receptor-1 is a novel inhibitory receptor for surfactant protein D. *J Leukoc Biol.* (2014) 96:105–11. doi: 10.1189/jlb.3AB0213-092RR
102. Meyaard L, Hurenkamp J, Clevers H, Lanier LL, Phillips JH. Leukocyte-associated Ig-like receptor-1 functions as an inhibitory receptor on cytotoxic T cells. *J Immunol.* (1999) 162:5800–4.
103. Verbrugge A, Rijkers ES, de Ruiter T, Meyaard L. Leukocyte-associated Ig-like receptor-1 has SH2 domain-containing phosphatase-independent function and recruits C-terminal Src kinase. *Eur J Immunol.* (2006) 36:190–8. doi: 10.1002/eji.200535226
104. Ouyang W, Xue J, Liu J, Jia W, Li Z, Xie X, et al. Establishment of an ELISA system for determining soluble LAIR-1 levels in sera of patients with HFRS and kidney transplant. *J Immunol Methods.* (2004) 292:109–17. doi: 10.1016/j.jim.2004.06.005
105. Lebbink RJ, van den Berg MC, de Ruiter T, Raynal N, van Roon JA, Lenting PJ, et al. The soluble leukocyte-associated Ig-like receptor (LAIR)-2 antagonizes the collagen/LAIR-1 inhibitory immune interaction. *J Immunol.* (2008) 180:1662–9. doi: 10.4049/jimmunol.180.3.1662
106. Bachelet I, Munitz A, Levi-Schaffer F. Abrogation of allergic reactions by a bispecific antibody fragment linking IgE to CD300a. *J Allergy Clin Immunol.* (2006) 117:1314–20. doi: 10.1016/j.jaci.2006.04.031
107. Borrego F. The CD300 molecules: an emerging family of regulators of the immune system. *Blood.* (2013) 121:1951–60. doi: 10.1182/blood-2012-09-435057
108. Clark GJ, Ju X, Tate C, Hart DN. The CD300 family of molecules are evolutionarily significant regulators of leukocyte functions. *Trends Immunol.* (2009) 30:209–17. doi: 10.1016/j.it.2009.02.003
109. Martinez-Barriocanal A, Arcas-Garcia A, Magallon-Lorenz M, Ejarque-Ortiz A, Negro-Demontel ML, Comas-Casellas E, et al. Effect of specific mutations in Cd300 complexes formation; potential implication of Cd300f in multiple sclerosis. *Sci Rep.* (2017) 7:13544. doi: 10.1038/s41598-017-12881-8
110. Murakami Y, Tian L, Voss OH, Margulies DH, Krzewski K, Coligan JE. CD300b regulates the phagocytosis of apoptotic cells via phosphatidylserine recognition. *Cell Death Differ.* (2014) 21:1746–57. doi: 10.1038/cdd.2014.86
111. Vitalle J, Terren I, Orrantia A, Zenarruzabeitia O, Borrego F. CD300 receptor family in viral infections. *Eur J Immunol.* (2019) 49:364–74. doi: 10.1002/eji.201847951
112. Voss OH, Murakami Y, Pena MY, Lee HN, Tian L, Margulies DH, et al. Lipopolysaccharide-induced CD300b receptor binding to toll-like receptor 4 alters signaling to drive cytokine responses that enhance septic shock. *Immunity.* (2016) 44:1365–78. doi: 10.1016/j.immuni.2016.05.005
113. Alvarez Y, Tang X, Coligan JE, Borrego F. The CD300a (IRp60) inhibitory receptor is rapidly up-regulated on human neutrophils in response to inflammatory stimuli and modulates CD32a (FcgammaRIIa) mediated

signaling. *Mol Immunol.* (2008) 45:253–8. doi: 10.1016/j.molimm.2007.05.006

114. Bachelet I, Munitz A, Moretta A, Moretta L, Levi-Schaffer F. The inhibitory receptor IRp60 (CD300a) is expressed and functional on human mast cells. *J Immunol.* (2005) 175:7989–95. doi: 10.4049/jimmunol.175.12.7989
115. Silva R, Moir S, Kardava L, Debell K, Simhadri VR, Ferrando-Martinez S, et al. CD300a is expressed on human B cells, modulates BCR-mediated signaling, and its expression is down-regulated in HIV infection. *Blood.* (2011) 117:5870–80. doi: 10.1182/blood-2010-09-310318
116. Lopez-Sejas N, Campos C, Hassouneh F, Sanchez-Correa B, Tarazona R, Pera A, et al. Effect of CMV and Aging on the Differential Expression of CD300a, CD161, T-bet, and Eomes on NK Cell Subsets. *Front Immunol.* (2016) 7:476.
117. Lankry D, Simic H, Klieger Y, Levi-Schaffer F, Jonjic S, Mandelboim O. Expression and function of CD300 in NK cells. *J Immunol.* (2010) 185:2877–86. doi: 10.4049/jimmunol.0903347
118. Birge RB, Boeltz S, Kumar S, Carlson J, Wanderley J, Calianese D, et al. Phosphatidylserine is a global immunosuppressive signal in efferocytosis, infectious disease, and cancer. *Cell Death Differ.* (2016) 23:962–78. doi: 10.1038/cdd.2016.11
119. Lankry D, Rovis TL, Jonjic S, Mandelboim O. The interaction between CD300a and phosphatidylserine inhibits tumor cell killing by NK cells. *Eur J Immunol.* (2013) 43:2151–61. doi: 10.1002/eji.201343433
120. Simhadri VR, Andersen JF, Calvo E, Choi SC, Coligan JE, Borrego F. Human CD300a binds to phosphatidylethanolamine and phosphatidylserine, and modulates the phagocytosis of dead cells. *Blood.* (2012) 119:2799–809. doi: 10.1182/blood-2011-08-372425
121. Zenarruzabeitia O, Vitalle J, Eguizabal C, Simhadri VR, Borrego F. The Biology and disease relevance of CD300a, an inhibitory receptor for phosphatidylserine and phosphatidylethanolamine. *J Immunol.* (2015) 194:5053–60. doi: 10.4049/jimmunol.1500304
122. Martinez-Martin N, Ramani SR, Hackney JA, Tom I, Wranik BJ, Chan M, et al. The extracellular interactome of the human adenovirus family reveals diverse strategies for immunomodulation. *Nat Commun.* (2016) 7:11473. doi: 10.1038/ncomms11473
123. Sun X, Huang S, Wang X, Zhang X, Wang X. CD300A promotes tumor progression by PECAM1, ADCY7 and AKT pathway in acute myeloid leukemia. *Oncotarget.* (2018) 9:27574–84. doi: 10.18632/oncotarget.24164
124. Jiang L, Xu Y, Zeng X, Fang J, Morse HC III, Zhou JX. Suppression of CD300A inhibits the growth of diffuse large B-cell lymphoma. *Oncotarget.* (2015) 6:31191–202. doi: 10.18632/oncotarget.5152
125. Raggi F, Blengio F, Eva A, Pende D, Varesio L, Bosco MC. Identification of CD300a as a new hypoxia-inducible gene and a regulator of CCL20 and VEGF production by human monocytes and macrophages. *Innate Immun.* (2014) 20:721–34. doi: 10.1177/1753425913507095
126. Schumann T, Adhikary T, Wortmann A, Finkernagel F, Lieber S, Schnitzer E, et al. Deregulation of PPARbeta/delta target genes in tumor-associated macrophages by fatty acid ligands in the ovarian cancer microenvironment. *Oncotarget.* (2015) 6:13416–33. doi: 10.18632/oncotarget.3826

Conflict of Interest: The authors declare that the research was conducted in the absence of any commercial or financial relationships that could be construed as a potential conflict of interest.

frontiers in Immunology

ORIGINAL RESEARCH
published: 29 September 2020
doi: 10.3389/fimmu.2020.576310

Shp1 Loss Enhances Macrophage Effector Function and Promotes Anti-Tumor Immunity

*Darienne R. Myers[1†], Clare L. Abram[2†], David Wildes[1], Amira Belwafa[1], Alia M. N. Welsh[2], Christopher J. Schulze[1], Tiffany J. Choy[1], Tram Nguyen[1], Neil Omaque[1], Yongmei Hu[2], Mallika Singh[1], Rich Hansen[1], Mark A. Goldsmith[1], Elsa Quintana[1], Jacqueline A. M. Smith[1] and Clifford A. Lowell[2]**

[1] Revolution Medicines, Inc., Redwood City, CA, United States, [2] Department of Laboratory Medicine, University of California, San Francisco, San Francisco, CA, United States

OPEN ACCESS

Edited by:
Ali A. Zarrin,
TRex Bio, United States

Reviewed by:
Dalil Hannani,
UMR5525 Techniques de l'Ingénierie Médicale et de la Complexité Informatique, Mathématiques et Applications (TIMC-IMAG), France
Keehoon Jung,
Seoul National University, South Korea

***Correspondence:**
Clifford A. Lowell
clifford.lowell@ucsf.edu

[†]These authors have contributed equally to this work

Specialty section:
This article was submitted to Molecular Innate Immunity, a section of the journal Frontiers in Immunology

Received: 25 June 2020
Accepted: 27 August 2020
Published: 29 September 2020

Citation:
Myers DR, Abram CL, Wildes D, Belwafa A, Welsh AMN, Schulze CJ, Choy TJ, Nguyen T, Omaque N, Hu Y, Singh M, Hansen R, Goldsmith MA, Quintana E, Smith JAM and Lowell CA (2020) Shp1 Loss Enhances Macrophage Effector Function and Promotes Anti-Tumor Immunity. Front. Immunol. 11:576310. doi: 10.3389/fimmu.2020.576310

Shp1, encoded by the gene *Ptpn6*, is a protein tyrosine phosphatase that transduces inhibitory signals downstream of immunoreceptors in many immune cell types. Blocking Shp1 activity represents an exciting potential immunotherapeutic strategy for the treatment of cancer, as Shp1 inhibition would be predicted to unleash both innate and adaptive immunity against tumor cells. Antibodies blocking the interaction between CD47 on tumor cells and SIRPα on macrophages enhance macrophage phagocytosis, show efficacy in preclinical tumor models, and are being evaluated in the clinic. Here we found that Shp1 bound to phosphorylated peptide sequences derived from SIRPα and transduced the anti-phagocytic signal, as Shp1 loss in mouse bone marrow-derived macrophages increased phagocytosis of tumor cells *in vitro*. We also generated a novel mouse model to evaluate the impact of global, inducible *Ptpn6* deletion on anti-tumor immunity. We found that inducible Shp1 loss drove an inflammatory disease in mice that was phenotypically similar to that seen when *Ptpn6* is knocked out from birth. This indicates that acute perturbation of Shp1 *in vivo* could drive hyperactivation of immune cells, which could be therapeutically beneficial, though at the risk of potential toxicity. In this model, we found that Shp1 loss led to robust anti-tumor immunity against two immune-rich syngeneic tumor models that are moderately inflamed though not responsive to checkpoint inhibitors, MC38 and E0771. Shp1 loss did not promote anti-tumor activity in the non-inflamed B16F10 model. The observed activity in MC38 and E0771 tumors was likely due to effects of both innate and adaptive immune cells. Following Shp1 deletion, we observed increases in intratumoral myeloid cells in both models, which was more striking in E0771 tumors. E0771 tumors also contained an increased ratio of effector to regulatory T cells following Shp1 loss. This was not observed for MC38 tumors, though we did find increased levels of IFNγ, a cytokine produced by effector T cells, in these tumors. Overall, our preclinical data suggested that targeting Shp1 may be an attractive therapeutic strategy for boosting the immune response to cancer via a mechanism involving both innate and adaptive leukocytes.

Keywords: tyrosine phosphatase, phagocytosis, PTPN6, immuno-oncology, SIRPα, inflammation

INTRODUCTION

The tumor immune microenvironment is a complex milieu comprised of both innate and adaptive immune cells. Activation of innate or adaptive immune cells can enhance an anti-tumor response. For example, enhancing the ability of effector T lymphocytes to kill tumor cells using checkpoint inhibitors has achieved success in the clinic (1). Therapies that enhance macrophage effector function, such as by targeting the "don't eat me" molecule CD47 on tumor cells to enhance macrophage phagocytosis, are being evaluated in clinical trials and are showing signs of activity in hematological malignancies in combination with opsonizing antibodies (2–5). Promotion of macrophage phagocytosis is a major mechanism of action of many antibodies in cancer therapies (6). The simultaneous targeting of both innate and adaptive immune cells to increase antitumor immunity represents as an exciting and promising therapeutic strategy for cancer.

The protein tyrosine phosphatase Src homology region 2 domain-containing phosphatase-1 (Shp1) is a potential immunotherapeutic target (7, 8). Shp1 is broadly expressed in the hematopoietic compartment and acts as a negative regulator of signaling in both innate and adaptive immune cells (9, 10). Thus, alterations in Shp1 have the potential to impact an anti-tumor immune response in several different ways. Shp1 exerts its inhibitory signaling function by binding to phosphorylated immunoreceptor tyrosine-based inhibitory motifs (ITIMs) on a variety of immunoreceptors. Upon binding and activation, Shp1 dephosphorylates its substrates, thereby transducing inhibitory signals that restrict immune cell function (9, 10). Consistent with this, mouse models with spontaneous mutations in the gene encoding Shp1, *Ptpn6*, that affect its expression or function develop an inflammatory/autoimmune disease associated with hyperactivation of multiple types of immune cells. The *motheaten* ($Ptpn6^{me/me}$) mouse was the first *Ptpn6*-mutant mouse model described, and the *me* mutation results in loss of Shp1 protein (11). *Motheaten* mice are runted and die within a few weeks of life from lethal pneumonitis, and the animals also present with a number of other disease features that reflect dysregulation of both innate and adaptive immune cells, such as myelopoiesis, splenomegaly, skin inflammation, and anti-nuclear antibody production (9, 11). Mice with other spontaneous mutations of *Ptpn6*, such as *motheaten-viable* ($Ptpn6^{me-v/me-v}$), $Ptpn6^{spin/spin}$ and $Ptpn6^{meB2/meB2}$ give rise to similar, yet milder inflammatory disease phenotypes (12–14). This has led to the hypothesis that loss of Shp1 activity would promote immune cell activation and enhance effector function in the tumor microenvironment. However, this question has been challenging to address with existing genetic mouse models, as the short lifespan and early-onset disease in *motheaten* and *motheaten-viable* mice would be incompatible with the kinetics of a tumor challenge study. Additionally, there is no selective Shp1 inhibitor available with properties that would enable the pharmacological assessment of Shp1 loss of function on tumor growth. Small molecule Shp1 inhibitors, including TPI-1 and SSG, have been reported (8, 15), but the selectivity and specificity of these inhibitors has not been fully established. Both molecules exhibit relatively low potency and have characteristics consistent with promiscuous Pan-Assay Interference Compounds (PAINS) (16). Specifically, the quinone moiety in TPI-1 and the metal (antimony) in SSG are both capable of non-specific reactivity with cysteine residues, which may account for their apparent inhibitory activity on the cysteine active site of Shp1, but also likely impact many other cellular targets. A recent evaluation of inhibitors of the related receptor tyrosine phosphatase Shp2 using cells that lack Shp2 protein revealed off-target effects (17). Until similar investigations are completed for Shp1 inhibitors, we believe cellular and *in vivo* experiments with these compounds should be interpreted with caution.

The complex *motheaten* phenotype does not arise from loss of Shp1 in any single immune cell subset, as deletion of *Ptpn6* in distinct cell lineages, achieved by crossing a floxed *Ptpn6* mouse to cell type-specific Cre driver lines, does not fully recapitulate the *motheaten* disease features (18–26). However, loss of Shp1 in myeloid cells is required to drive inflammation (9, 18, 27). Shp1 has been proposed to transduce anti-phagocytic "don't eat me" signals downstream of the signal regulatory protein alpha (SIRPα), which is expressed on dendritic cells (DCs) and macrophages, the primary phagocytic cells of the immune system (28, 29). Upon recognition of its ligand CD47, the ITIMs of SIRPα become phosphorylated. This allows for recruitment of Shp1 and activation of its phosphatase activity, leading to downregulation of signals from phagocytic receptors such as Fc receptors, thereby inhibiting phagocytosis (30, 31). Consistent with this, it has been shown that alveolar macrophages from *me* mice exhibit increased phagocytosis of apoptotic cells (32), suggesting that Shp1 loss enhances phagocytic activity. Whether Shp1-deficient macrophages from other anatomical sites also exhibit increased phagocytosis has yet to be determined. Furthermore, it is unknown whether Shp1 loss can augment phagocytosis to a similar degree as antibody blockade of the CD47-SIRPα interaction, or even have an additive effect in combination with pro-phagocytic signaling that is stimulated by the Fc portion of the blocking antibodies binding to Fc receptors on phagocytes. We aimed to address these questions herein and found that Shp1 could bind to phosphorylated peptide sequences derived from SIRPα in a manner that activated its phosphatase activity, and that Shp1-deficient macrophages exhibited enhanced phagocytosis in a manner comparable to that of CD47-SIRPα blockade. There is strong preclinical evidence that blocking the CD47-SIRPα interaction with an antibody enhances phagocytosis and restricts the growth of tumors *in vivo* (5, 33, 34) but whether Shp1 loss in tumor-infiltrating immune cells would similarly enhance anti-tumor immunity remains an open question.

Here we report on the generation of a novel mouse model that facilitated global, inducible deletion of *Ptpn6* in adult mice, and we used this model to uncover a role for Shp1 in anti-tumor immunity. We found that a *motheaten*-like disease consistent with hyperactivation of immune cells occurred when *Ptpn6* deletion was induced in adult mice. Lastly, we report that inducible deletion of *Ptpn6* drove anti-tumor immunity against several syngeneic tumor cell lines, with corresponding alterations in the frequency and/or activity of both myeloid and T

lymphocytes in the tumor immune microenvironment. Overall, our data suggest that Shp1 restricts immune cell activity in the tumor microenvironment, and that pharmacological inhibition of Shp1 could lead to activation of both innate and adaptive immune cells to promote anti-tumor immunity.

MATERIALS AND METHODS

Mice

Ptpn6$^{fl/fl}$, Cx3cr1-Cre, and Rosa26$^{LSL-YFP}$ mice have been described elsewhere (25, 35, 36). Rosa26-CreERT2 and dLck-Cre mice were obtained from the Jackson Laboratory (37, 38). C57BL/6 mice used for controls were obtained from Jackson Laboratories or Envigo. Mice were kept in specific pathogen-free facilities at the University of California, San Francisco (UCSF), Revolution Medicines or Taconic Biosciences, and cared for in accordance with institutional guidelines. All genotypes of mouse strains used were confirmed by PCR analysis of tail DNA.

Cell Lines

DLD1, Raji, THP-1 and B16F10 cells were obtained from the ATCC. DLD1 and Raji cells were cultured in RPMI with 10% FCS and 1% penicillin/streptomycin. THP-1 cells were cultured in RPMI with 10% FCS, 1% penicillin/streptomycin and 100 μg/ml Normocin. B16F10 cells were cultured in DMEM with GlutaMAX™ (Gibco) containing 10% FCS (Gibco). MC38 cells were obtained from Kerafast and were used in all studies except those in **Supplementary Figure 7**, which employed cells that were a gift from Jim Allison (UT MD Anderson Cancer Center), and grown in DMEM with GlutaMAX™ (Gibco) containing 10% FCS (Gibco) and penicillin/streptomycin. E0771 cells were obtained from CH3 Biosystems and cultured in RPMI 1640 with GlutaMAX™ (Gibco) containing 10% FCS (Gibco) and 20 mM HEPES. All cell lines were confirmed to be negative for Mycoplasma species by PCR (IDEXX Bioanalytics) and kept in a humidified incubator with 5% CO_2 at 37°C.

Biochemical Phosphatase Assay

Full length wild type SHP1 and all mutants were expressed with C-terminal 6-His tags in E. coli and purified by nickel affinity chromatography using standard techniques (ATUM, Newark, CA). The SIRPα di-phosphopeptide corresponding to residues 427 to 460 of human SIRPα (H_2N- ITpYADLNLP-PEG8-HTEpYASIQTSK-NH_2) was synthesized by ThermoFisher Custom Peptides (Carlsbad, CA). The catalytic activity of SHP1 was monitored using the fluorogenic small molecule substrate DiFMUP (ThermoFisher) in 96-well, black polystyrene plates (Corning). The assay was performed in 55 mM HEPES pH 7.2, 100 mM NaCl, 0.5 mM EDTA, 1 mM DTT, 0.001% Brij35, 0.002% BSA, 0.1% DMSO, 20 μM DiFMUP, 0.039 to 5.0 nM enzyme, and 0 to 3,000 nM SIRPα peptide, mixed immediately prior to reading the plate in kinetic mode on a SpectraMax M5 plate reader (Molecular Devices) for 6 min using excitation and emission wavelengths of 340 nm and 450 nm. Plots of initial velocity vs. [SHP1] were fit using linear regression to determine specific activity. Plots of specific activity vs. [SIRPα peptide] were fit using a 4-parameter concentration-response model in GraphPad Prism 8.42, with the upper baseline constrained to the specific activity of the fully activated SHP1 mutant E74K.

Generation and Polarization of Mouse Bone Marrow-Derived Macrophages

Bone marrow was flushed from mouse femurs and tibias with Ca^{2+} and Mg^{2+}-free Hepes-buffered saline solution (HBSS). Pellets were stored at −80°C for protein analysis by western blot, or were frozen in liquid nitrogen in 10% DMSO/90% FCS for cell culture experiments. For *in vitro* differentiation of bone marrow-derived macrophages, the method was adapted from (39). Cells were plated at 2×10^6 cells per 10 cm dish in 10 ml macrophage media consisting of αMEM (Gibco) supplemented with 10% FCS, 1% penicillin/streptomycin, 2 mM L-glutamine and 10 ng/ml M-CSF (Peprotech). Functional assays were performed starting on day 7 of culture. For polarization, macrophages were removed from plates using Cell Dissociation Buffer (Gibco), washed, and plated in either M0 conditions (macrophage media), M1-polarizing conditions (macrophage media supplemented with 100 ng/ml LPS and 20 ng/ml recombinant IFNγ) or M2-polarizing conditions (macrophage media supplemented with 20 ng/ml recombinant murine IL-4) for 24 h before analysis. To measure CD206 expression on M2 polarized mouse macrophages, cells were removed from plates using Cell Dissociation Buffer (Gibco) and stained for subsequent analysis by flow cytometry as outlined below. To measure cytokine production by M1 polarized macrophages, supernatants were harvested and analyzed by multiplexed ELISA.

Generation and Polarization of Human Monocyte-Derived Macrophages

Human monocytes were isolated from peripheral blood mononuclear cells using Miltenyi Biotech Classical Monocyte Isolation kit #130-117-337 or Miltenyi Biotec CD14 MicroBeads #130-050-201. Monocytes were cultured in RPMI (Sigma) supplemented with 10% heat-inactivated FCS (Gibco), 50 μM β-mercaptoethanol (Gibco) and 50 ng/ml M-CSF (R&D Systems). Cells were cultured for 5–6 days in 6-well plates (Costar). For siRNA-mediated knockdown of *PTPN6*, cells were washed and resuspended in antibiotic-free macrophage medium. siRNA oligos were obtained from Horizon Discovery (SMARTpool ON-TARGETplus human PTPN6 #L-009778-00-0020 and ON-TARGETplus non-targeting pool #D-001810-10-20). siRNAs and the transfection reagent RNAi Max (Invitrogen) were added to Opti-MEM medium (Gibco) and incubated for 15 min before drop-wise addition to cells. Cells were incubated with transfection mixture for 6 h at 37°C and were analyzed on day 6. For macrophage polarization, macrophage media was supplemented with the following factors 2 days after siRNA transfection: for M1, 20 ng/ml recombinant human IFNγ (R&D Systems) and 100 ng/ml LPS (Sigma) and for M2, 20 ng/ml recombinant human IL-4 (R&D Systems) and 10 ng/ml recombinant human IL-13 (R&D Systems). Supernatants were harvested from polarized macrophages and secreted cytokines were measured by Luminex Multiplex Immunoassay

(Bio-Rad) with reagent kits for IL-12p70 (171B5011M), TNFα (171B5026M), IL-6 (171B5006M), and IL-10 (171B5010M). CD206 expression on M2 polarized human macrophages was determined by fixation with 4% formaldehyde and staining with anti-CD206 (Abcam #Ab64693), followed by Alexa Fluor 647-conjugated secondary antibody. Cells were co-stained with Hoescht 33342 staining solution and Alexa Fluor 488-Phalloidin (Thermofisher). Fluorescent imaging was performed with the IN Cell Analyzer 2200 (GE Healthcare) and average fluorescence intensity was quantified.

Phagocytosis Assay

For assays with murine bone marrow-derived macrophages, cells were harvested from tissue culture dishes using Cell Dissociation Buffer (Gibco) or Accutase (Corning) and resuspended in RPMI. Target cells were cultured as previously described and labeled with 25 nM CellTrace Far Red proliferation dye (ThermoFisher) for 20 min at 37°C, at a density of 1×10^6 cells/ml. Dye was quenched and cells were resuspended in RPMI. Target cells were pre-incubated with opsonizing antibodies (anti-CD47 clone B6H12, eBioscience; mouse IgG1k isotype control, clone P3.6.2.8.1, Thermo Fisher; anti-CD20, Selleckchem), and macrophages were pre-incubated with Fc block (anti-CD16/32, BD Biosciences, clone 2.4G2) as indicated. Macrophages and labeled target cells were co-cultured for 4 h at 37°C in low-adherence 96-well plates at a ratio of 1:2, respectively. Cells were then washed and stained with 4′,6′-Diamidino-2-Phenylindole, Dihydrochloride (DAPI) prior to analysis by flow cytometry (Cytoflex, Beckman Coulter).

For phagocytosis assays with human macrophages treated with siRNA, macrophages were harvested by scraping and incubated with target cells that were pre-labeled with CellTrace Violet proliferation dye (ThermoFisher) for 4 h at 37°C. Cells were stained with LIVE/DEAD™ Fixable Far Red (Invitrogen) and anti-human CD11b (Biolegend, clone ICRF44) prior to analysis by flow cytometry. Phagocytic index was determined by gating on live, single cells, and identifying CellTrace Far Red$^+$ YFP$^+$ (mouse) or CellTrace Violet$^+$ CD11b$^+$ (human) macrophages.

Generation and Analysis of *PTPN6*-Deficient THP-1 Cells

PTPN6-deficient THP-1 cell pools were generated by transfection of Cas9RNPs targeting the *PTPN6* locus. Cas9RNP production and nucleofection was performed as previously described (40). The *PTPN6* locus was targeted using the following sgRNA sequence: TCACGCACAAGAAACGTCCA and a non-targeting (NT) sgRNA was used to generate a control cell line. Single cell clones were selected by limiting dilution and SHP1 loss was verified in monoclonal THP-1 cell lines by Western blot analysis.

To measure cytokine production, control and *PTPN6*-deficient THP-1 cell lines were plated at a density of 5×10^4 cells per well in a 96-well plate and rested at 37°C for 1 h before adding 1 μg/ml LPS (from E. coli 0111:B4, Invivogen). Cells were incubated at 37°C for 20 h, after which supernatant was removed and frozen at −80°C. Supernatants were thawed and assayed for TNF-α, IL-1β, IL-6, and IFNγ using a V-Plex Human ProInflammatory Panel I Kit on the Meso Scale Discovery (MSD) platform.

Western Blot Analysis

Tissue lysates were prepared from tissues snap-frozen in liquid nitrogen and powdered using a mortar and pestle. Powdered tissue was lysed in NP40 buffer supplemented with protease/phosphatase inhibitor cocktail (ThermoFisher, #78446) for 30 min on ice, then centrifuged at 4°C for 15 min at 21,000 × g to remove insoluble material. For peripheral blood lysates, blood was collected in K2-EDTA tubes (BD Biosciences), washed with PBS, and centrifuged for 5 min at 400 × g. Red blood cells in the pellet were lysed using RBC lysis solution (Miltenyi Biotec) following the manufacturer's protocol, or using ACK lysis buffer (150 mM NH_4Cl, 10 mM $KHCO_3$, 0.1 mM EDTA pH 7.2–7.4), and centrifuged for 5 min at 400 × g. The leukocyte-containing pellet was lysed in NP40 buffer as detailed above or lysed directly in Laemmli sample buffer. Total protein concentration of cell lysates was determined using the Pierce BCA Protein Assay kit (ThermoFisher). Equal amounts of protein were loaded onto 4–12% SDS-PAGE gradient gels for separation, transferred to nitrocellulose or PVDF membranes, blocked, and immunoblotting was performed using the following primary antibodies: anti-SHP1 (Abcam, clone Y476 #ab325599), anti-Shp1 (Santa Cruz, C19 #sc-287), anti-Shp1 (LSBio, #LS-C358839), anti-Erk1/2 (Cell Signaling, clone L34F12 #4696), or anti-Erk2 (Santa Cruz, D2 #sc1647) at 4°C overnight. Blots were probed with secondary antibodies: goat anti-rabbit IgG (LI-COR, 800CW) and goat anti-mouse IgG (LI-COR, 680RD), washed and scanned using the LI-COR Odyssey CLx. Protein bands were quantified using LI-COR Image Studio Acquisition Software.

Inducible Mouse Model of *Ptpn6* Deletion

For maximum Cre-mediated loss of Shp1, *Ptpn6*$^{fl/fl}$, and *Ptpn6*$^{fl/fl}$ ERT2-cre mice were treated with tamoxifen (Toronto Research Chemicals) at 200 mg/kg bid for 4 days by oral gavage. Tamoxifen was dissolved in corn oil (Sigma) at 20 mg/ml by incubation at 37°C for 8–12 h. Mouse bodyweight was monitored every 2–3 days.

PrimeFlow Analysis

Probes for murine *Ptpn6* (AF647 conjugate, Assay ID: VB1-3030134-PF) and murine beta-actin (AF750 conjugate, Assay ID: VB6- 12823-PF) were from ThermoFisher Scientific. Single cell suspensions of splenocytes were prepared and 2×10^6 cells were plated per well of a 96-well V-bottom plate. Cells were stained with LIVE/DEAD™ Fixable Aqua (ThermoFisher), blocked with anti-CD16/32 (BD Biosciences) and stained with the following antibodies to surface markers: Panel 1: NKp46 FITC, TCRβ PE-Cy7, CD25 PE, B220 BV421, CD8 BV650, CD4 BV711 or Panel 2: F4/80 FITC, Ly6g PE-Cy7, CD11c PE, CD11b e450, MHCII BV711 in Superbright staining buffer (ThermoFisher). Cells were fixed and permeabilized using PrimeFlow Assay Kit buffers following the manufacturer's instructions (ThermoFisher). Target probes were hybridized for 2 h at 40°C then cells were washed and stored overnight at 4°C in PrimeFlow RNA Wash Buffer with RNase Inhibitor 1. The following day, signal amplification

steps were performed according to manufacturer's protocol and cells were analyzed by flow cytometry on a BD Fortessa flow cytometer. Data was analyzed using FlowJo (Treestar) and the mean fluorescence intensity (MFI) of the *Ptpn6* mRNA probe was determined in the following cell types: PMNs ($CD11b^+$ $Ly6g^+$), Tregs ($B220^-$ $TCR\beta^+$ $CD4^+$ $CD25^+$ $FoxP3^+$), $CD4^+$ T cells ($B220^-$ $TCR\beta^+$ $CD4^+$ $CD8^-$), and $CD8^+$ T cells ($B220^-$ $TCR\beta^+$ $CD4^-$ $CD8^+$).

Flow Cytometry Analysis

For confirmation of CD47 expression on target cell lines, DLD1 and Raji cells were stained with anti-human CD47 clone B6H12 or mouse $IgG1_k$ isotype control. MC38 cells were stained with anti-mouse CD47 clone miap301 or rat $IgG2a_k$ isotype control.

To assess CD206 staining on polarized mouse macrophages, cells were detached using Cell Dissociation Buffer as previously described. Cells were stained with a fixable viability dye (ThermoFisher) according to the manufacturer's protocol, blocked with anti-mouse IgG and anti-CD16/32 (BD Biosciences, clone 2.4G2,) and stained with antibodies to surface markers. Cells were then fixed in FoxP3 fixation buffer (eBiosciences) and stained with anti-CD206-PE (Biolegend, clone C068C2). Cells were analyzed using a Cytoflex flow cytometer (Beckman Coulter).

Single cell suspensions of splenocytes were prepared by homogenizing spleens between two frosted microscope slides, followed by passage through a 70 μM cell strainer. Bronchoalveolar lavage (BAL) cells were obtained with five 1 ml flushes of the lungs with ice-cold 5 mM EDTA in PBS. Red blood cells were removed from cell suspensions by lysis with ACK buffer (150 mM NH_4Cl, 10 mM $KHCO_3$, 0.1 mM EDTA pH 7.2–7.4). Cells were resuspended in HBSS containing 2% (vol/vol) FCS, 20 mM HEPES and 1 mM EDTA and maintained at 4°C. Cell numbers were determined by using a Nucleocounter™ (Chemometec). Tumors were disaggregated using the GentleMACS Mouse Tumor Dissociation kit (Miltenyi Biotech) and resuspended in HBSS containing 2% FCS, 20 mM HEPES and 1 mM EDTA. For surface staining, cells were pre-incubated with 0.5 μg anti-CD16/32 antibody (clone 2.4G2, UCSF Hybridoma core) and 100 μg mouse IgG (Sigma) for 15 min to block non-specific binding, followed by addition of the following fluorescently-conjugated antibodies: From BD Biosciences; anti-mouse γδTCR FITC (Clone GL3, Cat# 553177), anti-mouse CD11c PE (Clone HL3, Cat# 553802), anti-mouse NK1.1 PE-Cy7 (Clone PK136, Cat# 553165), anti-mouse CD45R (B220) AF700 (Clone RA3-6B2 Cat# 557957), anti-mouse Ly6c AF780 (Clone AL-21 Cat# 560596), anti-mouse CD8 BV650 (Clone 53-6.7 Cat# 563234), anti-mouse I-A/I-E BV711 (Clone M5/114 Cat# 563414), anti-mouse TCRβ BV711 (H57-597 Cat# 563135), anti-mouse CD4 BV786 (Clone GK1.5 Cat# 563331), anti-mouse CD11b BUV395 (Clone M1/70 Cat# 563553). From Thermo Fisher; anti-mouse TCRβ PerCP-Cy5.5 (Clone H57-597, Cat# 45-5961), anti-mouse CD45R (B220) PerCP-Cy5.5 (Clone RA3-6B2, Cat# 45-0452), anti-mouse FoxP3 PE (Clone FJK-16S, Cat# 12-5773), anti-mouse CD25 APC (Clone PC61.5 Cat# 17-0251), anti-mouse CD3 AF780 (Clone 145-2C11 Cat# 47-0031), anti-mouse CD44 eFluor450 (Clone IM7 Cat# 48-0441). From Bio-Rad; anti-mouse F4/80 AF647 (Clone CI:A3-1, Cat# MCA497A647). From Biolegend; anti-mouse Ly6g Pacific Blue (Clone 1A8 Cat# 127612), anti-mouse CD45 BV605 (Clone 30-F11 Cat# 103139). Viability was assessed by staining with Live/Dead fixable Aqua (Thermo Fisher) or DAPI exclusion. Cells were fixed and permeabilized for intracellular staining using the FoxP3/Transcription Factor staining kit (Thermo Fisher). AccuCheck Counting Beads (Thermo Fisher) were added to samples prior to acquisition to obtain cell counts in some cases. All flow cytometry of material from the inducible mouse model was performed on a BD Fortessa flow cytometer. Analysis of flow cytometry data was done using Flowjo (Treestar). Tumor immune cell populations were identified by the gating strategy shown in **Supplementary Figure 8**.

Histology and Immunohistochemistry

Mouse lung lobes were inflated with formalin and fixed for 48 h prior to paraffin embedding, sectioning and staining with H&E. Images were collected using a Zeiss Axio Imager M2 and Zen Pro software. For staining with anti-F4/80 (Cell Signaling, Cat. #70076), lung lobes were fixed with formalin for 24 h prior to paraffin embedding and sectioning. Citrate-based pH 6.2 Heat-Induced Epitope Retrieval was used on the Biocare *intelliPATH* automated staining platform using the manufacturer's recommended settings. The sections were incubated with Biocare Peroxidase Blocker (Biocare, Cat. #PX968) and Background Punisher (Biocare, Cat. #BP974M) to block non-specific background staining. For the detection of rabbit primary antibodies, MACH4 HRP-polymer Detection System (Biocare, Cat. #MRH534) was used. The chromogenic detection and counterstaining kits IntelliPATH FLX DAB chromogen (Biocare, Cat. #IPK5010) and IntelliPATH Hematoxylin (Biocare Medical, Cat. #XMF963) were used.

Tumors were dissected from mice, bisected lengthwise, and formalin fixed for 24 h prior to paraffin embedding, sectioning and staining with H&E, or anti-mouse CD8 (Cell Signaling, Cat. #98941) as detailed above. Stained slides were digitized with a TissueScope LE whole slide scanner (Huron Digital Pathology) and images captured with Huron Viewer software. Quantification of CD8 staining was performed with the HALO® Image Analysis software from Indica labs using the CytoNuclear module.

Growth of Syngeneic Tumor Lines *in vivo*

Cells for *in vivo* use were maintained under limited passage (<5) from original stocks.

5×10^4 B16F10 cells in PBS were mixed 1:1 with ice cold Matrigel (Corning) and 100μl was injected subcutaneously into the inguinal area. 1×10^6 E0771 cells in 100μl PBS were injected into the mammary fat pad. 5×10^5 MC38 cells in 200μl HBSS were injected subcutaneously into the inguinal area or flank except for **Supplementary Figure 7** where 5×10^5 MC38 cells in 100μl 1:1 Matrigel:PBS were injected. Tumor volume was measured with digital calipers using the formulas ($width^2 \times length$) for **Figures 4B,E** and **Supplementary Figures 6A,7B**, or ($width^2 \times length/2$) for **Figure 4H** and **Supplementary Figures 6B,C**. Mice were

sacrificed when tumor volume >2,000 mm^3 or body weight dropped below 80% of initial weight.

Antibody Treatment *in vivo*

For studies with MC38 tumors, wild type C57BL/6 mice were implanted with MC38 cells as described above. When tumor volume reached an average of 75 mm^3, mice were randomized into groups of $n = 15$ mice. For studies with E0771 tumors, *Ptpn6*$^{fl/fl}$ mice were implanted as described above. For anti-PD1 studies: mice were dosed intraperitoneally (IP) with anti-PD1 (clone RMP1-14, BioXCell) or rat IgG2a isotype control (clone 2A3, BioXCell) at 10 mg/kg twice weekly (BIW). For anti-CD47 studies, mice were dosed IP with anti-CD47 (clone miap301, BioXCell) or rat IgG2a isotype control (clone 2A3, BioXCell) at 20 mg/kg BIW for 2 weeks as described in Liu et al. (41).

Analysis of Cytokine Levels in Murine Tumor Lysates

Snap-frozen tumors (0.1 g) were homogenized in 1 ml of buffer containing protease inhibitors using a Precellys homogenizer. Total protein concentration of the homogenates was determined using a BCA assay. Equal volumes of the homogenates were immediately assessed for cytokine/chemokine protein expression using a multiplex bead assay (Luminex, MILLIPLEX MAP Mouse Cytokine/Chemokine Magnetic Bead Panel). Results were normalized to the total concentration of protein as determined by BCA assay.

Statistical Analysis

Statistical analysis was performed using GraphPad Prism (GraphPad Software). Data were analyzed by unpaired *t*-test. For multiple group comparisons, an Analysis of Variance (ANOVA) was performed. The *p*-values for ANOVA analysis were calculated using Dunnett's test. Data were presented as mean ± SEM unless stated otherwise. Statistical significance was indicated as $^{*}p < 0.05$, $^{**}p < 0.01$, $^{***}p < 0.001$, and $^{****}p < 0.0001$.

RESULTS

Shp1 Phosphatase Transduces the "Don't Eat Me" Signal Downstream of SIRPα

Shp1 has a similar domain arrangement and tertiary structure to its paralog Shp2, which is known to adopt an autoinhibited conformation that is activated by binding of both SH2 domains to bis-phosphorylated, tyrosine containing sequence motifs (e.g., ITIMs and ITAMs) (30, 31). We investigated whether the activity of human SHP1 protein was similarly regulated by binding to phosphorylated motifs of interacting proteins such as SIRPα. First, we determined whether SHP1 adopted an autoinhibited conformation in the absence of SH2 domain binding. Multiple activating mutants of SHP2 occur in the inherited disorder Noonan Syndrome and sporadically in cancer genomes, including A72V, E76K, and G503V. Many of these mutations activate SHP2 by destabilizing the autoinhibited conformation (42). We made the same substitutions at homologous positions in SHP1 (A70V, E74K, and G497V). Compared to wild type SHP1, all three variants exhibited >40-fold increased activity on the fluorogenic synthetic substrate 6,8-Difluoro-4-Methylumbelliferyl Phosphate (DiFMUP) (**Figure 1A**), indicating that these mutations disrupted an autoinhibited conformation of SHP1 similar to that of SHP2. We then investigated whether SHP1 could be activated by binding of phosphotyrosine-containing sequence motifs from SIRPα, using a synthetic peptide comprised of the sequence motifs surrounding phosphorylated tyrosines 429 and 453 of human SIRPα, separated by a flexible PEG8 linker. SHP1 activity on DiFMUP increased in a concentration dependent manner with SIRPα peptide, up to 35-fold at the highest concentration tested (3 μM) (**Figure 1B**). To investigate the role of specific interactions with the SH2 domains of SHP1 in this activation, we replaced an arginine residue critical for phosphotyrosine binding (43) with glutamine in the N-SH2 domain (SHP1 R30Q), C-SH2 domain (SHP1 R136Q) and both domains (SHP1 R30Q R136Q). All engineered variants had catalytic activity, indicating properly folded protein (**Figure 1A**). The basal activity of R136Q was similar to wild type, whereas the activity of R30Q and the double mutant was ∼10-fold higher than wild type, possibly due to allosteric disruption of the autoinhibited conformation by the N-SH2 domain binding site mutation. Mutations in the SH2 domains greatly attenuated activation by SIRPα peptide binding; activity of SHP1 R136Q increased 3.5-fold, R30Q 1.8-fold, and R30Q R136Q 1.1-fold at 3 μM SIRPα peptide (**Figure 1B**). Taken together, these observations suggested that SHP1 adopts an autoinhibited conformation similar to SHP2, and that SHP1 phosphatase activity can be induced by binding to phosphorylated SIRPα.

We next wanted to test the hypothesis that Shp1 loss, and thus loss of the anti-phagocytic signal downstream of SIRPα, could enhance macrophage phagocytosis. To obtain *Ptpn6*-deficient macrophages, we crossed *Ptpn6*$^{fl/fl}$ mice to Cx3cr1-Cre Rosa26$^{LSL-YFP}$ and generated YFP^{+} bone marrow-derived macrophages (BMDMs) from these animals as well as from wild type (WT) control mice (*Ptpn6*$^{+/+}$ Cx3cr1-Cre Rosa26$^{LSL-YFP}$). We consistently achieved >85% reduction in Shp1 protein levels in *Ptpn6*-deleted BMDMs (**Supplementary Figure 1A**). To evaluate phagocytosis, we adapted a flow cytometry-based assay (44) wherein YFP-expressing macrophages were co-cultured with fluorescently-labeled cancer target cells, and the frequency of dual-labeled macrophages in the culture was measured, indicative of target cell uptake and referred to as "phagocytic index" (**Supplementary Figure 1B**). All target cell lines tested, which included both epithelial and hematopoietic cancer cell lines (DLD1, Raji, MC38) expressed the SIRPα ligand CD47 (**Supplementary Figure 1C**). *Ptpn6*-deficient BMDMs exhibited a 2–3-fold increase in phagocytic index compared to WT macrophages when co-cultured with DLD1 or Raji human cancer cells as well as the murine syngeneic colon tumor line MC38 (**Figure 1C**). Similar results were observed with human peripheral blood monocyte-derived macrophages transduced with *PTPN6*-targeted siRNA compared to macrophages transduced with a non-targeting siRNA (**Figure 1D**). Pre-incubation of murine and human macrophages with anti-CD47 in order to block the "don't eat me" signal led to increased phagocytosis by

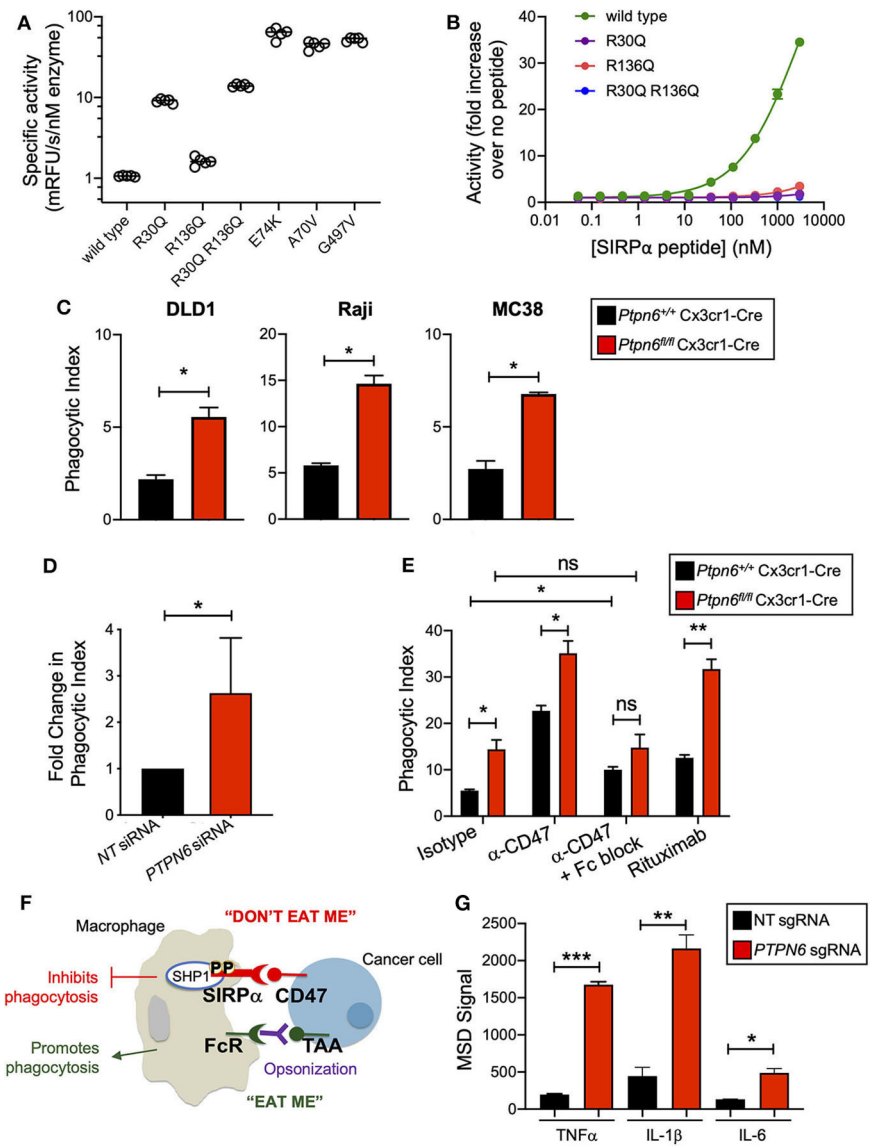

FIGURE 1 | Shp1 phosphatase transduces the "don't eat me" signal downstream of SIRPα. **(A)** Specific activity on the fluorogenic small molecule DiFMUP of purified, full-length, wild-type SHP1, phosphotyrosine binding-deficient mutants (R30Q, R136Q, and R30Q R136Q), and substitutions homologous to known activating mutations in SHP2 (E74K, A70V, and G497V) in the absence of activating concentrations of SIRPα peptide. **(B)** Increase in biochemical activity of SHP1 upon titration with a synthetic peptide corresponding to residues 427–460 of SIRPα, with tyrosines 429 and 453 phosphorylated. Shown are wild type SHP1 (green) and mutants that eliminate phosphotyrosine binding to the N-SH2 (R30Q, purple) and C-SH2 (R136Q, red) domains, and the double mutant (R30Q R136Q, blue). Lines represent fit to a 4-parameter concentration response model. **(C)** Flow cytometry-based *in vitro* phagocytosis assay. Murine bone marrow-derived macrophages (BMDMs) were co-cultured with DLD1, Raji, or MC38 target cells for 4 h prior to analysis by flow cytometry. Phagocytic index is defined as the number of macrophages that had taken up target cells divided by the total number of macrophages. Data is representative of 5 independent experiments with 2 mice/group. **(D)** as in **(C)** but with human peripheral blood monocyte-derived macrophages with *PTPN6* knockdown by siRNA, compared to non-targeting siRNA control. DLD1 were used as target cells. Data is normalized and combined from 4 independent experiments with 1–2 donors per experiment. **(E)** As in **(C)**, but target cells were pre-incubated with antibodies (isotype control, anti-CD47, rituximab, where indicated) and murine BMDMs were pre-incubated with Fc block (where indicated) prior to coculture. Raji were used as target cells. Data is representative of two to five independent experiments with 2 mice/group. **(F)** Cartoon schematic of the balance of signals that impact macrophage phagocytosis. Interaction of SIRPα on the macrophage with CD47 on the cancer target cell leads to an anti-phagocytic "don't eat me" signal that is transduced by SHP1. Macrophages can also receive pro-phagocytic "eat me" signals via stimulation of certain Fc receptors. This can occur when a tumor-associated antigen (TAA) is bound by an antibody, opsonizing the tumor target cell. The Fc portion of the opsonizing antibody can bind to macrophage Fc receptors, driving the "eat me" signal. **(G)** Immunoassay (MSD) for cytokine secretion by wild type (non-targeting, NT, sgRNA) and SHP1 knockout (*PTPN6* sgRNA) THP1 cells. Cells were stimulated with 1μg/ml LPS for 20 h prior to harvesting of culture supernatants. Data is representative of four independent experiments with 3 technical replicates per condition per experiment. Error bars represent SEM, $^{*}p < 0.05$, $^{**}p < 0.01$, $^{***}p < 0.001$.

both WT and *Ptpn6*-deficient macrophages (**Figure 1E**, **Supplementary Figure 1B)**. Phagocytosis is governed by a combination of anti-phagocytic "don't eat me" signals, such as the one driven by CD47 binding to SIRPα, and by "eat me" signals that come from crosslinking of Fc receptors on macrophages; this triggers a signaling pathway that is pro-phagocytic and leads to engulfment of the target cell [(29); schematized in **Figure 1F**]. In the experiments shown in **Figure 1E**, we used an intact anti-CD47 antibody: this can disrupt both the CD47-SIRPα interaction via the variable region of the antibody binding to CD47, and can also bind to macrophage Fc receptors which would enhance phagocytic uptake by triggering the described pro-phagocytic "eat me" signaling pathway. To uncouple the effect of blocking "don't eat me" signals from promoting "eat me" signals, we first pre-incubated macrophages with an antibody that blocks Fc receptors ("Fc block," α-CD16/32). Here, any increase in phagocytosis would be due to blocking the "don't eat me" CD47-SIRPα signal alone. Consistent with this, pretreating WT macrophages with "Fc block" prior to incubation with target cells and anti-CD47 led to increased phagocytosis compared to cocultures with isotype antibody (**Figure 1E**). In contrast, *Ptpn6*-deleted macrophages pretreated with Fc block did not drive a further increase in phagocytosis compared to isotype control antibody treatment (**Figure 1E**). This demonstrated that Shp1 transduced the "don't eat me" signal, and that Shp1 loss-of-function in macrophages drove a similar increase in phagocytosis to that observed with CD47 blockade. Of note, we observed the highest phagocytic index when we combined Shp1 loss with an opsonizing antibody that stimulates an "eat me" signal through macrophage Fc receptors, such as anti-CD47 or anti-CD20 (rituximab) (**Figure 1E**). This is consistent with the emergent clinical success of combining a non-opsonizing anti-CD47 antibody with rituximab in treating $CD20^+$ B cell lymphomas (45).

We also found that SHP1 deletion induced phenotypic changes in macrophages, making them more pro-inflammatory. We knocked out SHP1 in the human monocytic cell line THP-1 using CRISPR-Cas9 and found that clonal SHP1-deficient cells stimulated with lipopolysaccharide (LPS) produced higher levels of the inflammatory cytokines TNFα, IL-1β, and IL-6 compared to THP-1 cells that received a non-targeting (NT) control sgRNA (**Figure 1G**). We next evaluated the impact of Shp1 loss on BMDMs polarized to the proinflammatory "M1" and alternatively-activated "M2" subtypes by incubation with either LPS and IFNγ, or IL-4, respectively, in addition to the non-polarized "M0" BMDMs used in previous experiments. *Ptpn6*-deficient M0 macrophages expressed lower levels of the mannose receptor CD206 (MRC1), an M2-associated marker that plays a major role in the progression of solid tumors due to immunosuppressive effects and impacts on angiogenesis and metastasis (46, 47). This suggested that *Ptpn6*-deficient macrophages were phenotypically less "M2-like" compared to WT macrophages (**Supplementary Figure 1D**). We also observed a reduction in CD206 levels on *Ptpn6*-deficient M2 macrophages (**Supplementary Figure 1D**). Human *PTPN6*-knockdown M2-polarized macrophages also exhibited lower CD206 levels, consistent with our findings in murine macrophages (**Supplementary Figure 1E**). *PTPN6*-deficient human M1 macrophages trended toward increased secretion of the proinflammatory cytokines IL-6 and TNFα (**Supplementary Figure 1F**), consistent with published literature (48). We also observed a trend toward increased IL-1β and IL-10 in mouse M1 macrophages, and reduced IL-12p70 (**Supplementary Figure 1G**), however differences in the experimental methodologies for Shp1 perturbation (siRNA knockdown for human cells and Cre-mediated DNA deletion in the mouse cells) make it hard to draw direct comparisons between our findings in the mouse and human cells. Overall, we found that Shp1 loss in macrophages resulted in a more proinflammatory phenotype and enhanced phagocytic effector function.

Generation of a Genetically-Engineered Mouse Model for Global, Inducible Deletion of *Ptpn6*

Given that enhancing macrophage phagocytosis has been demonstrated to increase anti-tumor activity in preclinical models (6), we wanted to evaluate the impact of Shp1 loss on tumor growth. *Ptpn6*$^{me/me}$ *or* *Ptpn6*$^{mev/mev}$ mice have constitutive mutations in Shp1 and could not be used for tumor growth studies because these animals succumb to *motheaten* disease too rapidly to allow for evaluation of tumor growth (9, 11, 14). Thus, to test the effect of Shp1 loss on tumor growth, we generated a model for global, inducible deletion of *Ptpn6*. To achieve this, we crossed the *Ptpn6*$^{fl/fl}$ mice (25) to the *Rosa26*$^{Cre/ERT2}$ strain (37): with this model (referred to as *Ptpn6*$^{fl/fl}$ERT2-Cre), the Cre was sequestered in the cytosol by virtue of its fusion with the estrogen receptor (ER), and could only translocate to the nucleus and recombine out the loxP-flanked *Ptpn6* DNA upon administration of the ER ligand tamoxifen (49). We developed a tamoxifen dosing regimen that led to a 70–80% reduction in Shp1 protein levels in peripheral blood cells as measured by immunoblot for Shp1 (**Figures 2A,B**). This degree of deletion was detectable 2 days following the last dose of tamoxifen treatment and was sustained for 40 days following initial tamoxifen dosing (**Figure 2A**). Deletion was equivalent in both male and female mice (**Supplementary Figure 2**). Of note, Shp1 protein levels in the peripheral blood began to increase beyond 40 days post-tamoxifen treatment, approaching wild type levels (**Figure 2A**). It is possible that *Ptpn6* was not effectively deleted in progenitor cells following tamoxifen treatment, leading to the observed restoration of detectable Shp1 protein. We determined that *Ptpn6* was knocked out in both innate and adaptive immune cells using a flow cytometry assay that enables detection of mRNA as a surrogate for protein expression because there is no available antibody that detects Shp1 protein by flow cytometry. Using mRNA flow cytometry, we could detect reduced *Ptpn6* mRNA levels in several different immune cell subsets, including neutrophils (PMN), $CD8^+$ T cells, and both effector and regulatory

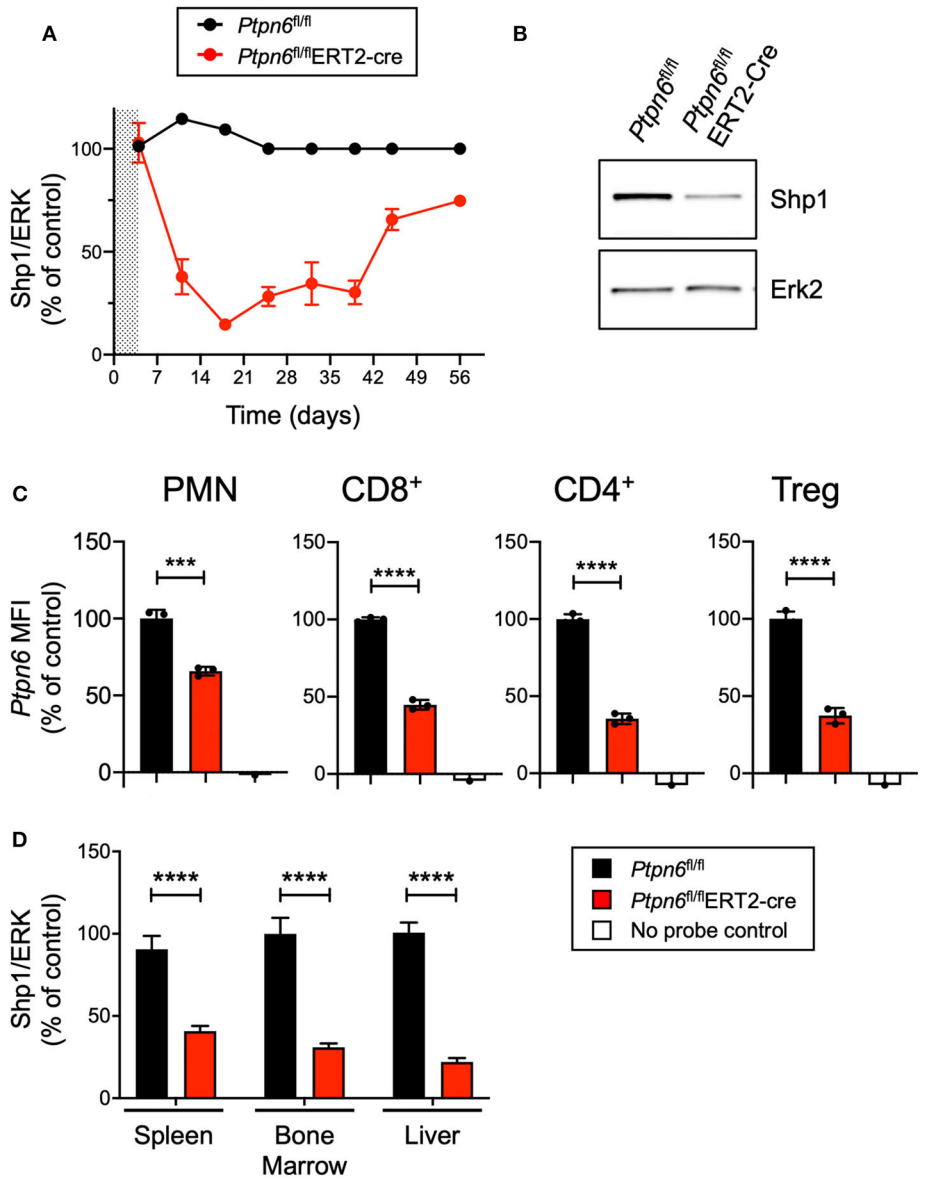

FIGURE 2 | Generation of a genetically-engineered mouse model for global, inducible deletion of *Ptpn6*. **(A)** Shp1 protein relative to total Erk2 protein in peripheral blood cells analyzed over time, from *Ptpn6*$^{fl/fl}$ and *Ptpn6*$^{fl/fl}$ ERT2-Cre mice that had been treated with tamoxifen (200 mg/kg bid for 4 days, represented by shaded area). Data is representative of at least three independent experiments with 4–5 mice pre group. **(B)** Representative immunoblot from A of Shp1 and Erk2 protein levels in whole cell lysates of peripheral blood cells from indicated mice on day 18 following tamoxifen treatment. Lysates were analyzed by SDS-PAGE followed by immunoblotting with indicated antibodies. **(C)** Flow cytometric analysis of *Ptpn6* mRNA levels in the indicated subsets of immune cells from *Ptpn6*$^{fl/fl}$ and *Ptpn6*$^{fl/fl}$ ERT2-Cre mouse spleens on day 12 after MC38 tumor implant (day 19 after initial tamoxifen dose). Data is from one experiment with $n = 3$ mice/group. **(D)** Analysis of Shp1 protein levels by immunoblot in mouse spleen, bone marrow, and liver tissue lysates. Organs were isolated from MC38 tumor-bearing *Ptpn6*$^{fl/fl}$ and *Ptpn6*$^{fl/fl}$ ERT2-Cre mice at study endpoint and tissue lysates were homogenized, then analyzed by SDS-PAGE followed by immunoblotting with indicated antibodies. Quantitated Shp1 protein was normalized to total Erk protein. Data is representative of three independent experiments with 4–10 mice/group. Error bars represent SEM, $^{***}p < 0.001$, $^{****}p < 0.0001$.

(Treg) CD4$^+$ T cells in the spleens of *Ptpn6*$^{fl/fl}$ERT2-Cre mice 19 days following tamoxifen administration (**Figure 2C**). The reduction in mRNA levels was concordant with the reduction in protein observed in total peripheral blood cells in **Figure 2A**. Loss of Shp1 protein was also detected in the peripheral tissues of tamoxifen-treated *Ptpn6*$^{fl/fl}$ERT2-Cre mice, including the spleen, bone marrow, and liver (**Figure 2D**). Overall, we were able to generate a mouse model that allowed for inducible deletion of *Ptpn6* in adult mice and developed an assay to monitor Shp1 protein levels over time in mouse peripheral in blood cells, as well as at study endpoint in peripheral tissues.

Global, Inducible Deletion of *Ptpn6* Leads to Features of the *Motheaten* Phenotype

Before challenging *Ptpn6* inducible knockout mice with tumors, we wanted to determine the impact of Shp1 loss in non-tumor-bearing mice. In particular, we were intrigued as to whether we would observe the broad immune cell hyper-activation seen in *motheaten* mice using our model, wherein the hematopoietic compartment was allowed to develop normally prior to Shp1 loss. Strikingly, we found that mice with inducible *Ptpn6* deletion developed several features reminiscent of the *motheaten* phenotype. All mice lost weight in the 10 days following tamoxifen administration (**Figure 3A**), likely as a result of tamoxifen-induced adverse effects (50). Mice recovered weight to baseline within 2 weeks after treatment. However, at day 20, *Ptpn6*$^{fl/fl}$ERT2-Cre mice begin to exhibit weight loss (**Figure 3A**) that was not observed in control *Ptpn6*$^{fl/fl}$ mice. The transient reduction in Shp1 levels did not result in lethal disease as *Ptpn6*$^{fl/fl}$ERT2-cre mice began to regain some weight over time (**Supplementary Figure 3A**), concomitant with the increase of Shp1 protein in peripheral blood shown in **Figure 2A**. Expansion of myeloid cells (CD11b^{+}) was observed in the peripheral blood of *Ptpn6*$^{fl/fl}$ERT2-Cre by day 14 (**Figure 3B**). We observed splenomegaly in the *Ptpn6*$^{fl/fl}$ERT2-Cre mice following tamoxifen treatment, which was due to an increased number of CD11b^{+} myeloid cells (**Figure 3C**) comprised of both PMNs and Ly6c high and low monocytes (**Supplementary Figure 3B**). Lung inflammation is a key feature of the *motheaten* phenotype (9); consistent with this, we observed both a time- and dose-dependent increase of total cells within the bronchoalveolar lavage (BAL) fluid of tamoxifen-treated *Ptpn6*$^{fl/fl}$ERT2-Cre mice (**Figures 3D,E**). Whereas BAL fluid harvested from lungs of control mice contained >85% of CD45^{+} CD11c^{hi} alveolar macrophages, the large increase of cells in the BAL fluid from *Ptpn6*$^{fl/fl}$ERT2-Cre mice was comprised almost entirely of CD45^{+} CD11b^{+} CD11c^{-} myeloid cells (**Figure 3F**). Analysis of lung tissue sections from tamoxifen-treated *Ptpn6*$^{fl/fl}$ERT2-Cre mice revealed extensive inflammatory cell infiltration (**Figure 3G**). These data confirmed that deletion of Shp1 in adult mice was sufficient to induce a *motheaten*-like phenotype.

Ptpn6 Deletion Drives Robust Anti-Tumor Immunity in Two Immune-Rich Syngeneic Tumor Lines

We next wanted to leverage this novel mouse model to determine the impact of Shp1 loss on tumor growth *in vivo*. We administered tamoxifen according to the regimen outlined in **Figure 2A** and implanted syngeneic mouse tumor cells 3 days after the final tamoxifen dose, a time selected to coincide with initial Shp1 protein loss in mouse peripheral blood cells. As shown in **Figure 2A**, reduction in Shp1 protein levels was observed for ∼30 days following tamoxifen treatment, which is a sufficient window of time for the syngeneic mouse tumor lines B16F10, E0771, and MC38 to reach endpoint (volume > 2,000 mm^3). Thus, we reasoned that our model would allow us to interrogate tumor growth co-incident with Shp1 protein loss in the host animals.

B16F10 melanoma is a poorly immunogenic cell line, with <1% of the tumor being comprised of CD45^{+} immune cells (**Figure 4A**). As such, it is challenging to observe tumor growth inhibition when treating these tumors with single agent immunotherapies (51). Unsurprisingly, we did not observe any difference in tumor growth upon implantation of B16F10 cells into tamoxifen-treated *Ptpn6*$^{fl/fl}$ERT2-Cre and *Ptpn6*$^{fl/fl}$ mice, suggesting that Shp1 loss alone is not sufficient to drive anti-tumor immunity in this "immune desert" tumor (**Figure 4B**). Immunophenotyping of these tumors did not show any significant changes in the composition of the tumor immune microenvironment (**Supplementary Figures 4A,B**). All mice reached tumor endpoint by day 15 of the study (**Figure 4B**) and maintained bodyweight following an initial loss upon tamoxifen administration (**Supplementary Figure 4C**). We confirmed that Shp1 protein was reduced by 50% in peripheral blood cells of tumor-bearing mice upon tamoxifen treatment (**Figure 4C**).

Given that Shp1 loss in myeloid cells drives an inflammatory, pro-phagocytic phenotype [(9), **Figures 1C–G** and **Supplementary Figure 1F**], we next tested the impact of Shp1 loss on the growth of two syngeneic tumor cell lines that develop a more immune-rich microenvironment, the breast adenocarcinoma E0771 and the colon adenocarcinoma MC38. Myeloid cells made up 80% of tumor-infiltrating leukocytes (CD45^{+} cells) in both E0771 tumors (**Supplementary Figure 5A**) and MC38 tumors (**Supplementary Figure 5B**). We did not detect any difference in the total number of live CD45^{+} cells infiltrating the E0771 tumors (∼5%) when Shp1 levels were reduced (**Figure 4D**). However, we observed reduced growth of E0771 tumors in tamoxifen-treated *Ptpn6*$^{fl/fl}$ERT2-cre mice relative to control *Ptpn6*$^{fl/fl}$ mice (**Figure 4E**), as well as reduced tumor weight (**Supplementary Figure 5C**), suggesting that loss of Shp1 could drive anti-tumor immunity. We observed a 40% reduction in Shp1 protein levels in peripheral blood cells from tumor-bearing *Ptpn6*$^{fl/fl}$ ERT2-Cre mice following tamoxifen treatment (**Figure 4F**), and mice began to show bodyweight loss consistent with development of the *motheaten* phenotype (**Supplementary Figure 5D**).

Analysis of MC38 tumors implanted into our mouse model revealed a higher frequency of CD45^{+} immune cell infiltration (∼10–15%) relative to E0771 tumors, but like E0771 we did not observe a significant difference in the overall immune cell infiltrate (% CD45^{+} cells) between mice with reduced Shp1 protein compared to WT controls (**Figure 4G**). We observed significant MC38 tumor growth inhibition in tamoxifen-treated *Ptpn6*$^{fl/fl}$ERT2-cre mice compared to *Ptpn6*$^{fl/fl}$ control mice (**Figure 4H**). We confirmed that Shp1 protein was reduced in the peripheral blood of tamoxifen-treated *Ptpn6*$^{fl/fl}$ERT2-cre mice (**Figure 4I**). We could also detect a 50% reduction of Shp1 protein in MC38 tumor lysates from mice with inducible Shp1 deletion compared to control mice (**Supplementary Figure 5E**).

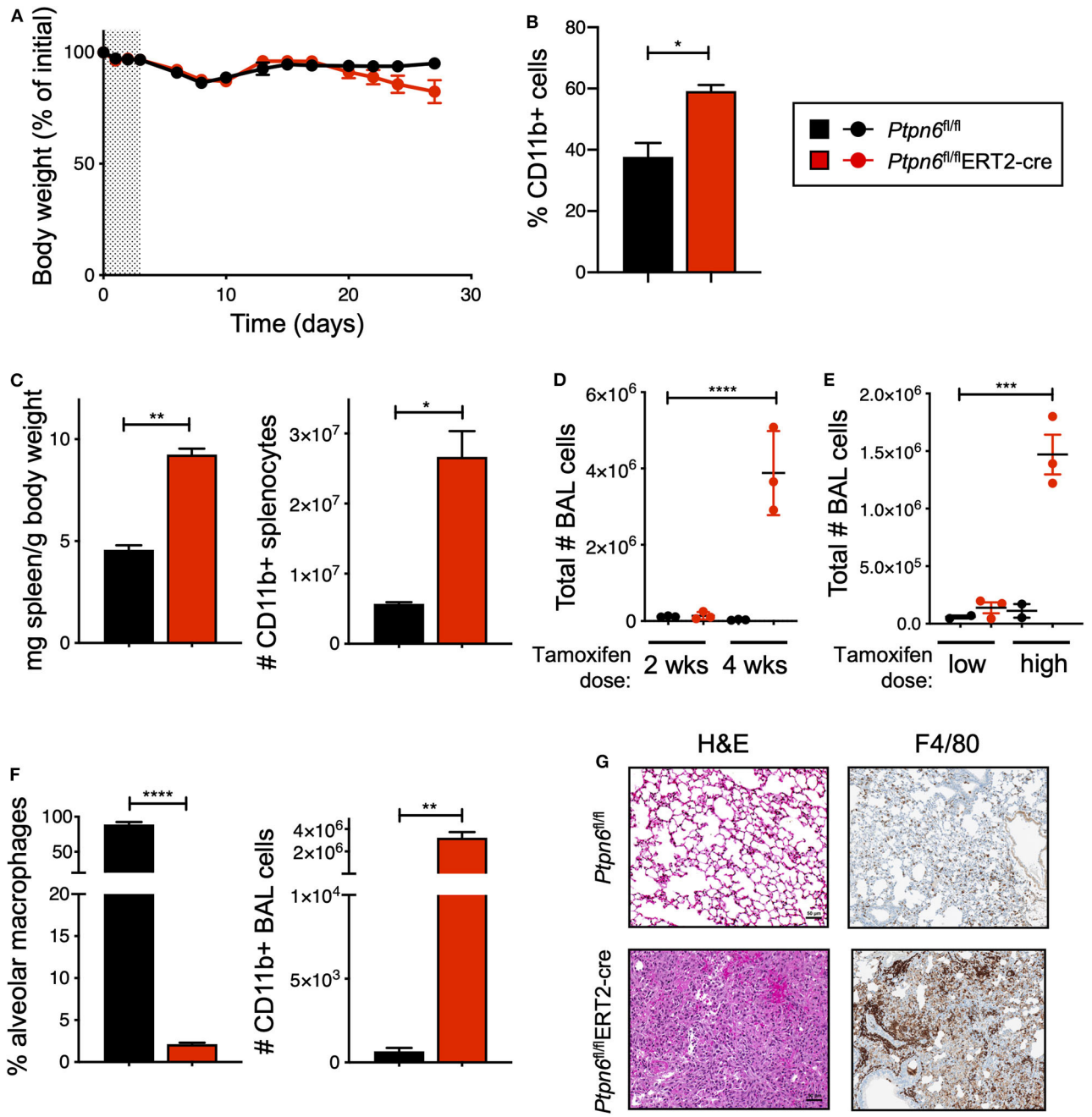

FIGURE 3 | Global, inducible deletion of *Ptpn6* leads to features of the *motheaten* phenotype. **(A)** Body weight of mice of the indicated genotypes, given as % of initial mouse weight, measured over time following treatment with 200 mg/kg tamoxifen bid for 4 days (shaded area). Data is from $n = 9$–10 mice per group. **(B)** Flow cytometric analysis of $CD11b^+$ cells in peripheral blood taken 14 days after initial tamoxifen dose, data shown as % of live $CD45^+$ cells. **(C)** Spleen weight relative to mouse body weight (left), and flow cytometric analysis of $CD11b^+$ splenocytes (right) measured 50 days after initial tamoxifen dose. **(D,E)** total number of bronchoalveolar lavage (BAL) cells from mice of the indicated genotypes measured at either day 14 (2 wks) and 28 (4 wks) following 200 mg/kg tamoxifen bid for 4 days **(D)**, or day 50 following 5 days of 200 mg/kg/day (low dose) or 4 days of 200 mg/kg bid (high dose) **(E)**. **(F)** Flow cytometric analysis of BAL cells at day 28 after initial tamoxifen dose of 200 mg/kg tamoxifen bid for 4 days. Data is graphed as % of $CD45^+$ live cells. **(G)** Representative H&E and anti-F4/80-stained sections of lung lobes from mice of the indicated genotypes. H&E stained sections were from lungs harvested 4 weeks after initial tamoxifen dose of 200 mg/kg tamoxifen bid for 4 days, two independent experiments with 4–7 mice/group. Anti-F4/80 staining is from one experiment with 5 mice/group; lungs were collected day 27 after tumor implantation. Error bars represent SEM, $^*p < 0.05$, $^{**}p < 0.01$, $^{***}p < 0.001$, $^{****}p < 0.0001$.

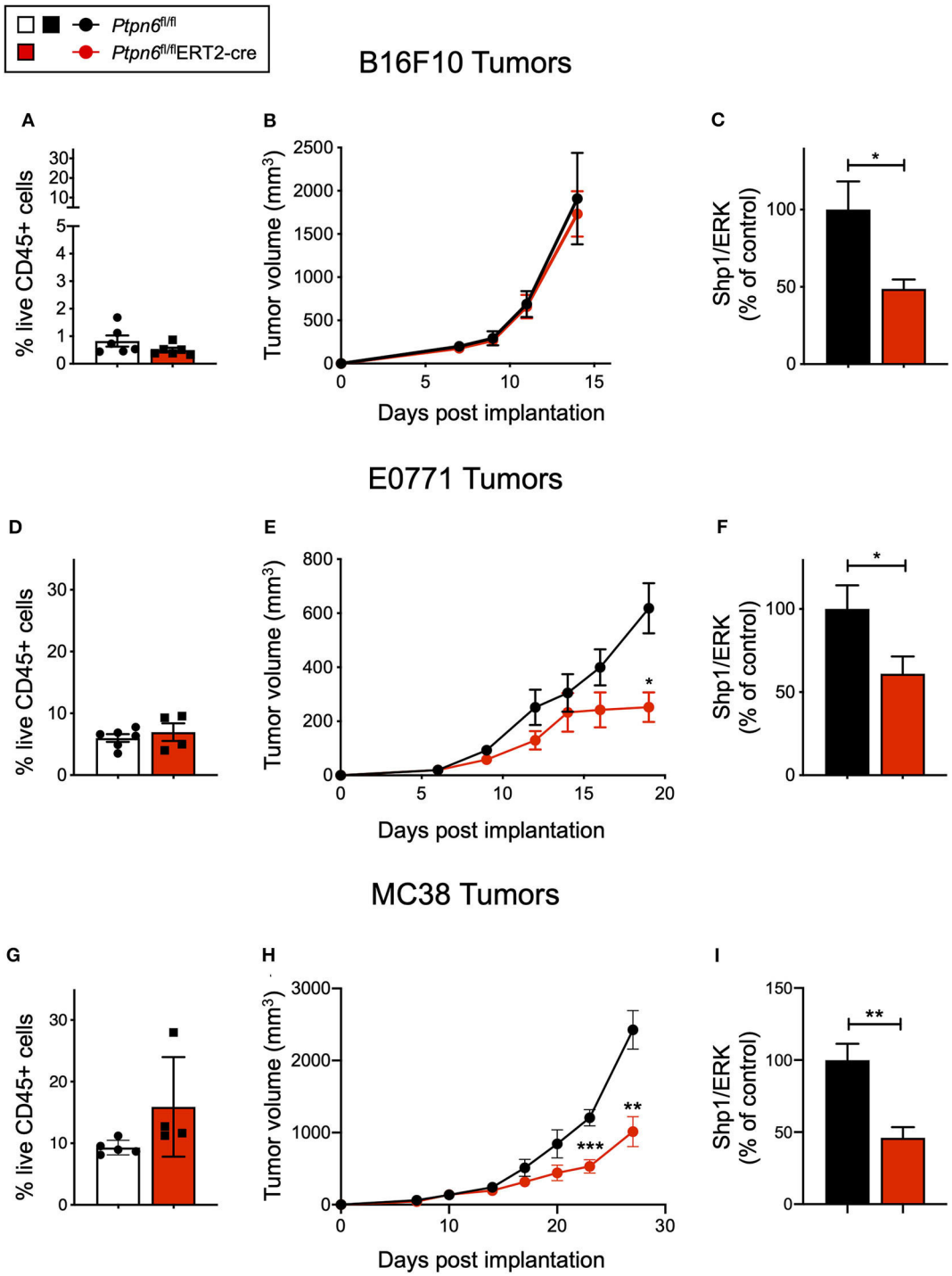

FIGURE 4 | *Ptpn6* deletion drives robust anti-tumor immunity in two immune-rich syngeneic tumor lines. **(A)** Flow cytometric analysis of live CD45$^+$ cells from B16F10 melanoma tumors isolated from tamoxifen-treated *Ptpn6*$^{fl/fl}$ and *Ptpn6*$^{fl/fl}$ERT2-cre mice at day 14 post tumor implantation. **(B)** B16F10 tumor volume measurements in tamoxifen-treated *Ptpn6*$^{fl/fl}$ERT2-cre and *Ptpn6*$^{fl/fl}$ mice. Each data point represents the average tumor volume of all mice in a given group. Data is representative of three independent experiments with 5–7 mice/group. **(C)** Shp1 protein relative to total Erk2 protein in peripheral blood cells from indicated mice 14 days after initial tamoxifen dose (200 mg/kg bid for 4 days) and 7 days after B16F10 tumor cells were implanted. Data is representative of at least three independent experiments with 5–7 mice per group. **(D)** Flow cytometric analysis of live CD45$^+$ cells from E0771 tumors isolated from tamoxifen-treated *Ptpn6*$^{fl/fl}$ and *Ptpn6*$^{fl/fl}$ERT2-cre mice at day 19 post tumor implantation. **(E)** E0771 tumor volume measurements in tamoxifen-treated *Ptpn6*$^{fl/fl}$ERT2-cre and *Ptpn6*$^{fl/fl}$ mice. Each data point represents the average tumor volume of all mice in a given group. Data is representative of three independent experiments with 4–5 mice per group. Statistical significance was

(Continued)

FIGURE 4 | calculated at each time point using an unpaired *t*-test. **(F)** Shp1 protein relative to total Erk2 protein in peripheral blood cells from indicated mice 14 days after initial tamoxifen dose (200 mg/kg bid for 4 days) and 7 days after E0771 tumor cells were implanted. Data is representative of at least three independent experiments with 4–5 mice per group. **(G)** Flow cytometric analysis of live $CD45^+$ cells from MC38 tumors isolated from tamoxifen-treated *Ptpn6*$^{fl/fl}$ and *Ptpn6*$^{fl/fl}$ERT2-cre mice at day 29 post tumor implantation. **(H)** MC38 tumor volume measurements in tamoxifen-treated *Ptpn6*$^{fl/fl}$ERT2-cre and *Ptpn6*$^{fl/fl}$ mice. Each data point represents the average tumor volume of all mice in a given group ($n = 10$ *Ptpn6*$^{fl/fl}$ and $n = 9$ *Ptpn6*$^{fl/fl}$ERT2cre, except for days 23 and 27 post tumor implantation, when data collected was from $n = 9$ *Ptpn6*$^{fl/fl}$ and $n = 7$ *Ptpn6*$^{fl/fl}$ERT2-cre/group). Data are representative of two independent experiments with $n =$ 9–10 or 4–5 mice per group. Statistical significance was calculated at each time point using an unpaired *t*-test. **(I)** Shp1 protein relative to total Erk2 protein in peripheral blood cells from indicated mice at day 13 post tumor implantation. Mice had been treated with tamoxifen (200 mg/kg bid for 4 days) prior to implantation with MC38 cells. Data is representative of two independent experiments with at least 4 mice/group. Error bars represent SEM, $^*p < 0.05$, $^{**}p < 0.01$, $^{***}p < 0.001$.

Given that MC38 tumor cells do not express Shp1 (**Supplementary Figure 5E**), we attributed the observed reduction in Shp1 protein level to host tumor-infiltrating cells. As expected, MC38 tumor-bearing *Ptpn6*$^{fl/fl}$ERT2-cre mice lost weight, consistent with development of the *motheaten* phenotype (**Supplementary Figure 5F**).

Multiple Cell Types Contribute to Anti-Tumor Immunity in Mice With Inducible *Ptpn6* Deletion

Immunophenotyping of the E0771 tumors from *Ptpn6*$^{fl/fl}$ERT2-cre and *Ptpn6*$^{fl/fl}$ mice at the study endpoint revealed a significant increase in both the numbers of M1 and M2 macrophages (**Figures 5A,B**) and a trend toward an increased M1/M2 ratio (**Figure 5C**). Although we saw no effect on the frequency of αβ T cells (**Supplementary Figure 5A**), we observed evidence of increased T cell activation: E0771 tumors from *Ptpn6*$^{fl/fl}$ERT2-cre mice contained a higher frequency of activated, antigen-experienced ($CD44^{hi}$) $CD4^+$ and $CD8^+$ T cells, and an increase in the ratio of effector $CD4^+$ and $CD8^+$ T cells to Tregs (**Figure 5D**), consistent with an anti-tumor response.

Immunophenotyping of MC38 tumors collected near study endpoint from tamoxifen-treated *Ptpn6*$^{fl/fl}$ERT2-cre and *Ptpn6*$^{fl/fl}$ mice did not reveal any significant differences in the composition of the immune cell infiltrate (**Figure 5E**), though there was a trend toward increased M1 macrophages with no effect on the frequency of M2 macrophages (**Supplementary Figure 5G**). As such, there was a trend toward an increased M1/M2 ratio (**Supplementary Figure 5H**), though this did not reach statistical significance. Despite not seeing an increase in T cell frequency by flow cytometry (**Supplementary Figure 5B**) nor any difference in $CD8^+$ effector T cell to Treg ratio (**Supplementary Figure 5I**), immunohistochemistry analysis of tumor sections did reveal a significant increase in $CD8^+$ T cells in MC38 tumors from *Ptpn6*$^{fl/fl}$ERT2-cre mice relative to controls. Importantly, the increase in $CD8^+$ T cell infiltration was observed in the core of the tumors (**Figure 5F**). We hypothesized that differences in immune cell function, in addition to immune cell abundance, might be contributing to the MC38 tumor growth inhibition observed in **Figure 4H**. To address this, we analyzed cytokine levels in MC38 tumor lysates from tamoxifen-treated *Ptpn6*$^{fl/fl}$ERT2-cre and *Ptpn6*$^{fl/fl}$ mice at study endpoint and observed increased levels of the proinflammatory, myeloid-derived cytokines IL-1β, and IL-12p70 (**Figure 5G**). IL-12p70 production by myeloid cells drives differentiation of T helper 1 (Th1) cells and stimulates production of IFNγ from T and NK cells (52, 53). Consistent with this, we also observed increased IFNγ in MC38 tumor lysates from *Ptpn6*$^{fl/fl}$ERT2-cre mice (**Figure 5G**). Overall, these data demonstrate that Shp1 loss drives robust anti-tumor immunity against two immune-rich syngeneic tumor lines.

The E0771 and MC38 cell lines we used for these studies were not sensitive to immune checkpoint blockade, as implantation of these cells into wild type mice followed by treatment with anti-PD1 did not affect tumor growth (**Supplementary Figures 6A,B**). The MC38 line was also insensitive to anti-CD47 treatment (**Supplementary Figure 6C**), even though the tumor cells did express CD47 at the cell surface (**Supplementary Figure 1C**). That we were able to see immunomodulation and anti-tumor activity upon Shp1 deletion in these two models is significant given that neither tumor line responded to checkpoint inhibitor blockade, the standard of care immunotherapy treatment. Overall, these results demonstrated that Shp1 loss in the host mouse can impair growth of two distinct immunogenic tumor cell lines *in vivo*, but cannot drive anti-tumor activity in a tumor line that is non-immunogenic (B16F10). Our immunophenotyping data suggest that the observed activity likely comes from effects of Shp1 loss on multiple immune cell types including macrophages and T cells. Furthermore, the contribution of these cells to the anti-tumor response may be distinct among different tumor histotypes.

Loss of Shp1 Exclusively in the T Cell Compartment Is Insufficient to Drive Anti-Tumor Immunity

We investigated whether loss of Shp1 in the T cell compartment alone was sufficient to cause a reduction in tumor growth. This was achieved by crossing *Ptpn6*$^{fl/fl}$ mice with the T-cell specific distal Lck-Cre strain. T cells from these mice show an increase in the expression of the activation marker CD44, but the mice do not show any sign of inflammation or autoimmune disease (**Supplementary Figure 7A)** (21). We did not observe any reduction of MC38 tumor growth in these mice (**Supplementary Figure 7B**). Similar to the *motheaten* mice, mice with loss of Shp1 exclusively in the myeloid compartment (crossing the *Ptpn6*$^{fl/fl}$ mice to the CD11c-Cre strain to target DCs or the MRP8-Cre strain to target neutrophils) results in substantial immune activation in young mice (18), which confounded studies analyzing the immune response to tumors in these animals (unpublished observations). As such, we were unable to assess the effect

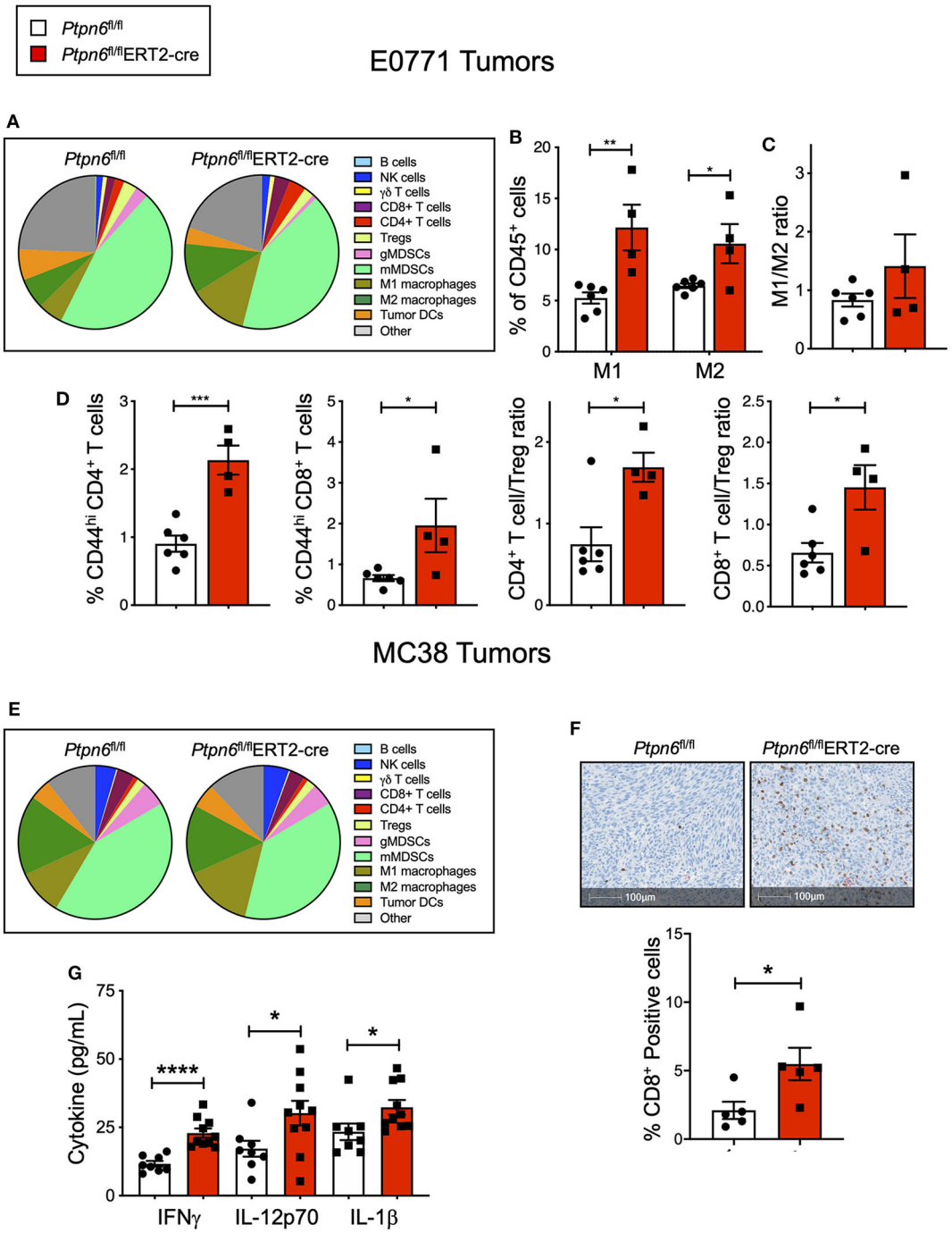

FIGURE 5 | Multiple cell types contribute to anti-tumor immunity in mice with inducible *Ptpn6* deletion. **(A)** Flow cytometric analysis of E0771 tumors isolated from tamoxifen-treated *Ptpn6*$^{fl/fl}$ and *Ptpn6*$^{fl/fl}$ERT2-cre mice at day 19 post tumor implantation. Cells were gated on live CD45$^+$ cells and individual populations were identified by the gating strategy outlined in the Methods and **Supplementary Figure 8**. Data is representative of two experiments with 4–5 mice per group. **(B,C)** Flow cytometric analysis of M1 and M2 macrophages in E0771 tumors from tamoxifen-treated mice, gated based on strategy outlined in Methods and **Supplementary Figure 8**, represented as % CD45$^+$ cells **(B)**, and the ratio of M1 to M2 macrophages **(C)**. **(D)** Flow cytometric analysis of T cell subsets isolated from E0771 tumors from tamoxifen-treated *Ptpn6*$^{fl/fl}$ and *Ptpn6*$^{fl/fl}$ ERT2-cre mice at day 19, represented as %CD45+ cells. Data is representative of two experiments with 4–5 mice per group. **(E)** Flow cytometric analysis of MC38 tumors isolated from tamoxifen-treated *Ptpn6*$^{fl/fl}$ and *Ptpn6*$^{fl/fl}$ERT2-cre mice at day 29 post tumor-implantation. Cells were gated on live CD45$^+$ cells and individual populations were identified by the gating strategy outlined in the Methods and **Supplementary Figure 8**. Data is from one experiment with $n = 4$–5 mice per group. **(F)** Representative image of immunohistochemical analysis of CD8$^+$ T cells in MC38 tumors from tamoxifen-treated *Ptpn6*$^{fl/fl}$ and *Ptpn6*$^{fl/fl}$ERT2-cre mice (left), and quantitation of CD8$^+$ positive cells in the images (right). Tumors were collected on day 27 post implantation. Data is from one experiment. **(G)** Multiplexed immunoassay (Luminex) analysis of cytokine levels in lysates of MC38 tumor isolated from tamoxifen-treated *Ptpn6*$^{fl/fl}$ and *Ptpn6*$^{fl/fl}$ERT2-cre mice at day 27 post tumor-implantation. Lysates were prepared and analyzed from $n = 8$ *Ptpn6*$^{fl/fl}$ and $n = 10$ *Ptpn6*$^{fl/fl}$ERT2-cre mice. Error bars represent SEM, and $^*p < 0.05$, $^{**}p < 0.01$, $^{***}p < 0.005$, $^{****}p < 0.001$.

of *Ptpn6* deletion specifically in myeloid cells on tumor growth. This highlights the need for models that permit cell type-specific inducible deletion, or a specific pharmacological inhibitor of Shp1 that would acutely perturb Shp1 activity in mice.

DISCUSSION

Enhancing anti-tumor effector functions in immune cells has emerged as a successful therapeutic strategy in cancer. Both innate and adaptive immune cells are present in the tumor immune microenvironment: therapies that target innate cells such as agents that block the CD47-SIRPα interaction are being evaluated in the clinic, and checkpoint inhibitor blockade treatments that promote T cell activity are now FDA-approved for several tumor histotypes (1, 3–5). Enhancing anti-tumor immunity by combining different approaches that engage both innate and adaptive immune cells is thus an attractive strategy. As such, the protein tyrosine phosphatase Shp1 is a promising target owing to its broad hematopoietic expression and its regulation of many immune cell signaling pathways. Here we report a novel mouse model of inducible *Ptpn6* deletion that allowed us to investigate how loss of Shp1 in host immune cells could impact tumor growth. This model demonstrated for the first time that deletion of *Ptpn6* in adult mice drove the same inflammatory phenotype as that seen with constitutive *Ptpn6* deletion. Animals with inducible *Ptpn6* deletion exhibited immune cell infiltration in the spleen, lungs and BAL, along with weight loss. This suggests that the *motheaten* phenotype does not arise from aberrant immune cell development and differentiation.

Loss of Shp1 drove anti-tumor immunity against two independent tumor lines, E0771 and MC38, that induce relatively immune cell-rich tumors containing a high frequency of myeloid cells and are insensitive to anti-PD1 checkpoint inhibitor therapy. We found that Shp1 loss in macrophages enhanced their ability to perform phagocytosis *in vitro*, which could be one mechanism that contributed to the observed increase in anti-tumor immunity following induced deletion of *Ptpn6*. Whether *Ptpn6*-deficient macrophages exhibit increased phagocytosis in the tumor microenvironment, and therefore could increase the activity of anti-tumor antibody therapies remains an exciting open research question. Going forward, it would be important to test this hypothesis in a tumor model responsive to agents that enhance pro-phagocytic signaling via opsonization.

Our *in vivo* data support a mechanism of tumor growth inhibition that involves several immune cell types. We observed evidence of both macrophage expansion and T cell activation, with a shift in the balance of effector vs. regulatory T cells. In addition, we observed increased levels of the myeloid-derived cytokines IL-1β and IL-12p70, which are produced by activated macrophages and DCs. These cytokines promote the differentiation of $CD4^+$ T cells toward Th1, and production of IFNγ by cytotoxic innate immune cells (natural killer cells) as well as cytotoxic $CD8^+$ T lymphocytes and $CD4^+$ Th1 cells (52, 53).

We and others have shown that deletion of Shp1 leads to activation of DCs. DCs from *mev* mice exhibit enhanced secretion of the pro-inflammatory cytokine TNFα in response to stimulation (54), and Shp1-deficient dendritic cells derived from $Ptpn6^{fl/fl}$CD11c-Cre mice secrete more of the proinflammatory cytokines IL-6, IL-1β, and TNFα (18, 22). Knocking down *Ptpn6* with shRNA leads to enhanced antigen uptake and priming of T cells, and enhanced activity in an *in vivo* vaccination model of B16F10 melanoma (55). Increased priming of T cells could enhance their response to tumor-specific antigens. Previous studies have also demonstrated an effect of Shp1 loss in T lymphocytes. *Ptpn6*-deficient $CD4^+$ and $CD8^+$ T cells exhibit increased proliferation (20, 21, 56) and are less sensitive to suppression by regulatory T cells (57). A recent genome-wide CRISPR screen in primary human CD4+ T cells identified *PTPN6* as a negative regulator of T cell proliferation (58). *Ptpn6*-deficient CD8 T cells exhibit enhanced killing, and transfer of *Ptpn6*-deficient CD8 T cells into mice with systemic leukemia improves disease outcome (56). It is attractive to hypothesize that the anti-tumor immunity observed in mice with inducible *Ptpn6* deletion is due in part to enhanced T cell priming by DCs and increased effector T cell activity. Shp1 loss can also impact other cell types that are relevant to tumor immunology, such as B cells, natural killer cells, and neutrophils (18, 25, 26). While we did not detect significant differences in the numbers of these cells in tumors from tamoxifen-treated $Ptpn6^{fl/fl}$ERT2-cre mice, it is possible that Shp1 loss alters the activity of these cells in the tumor microenvironment. Examination of other tumor models, that generate different tumor immune microenvironments compared to the models presented in this study, may reveal different responses to genetic deletion of Shp1, either alone or in combination with other therapies.

While our *in vivo* tumor growth data provide a strong rationale for pharmacological inhibition of Shp1 as a potential therapeutic approach for cancer, the development of a *motheaten*-like disease may represent a challenge with respect to tolerability. The current findings highlight the need for Shp1-selective pharmacological agents that can provide transient and reversible inhibition of Shp1 activity, in contrast to the genetic deletion we used in this study, and therefore provide more translatable insights into the tolerability risks. It will be important to determine whether a therapeutic window exists wherein emergent toxicities can be managed or mitigated, while preserving robust anti-tumor activity. If this is the case, then modulation of Shp1 activity with a pharmacological agent represents an attractive immunotherapeutic strategy for the treatment of cancer.

DATA AVAILABILITY STATEMENT

All datasets presented in this study are included in the article/**supplementary material**.

ETHICS STATEMENT

The animal studies were reviewed and approved by the Institutional Animal Care and Use Committees (IACUC) of the University of California, San Francisco (UCSF) or Revolution Medicines.

AUTHOR CONTRIBUTIONS

DM, CA, EQ, MS, RH, MG, JS, and CL conceptualized the study. DM, CA, DW, AB, AW, CS, TC, TN, NO, and YH performed the experiments. DM, CA, DW, AB, AW, CS, TC, and NO analyzed the data. DM, CA, DW, AB, EQ, JS, and CL contributed to writing. All authors contributed to the article and approved the submitted version.

FUNDING

This work was funded by grants CRR-20-636450 (UC Cancer Research Coordinating Committee) and RO1AI13272 (NIH) to CL, a DRC Center Grant P30 DK063720 (NIH) for flow cytometry, and a Sponsored Research Agreement between Revolution Medicines and the Lowell Laboratory at UCSF.

ACKNOWLEDGMENTS

The authors thank the employees of Revolution Medicines, members of the Lowell lab, Dr. Dong Lee, and Dr. Arthur Weiss for helpful discussions. We thank the respective research teams at the following contract research organizations for the conduct of *in vitro* studies: Charles River Laboratories (Harlow, UK), KWS BioTest (Portishead, UK), Taconic Biosciences (Rensselaer, New York, USA), DC3 Therapeutics (South San Francisco, California, USA), and Ensigna Biosystems (Brisbane, California, USA). We also thank Nori Ueno and Anthony Jose at ThermoFisher Scientific for technical support for the PrimeFlow assay, the UCSF flow cytometry core (DRC Center Grant NIH P30 DK063720), and the UCSF mouse pathology core.

SUPPLEMENTARY MATERIAL

The Supplementary Material for this article can be found online at: https://www.frontiersin.org/articles/10.3389/fimmu.2020.576310/full#supplementary-material

REFERENCES

1. Wei SC, Duffy CR, Allison JP. fundamental mechanisms of immune checkpoint blockade therapy. *Cancer Discov.* (2018) 8:1069–86. doi: 10.1158/2159-8290.CD-18-0367
2. Guerriero JL. Macrophages: the road less traveled, changing anticancer therapy. *Trends Mol Med.* (2018) 24:472–89. doi: 10.1016/j.molmed.2018.03.006
3. McCracken MN, Cha AC, Weissman IL. Molecular pathways: activating t cells after cancer cell phagocytosis from blockade of CD47 "don't eat me" signals. *Clin Cancer Res.* (2015) 21:3597–601. doi: 10.1158/1078-0432.CCR-14-2520
4. Weiskopf K. Cancer immunotherapy targeting the CD47/SIRPalpha axis. *Eur J Cancer.* (2017) 76:100–9. doi: 10.1016/j.ejca.2017.02.013
5. Chao MP, Alizadeh AA, Tang C, Myklebust JH, Varghese B, Gill S, et al. Anti-CD47 antibody synergizes with rituximab to promote phagocytosis and eradicate non-Hodgkin lymphoma. *Cell.* (2010) 142:699–713. doi: 10.1016/j.cell.2010.07.044
6. Weiskopf K, Weissman IL. Macrophages are critical effectors of antibody therapies for cancer. *MAbs.* (2015) 7:303–10. doi: 10.1080/19420862.2015.1011450
7. Dempke WCM, Uciechowski P, Fenchel K, Chevassut T. Targeting SHP-1, 2 and SHIP pathways: a novel strategy for cancer treatment? *Oncology.* (2018) 95:257–69. doi: 10.1159/000490106
8. Watson HA, Wehenkel S, Matthews J, Ager A. SHP-1: the next checkpoint target for cancer immunotherapy? *Biochem Soc Trans.* (2016) 44:356–62. doi: 10.1042/BST20150251
9. Abram CL, Lowell CA. Shp1 function in myeloid cells. *J Leukoc Biol.* (2017) 102:657–75. doi: 10.1189/jlb.2MR0317-105R
10. Lorenz U. SHP-1 and SHP-2 in T cells: two phosphatases functioning at many levels. *Immunol Rev.* (2009) 228:342–59. doi: 10.1111/j.1600-065X.2008.00760.x
11. Green MC, Shultz LD. Motheaten, an immunodeficient mutant of the mouse. *I. Genetics and pathology. J Hered.* (1975) 66:250–8. doi: 10.1093/oxfordjournals.jhered.a108625
12. Croker BA, Lawson BR, Rutschmann S, Berger M, Eidenschenk C, Blasius AL, et al. Inflammation and autoimmunity caused by a SHP1 mutation depend on IL-1, MyD88, and a microbial trigger. *Proc Natl Acad Sci USA.* (2008) 105:15028–33. doi: 10.1073/pnas.0806619105
13. Nesterovitch AB, Szanto S, Gonda A, Bardos T, Kis-Toth K, Adarichev VA, et al. Spontaneous insertion of a b2 element in the ptpn6 gene drives a systemic autoinflammatory disease in mice resembling neutrophilic dermatosis in humans. *Am J Pathol.* (2011) 178:1701–14. doi: 10.1016/j.ajpath.2010.12.053
14. Shultz LD, Coman DR, Bailey CL, Beamer WG, Sidman CL. "Viable motheaten," a new allele at the motheaten locus. I. Pathology. *Am J Pathol.* (1984) 116:179–92.
15. Kundu S, Fan K, Cao M, Lindner DJ, Zhao ZJ, Borden E, et al. Novel SHP-1 inhibitors tyrosine phosphatase inhibitor-1 and analogs with preclinical anti-tumor activities as tolerated oral agents. *J Immunol.* (2010) 184:6529–36. doi: 10.4049/jimmunol.0903562
16. Davis BJ, Erlanson DA. Learning from our mistakes: the 'unknown knowns' in fragment screening. *Bioorg Med Chem Lett.* (2013) 23:2844–52. doi: 10.1016/j.bmcl.2013.03.028
17. Tsutsumi R, Ran H, Neel BG. Off-target inhibition by active site-targeting SHP2 inhibitors. *FEBS Open Bio.* (2018) 8:1405–11. doi: 10.1002/2211-5463.12493
18. Abram CL, Roberge GL, Pao LI, Neel BG, Lowell CA. Distinct roles for neutrophils and dendritic cells in inflammation and autoimmunity in motheaten mice. *Immunity.* (2013) 38:489–501. doi: 10.1016/j.immuni.2013.02.018
19. Ando T, Xiao W, Gao P, Namiranian S, Matsumoto K, Tomimori Y, et al. Critical role for mast cell Stat5 activity in skin inflammation. *Cell Rep.* (2014) 6:366–76. doi: 10.1016/j.celrep.2013.12.029
20. Fowler CC, Pao LI, Blattman JN, Greenberg PD. SHP-1 in T cells limits the production of CD8 effector cells without impacting the formation of long-lived central memory cells. *J Immunol.* (2010) 185:3256–67. doi: 10.4049/jimmunol.1001362
21. Johnson DJ, Pao LI, Dhanji S, Murakami K, Ohashi PS, Neel BG. Shp1 regulates T cell homeostasis by limiting IL-4 signals. *J Exp Med.* (2013) 210:1419–31. doi: 10.1084/jem.20122239
22. Kaneko T, Saito Y, Kotani T, Okazawa H, Iwamura H, Sato-Hashimoto M, et al. Dendritic cell-specific ablation of the protein tyrosine phosphatase Shp1 promotes Th1 cell differentiation and induces autoimmunity. *J Immunol.* (2012) 188:5397–407. doi: 10.4049/jimmunol.1103210
23. Li YF, Xu S, Ou X, Lam KP. Shp1 signalling is required to establish the long-lived bone marrow plasma cell pool. *Nat Commun.* (2014) 5:4273. doi: 10.1038/ncomms5273

24. Mazharian A, Mori J, Wang YJ, Heising S, Neel BG, Watson SP, et al. Megakaryocyte-specific deletion of the protein-tyrosine phosphatases Shp1 and Shp2 causes abnormal megakaryocyte development, platelet production, and function. *Blood.* (2013) 121:4205–20. doi: 10.1182/blood-2012-08-449272
25. Pao LI, Lam KP, Henderson JM, Kutok JL, Alimzhanov M, Nitschke L, et al. B cell-specific deletion of protein-tyrosine phosphatase Shp1 promotes B-1a cell development and causes systemic autoimmunity. *Immunity.* (2007) 27:35–48. doi: 10.1016/j.immuni.2007.04.016
26. Viant C, Fenis A, Chicanne G, Payrastre B, Ugolini S, Vivier E. SHP-1-mediated inhibitory signals promote responsiveness and anti-tumour functions of natural killer cells. *Nat Commun.* (2014) 5:5108. doi: 10.1038/ncomms6108
27. Yu CC, Tsui HW, Ngan BY, Shulman MJ, Wu GE, Tsui FW. B and T cells are not required for the viable motheaten phenotype. *J Exp Med.* (1996) 183:371–80. doi: 10.1084/jem.183.2.371
28. Chen J, Zhong MC, Guo H, Davidson D, Mishel S, Lu Y, et al. SLAMF7 is critical for phagocytosis of haematopoietic tumour cells via Mac-1 integrin. *Nature.* (2017) 544:493–7. doi: 10.1038/nature22076
29. Veillette A, Chen J. SIRPalpha-CD47 immune checkpoint blockade in anticancer therapy. *Trends Immunol.* (2018) 39:173–84. doi: 10.1016/j.it.2017.12.005
30. Wang W, Liu L, Song X, Mo Y, Komma C, Bellamy HD, et al. Crystal structure of human protein tyrosine phosphatase SHP-1 in the open conformation. *J Cell Biochem.* (2011) 112:2062–71. doi: 10.1002/jcb.23125
31. Yang J, Liu L, He D, Song X, Liang X, Zhao ZJ, et al. Crystal structure of human protein-tyrosine phosphatase SHP-1. *J Biol Chem.* (2003) 278:6516–20. doi: 10.1074/jbc.M210430200
32. Janssen WJ, McPhillips KA, Dickinson MG, Linderman DJ, Morimoto K, Xiao YQ, et al. Surfactant proteins A and D suppress alveolar macrophage phagocytosis via interaction with SIRP alpha. *Am J Respir Crit Care Med.* (2008) 178:158–67. doi: 10.1164/rccm.200711-1661OC
33. Weiskopf K, Ring AM, Ho CC, Volkmer JP, Levin AM, Volkmer AK, et al. Engineered SIRPalpha variants as immunotherapeutic adjuvants to anticancer antibodies. *Science.* (2013) 341:88–91. doi: 10.1126/science.1238856
34. Weiskopf K, Jahchan NS, Schnorr PJ, Cristea S, Ring AM, Maute RL, et al. CD47-blocking immunotherapies stimulate macrophage-mediated destruction of small-cell lung cancer. *J Clin Invest.* (2016) 126:2610–20. doi: 10.1172/JCI81603
35. Abram CL, Roberge GL, Hu Y, Lowell CA. Comparative analysis of the efficiency and specificity of myeloid-Cre deleting strains using ROSA-EYFP reporter mice. *J Immunol Methods.* (2014) 408:89–100. doi: 10.1016/j.jim.2014.05.009
36. Srinivas S, Watanabe T, Lin CS, William CM, Tanabe Y, Jessell TM, et al. Cre reporter strains produced by targeted insertion of EYFP and ECFP into the ROSA26 locus. *BMC Dev Biol.* (2001) 1:4. doi: 10.1186/1471-213X-1-4
37. Ventura A, Kirsch DG, McLaughlin ME, Tuveson DA, Grimm J, Lintault L, et al. Restoration of p53 function leads to tumour regression *in vivo*. *Nature.* (2007) 445:661–5. doi: 10.1038/nature05541
38. Wang Q, Strong J, Killeen N. Homeostatic competition among T cells revealed by conditional inactivation of the mouse Cd4 gene. *J Exp Med.* (2001) 194:1721–30. doi: 10.1084/jem.194.12.1721
39. Marim FM, Silveira TN, Lima DS Jr., Zamboni DS. A method for generation of bone marrow-derived macrophages from cryopreserved mouse bone marrow cells. *PLoS ONE.* (2010) 5:e15263. doi: 10.1371/journal.pone.0015263
40. Hultquist JF, Hiatt J, Schumann K, McGregor MJ, Roth TL, Haas P, et al. CRISPR-Cas9 genome engineering of primary CD4(+) T cells for the interrogation of HIV-host factor interactions. *Nat Protoc.* (2019) 14:1–27. doi: 10.1038/s41596-018-0069-7
41. Liu X, Pu Y, Cron K, Deng L, Kline J, Frazier WA, et al. CD47 blockade triggers T cell-mediated destruction of immunogenic tumors. *Nat Med.* (2015) 21:1209–15. doi: 10.1038/nm.3931
42. Tartaglia M, Gelb BD. Germ-line and somatic PTPN11 mutations in human disease. *Eur J Med Genet.* (2005) 48:81–96. doi: 10.1016/j.ejmg.2005.03.001
43. Waksman G, Kominos D, Robertson SC, Pant N, Baltimore D, Birge RB, et al. Crystal structure of the phosphotyrosine recognition domain SH2 of v-src complexed with tyrosine-phosphorylated peptides. *Nature.* (1992) 358:646–53. doi: 10.1038/358646a0
44. Tseng D, Volkmer JP, Willingham SB, Contreras-Trujillo H, Fathman JW, Fernhoff NB, et al. Anti-CD47 antibody-mediated phagocytosis of cancer by macrophages primes an effective antitumor T-cell response. *Proc Natl Acad Sci USA.* (2013) 110:11103–8. doi: 10.1073/pnas.1305569110
45. Advani R, Flinn I, Popplewell L, Forero A, Bartlett NL, Ghosh N, et al. CD47 blockade by Hu5F9-G4 and rituximab in non-hodgkin's lymphoma. *N Engl J Med.* (2018) 379:1711–21. doi: 10.1056/NEJMoa1807315
46. DeNardo DG, Ruffell B. Macrophages as regulators of tumour immunity and immunotherapy. *Nat Rev Immunol.* (2019) 19:369–82. doi: 10.1038/s41577-019-0127-6
47. Jaynes JM, Sable R, Ronzetti M, Bautista W, Knotts Z, Abisoye-Ogunniyan A, et al. Mannose receptor (CD206) activation in tumor-associated macrophages enhances adaptive and innate antitumor immune responses. *Sci Transl Med.* (2020) 12:aax6337. doi: 10.1126/scitranslmed.aax6337
48. Christophi GP, Panos M, Hudson CA, Christophi RL, Gruber RC, Mersich AT, et al. Macrophages of multiple sclerosis patients display deficient SHP-1 expression and enhanced inflammatory phenotype. *Lab Invest.* (2009) 89:742–59. doi: 10.1038/labinvest.2009.32
49. Feil S, Valtcheva N, Feil R. Inducible Cre mice. *Methods Mol Biol.* (2009) 530:343–63. doi: 10.1007/978-1-59745-471-1_18
50. Huh WJ, Khurana SS, Geahlen JH, Kohli K, Waller RA, Mills JC. Tamoxifen induces rapid, reversible atrophy, and metaplasia in mouse stomach. *Gastroenterology.* (2012) 142:21–4 e7. doi: 10.1053/j.gastro.2011.09.050
51. Mosely SI, Prime JE, Sainson RC, Koopmann JO, Wang DY, Greenawalt DM, et al. Rational selection of syngeneic preclinical tumor models for immunotherapeutic drug discovery. *Cancer Immunol Res.* (2017) 5:29–41. doi: 10.1158/2326-6066.CIR-16-0114
52. Lu X. Impact of IL-12 in Cancer. *Curr Cancer Drug Targets.* (2017) 17:682–97. doi: 10.2174/1568009617666170427102729
53. Teng MW, Bowman EP, McElwee JJ, Smyth MJ, Casanova JL, Cooper AM, et al. IL-12 and IL-23 cytokines: from discovery to targeted therapies for immune-mediated inflammatory diseases. *Nat Med.* (2015) 21:719–29. doi: 10.1038/nm.3895
54. An H, Hou J, Zhou J, Zhao W, Xu H, Zheng Y, et al. Phosphatase SHP-1 promotes TLR- and RIG-I-activated production of type I interferon by inhibiting the kinase IRAK1. *Nat Immunol.* (2008) 9:542–50. doi: 10.1038/ni.1604
55. Ramachandran IR, Song W, Lapteva N, Seethammagari M, Slawin KM, Spencer DM, et al. The phosphatase SRC homology region 2 domain-containing phosphatase-1 is an intrinsic central regulator of dendritic cell function. *J Immunol.* (2011) 186:3934–45. doi: 10.4049/jimmunol.1001675
56. Stromnes IM, Fowler C, Casamina CC, Georgopolos CM, McAfee MS, Schmitt TM, et al. Abrogation of SRC homology region 2 domain-containing phosphatase 1 in tumor-specific T cells improves efficacy of adoptive immunotherapy by enhancing the effector function and accumulation of short-lived effector T cells *in vivo*. *J Immunol.* (2012) 189:1812–25. doi: 10.4049/jimmunol.1200552
57. Mercadante ER, Lorenz UM. T cells deficient in the tyrosine phosphatase shp-1 resist suppression by regulatory t cells. *J Immunol.* (2017) 199:129–37. doi: 10.4049/jimmunol.1602171
58. Shifrut E, Carnevale J, Tobin V, Roth TL, Woo JM, Bui CT, et al. Genome-wide CRISPR Screens in primary human t cells reveal key regulators of immune function. *Cell.* (2018) 175:1958–71.e15. doi: 10.1016/j.cell.2018.10.024

Conflict of Interest: DM, DW, AB, CS, TC, TN, NO, MS, RH, MG, EQ, and JS are full time employees and stockholders of Revolution Medicines.

The remaining authors declare that the research was conducted in the absence of any commercial or financial relationships that could be construed as a potential conflict of interest.

frontiers in Immunology

ORIGINAL RESEARCH
published: 09 October 2020
doi: 10.3389/fimmu.2020.570963

SIRPα on Mouse B1 Cells Restricts Lymphoid Tissue Migration and Natural Antibody Production

*Katka Franke[1], Saravanan Y. Pillai[2], Mark Hoogenboezem[3], Marion J. J. Gijbels[4,5], Hanke L. Matlung[1], Judy Geissler[1], Hugo Olsman[1], Chantal Pottgens[4], Patrick J. van Gorp[4], Maria Ozsvar-Kozma[6], Yasuyuki Saito[7], Takashi Matozaki[7], Taco W. Kuijpers[1,8], Rudi W. Hendriks[2], Georg Kraal[9], Christoph J. Binder[6], Menno P. J. de Winther[4,10] and Timo K. van den Berg[1,9]**

[1] Sanquin Research and Landsteiner Laboratory, Department of Blood Cell Research, Amsterdam UMC, University of Amsterdam, Amsterdam, Netherlands, [2] Department of Pulmonary Medicine, Erasmus MC, Rotterdam, Netherlands, [3] Sanquin Research and Landsteiner Laboratory, Department of Plasma Protein, Amsterdam UMC, University of Amsterdam, Amsterdam, Netherlands, [4] Department of Medical Biochemistry, Experimental Vascular Biology, Amsterdam UMC, University of Amsterdam, Amsterdam, Netherlands, [5] Department of Pathology, CARIM, Cardiovascular Research Institute Maastricht, GROW-School for Oncology and Developmental Biology, Maastricht University, Maastricht, Netherlands, [6] Department of Laboratory Diagnostics, Medical University of Vienna, Vienna, Austria, [7] Division of Molecular and Cellular Signaling, Department of Biochemistry and Molecular Biology, Kobe University Graduate School of Medicine, Kobe, Japan, [8] Department of Pediatric Hematology, Immunology and Infectious Disease, Emma Children's Hospital, Academic Medical Center, University of Amsterdam, Amsterdam, Netherlands, [9] Department of Molecular Cell Biology and Immunology, Amsterdam UMC, Vrije Universiteit Amsterdam, Amsterdam Infection and Immunity Institute, Amsterdam, Netherlands, [10] Institute for Cardiovascular Prevention (IPEK), Munich, Germany

The inhibitory immunoreceptor SIRPα is expressed on myeloid and neuronal cells and interacts with the broadly expressed CD47. CD47-SIRPα interactions form an innate immune checkpoint and its targeting has shown promising results in cancer patients. Here, we report expression of SIRPα on B1 lymphocytes, a subpopulation of murine B cells responsible for the production of natural antibodies. Mice defective in SIRPα signaling (SIRPα$^{\Delta CYT}$ mice) displayed an enhanced CD11b/CD18 integrin-dependent B1 cell migration from the peritoneal cavity to the spleen, local B1 cell accumulation, and enhanced circulating natural antibody levels, which was further amplified upon immunization with T-independent type 2 antigen. As natural antibodies are atheroprotective, we investigated the involvement of SIRPα signaling in atherosclerosis development. Bone marrow (SIRPα$^{\Delta CYT}$>LDLR$^{-/-}$) chimaeric mice developed reduced atherosclerosis accompanied by increased natural antibody production. Collectively, our data identify SIRPα as a unique B1 cell inhibitory receptor acting to control B1 cell migration, and imply SIRPα as a potential therapeutic target in atherosclerosis.

Keywords: B1 cells, natural antibodies, atherosclerosis, immune checkpoint, inhibitory receptor, SIRPα, CD47, CD11b/CD18-integrin

OPEN ACCESS

Edited by:
Ali A. Zarrin, TRex Bio, United States

Reviewed by:
Marc Seifert, Essen University Hospital, Germany
Lars Nitschke, University of Erlangen Nuremberg, Germany
Andre Veillette, Institute of Clinical Research De Montreal (IRCM), Canada

***Correspondence:**
Timo K. van den Berg
t.k.vandenberg@sanquin.nl

Specialty section:
This article was submitted to Molecular Innate Immunity, a section of the journal Frontiers in Immunology

Received: *09 June 2020*
Accepted: *17 September 2020*
Published: *09 October 2020*

Citation:
Franke K, Pillai SY, Hoogenboezem M, Gijbels MJJ, Matlung HL, Geissler J, Olsman H, Pottgens C, van Gorp PJ, Ozsvar-Kozma M, Saito Y, Matozaki T, Kuijpers TW, Hendriks RW, Kraal G, Binder CJ, de Winther MPJ and van den Berg TK (2020) SIRPα on Mouse B1 Cells Restricts Lymphoid Tissue Migration and Natural Antibody Production. Front. Immunol. 11:570963. doi: 10.3389/fimmu.2020.570963

INTRODUCTION

Signal regulatory protein alpha (SIRPα) is an inhibitory immunoreceptor known to be expressed on myeloid and neuronal cells. SIRPα interacts with the broadly expressed cell surface ligand CD47 present on most cells in the body, including both hematopoietic and non-hematopoietic cells (1). Binding of CD47 to SIRPα generates intracellular inhibitory signals *via* immunoreceptor tyrosine-based inhibitory motifs (ITIM) in the cytoplasmic tail of SIRPα. Upon phosphorylation the SIRPα ITIM act to recruit and activate the tyrosine phosphatases SHP-1 and/or SHP-2, which inhibit tyrosine-phosphorylation-dependent signaling events and the resultant downstream cellular effector functions, including, e.g., phagocytosis (1). As such, the CD47-SIRPα axis forms an important innate immune checkpoint, with CD47 acting as so-called "don't-eat-me" signal, which prevents the engulfment of healthy cells by myeloid cells (2). However, aberrant cells, such as cancer cells, may also exploit this pathway by (over) expressing CD47 and thus escaping immune-mediated destruction. Therapeutic targeting of the CD47-SIRPα checkpoint has been most intensively explored in the context of cancer. In fact, recent first in-human studies of agents interfering with this pathway demonstrate a favorable safety profile and promising therapeutic potential (3).

Based on their functions, anatomical location and phenotypical properties B lymphocytes can be divided into conventional B cells, also known as B2 cells, representing the majority of B cells, and into a smaller population of unconventional B1 cells. In mice, B1 cells are produced in the fetal liver before birth and afterward reside mainly in the pleural and peritoneal cavities where they are maintained by self-renewal (4). In addition, small proportions (<1%), but significant numbers, of these cells can be found in spleen and bone marrow (4–6). B1 cells residing in body cavities have a limited capacity to produce natural antibodies. However, after stimulation, by, e.g., LPS or viral infection, they migrate to the secondary lymphoid tissues, including the spleen, where they differentiate into plasma cells forming the major systemic source of natural antibodies (7, 8). This conditional migration is governed by the CD11b/CD18 integrin (7, 9). B1 cells that have arrived to the spleen gradually lose expression of CD11b/CD18 integrin, with hardly detectable levels after 6 days (9). Peritoneal B1 cells represent about 35%–70% of all $CD19^+$ cells present in the peritoneal cavity and can be further divided into B1a ($CD19^+CD11b^+CD5^+$) and B1b ($CD19^+CD11b^+CD5^-$) cells (4). Unlike B2 cells, B1 cells in the spleen constitutively secrete natural antibodies, which are IgM antibodies commonly targeting, e.g., phospholipid and polysaccharide antigens, such as phosphorylcholine, phosphatidylcholine and lipopolysaccharide (4). Notably, a large part of the natural IgM antibodies is directed against epitopes created through lipid peroxidation (so called oxidation-specific epitopes, OSE), expressed amongst others on apoptotic cells and modified lipoproteins (10). Protective effects of natural antibodies against oxidized lipids have been well established in atherosclerosis (11–14), a chronic inflammatory disease characterized by accumulation of modified (oxidized) lipids in big and medium sized arteries (15). The atheroprotective capacity of IgM antibodies is explained by their binding to oxLDL, thereby preventing oxLDL uptake by macrophages, which as a consequence reduces foam cell formation and lesion development (11, 16). Additionally, natural antibodies are produced to promote clearance of apoptotic cells, which carry the same OSE as oxLDL (14).

It is known that B1 cell responses are restricted by different inhibitory immunoreceptors expressed on these cells, including, e.g., CD5 (17), CD22 (18), Fc gamma receptor IIb (FcγRIIb) (19, 20), and Siglec-G (21, 22). CD5 has been strongly linked to inhibition of BCR signaling, which prevents unwanted self-reactivity of B1 cells (23). B1 cells from mice lacking Siglec-G show a dramatic increase in Ca^{2+} flux upon anti-IgM treatment (22) and increased natural antibody production (24), also suggesting a role of Siglec-G in BCR signaling. All these receptors commonly exhibit their inhibitory functions through intracellular immunoreceptor tyrosine-based inhibitory motifs (ITIM), which upon tyrosine phosphorylation recruit and activate the cytosolic tyrosine phosphatases SHP-1 and/or SHP-2. In the case of FcγRIIb, the inositol phosphatases SHIP-1 and/or SHIP-2 play a prominent role as mediators of inhibitory signaling (25).

Here, we describe another inhibitory receptor, SIRPα, which is expressed on B1 cells in mice. We demonstrate that, in contrast to other currently known inhibitory receptors, SIRPα on B1 cells negatively regulates their migration, B1 cell numbers in the spleen, and systemic natural antibody production, without directly affecting B1 cell activation. Mice lacking the cytoplasmic tail of SIRPα ($SIRP\alpha^{\Delta CYT}$ mice) in their hematopoietic compartment are protected against atherosclerosis with increased natural antibody levels against oxidized lipids. This identifies SIRPα as a novel immunoinhibitory receptor on B1 cells with unique regulatory functions and potential for therapeutic targeting in atherosclerosis.

MATERIALS AND METHODS

Mice

$SIRP\alpha^{-/-}$ mice maintained on a C57BL/6 background have been described and were maintained in the Institute for Experimental Animals at Kobe University Graduate School of Medicine under specific-pathogen free conditions (26). C57BL/6 mice with a targeted deletion of the SIRPα cytoplasmic region have been described previously (27, 28). The mice that were originally generated onto the 129/Sv background were backcrossed onto C57BL/6 mice for at least 13 generations. Wild-type (wt) C57BL/6 mice of the same genetic background were maintained under specific pathogen-free conditions together with the $SIRP\alpha^{\Delta CYT}$ mice in the breeding facility of The Netherlands Cancer Institute, Amsterdam, The Netherlands or the VU Medical Center, Amsterdam, The Netherlands. Unless indicated otherwise littermates from heterozygous breedings were used for both wild type and mutant mice. Bone marrow was isolated and used for transplantation at the animal facility of Maastricht University, Maastricht, The Netherlands. Animals were housed in ventilated cages and treated according to European Commission guidelines. They were euthanized using combination of isofluran and CO_2. All animal experiments were approved by the Animal Welfare Committee of the VU Medical Center Amsterdam, The

Netherlands, Maastricht University, Maastricht, The Netherlands, and The Netherlands Cancer Institute, Amsterdam, The Netherlands. $LDLR^{-/-}$ mice on C57BL/6J background were obtained from Jackson Laboratory (Bar Harbor, ME, USA).

Flow Cytometric Analysis of SIRPα Expression on Mouse B Cells

Mouse B cells were isolated from the peritoneal cavity by peritoneal lavage of 8–12 weeks old $SIRP\alpha^{\Delta CYT}$ mice and age matched wt mice. Mice were sacrificed and immediately after that 5 ml of cold PBS containing 3% of fetal calf serum (FCS) and 3mM EDTA was injected into their peritoneal cavity. After gentle massage, cells were collected and used for analysis of SIRPα expression. Additionally, bone marrow and spleens of the same mice were isolated and blood samples were taken to analyze for expression of SIRPα. Fetal livers were isolated from mice of FVB background at E12. Single cell suspensions of splenocytes were prepared after the spleens were homogenized through 100μm filter (BD Biosciences, Bedford, MA, USA), lysed with lysis buffer and washed twice with cold PBS. For blood analysis whole blood was first spun down at 2,000 rpm at 4°C for 10 min and plasma was collected and stored at −80°C for later analysis of antibodies level. Erythrocytes were lysed using cold lysis buffer containing 155mM NH_4Cl, 10mM $KHCO_3$, and 0.1mM EDTA (ethylene diamine tetra acetic acid), pH 7.4. For flow cytometry analysis first Fc receptors were blocked using α-CD16/CD32 antibody (clone 2.4G2, BD Biosciences, Bedford, MA, USA). The cells were subsequently washed and stained for following surface markers with directly conjugated antibodies against CD19/B220 (PerCP Cy5.5 or eFluor 450), CD11b (Alexa Fluor 488), CD5 (PE), IgM (PE), SIRPα (APC or PerCP 710) (all antibodies purchased from eBioscience, San Diego, CA, USA), and CD43 (APC Cy7, BioLegend, San Diego, CA, USA). Expression of proteins was measured using FACS Canto II HTS (BD Biosciences, Bedford, MA, USA) and analyzed using FlowJo software (FlowJo LLC, Ashland, OR, USA). To reliably detect SIRPα expression and separate it from autofluorescence, fluorescence minus one (FMO) control was applied, when cells were stained for all determinants except SIRPα (9).

Quantitative RT-PCR to Determine SIRPα mRNA Expression

RNA was isolated from FACS sorted mouse B1a and B2 cells based on markers listed above with QIAamp RNA Blood mini kit according to manufacturer's instructions (Qiagen, Venlo, The Netherlands). RNA was eluted with 30 μl H2O, to obtain as high as possible concentration of RNA. Total RNA was reverse transcribed using the III first-strand synthesis system for RT-PCR (Invitrogen, Breda, The Netherlands). In short, 8-μl RNA was primed with 2.5 μM oligo-dT primer which specifically targets mRNA and 0.5 mM dNTP for 5 min at 65°C. Reverse transcription was performed with 10 U/μl Superscript III in the presence of 5 mM $MgCl_2$, 20 mM Tris-HCL, and 50 mM KCl, pH 8.4 (RT buffer), 2 U/μl RNAseOUT™, lacking DTT for reasons described before (29) for 50 min at 50°C. After that, Superscript III was inactivated by incubation for 5 min at 85°C, followed by chilling on ice. Immediately thereafter, 2 U RNase H was added and incubated at 37°C for 20 min. Subsequently cDNA was stored at −20°C until further use. Amplification by PCR was performed on a LightCycler instrument (Roche, Almere, The Netherlands), with software version 3.5. The reaction was performed with Lightcycler FastStart DNA Master^{PLUS} SYBR Green I (Roche, Almere, The Netherlands). The annealing temperature used for all primers was 60°C. The reaction mix consisted of 4 μl of cDNA, 1 μM of each primer combination and 4 μl of Lightcycler FastStart DNA Master^{PLUS} SYBR Green I (Roche) in a total volume of 20 μl. After an incubation step for 10 min at 95°C, the template was amplified for 45 cycles at 95°C, annealing of the primers was performed at 60°C for 30 s, followed by extension at 72°C for 15 s. At the end of the 45 cycles, a melting curve was generated to determine the unique features of the DNA amplified. cDNA of control wt animals was used as a standard curve with a serial 10-fold dilution. Musculus Ubiquitin C was used as a reference gene. The product was sequenced by Big-dye Terminator Sequencing and ABI Prism software (Applied Biosystems, Foster City, USA). The sequence obtained was verified with BLAST (http://www.ncbi.nlm.nih.gov/BLAST/) to determine specificity. Primer sequences are available upon request.

Binding of Phosphatidylcholine by Primary Mouse B Cells

B cells were isolated and labeled with antibodies against surface CD5 and B220 as described above along with fluorescein-labeled phosphatidylcholine (PtC) liposomes (DOPC/CHOL 55:45, Formumax Scientific Inc.). The cells were incubated on ice for 20 min followed by two washing steps, then cells were analyzed using an LSRII flow cytometer (BD Biosciences, Bedford, MA, USA) for binding of phosphatidylcholine and data were processed with FlowJo software (FlowJo LLC, Ashland, OR, USA).

Intracellular Calcium Mobilization Measurement in Primary Mouse B1a Cells

B cells were isolated from the peritoneal cavity of 8–12 weeks old $SIRP\alpha^{\Delta CYT}$ mice and aged matched wt mice using peritoneal lavage as described above. First, Fc receptors were blocked using α-CD16/CD32 antibody (clone 2.4G2, BD Biosciences, Bedford, MA, USA). The cells were then stained with directly labeled antibody against CD5 (APC) and B220 (APC Cy7, both BD Biosciences, Bedford, MA, USA) allowing identification of B1a cells. Calcium flux was determined as described before by flow cytometric determination (30). Briefly, intracellular fluxes of Ca^{2+} were measured using Fluo-3-AM and Fura Red-AM fluorogenic probes (Life Technologies, Carlsbad, CA, USA). The cells were incubated with 5μ Fluo3-AM and 5μM Fura Red-AM in loading buffer (Hank's balanced salt solution medium supplemented with 10 mM HEPES and 5% fetal calf serum) at 30°C for 30 min in the dark. Cells were then washed and resuspended in buffer (Hank's balanced salt solution medium with 10 mM HEPES, 5% fetal calf serum and 1 mM CaCl2) at room temperature. Cells were warmed to 37 °C for 5 min before acquisition of events. BCR-mediated $Ca2^{+}$ mobilization was measured for 60s after the cells were

stimulated either with 10 μg/ml F(ab′)2 of polyclonal goat anti-mouse IgM (Jackson ImmunoResearch, West Grove, PA, USA) or 0.5mM phosphatidylcholine (PtC) (F60103F-F, FormuMax USA). At the end of each Ca^{2+} measurement, cells were treated with ionomycine (Life Technologies, Eugene, OR, USA) as a positive control for calcium signaling. Data were acquired on an LSRII flow cytometer (BD Biosciences, Bedford, MA, USA) and data analysis was performed with the use of FlowJo software (FlowJo LLC, Ashland, OR, USA).

Immunization of Mice With DNP-Ficoll

For B1-specific immunization intraperitoneal injection of TI-2 antigen di-nitro phenyl (DNP)-Ficoll was used as described originally in (31). Briefly, mice were injected with 50 μg of DNP-Ficoll in 200-μl PBS solution or with 200 μl of PBS only as control. After 7 days animals were sacrificed and their blood was collected, plasma was harvested and stored at −80°C before analysis of IgM and IgG3 antibodies by ELISA.

Measurement of IgM and IgG With ELISA

Plasma levels of IgM antibodies against several OSE were determined by chemiluminescent ELISA (32). Dilutions of 1:100 [anti-phosphocholine (PC)-BSA IgM and all IgG antibodies], 1:500 [E06/T15id+ IgM, anti-malondialdehyde (MDA-)LDL IgM, anti-Cu-OxLDL IgM], and 1:20.000 (total IgM) were used. Supernatants of peritoneal B1 cell cultures or plasma of mice were serially diluted to determine IgM production after 48 h of stimulation or IgM/IgG3 against DNP-Ficoll after 7-days immunization as previously described (33). Briefly, supernatants were measured by sandwich ELISA, using unlabeled for coating and peroxidase-labeled anti-mouse IgM/IgG antibody (total, or DNP-Ficoll specific, Southern Biotechnology, Birmingham, AL, USA) for detection, and azino-bis-ethylbenz-thiazoline sulfonic acid was used as the substrate. Antibody concentrations were calculated by using purified mouse IgM protein (IgM DNP-Ficoll and IgG3 DNP-Ficoll PMP52, Serotec, UK) as a standard.

Proliferation of B1 Cells

B cells were isolated from the peritoneal cavity of either wt or SIRPα$^{\Delta CYT}$ mice and either left unstimulated or incubated with various stimuli for 48h after labeling with CFSE dye. Dilution of the dye after cell division was determined by flow cytometry on B1a cells (gated for CD19+, CD5+, CD11b+ lymphocytes) and percentage of proliferating cells was calculated.

Stimulation of Peritoneal B1 Cell

Peritoneal B1a cells were obtained through negative magnetic-activated cell separation with a cocktail of antibodies depleting other than B1a cells achieving more than 90% purity in isolation (Miltenyi Biotec B.V., Utrecht, The Netherlands). B1a cells were subsequently counted and plated in IMDM medium (Invitrogen, Eugene, OR, USA) supplemented with 10% fetal calf-serum (FCS; Bodinco, Alkmaar, The Netherlands, 100 U/ml of penicillin, 100 mg/ml of streptomycin, and 2 mM L-glutamine (all Gibco Invitrogen, Breda, The Netherlands), and beta-mercapthoethanol (3.57×10^{-4}M; Millipore, Amsterdam, The Netherlands). Cells were plated in 96-well plate in density of 1×10^6/ml in 200 μl of medium and cultured at 37°C and 5% CO2 for 48h in presence of 5 μg of lipopolysaccharide (LPS, isolated from E. coli strain 055:B5, Sigma, St. Louis, MO, USA; LBP from R&D Systems, Abingdon, UK), isotype control (rat IgG2b, eBioscience, San Diego, CA, USA), anti-CD11b antibody (functional grade, eBioscience, San Diego, CA, USA), or anti-CD11a (functional grade, eBioscience, San Diego, CA, USA) in final concentration 10 μg/ml. After that supernatant was collected and stored at −80°C before measurement of IgM antibody by ELISA. Cells were harvested and processed for analysis by flow cytometry and imaging cytometry.

Image Stream Analysis of Aggregate Formation

LPS-stimulated B1a cells were stained with following antibodies: CD19 (PerCP Cy5.5), CD11b (Alexa Fluor 488), CD5 (PE), SIRPα (APC), (all antibodies purchased from eBioscience, San Diego, CA, USA) and analyzed imaging cytometry to detect formation of aggregates (Image Stream, (Image Stream, Amnis, EMD, Millipore, Seattle, WA, USA) with gating strategy as follows: all events were divided based on their size into single cells (1 cell); doublets (2 cells); doublets and small aggregates (2–3 cells); big aggregates (3–4 cells); and large aggregates (>4 cells). Analysis of data was performed using analysis software IDEAS (Amnis Corporation, Seattle, WA, USA) and depicted as percentage of all gated events.

Adoptive Transfer of Peritoneal B1 Cells

Either wt or SIRPα$^{\Delta CYT}$ animals were used as donors of peritoneal B1 cells for adoptive transfer. Cells were harvested by peritoneal lavage as described above. The cells were left in IMDM medium supplemented with 10% FCS (Bodinco, Alkmaar, The Netherlands, 100 U/ml of penicillin, 100 mg/ml of streptomycin, and 2 mM L-glutamine (all Gibco Invitrogen, Breda, The Netherlands) to rest for 30 min. After that the easy to detach and floating cells (excluding adherent peritoneal macrophages) were first incubated with Fc receptor blocking antibody (anti-CD16/CD32) and after washing incubated with either isotype control (rat IgG2b, eBioscience, San Diego, CA, USA) or anti-CD11b antibody (functional grade, eBioscience, San Diego, CA, USA) in concentration of 10 μg/ml for 30 min. Antibodies were washed away and wt and SIRPα$^{\Delta CYT}$ cells were labeled with membrane dye DiD and DiO, respectively (or vice versa, to exclude effect of the dye on cell properties). Cells were washed multiple times and mixed in 50:50 ratio based on a cell count. The actual ratio was additionally determined by analyzing a small sample of pooled cells on flow cytometer allowing later normalization of the cell input. Cells were then injected into the peritoneal cavity of either wt or SIRPα$^{\Delta CYT}$ recipient mice, left resting for 1 h, and followed by either 200-μl injection of PBS (control) or 10 μg of LPS in 200-μl PBS intraperitoneally to induce migration of B1 cells from the peritoneal cavity (7, 33). Peritoneal lavage of recipient mice was performed 3h after PBS/LPS injection. Lavage composition was analyzed by flow cytometry in CD19+ single cell population and percentage of cells with distinct membrane label was calculated. Percentage of cells was normalized for input of pooled cells as indicated above.

Bone Marrow Transplantation

One week before transplantation, female LDLR$^{-/-}$ mice were housed in filter top cages with neomycin (100 mg/L; Gibco, Breda, The Netherlands) and polymyxin B sulphate (66104 U/L; Gibco Breda, The Netherlands) in their acidified drinking water. The animals received 6 Gy of total body irradiation twice on consecutive days. Bone marrow isolated from SIRPα$^{\Delta CYT}$ and wt mice was injected intravenously to rescue the hematopoietic system of the irradiated mice as described previously (34). Briefly, one week before transplantation, female LDLR−/− mice were housed in filter-top cages and provided with acidified water containing neomycin (100mg/l; GIBCO, Breda, The Netherlands) and polymyxin B sulfate (6 × 104 U/l; GIBCO). The animals received 2 × 6 Gy total body irradiation on two consecutive days. On the second day, bone marrow was isolated from 6 SIRPα$^{\Delta CYT}$ and 6 wt littermates, and 10^7 cells/mouse were injected intravenously to rescue the hematopoietic system of the irradiated mice. Four weeks after the transplantation, mice were put on a high fat diet (0.15% cholesterol, 16% fat, Arie Blok, The Netherlands) for 10 weeks and level of chimerism was tested (reached 98.76% ± 0.73).

Mouse Blood Parameters

Blood was withdrawn at the indicated times during high fat diet period and plasma lipid levels were enzymatically measured using ELISA (Sigma Aldrich, Zwijndrecht, The Netherlands).

Atherosclerotic Lession Analysis

Transplanted animals were sacrificed and isolated hearts were cut perpendicularly to heart axis just below the atrial tips, as described before (35, 36). Briefly, tissue was frozen in tissue-tec (Shandon, Veldhoven, The Netherlands) with the base facing downward, and sectioning was performed toward the aortic valve area. Sections of 7 µm were collected, starting from where the atrioventricular valves were visible. Aortic lesion areas were quantified using serial cross-sections obtained every 42 µm, beginning at the start of the atrioventricular valves and spanning 250 µm. Serial cross sections were stained with toluidin blue and lesion areas were quantified using Adobe Photoshop software. Severity of lesions was scored as early, moderate and advanced, using criteria as described before (35, 36). In detail, early lesions were fatty streaks containing only foam cells; moderate (intermediate) lesions were characterized by the additional presence of a collagenous cap, and advanced lesions showed involvement of the media mostly accompanied by increased collagen content and necrosis of the plaque. Foam cell size within plaques was determined by dividing the size of an allocated foamy macrophage area by the number of macrophages.

Immunohistochemical Staining

Atherosclerotic lesions from aortic roots were stained with various antibodies to identify neutrophils (NIMP directed against Ly6G, a gift from P. Heeringa), T cells (KT3, directed against CD3) and newly recruited macrophages (ER-MP58, a gift from P. Leenen) followed by detection with biotin labeled rabbit anti-rat antibody and staining with ABC kit (Vector Labs, Burlingame, CA).

Statistical Analysis

Statistical analysis was performed using GraphPad Prism version 8.02 (GraphPad Software, San Diego, CA, USA). Data were evaluated by two-tailed student t-test if two columns were compared. If more columns were compared, one-way ANOVA followed by multiple comparison correction was applied.

RESULTS

SIRPα Is Expressed on B1 Cells

The inhibitory immunoreceptor SIRPα is considered to be present selectively on neuronal cells as well as on myeloid cells in the hematopoietic compartment (1, 37). It is thought to be lacking from lymphoid cells, at least under steady state conditions (38). However, a more detailed evaluation of B cell subsets revealed SIRPα expression on all B1 cells in the peritoneal cavity (PC) and on a subpopulation of B cells in the spleen (SP) of mice (**Figures 1A–C** and **Supplementary Figures 1A, B**). In particular, by using specific markers identifying B1a cells (i.e., CD19$^+$CD5$^+$CD11b$^+$) and B1b cells (i.e., CD19$^+$CD5$^-$CD11b$^+$) we could clearly demonstrate surface SIRPα expression on both of these PC B1 lymphocyte populations. PC B2 cells show much lower if any SIRPα expression. In the spleen we could detect expression of SIRPα only on a subset of B220$^+$/CD19$^+$CD43$^+$CD23$^-$ B1 cells. Relatively low levels of SIRPα staining were found on marginal zone B cells (B220$^+$/CD19$^+$CD43$^-$CD23$^-$) and minimal detectable expression was found on B220$^+$/CD19$^+$CD23$^+$CD43$^-$ follicular B cells. Consistent with other studies (38), we could not observe any SIRPα expression on circulating B cells in mice and no expression on B2 cells from the bone marrow (**Supplementary Figure 1C**). However, we could detect SIRPα on fetal liver B220$^+$/CD19$^+$CD43$^+$ B cells and B1 cells in the bone marrow (**Supplementary Figure 1C**). As a control staining was performed on B1 cells from the peritoneal cavity of mice deficient for SIRPα altogether (SIRPα$^{-/-}$ mice, **Supplementary Figure 2**) indicating that staining observed on B1 cells in wild type mice can indeed be solely attributed to SIRPα expression on those cells. Staining on B1 cells from SIRPα$^{\Delta CYT}$ mice showed a slightly reduced overall surface expression as has been reported for other cells expressing SIRPα (data not shown). Compared with peritoneal macrophages, we found substantially lower levels of both CD11b and SIRPα on B1 cells, clearly discriminating B1 cells from myeloid cells (**Figure 1D**). Expression of SIRPα mRNA was confirmed by qRT-PCR on FACS sorted peritoneal B1a cells (CD19$^+$CD5$^+$CD11b$^+$) (**Figure 1E**).

SIRPα Limits Natural IgM Antibody Levels *In Vivo*

Because SIRPα, like Siglec-G, is also a typical inhibitory immunoreceptor with cytoplasmic ITIM motifs signaling through SHP-1 and/or SHP-2, we tested whether the lack of SIRPα signaling would affect natural antibody generation as well. As can be seen in **Figure 2A** there was a prominent (~2-fold) enhancement in the plasma levels of total and OSE-reactive natural IgM antibodies in mice lacking the cytoplasmic tail of SIRPα (SIRPα$^{\Delta CYT}$ mice). This occurred for all OSE tested, including the so-called T15 epitope that

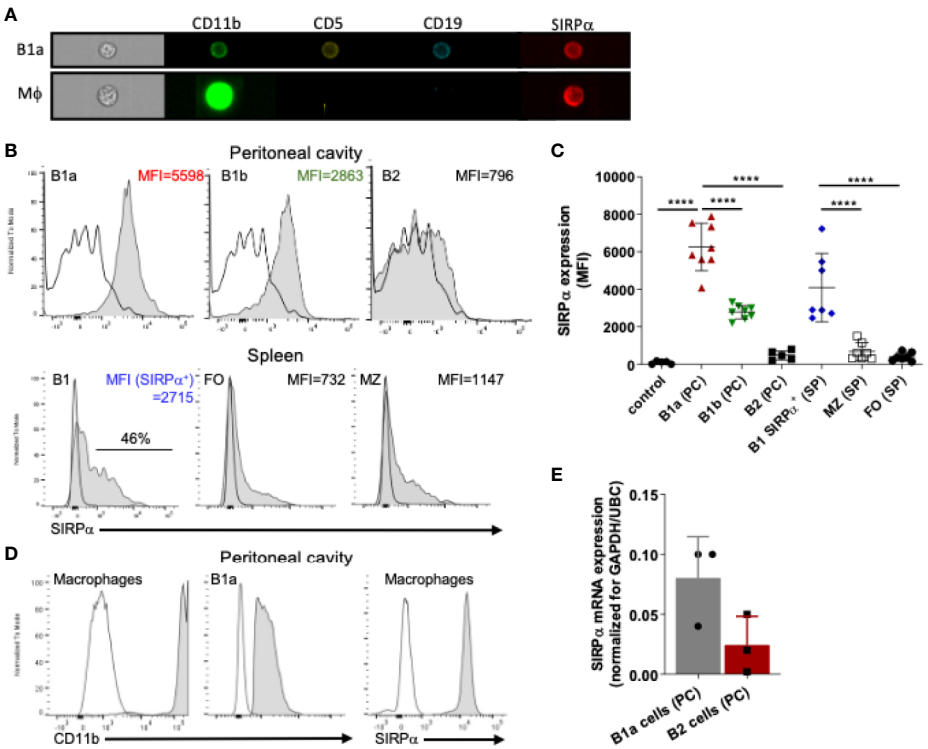

FIGURE 1 | SIRPα is expressed by B1 cells. **(A)** Imaging flow cytometry visualizing expression of SIRPα on CD19+CD5+CD11b+ B1a cells and CD11b+CD19– macrophages. Representative histograms **(B)** and synopsis **(C)** of SIRPα surface expression on defined B cell subpopulations as determined by flow cytometry (MFI, Mean fluorescence intensity). Note that the most prominent expression occurs on peritoneal cavity (PC) B1a and B1b cells, and on a subset of the splenic (SP) B1, with little or no expression on marginal zone (MZ) and follicular (FO) B cells. **(D)** Macrophages cells from the peritoneal cavity show relatively high levels of expression of both CD11b and SIRPα. **(E)** SIRPα mRNA expression on FACS sorted peritoneal cavity B1a and B2 cells. Data are in **(C, E)** are presented as mean ± SEM and represent measurements of 5–8 and 3 individual mice, respectively. Statistical analysis was performed by one-way ANOVA with Dunnett's multiple comparison corrrection, ****$p < 0.0001$.

defines PC-reactive EO6 type anti-OxLDL IgM antibodies with anti-atherogenic potential *in vivo* (11, 39), as well as phosphocholine (PC) and those against *ex vivo* oxidized LDL (i.e., MDA-LDL and Cu-OxLDL). Consistent with a specific B1 cell phenotype and a selective regulation of natural IgM levels the corresponding IgG levels were not altered (**Figure 2B**). When SIRPα$^{\Delta CYT}$ mice were immunized with a typical T-cell independent type 2 (TI-2) antigen, DNP-Ficoll, we observed robust and enhanced DNP-specific IgM and IgG3 immune responses (**Figure 2C**). Of interest, no enhanced antibody responses have been observed in SIRPα$^{\Delta CYT}$ mice upon immunization with the thymus-dependent antigen TNP-KLH (Y. Kaneko (Gunma University, Japan), personal communication). These results indicate that SIRPα signaling regulates natural antibody production as well as the response of B1 cells to antigenic stimulation.

SIRPα Increases Splenic B1 Cell Numbers Without Affecting B Cell Receptor Function

Next, we investigated whether the changes in B1-cell associated antibodies in SIRPα$^{\Delta CYT}$ mice could be related to changes in B1 cell numbers in the peritoneal cavity or the spleen of these mice (**Figure 2D**, **Supplementary Figures 3A–G**). We did not detect significant differences in proportions or the absolute numbers of peritoneal cavity B1a and B1b cells. In contrast, proportions and absolute numbers of B1 cells in the spleen of SIRPα$^{\Delta CYT}$ mice were significantly (~2-fold) increased compared to wt animals. There were no significant differences in total cell numbers or proportions of other splenic B cell subsets, indicating that the effects were specific for B1 cells. We next asked how SIRPα might contribute to the increase in splenic B cell numbers and natural antibody levels. One possibility was that SIRPα was controlling the activation and expansion of B1 cells. First, we tested whether antigen recognition by B1 cells might be altered, as a consequence of potential differences in BCR expression, but we observed no difference in, e.g., the binding of a typical B1a cell antigen phosphatidylcholine (PtC) (40) to B1a cells (**Figure 3A** and **Supplementary Figure 3H**). Next, we explored potential differences in B1a cell activation capacity. This included measuring Ca^{2+} flux upon cross-linking of BCR (**Figure 3B**), and monitoring sorted PC B1a cell IgM secretion upon stimulation with LPS *in vitro* (**Figure 3C**), a potent and typical B1 cell activation stimulus (7). Both read-outs showed comparable activation capacity of wt and SIRPα$^{\Delta CYT}$ B1a cells.

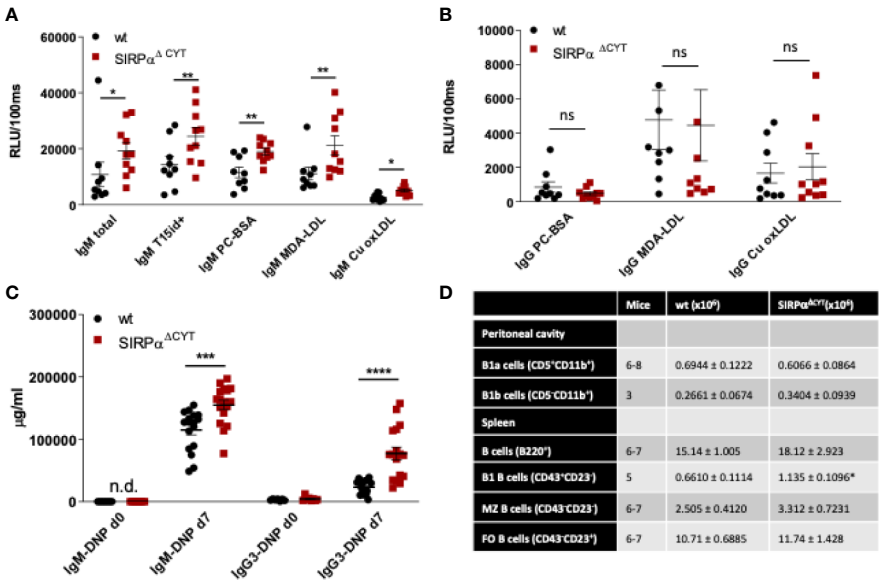

FIGURE 2 | Loss of SIRPα signaling promotes B1 cell accumulation in the spleen and natural IgM antibody formation *in vivo*. Defective SIRPα signaling in mice lacking the SIRPα cytoplasmic tail (SIRPα$^{\Delta CYT}$) results in increased plasma levels of natural IgM **(A)** but not IgG **(B)** antibodies directed against the indicated oxidation-specific epitopes under steady-state conditions; wt, wild-type mice; RLU/100 ms, Relative Luminescence per 100 ms. **(C)** Immunization with the haptenated TI-2 antigen DNP-Ficoll triggers increased production of both IgM and IgG3 antibodies against DNP in SIRPα$^{\Delta CYT}$ mice. Data are presented as mean ± SEM and are representative of 9-10 **(A)**, 8 **(B)**, 17 **(C)** individual mice. **(D)** B cell numbers in peritoneal cavity and spleen of wt and SIRPα$^{\Delta CYT}$ mice. Absolute number of different B cell populations was determined in the peritoneal cavity and the spleen of young adult mice (8–12 weeks) under steady state conditions. For further details see **Supplementary Figures 2A–G**. Statistical analysis was performed by unpaired Student t-test, corrected for multiple comparisons with Holm-Sedak method where applicable, *p < 0.05; **p < 0.01, ***p < 0.001, ****p < 0.0001.; ns, non-significant; n.d., not detectable.

Finally, there were apparently no differences in B1a cell proliferation (**Supplementary Figure 4**). Taken together, these findings support the idea that SIRPα signaling controls splenic B1 cell accumulation and, likewise as a consequence, also the levels of naturally occurring antibodies, but this was apparently not linked to a generalized regulation of BCR- or TLR-mediated B1 cell activation.

SIRPα Regulates CD11b/CD18 Integrin Function and B1 Cell Migratory Capacity

Notably, when analyzing LPS-stimulated B1 cells by flow cytometry, we observed the presence of cell clusters in the cultures that appeared larger for SIRPα$^{\Delta CYT}$ B1a cells relative to their wt counterparts (**Supplementary Figure 5A**). This prompted us to visualize and quantify this aggregate formation of B1a cells by imaging flow cytometry, which indeed consistently demonstrated a substantially increased proportion of large aggregates (i.e., consisting of more than 4 cells) in SIRPα$^{\Delta CYT}$ peritoneal B1a cells as compared to wt B1a cells after LPS stimulation (**Figure 4A** and **Supplementary Figures 5B, C**). In contrary, we could not observe comparable aggregates when sorted splenic B1 cells were cultured in a similar manner (**Figure 4B**). Interestingly, such doublets and large aggregates specific for CD11b^{+} B1 cells have been previously reported by Ghosn et al. and their formation seems to be dependent on CD11b (9). Furthermore, SIRPα inhibitory signaling has been previously linked to integrin function in other cells (28). We therefore hypothesized that SIRPα may serve as a negative regulator of CD11b/CD18 integrin function in B1 cells. To test this, we stimulated sorted peritoneal B1a cells with LPS in the presence of a blocking anti-CD11b antibody. Clearly, the increased formation of large aggregates triggered by LPS in mice lacking SIRPα signaling could be partially prevented by blocking CD11b, but not by blocking CD11a (**Figure 4C**). Next, we asked whether B1 cell aggregate formation through CD11b/CD18 integrin could be a prerequisite for production of natural antibodies. We tested supernatants of B1a cells that were activated by LPS in the presence of blocking CD11b antibody or blocking CD11a antibody. It appeared that SIRPα$^{\Delta CYT}$ B1a cells have comparable antibody production as wt B1 cells *in vitro*, independently of CD11b or CD11a function (**Figure 4D**). Thus, whereas CD11b-mediated formation of large aggregates did not regulate natural antibody production *in vitro*, such B1 cell aggregate formation, which was promoted upon disruption of SIRPα signaling, nevertheless appeared a read-out for CD11b/CD18 activation. This suggested that SIRPα signaling was negatively regulating B1 cell integrin function. Of interest, Waffarn et al. have shown, that CD11b/CD18, unlike CD11a/CD18, is indispensable for migration of stimulated B1 cells from cavities to secondary lymphoid tissues where they mature into natural antibody producing plasma cells (8). This led us to propose that SIRPα could actually regulate CD11b/CD18 function during migration of B1 cells to the secondary lymphoid tissues, which would provide an explanation for the

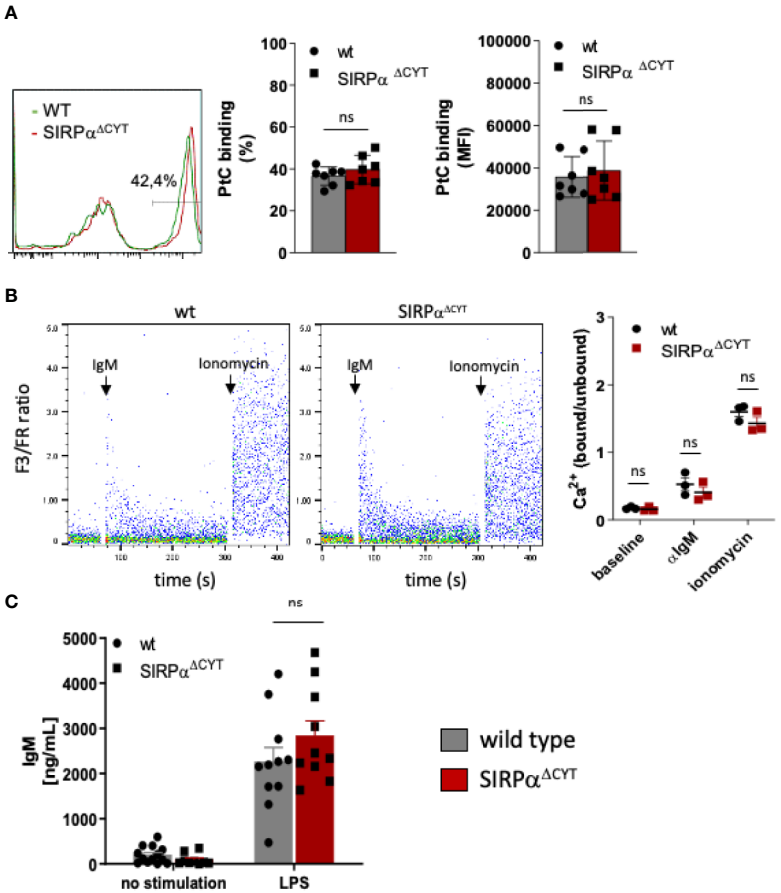

FIGURE 3 | Loss of SIRPα signaling does not have a generalized effect on B1 cell activation. **(A)** Comparable frequency (FACS plot of representative example, left panel; % positivity, middle panel) and magnitude (MFI, right panel) of phosphatidylcholine (PtC; a typical B1a antigen) antigen binding by wt and SIRPα$^{\Delta CYT}$ peritoneal cavity B1a cells (n = 7 mice/group). **(B)** Similar levels of B1a cell surface IgM signaling, as determined by intracellular Ca^{2+} mobilization, in wt and SIRPα$^{\Delta CYT}$ peritoneal cavity B1 cells triggered by anti-IgM antibodies; responses with ionomycin are shown as a positive control; left panels: representative examples of Ca^{2+}-responses in wt and SIRPα$^{\Delta CYT}$ **(B)**; right panels: average values of B1a cells from n = 3 mice/group. **(C)** Comparable levels of LPS-stimulated IgM production in B1a cells isolated from SIRPα$^{\Delta CYT}$ and wt mice (n = 10–11 mice/group); ns, non-significant.

increased numbers of B1 cells in the spleens of SIRPα$^{\Delta CYT}$ mice. To directly test the effect of SIRPα signaling on the capacity of B1 cells to migrate from the peritoneal cavity we performed adoptive transfer experiments. To confirm integrin-dependence, B1 cells of both wt and SIRPα$^{\Delta CYT}$ donor mice were in parallel pre-incubated with blocking CD11b antibody, excessive amount of the antibody was removed, and then, the cells were labeled with unique membrane dyes, mixed in 1:1 ratio, and injected to either wt or SIRPα$^{\Delta CYT}$ recipients (**Figure 4E**). This set-up allowed us to selectively monitor, in individual animals, the effect of SIRPα and CD11b/CD18 on the migration of B1 cells from the peritoneal cavity to the spleen. As expected, B1 cells that lack inhibitory cytoplasmic tail of SIRPα showed increased efflux from the peritoneal cavity (**Figure 4F**). The enhanced exit of SIRPα$^{\Delta CYT}$ B1 cells was fully dependent on CD11b/CD18, as it could be completely inhibited by antibody blocking. Taken together, our data strongly suggest that CD11b/CD18 function in B1 cells is under negative control of SIRPα and that in absence of SIRPα signaling B1 cells have a higher propensity to leave the peritoneal cavity, thereby contributing to an accumulation of B1 cells in the spleen and an enhanced systemic production of natural antibodies.

Lack of SIRPα Signaling Protects Mice From Atherosclerosis

In order to further establish the potential pathological/clinical relevance of the regulation of natural IgM antibody production by SIRPα *in vivo*, we decided to explore the role of SIRPα in atherosclerosis. Natural IgM antibodies produced by B1a cells have a well-established protective role in various diseases, and particularly in atherosclerosis, a feature which is apparently due to their capacity to neutralize oxLDL uptake and enhance apoptotic cell clearance by macrophages (11–13). To directly address the role of SIRPα in atherosclerosis in mice, we transplanted wt and SIRPα$^{\Delta CYT}$ bone marrow into atherosclerosis-prone LDLR$^{-/-}$ recipient mice. This well-established atherosclerosis model includes the replacement of peritoneal B cell populations (including B1 cells) by the donor cells (11, 12, 21, 22, 41–43).

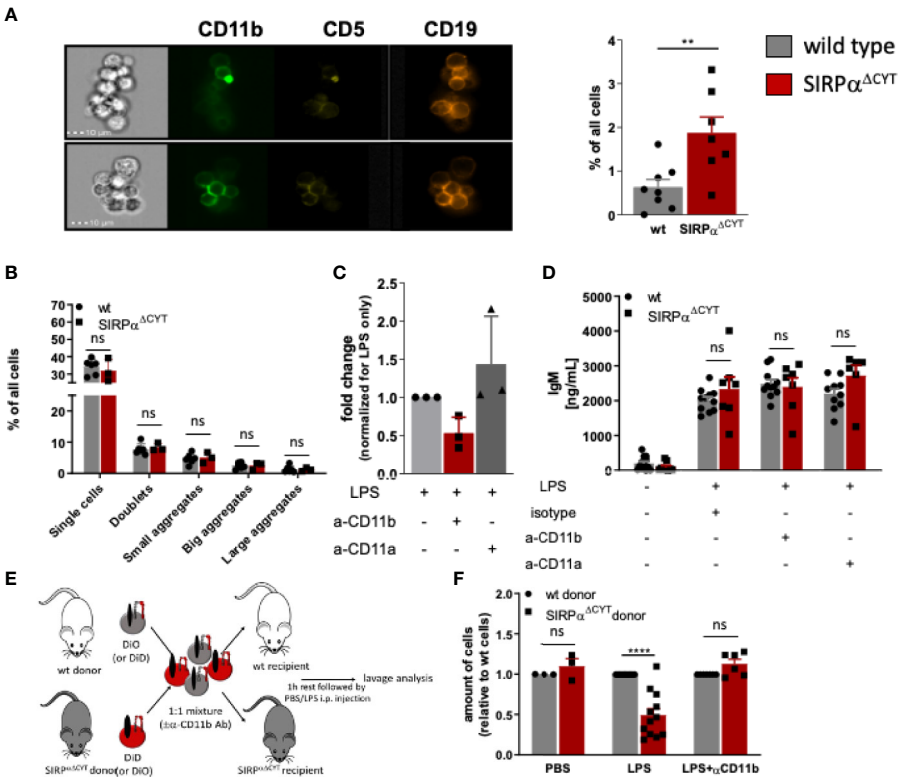

FIGURE 4 | Loss of SIRPα signaling promotes LPS-induced CD11b/CD18 integrin-dependent B1 cell efflux from the peritoneal cavity. **(A, B)** Lack of SIRPα signaling promotes the formation of large aggregates in isolated SIRPα$^{\Delta CYT}$ peritoneal cavity **(A)** but not splenic **(B)** B1a cells (n = 6–8 mice/group). **(C)** Enhanced frequency of B1 cell large aggregates in SIRPα$^{\Delta CYT}$ peritoneal cavity B1a cells relative to wt cells is CD11b/CD18-integrin-dependent as it is reduced by blocking anti-CD11b, but not anti-CD11a antibodies. **(D)** Blockade of CD11b/CD18 or CD11a/CD18 integrins has no effect on IgM antibody production by peritoneal cavity B1 cells upon LPS stimulation. **(E)** Experimental design of egress of adoptively transferred mixed SIRPα$^{\Delta CYT}$/wt B1 cells from the peritoneal cavity. **(F)** Evaluation of adoptively transferred mixed SIRPα$^{\Delta CYT}$/wt B1 cells shows increased efflux of SIRPα$^{\Delta CYT}$ B1 cells relative to wt from the peritoneal cavity upon LPS stimulation and this enhanced egress is CD11b/CD18 dependent (n = 3–12 mice/group). Similar data were obtained for SIRPα$^{\Delta CYT}$ recipients (not shown). Data are presented as mean ± SEM. Statistical analysis was performed by unpaired Student t-test, corrected for multiple comparisons with Holm-Sedak method where applicable, **p < 0.01, ****p < 0.0001; ns, non-significant.

Mice transplanted with wt or SIRPα$^{\Delta CYT}$ cells, and subjected to a high-fat diet, showed neither differences in weight, plasma cholesterol and triglyceride levels nor prominent changes in blood cell composition (**Supplementary Figures 6A–E**). However, when the atherosclerotic lesions of these mice were evaluated, it became apparent that mice transplanted with SIRPα$^{\Delta CYT}$ cells developed much smaller lesions (**Figure 5A**) with a substantially less severe phenotype (**Figure 5B**) compared to wt chimeras. Additionally, when the plasma of atherosclerotic mice was analyzed for the presence of antibodies against oxLDL, in mice transplanted with SIRPα$^{\Delta CYT}$ cells elevated levels of T15/E06 IgM (**Figure 5C**), an oxLDL neutralizing antibody, being particularly critical in the protection against atherosclerosis, were found. (11, 39, 44). Similar to the steady state situation, levels of IgG targeting OSE remained unaltered (**Supplementary Figure 6F**). A more detailed evaluation of the cellular composition of the lesions showed an increase in the number of newly recruited ERMP58+ myeloid cells (**Figure 5D**), which was associated with a significantly decreased mRNA for CD68^{+} macrophages (**Figure 5E**) and size of the area occupied by foam cells in mice transplanted with SIRPα$^{\Delta CYT}$ cells (**Figure 5F**), consistent with the proposed mechanism of IgM-mediated inhibition of foam cell formation (11, 16, 45). There were no significant differences observed in numbers of other immune cells known to be involved in pathogenesis of atherosclerosis, such as T-lymphocytes and neutrophils (**Supplementary Figures 6G, H**).

DISCUSSION

In this study, we provide evidence for the expression and functional relevance of the inhibitory receptor SIRPα on B1 cells in mice. Our results demonstrate that SIRPα is an inhibitory receptor on B1 cells that controls the numbers of splenic B1 cells, thereby most likely affecting systemic natural antibody levels. The increase in splenic B1 cell numbers in the absence of SIRPα signaling occurs most probably because of the absence of an inhibitory effect of on CD11b/CD18 integrin activation, which promotes the migration of these B1 cells from the peritoneal cavity to the spleen. We also show that a lack of

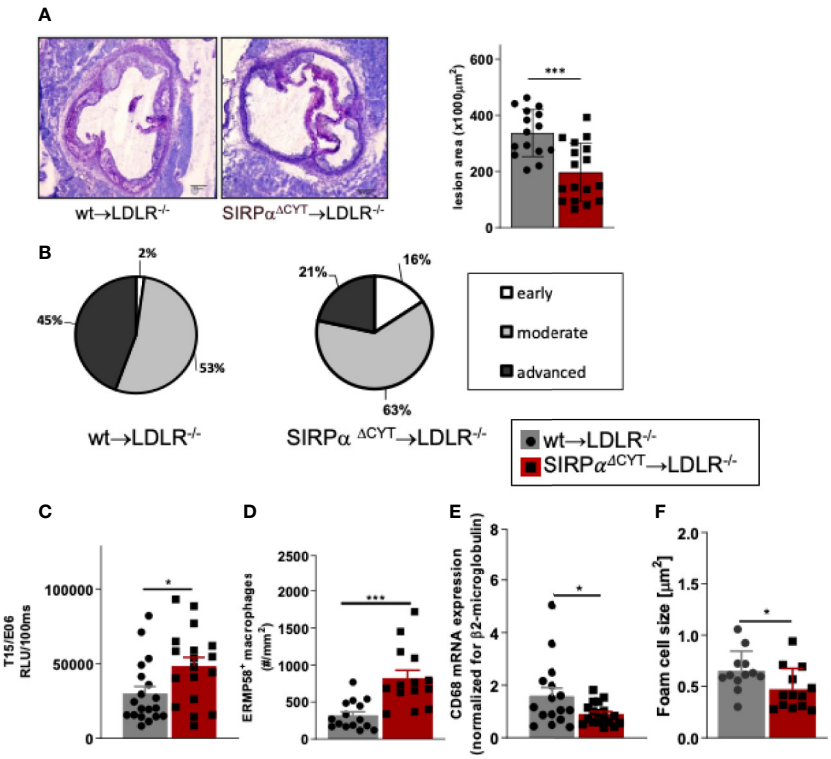

FIGURE 5 | Loss of SIRPα signaling protects mice from atherosclerosis. **(A, B)** Bone marrow chimeras carrying dysfunctional SIRPα in their hematopoietic compartment are protected from atherosclerosis, showing **(A)** smaller and **(B)** less severe aortic lesions. **(C)** Atheroprotection in SIRPα$^{\Delta CYT}$>LDLR$^{-/-}$ chimeras is associated with increased levels of oxLDL-targeting natural antibody T15/E06 in plasma. **(D–F)** Atherosclerotic lesions of SIRPα$^{\Delta CYT}$>LDLR$^{-/-}$ chimeras contain more small macrophages **(D)**, less CD68+ macrophages **(E)**, and a smaller foam cell area **(F)** as compared to wt chimeras. Data are presented as mean ± SEM and are representative of 15-17 **(A, B)**, 18-19 **(C)**, and 12-16 **(D–F)** individual mice. Statistical analysis was performed by unpaired Student t-test used per variable, corrected for multiple comparisons with Holm-Sedak method, *p < 0.05; ***p < 0.001 or Chi-square test **(B)**, *p < 0.05.

inhibitory SIRPα signaling in atherosclerotic mice leads to selectively elevated plasma levels of oxLDL-neutralizing natural antibodies and propose that this directly contributes to the atheroprotective effect of SIRPα mutation. The latter is in agreement with the well-established regulatory role of such antibodies in atherosclerosis (46).

SIRPα is one of the most abundant inhibitory receptors on myeloid cells including neutrophils, monocytes, the majority of tissue macrophages and CD4$^+$ dendritic cells, affecting a variety of cell functions in a primarily negative fashion (1, 2). SIRPα has, as yet, not been reported to be expressed by any B cells. Recently, SIRPα was also reported to be selectively expressed on a small subset of T lymphocytes, i.e., exhausted CD8+ memory T cells emerging after chronic viral infection (47). For a long time, the general assumption has been that SIRPα is, at least among hematopoietic cells, restricted to the myeloid lineage (37, 48). Most of the studies based the absence of SIRPα from lymphocytes on staining of blood cells in rodents (37, 38) while other, less accessible or more obscure subpopulations of lymphoid origin remained unexplored. We found expression of SIRPα exclusively on B1 cells in the peritoneal cavity and on a minor subset of B cells in the spleen. We also observed that the population of steady-state splenic B1 cells is roughly doubled in mice lacking SIRPα signaling. This increase in splenic B1 cells may well explain the (also ~2-fold) higher IgM plasma levels found in SIRPα$^{\Delta CYT}$ mice. Antigens with repetitive patterns, such as lipids and glycolipids, including self-antigens that are generated, e.g., upon oxidation or apoptosis can induce multivalent antigen crosslinking of specific BCR on B1 cells and induce TI-2 responses. Due to this self- and poly- reactivity of B1 cells, their functions have to be tightly regulated to avoid autoimmunity. Several inhibitory receptors that regulate various aspects of B1 cell function are already known to be instrumental in this. We have observed that lack of SIRPα on B1 cells has no measurable effect on calcium flux and IgM secretion, which may suggest that Siglec-G and CD5, which have previously shown to regulate these parameters, comprise the major regulators of BCR signaling in B1 cells (17). SIRPα$^{\Delta CYT}$ mice have moderately increased numbers of B1 cells only in the spleen with the peritoneal population virtually unaltered. Also, B1-associated antibody levels are elevated in SIRPα$^{\Delta CYT}$ mice, both at baseline and after TI-2 antigen exposure. Natural antibodies are predominantly produced by B1 cells in secondary lymphoid organs such as spleen (4) or specific (e.g., mediastinal) lymph nodes (8). Egress of B1 cells residing in the body cavities (peritoneal or pleural) into the secondary lymphoid organs has been demonstrated to depend on the CD11b/CD18 integrin (8). CD11b can function only in heterodimer with CD18 integrin, forming together CD11b/CD18 (also known as CR3, Mac-1,

Integrin alpha M, or $\alpha_M\beta_2$ integrin). B1 cells are known to express various integrin molecules, but B1 cells are the only B cells that express CD11b/CD18 integrin and until now no direct regulator of its function has been described. We show here that SIRPα negatively regulates capacity of B1 cells to exit the peritoneal cavity through CD11b/CD18 integrin, identifying this inhibitory immunoreceptor as the first *bona fide* regulator of B1 migratory function. It should be emphasized that we cannot formally attribute the *in vivo* phenotype of the SIRPα-mutant mice to B1 cell-intrinsic effects of SIRPα signaling, since also other cells, such as myeloid cells, in these mice have a defect in SIRPα signaling as well. Taken together, a picture emerges where different B1 cell functions appear to be regulated by distinct inhibitory receptors, with SIRPα more or less specifically controlling their migratory behavior, whereas others, e.g., Siglec-G and CD5 may control B1 cell activation in a more generalized fashion.

The homeostatic function of IgM antibodies has been well documented in atherosclerosis (11–13, 49). Mice lacking SIRPα signaling in the hematopoietic compartment showed increased plasma levels of T15/E06 IgM and show smaller and less severe atherosclerotic lesions. This is consistent with observations in Siglec $G^{-/-}$ bone marrow chimeras, where the lack of inhibitory signaling by Siglec G led to increased OSE-specific natural IgM antibody levels and decreased atherosclerosis development (24). Increased plasma level of T15/E06 IgM is a very likely mechanism of atheroprotection in $SIRP\alpha^{\Delta CYT}$ chimeras. However, transplantation of $SIRP\alpha^{\Delta CYT}$ and wt bone marrow resulted in replacement of both myeloid and lymphoid lineage in the donor $LDLR^{-/-}$ mice. As macrophages are important players in development of atherosclerosis we cannot exclude their contribution to the observed phenotype, especially since the SIRPα counter-receptor CD47 appears involved in pathogenesis of atherosclerosis through inhibition, e.g., macrophage efferocytosis (50). Furthermore, whether blocking antibodies targeting SIRPα, rather than CD47, would show similar effect still remains to be confirmed, also because the CD47 monoclonal antibody miap410 used in the study of Kojima (50) has prominent opsonizing capacity and a less convincing ability to actually block the CD47-SIRPα axis (51).

Importantly, it is well established that humans, like mice, have "natural" antibodies targeting, e.g., OSE, which are atheroprotective, and these even appear to have prognostic value for the development of cardiovascular disease (52). Based on our current findings in mice, the prediction would therefore be that the human natural antibody producing B cells would also express SIRPα and would consequently also be subject to regulation *via* the CD47-SIRPα axis. The problem is, however, that the B1 cell equivalent subset responsible for natural antibody production in humans has not been properly identified, and this is in fact a heavily debated issue in the B1 cell field. For instance, the reported identification of human B1 cells in blood defined as $CD20^+CD27^+CD43^+CD70^-$ (53) is quite controversial and has been challenged by several other studies suggesting that these cells are rather result of a technical artefact (54–56). Further studies are clearly needed to resolve this issue and to establish SIRPα expression and function on these putative human B1 cells.

Collectively, our data identify SIRPα as a novel B1 cell immune checkpoint, which functions to control B1 cell migration to lymphoid tissues and natural antibody generation. Our findings also imply SIRPα as a potential therapeutic target in atherosclerosis. The CD47-SIRPα innate immune checkpoint is currently extensively studied in the context of cancer immunotherapy (2, 57), with a number of different agents in preclinical and/or clinical development, and ~35 ongoing clinical trials, carving out a path for potential therapeutic targeting of the CD47-SIRPα axis also in other diseases, including cardiovascular disease.

AUTHOR'S NOTE

This manuscript has been released as a preprint at BioRxiv, doi: https://doi.org/10.1101/2020.05.13.092494.

DATA AVAILABILITY STATEMENT

The raw data supporting the conclusions of this article will be made available by the authors, without undue reservation.

ETHICS STATEMENT

The animal study was reviewed and approved by Animal Welfare Committees of the VU Medical Center Amsterdam, The Netherlands; Maastricht University, Maastricht, The Netherlands; and The Netherlands Cancer Institute, Amsterdam, The Netherlands.

AUTHOR CONTRIBUTIONS

KF, SP, MH, MG, HM, JG, HO, CP, PG, MO-K, and YS performed experiments and analyzed data. TM, TK, RH, GK, CB, MW, and TB provided reagents and facilities and designed research and/or evaluated data. KF and TB wrote the paper. All authors contributed to the article and approved the submitted version.

FUNDING

This work was supported by NWO-TOP grant (#91208001) awarded to GK, MW, and TB.

ACKNOWLEDGMENTS

The authors thank Martijn A. Nolte and Rene A.W. van Lier for useful discussions.

SUPPLEMENTARY MATERIAL

The Supplementary Material for this article can be found online at: https://www.frontiersin.org/articles/10.3389/fimmu.2020.570963/full#supplementary-material

REFERENCES

1. Barclay AN, van den Berg TK. The interaction between signal regulatory protein alpha (SIRPalpha) and CD47: structure, function, and therapeutic target. *Annu Rev Immunol* (2014) 32:25–50. doi: 10.1146/annurev-immunol-032713-120142
2. Matlung HL, Szilagyi K, Barclay NA, van den Berg TK. The CD47-SIRPalpha signaling axis as an innate immune checkpoint in cancer. *Immunol Rev* (2017) 276(1):145–64. doi: 10.1111/imr.12527
3. Advani R, Flinn I, Popplewell L, Forero A, Bartlett NL, Ghosh N, et al. CD47 Blockade by Hu5F9-G4 and Rituximab in Non-Hodgkin's Lymphoma. *N Engl J Med* (2018) 379(18):1711–21. doi: 10.1056/NEJMoa1807315
4. Baumgarth N. The double life of a B-1 cell: self-reactivity selects for protective effector functions. *Nat Rev Immunol* (2011) 11(1):34–46. doi: 10.1038/nri2901
5. Choi YS, Dieter JA, Rothaeusler K, Luo Z, Baumgarth N. B-1 cells in the bone marrow are a significant source of natural IgM. *Eur J Immunol* (2012) 42 (1):120–9. doi: 10.1002/eji.201141890
6. Smith FL, Baumgarth N. B-1 cell responses to infections. *Curr Opin Immunol* (2019) 57:23–31. doi: 10.1016/j.coi.2018.12.001
7. Yang Y, Tung JW, Ghosn EE, Herzenberg LA, Herzenberg LA. Division and differentiation of natural antibody-producing cells in mouse spleen. *Proc Natl Acad Sci U S A* (2007) 104(11):4542–6. doi: 10.1073/pnas.0700001104
8. Waffarn EE, Hastey CJ, Dixit N, Soo Choi Y, Cherry S, Kalinke U, et al. Infection-induced type I interferons activate CD11b on B-1 cells for subsequent lymph node accumulation. *Nat Commun* (2015) 6:8991. doi: 10.1038/ncomms9991
9. Ghosn EE, Yang Y, Tung J, Herzenberg LA, Herzenberg LA. CD11b expression distinguishes sequential stages of peritoneal B-1 development. *Proc Natl Acad Sci U S A* (2008) 105(13):5195–200. doi: 10.1073/pnas.0712350105
10. Miller YI, Tsimikas S. Oxidation-specific epitopes as targets for biotheranostic applications in humans: biomarkers, molecular imaging and therapeutics. *Curr Opin Lipidol* (2013) 24(5):426–37. doi: 10.1097/MOL.0b013e328364e85a
11. Binder CJ, Horkko S, Dewan A, Chang MK, Kieu EP, Goodyear CS, et al. Pneumococcal vaccination decreases atherosclerotic lesion formation: molecular mimicry between Streptococcus pneumoniae and oxidized LDL. *Nat Med* (2003) 9(6):736–43. doi: 10.1038/nm876
12. Caligiuri G, Khallou-Laschet J, Vandaele M, Gaston AT, Delignat S, Mandet C, et al. Phosphorylcholine-targeting immunization reduces atherosclerosis. *J Am Coll Cardiol* (2007) 50(6):540–6. doi: 10.1016/j.jacc.2006.11.054
13. Faria-Neto JR, Chyu KY, Li X, Dimayuga PC, Ferreira C, Yano J, et al. Passive immunization with monoclonal IgM antibodies against phosphorylcholine reduces accelerated vein graft atherosclerosis in apolipoprotein E-null mice. *Atherosclerosis* (2006) 189(1):83–90. doi: 10.1016/j.atherosclerosis.2005.11.033
14. Grasset EK, Duhlin A, Agardh HE, Ovchinnikova O, Hagglof T, Forsell MN, et al. Sterile inflammation in the spleen during atherosclerosis provides oxidation-specific epitopes that induce a protective B-cell response. *Proc Natl Acad Sci U S A* (2015) 112(16):E2030–8. doi: 10.1073/pnas.1421227112
15. Libby P, Ridker PM, Hansson GK. Progress and challenges in translating the biology of atherosclerosis. *Nature* (2011) 473(7347):317–25.
16. Horkko S, Bird DA, Miller E, Itabe H, Leitinger N, Subbanagounder G, et al. Monoclonal autoantibodies specific for oxidized phospholipids or oxidized phospholipid-protein adducts inhibit macrophage uptake of oxidized low-density lipoproteins. *J Clin Invest* (1999) 103(1):117–28. doi: 10.1172/JCI4533
17. Bikah G, Carey J, Ciallella JR, Tarakhovsky A, Bondada S. CD5-mediated negative regulation of antigen receptor-induced growth signals in B-1 B cells. *Science* (1996) 274(5294):1906–9. doi: 10.1126/science.274.5294.1906
18. Nitschke L, Carsetti R, Ocker B, Kohler G, Lamers MC. CD22 is a negative regulator of B-cell receptor signalling. *Curr Biol* (1997) 7(2):133–43. doi: 10.1016/s0960-9822(06)00057-1
19. Amezcua Vesely MC, Schwartz M, Bermejo DA, Montes CL, Cautivo KM, Kalergis AM, et al. FcgammaRIIb and BAFF differentially regulate peritoneal B1 cell survival. *J Immunol* (2012) 188(10):4792–800. doi: 10.4049/jimmunol.1102070
20. Bagchi-Chakraborty J, Francis A, Bray T, Masters L, Tsiantoulas D, Nus M, et al. B Cell Fcgamma Receptor IIb Modulates Atherosclerosis in Male and Female Mice by Controlling Adaptive Germinal Center and Innate B1-Cell Responses. *Arterioscler Thromb Vasc Biol* (2019) 39:1379–89. doi: 10.1161/ATVBAHA.118.312272
21. Ding C, Liu Y, Wang Y, Park BK, Wang CY, Zheng P, et al. Siglecg limits the size of B1a B cell lineage by down-regulating NFkappaB activation. *PloS One* (2007) 2(10):e997. doi: 10.1371/journal.pone.0000997
22. Hoffmann A, Kerr S, Jellusova J, Zhang J, Weisel F, Wellmann U, et al. Siglec-G is a B1 cell-inhibitory receptor that controls expansion and calcium signaling of the B1 cell population. *Nat Immunol* (2007) 8(7):695–704. doi: 10.1038/ni1480
23. Hayakawa K, Hardy RR, Parks DR, Herzenberg LA. The "Ly-1 B" cell subpopulation in normal immunodefective, and autoimmune mice. *J Exp Med* (1983) 157(1):202–18. doi: 10.1084/jem.157.1.202
24. Gruber S, Hendrikx T, Tsiantoulas D, Ozsvar-Kozma M, Goderle L, Mallat Z, et al. Sialic Acid-Binding Immunoglobulin-like Lectin G Promotes Atherosclerosis and Liver Inflammation by Suppressing the Protective Functions of B-1 Cells. *Cell Rep* (2016) 14(10):2348–61. doi: 10.1016/j.celrep.2016.02.027
25. Smith KG, Clatworthy MR. FcgammaRIIB in autoimmunity and infection: evolutionary and therapeutic implications. *Nat Rev Immunol* (2010) 10 (5):328–43. doi: 10.1038/nri2762
26. Washio K, Kotani T, Saito Y, Respatika D, Murata Y, Kaneko Y, et al. Dendritic cell SIRPα regulates homeostasis of dendritic cells in lymphoid organs. *Genes Cells Devoted Mol Cell Mech* (2015) 20(6):451–63. doi: 10.1111/gtc.12238
27. Yamao T, Noguchi T, Takeuchi O, Nishiyama U, Morita H, Hagiwara T, et al. Negative regulation of platelet clearance and of the macrophage phagocytic response by the transmembrane glycoprotein SHPS-1. *J Biol Chem* (2002) 277 (42):39833–9. doi: 10.1074/jbc.M203287200
28. Inagaki K, Yamao T, Noguchi T, Matozaki T, Fukunaga K, Takada T, et al. SHPS-1 regulates integrin-mediated cytoskeletal reorganization and cell motility. *EMBO J* (2000) 19(24):6721–31. doi: 10.1093/emboj/19.24.6721
29. Lekanne Deprez RH, Fijnvandraat AC, Ruijter JM, Moorman AF. Sensitivity and accuracy of quantitative real-time polymerase chain reaction using SYBR green I depends on cDNA synthesis conditions. *Anal Biochem* (2002) 307 (1):63–9. doi: 10.1016/S0003-2697(02)00021-0
30. Muggen AF, Pillai SY, Kil LP, van Zelm MC, van Dongen JJ, Hendriks RW, et al. Basal Ca(2+) signaling is particularly increased in mutated chronic lymphocytic leukemia. *Leukemia* (2015) 29(2):321–8. doi: 10.1038/leu.2014.188
31. Maas A, Dingjan GM, Savelkoul HF, Kinnon C, Grosveld F, Hendriks RW. The X-linked immunodeficiency defect in the mouse is corrected by expression of human Bruton's tyrosine kinase from a yeast artificial chromosome transgene. *Eur J Immunol* (1997) 27(9):2180–7. doi: 10.1002/eji.1830270910
32. Chou MY, Fogelstrand L, Hartvigsen K, Hansen LF, Woelkers D, Shaw PX, et al. Oxidation-specific epitopes are dominant targets of innate natural antibodies in mice and humans. *J Clin Invest* (2009) 119(5):1335–49. doi: 10.1172/JCI36800
33. Ha SA, Tsuji M, Suzuki K, Meek B, Yasuda N, Kaisho T, et al. Regulation of B1 cell migration by signals through Toll-like receptors. *J Exp Med* (2006) 203 (11):2541–50. doi: 10.1084/jem.20061041
34. Goossens P, Gijbels MJ, Zernecke A, Eijgelaar W, Vergouwe MN, dM v, et al. Myeloid type I interferon signaling promotes atherosclerosis by stimulating macrophage recruitment to lesions. *Cell Metab* (2010) 12(2):142–53. doi: 10.1016/j.cmet.2010.06.008
35. Kanters E, Pasparakis M, Gijbels MJ, Vergouwe MN, Partouns-Hendriks I, Fijneman RJ, et al. Inhibition of NF-kappaB activation in macrophages increases atherosclerosis in LDL receptor-deficient mice. *J Clin Invest* (2003) 112(8):1176–85. doi: 10.1172/JCI18580
36. Kanters E, Gijbels MJ, van der Made I, Vergouwe MN, Heeringa P, Kraal G, et al. Hematopoietic NF-kappaB1 deficiency results in small atherosclerotic lesions with an inflammatory phenotype. *Blood* (2004) 103(3):934–40. doi: 10.1182/blood-2003-05-1450
37. Adams S, van der Laan LJ, Vernon-Wilson E, Renardel de LC, Dopp EA, Dijkstra CD, et al. Signal-regulatory protein is selectively expressed by myeloid and neuronal cells. *J Immunol* (1998) 161(4):1853–9.
38. Sato-Hashimoto M, Saito Y, Ohnishi H, Iwamura H, Kanazawa Y, Kaneko T, et al. Signal regulatory protein alpha regulates the homeostasis of T

lymphocytes in the spleen. *J Immunol* (2011) 187(1):291–7. doi: 10.4049/jimmunol.1100528
39. Que X, Hung MY, Yeang C, Gonen A, Prohaska TA, Sun X, et al. Oxidized phospholipids are proinflammatory and proatherogenic in hypercholesterolaemic mice. *Nature* (2018) 558(7709):301–6. doi: 10.1038/s41586-018-0198-8
40. Berland R, Wortis HH. Origins and functions of B-1 cells with notes on the role of CD5. *Annu Rev Immunol* (2002) 20:253–300. doi: 10.1146/annurev.immunol.20.100301.064833
41. Duber S, Hafner M, Krey M, Lienenklaus S, Roy B, Hobeika E, et al. Induction of B-cell development in adult mice reveals the ability of bone marrow to produce B-1a cells. *Blood* (2009) 114(24):4960–7. doi: 10.1182/blood-2009-04-218156
42. Holodick NE, Repetny K, Zhong X, Rothstein TL. Adult BM generates CD5+ B1 cells containing abundant N-region additions. *Eur J Immunol* (2009) 39 (9):2383–94. doi: 10.1002/eji.200838920
43. Jellusova J, Duber S, Guckel E, Binder CJ, Weiss S, Voll R, et al. Siglec-G regulates B1 cell survival and selection. *J Immunol* (2010) 185(6):3277–84. doi: 10.4049/jimmunol.1001792
44. Binder CJ, Hartvigsen K, Chang MK, Miller M, Broide D, Palinski W, et al. IL-5 links adaptive and natural immunity specific for epitopes of oxidized LDL and protects from atherosclerosis. *J Clin Invest* (2004) 114(3):427–37. doi: 10.1172/JCI200420479
45. Feng X, Zhang Y, Xu R, Xie X, Tao L, Gao H, et al. Lipopolysaccharide up-regulates the expression of Fcalpha/mu receptor and promotes the binding of oxidized low-density lipoprotein and its IgM antibody complex to activated human macrophages. *Atherosclerosis* (2010) 208(2):396–405. doi: 10.1016/j.atherosclerosis.2009.07.035
46. Binder CJ, Papac-Milicevic N, Witztum JL. Innate sensing of oxidation-specific epitopes in health and disease. *Nat Rev Immunol* (2016) 16(8):485–97. doi: 10.1038/nri.2016.63
47. Myers LM, Tal MC, Torrez Dulgeroff LB, Carmody AB, Messer RJ, Gulati G, et al. A functional subset of CD8(+) T cells during chronic exhaustion is defined by SIRPalpha expression. *Nat Commun* (2019) 10(1):794. doi: 10.1038/s41467-019-08637-9
48. Brooke GP, Parsons KR, Howard CJ. Cloning of two members of the SIRP alpha family of protein tyrosine phosphatase binding proteins in cattle that are expressed on monocytes and a subpopulation of dendritic cells and which mediate binding to CD4 T cells. *Eur J Immunol* (1998) 28 (1):1–11. doi: 10.1002/(SICI)1521-4141(199801)28:01<1::AID-IMMU1>3.0.CO;2-V
49. Gronwall C, Silverman GJ. Natural IgM: beneficial autoantibodies for the control of inflammatory and autoimmune disease. *J Clin Immunol* (2014) 34 Suppl 1:S12–21. doi: 10.1007/s10875-014-0025-4
50. Kojima Y, Volkmer JP, McKenna K, Civelek M, Lusis AJ, Miller CL, et al. CD47-blocking antibodies restore phagocytosis and prevent atherosclerosis. *Nature* (2016) 536(7614):86–90. doi: 10.1038/nature18935
51. Han X, Sterling H, Chen Y, Saginario C, Brown EJ, Frazier WA, et al. CD47, a ligand for the macrophage fusion receptor, participates in macrophage multinucleation. *J Biol Chem* (2000) 275(48):37984–92. doi: 10.1074/jbc.M002334200
52. Ravandi A, Boekholdt SM, Mallat Z, Talmud PJ, Kastelein JJ, Wareham NJ, et al. Relationship of IgG and IgM autoantibodies and immune complexes to oxidized LDL with markers of oxidation and inflammation and cardiovascular events: results from the EPIC-Norfolk Study. *J Lipid Res* (2011) 52(10):1829–36. doi: 10.1194/jlr.M015776
53. Griffin DO, Rothstein TL. A small CD11b(+) human B1 cell subpopulation stimulates T cells and is expanded in lupus. *J Exp Med* (2011) 208(13):2591–8. doi: 10.1084/jem.20110978
54. Reynaud CA, Weill JC. Gene profiling of CD11b$^+$ and CD11b$^-$ B1 cell subsets reveals potential cell sorting artifacts. *J Exp Med* (2012) 209(3):433–4. doi: 10.1084/jem.20120402
55. Descatoire M, Weill JC, Reynaud CA, Weller S. A human equivalent of mouse B-1 cells? *J Exp Med* (2011) 208(13):2563–4. doi: 10.1084/jem.20112232
56. Perez-Andres M, Grosserichter-Wagener C, Teodosio C, van Dongen JJ, Orfao A, van Zelm MC. The nature of circulating CD27+CD43+ B cells. *J Exp Med* (2011) 208(13):2565–6. doi: 10.1084/jem.20112203
57. van den Berg TK, Valerius T. Myeloid immune-checkpoint inhibition enters the clinical stage. *Nat Rev Clin Oncol* (2019) 16(5):275–6. doi: 10.1038/s41571-018-0155-3

Conflict of Interest: The authors declare that the research was conducted in the absence of any commercial or financial relationships that could be construed as a potential conflict of interest.

frontiers in Immunology

REVIEW
published: 14 October 2020
doi: 10.3389/fimmu.2020.575175

Roles for the FCRL6 Immunoreceptor in Tumor Immunology

*Randall S. Davis**

Departments of Medicine, Microbiology, and Biochemistry & Molecular Genetics, The Comprehensive Cancer Center, University of Alabama at Birmingham, Birmingham, AL, United States

Members of the Fc receptor-like (*FCRL1–6*) gene family encode transmembrane glycoproteins that are preferentially expressed by B cells and generally repress responses via cytoplasmic tyrosine-based regulation. Given their distribution and function, there is a growing appreciation for their roles in lymphoproliferative disorders and as immunotherapeutic targets. In contrast to FCRL1–5, FCRL6 is distinctly expressed outside the B lineage by cytotoxic T and NK lymphocytes. Its restricted expression by these orchestrators of cell-mediated immunity, along with its inhibitory properties and extracellular interactions with MHCII/HLA-DR, represent a newly appreciated axis with relevance in tolerance and cancer defense. The significance of FCRL6 in this arena has been recently demonstrated by its upregulation in HLA-DR$^+$ tumor samples from melanoma, breast, and lung cancer patients who relapsed following PD-1 blockade. These findings imply a potential mechanistic role for FCRL6 in adaptive evasion to immune checkpoint therapy. Here we review these new developments in the FCRL field and identify new evidence for the prognostic significance of FCRL6 in malignancies that collectively indicate its potential as a biomarker and therapeutic target.

Keywords: lymphocytes, inhibitory signaling, regulation, tumor immunology, cell-mediated immunity, FCRL family

OPEN ACCESS

Edited by:
Ali A. Zarrin,
TRex Bio, United States

Reviewed by:
Andreas Pircher,
Innsbruck Medical University, Austria
Nahum Puebla-Osorio,
University of Texas MD Anderson Cancer Center, United States

***Correspondence:**
Randall S. Davis
rsdavis@uab.edu

Specialty section:
This article was submitted to Cancer Immunity and Immunotherapy, a section of the journal Frontiers in Immunology

Received: *22 June 2020*
Accepted: *01 September 2020*
Published: *14 October 2020*

Citation:
Davis RS (2020) Roles for the FCRL6 Immunoreceptor in Tumor Immunology. Front. Immunol. 11:575175. doi: 10.3389/fimmu.2020.575175

INTRODUCTION

The immune system maintains a careful balance of activation vs. inhibition signals to coordinate restraint at homeostasis and promote effector responses when triggered. These cellular mechanisms establish tissue surveillance and stand ready to mount a vigorous immune defense, but must also suppress overzealous responses that could potentially harm the host. The growing significance of inhibitory receptors in immune regulation and human health is underscored by their roles in a variety of disorders including infectious diseases, autoimmunity, and cancer.

The discovery that malignancies have evolved mechanisms that exploit inhibitory receptors to circumvent elimination by immune cells is fundamentally impacting our understanding of tumor immunology and revolutionizing cancer therapy. Antibody (Ab)-mediated targeting of the PD-1/PD-L1 and CTLA-4/B7 immune checkpoint inhibitor (ICI) axes enables disruption of receptor-ligand interactions that shield tumors from infiltrating cytotoxic lymphocytes (1, 2). This selective approach has reinvigorated the field of tumor immunology and ignited extraordinary potential for new diagnostic, prognostic, and therapeutic strategies that deliver more targeted and effective patient care. As of 2018, it is estimated that ∼44% of cancer patients are eligible for ICI therapy (3). However, as treatment expands, many patients who enjoyed durable responses will relapse as the tumor adapts and becomes resistant to recognition and rejection by tumor infiltrating lymphocytes (TILs) (4, 5). Unfortunately, the mechanisms responsible for ICI resistance remain incompletely defined. This issue is becoming a growing barrier for cancer patients who have limited therapeutic options and require alternative strategies to overcome the tumor's adaptive resistance.

Here we review recent developments related to members of the Fc receptor-like (FCRL1–6) immunoregulatory family with a specific focus on the FCRL6 molecule in cell-mediated immunity and its newly appreciated roles in tumor immunology. Its restricted expression by cytotoxic NK and T cells, cytoplasmic tyrosine-based inhibitory properties, and extracellular interactions with MHCII/HLA-DR introduce a new axis with relevance in tolerance and cancer defense (**Figure 1**). Its importance was recently demonstrated in studies that identified its upregulation in HLA-DR$^+$ tumor samples from melanoma, breast, and lung cancer patients who had relapsed following PD-1 blockade (7). These findings imply a potential mechanistic role for FCRL6 in adaptive evasion to ICI therapy. By investigating its expression among The Cancer Genome Atlas (TCGA) tumor samples, we identify new evidence for the prognostic significance of FCRL6 in melanoma, breast, and lung cancer that collectively indicate its potential as a biomarker and therapeutic target.

FC RECEPTOR-LIKE MOLECULES (FCRL) IN B CELL REGULATION

An extended family of *FCRL1–6* genes in humans and mice encode type I transmembrane (TM) glycoproteins with cytoplasmic immunoreceptor tyrosine-based activation (ITAM)-like or inhibitory (ITIM) motifs [reviewed in (8, 9)]. FCRL1–5 are preferentially expressed by B lineage cells and modulate B cell antigen-receptor (BCR)-mediated signaling (10). Notably, FCRL3 is also detected outside the B lineage on subsets of T and NK cells (11–13). While FCRL1 is a pan B cell marker with ITAM-like motifs that promotes BCR activation in humans and mice [unpublished studies and (14–16)], signaling studies demonstrate that FCRL2–5 generally exert inhibitory function. Consistent with their possession of cytoplasmic ITIM sequences, following BCR cross-linking, FCRL2–5 are tyrosine phosphorylated (pY) and can repress global pY, Ca^{2+} flux, and MAP kinase activation via recruitment of the SHP-1 and/or SHP-2 phosphatases (17–21). In mice (m), mFCRL5 has similar inhibitory properties (22). However, the presence of both ITAM and ITIM in the FCRL2–5 representatives implies more complex signaling than the classical FCRs that are either activating or inhibitory (23). Accordingly, mFCRL5 has the ability to modulate BCR signaling in a binary fashion. However, its functional properties among B cell subsets vary according to the differential recruitment of the Lyn Src-family kinase (SFK) to an ITAM-like sequence and SHP-1 to an ITIM (21). The capacity for composite activating and inhibitory signaling is also present in human FCRL3 and FCRL4. These proteins possess dual regulatory properties that appear to differ according to the innate (Toll-like receptor/TLR) or adaptive (BCR) nature of B cell stimulation (24, 25). Molecular dissection of the FCRL4 cytoplasmic tail has demonstrated that its function is altered by the recruitment of at least two different SFKs. FCRL4 wields suppressive activity in B cells co-expressing FGR, but promotes activation in B cells co-expressing HCK p59 (26). Thus, as opposed to the classical FCR for IgG and IgE, these findings highlight that many FCRLs possess multifaceted regulatory potential.

Beyond their intracellular signaling capability, ligands have been identified for several FCRLs. The potential for Ig binding was initially detected for FCRL4 and FCRL5, but was confirmed in studies by Wilson et al. who found these receptors could interact with IgA and IgG (27, 28). However, unlike the classical IgG and IgE FCRs, IgG binding to FCRL5 is glycosylation dependent and requires both the Fab and Fc portions (29). Recent work has also identified secretory IgA as a ligand for FCRL3 and this relationship could impact inhibition in T regulatory cells (30). How these receptor-ligand interactions influence the systemic and cellular function of the lymphocytes that express them or contribute to disease pathogenesis remains ripe for future investigation.

RELEVANCE OF FCRL1-5 IN B CELL LYMPHOPROLIFERATIVE DISORDERS

The preferential expression of FCRL1–5 by B cells has made these molecules relevant clinical candidates in lymphoproliferative disorders such as leukemias and lymphomas. In fact their initial identification by the Dalla-Favera group as immunoglobulin superfamily receptor translocation-associated (IRTA) genes, resulted from the characterization of a t(1;14)(q21;q32) translocation breakpoint in a multiple myeloma cell line (28). These early studies also demonstrated dysregulated *FCRL5/IRTA2* transcript expression in follicular lymphoma and myeloma cell lines with 1q21 abnormalities (31). Variable upregulation of *FCRL1–5* in B cell malignancies was further revealed through the Lymphochip-based microarray analyses led by the Staudt group (32), but have now been expanded in ever-growing numbers of high-throughput RNA-seq studies. Following the development of monoclonal Abs (mAbs), several groups validated FCRL surface protein expression by malignant B cell lines as well as B cell chronic lymphocytic leukemia (CLL) cells, the most common leukemia in Western countries (11, 33, 34). An analysis of FCRL1–5 in a cohort of CLL patients well-characterized for standard prognostic factors, identified FCRL2 as a marker for a subgroup of CLL patients with a more indolent disease course as reflected by favorable progression free survival and overall survival (34, 35). By flow cytometry, FCRL2 was able to segregate CLL samples according to the mutation status of the *IGHV* gene expressed by the leukemic clone. Its upregulation by mutated *IGHV* CLL samples introduced a novel surface marker of this favorable disease subtype. This pattern of FCRL2 expression was in contrast to CD38, ZAP-70, and CD49d, which are chiefly upregulated in patients with unmutated CLL who experience a more aggressive disease course (10, 36, 37). The inhibitory function evident for FCRL2 in healthy B cells (19) implies that its upregulation by indolent *IGHV* mutated CLL might also contribute to biological suppression in this favorable CLL subtype. Thus, the expression of these regulatory proteins may not only have prognostic significance, but could also have physiological impact on the clinical disease course and pathogenesis of certain lymphoproliferative disorders.

The targetability of FCRL members in B cell malignancies is an area of active investigation and FCRL5 has become a promising

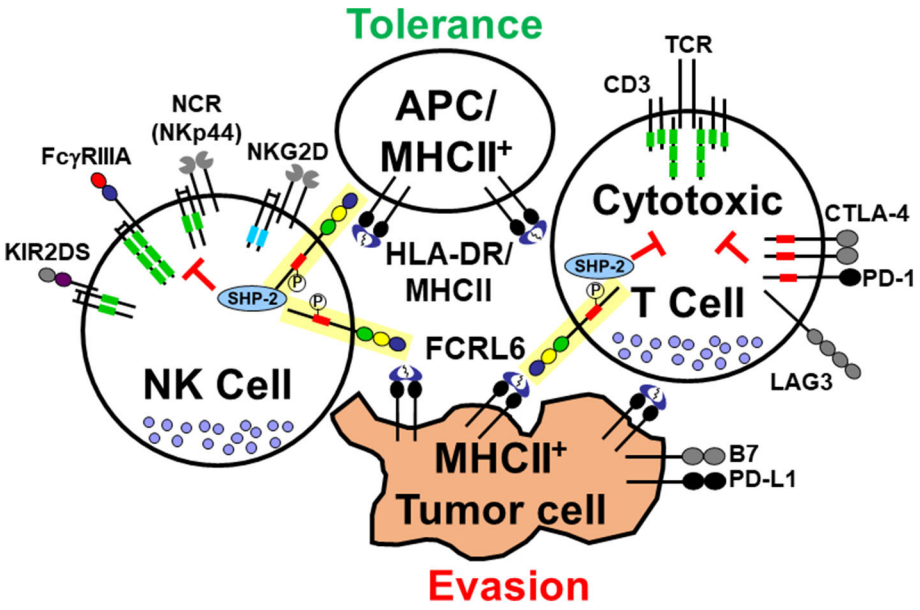

FIGURE 1 | Interactions of the cytotoxic lymphocyte-expressed FCRL6 immunoreceptor with MHCII-expressing cells. The schematic representation shows the FCRL6 receptor (yellow box), which is composed of three extracellular Ig-like domains, an uncharged transmembrane region, and a cytoplasmic tail with two tyrosines, including a consensus ITIM (red rectangle) that recruits the SHP-2 tyrosine phosphatase. FCRL6 is expressed by cytotoxic T and NK cells and has been found to interact with MHCII/HLA-DR. Other pertinent adaptor-associated activating (ITAM-bearing, green rectangles and DAP-10, blue rectangles) and immune checkpoint inhibitory (ICI) molecule pairs (CTLA-4/B7, PD-1/PD-L1, LAG3/MHCII, and NKp44/MHCII) highlight the regulatory balance of immune tolerance and tumor evasion between cytotoxic lymphocytes and APCs or tumor cells. Note NKp44 also has an inhibitory splice isoform (6).

therapeutic candidate. Analysis of blood and tissue samples by the Pastan laboratory identified elevated levels of soluble and surface bound FCRL5 in multiple myeloma, CLL, and mantle cell lymphoma patient samples (33). Studies targeting FCRL5 in myeloma have been conducted by investigators at Genentech (38–40). Two approaches have been pursued including a mAb drug conjugate and a T cell-dependent bispecific mAb. Pre-clinical xenograft models employing multiple myeloma samples indicated efficacy for a humanized IgG1 isotype FCRL5 mAb conjugated to monomethyl auristatin E (MMAE) (38). This microtubule inhibitor becomes active when surface receptors bound by the mAb-conjugate are internalized in target cells. A Phase 1 study of this anti-FCRL5-MMAE drug compound (DFRF4539A) in relapsed and refractory multiple myeloma patients ($n = 39$) showed tolerability as a single agent, but demonstrated limited activity and may not be a successful strategy for myeloma (39). The authors speculated that the low response rates in this study could be due to the unknown threshold for Ab-dependent cytotoxicity activity, shedding of the FCRL5 target, limited internalization, and a less effective role of MMAE in cells with a low proliferative index. However, preclinical studies with a bispecific FCRL5/CD3 mAb has shown encouraging activity against patient myeloma cells, can deplete B cells and bone marrow plasma cells in cynomolgus monkeys, and exhibits enhanced activity when combined with PD-L1 blockade (40). These studies indicate that immunotherapeutic targeting of FCRL5 and other FCRL family members expressed by B cells may have utility in a variety of lymphoproliferative disorders.

HUMAN FCRL6 IS AN IMMUNOREGULATORY PROTEIN RESTRICTED TO CYTOTOXIC T AND NK CELLS

Notably, the first member of the FCRL family identified was a rat FCRL6 ortholog, termed gp42, that was discovered in a search for markers of lymphokine activated killer (LAK) cells (41). Following the discovery of human FCRL1–5, we and others identified human and mouse *FCRL6*/*Fcrl6* counterparts, both of which encode type I TM glycoproteins (42–44). However, the structure and distribution of these FCRL6 molecules among lymphocytes has marked interspecies differences (43). Recent studies with receptor-specific mAbs identified the expression of mFCRL6, which has two Ig like extracellular domains and a short cytoplasmic tail lacking a consensus ITIM or ITAM, by subsets of progenitor B cells in the fetal liver and bone marrow (45). An analysis of pro B cell subsets purified according to the presence or absence of FCRL6 expression, revealed that FCRL6$^+$ progenitors have a distinct transcript signature, constrained diversity of their *IGHV* repertoires, and hydrophobic and charged CDR-H3 characteristics akin to innate-like B-1 cells that produce natural Abs (45). However, the regulatory role of mFCRL6 among these pro B cells is not yet defined. Despite syntenic genomic positions, the disparate structure and expression pattern of this family member presents some barriers for *in vivo* translational understanding of its human relative. In contrast, human FCRL6, which has three extracellular Ig-like domains, an uncharged TM

region, and a cytoplasmic tail featuring a consensus ITIM, is restricted to cytotoxic T and NK cells (44, 46).

The development of receptor-specific mAbs facilitated examination of its ontogeny and distribution in human tissues. FCRL6 is present on mature NK and T lymphocytes from adult spleen and blood, but not by these cells from primary developmental sites such as the fetal liver, bone marrow, or thymus (45). Inflammatory tonsillar tissue also lacks significant numbers of FCRL6$^+$ cells. Within the blood, FCRL6 marks more terminally differentiated cytotoxic CD16$^+$CD56^{dim} NK cells, a finding that correlates with cytoplasmic perforin and expression of the keratin sulfate-related lactosamine carbohydrate epitope, PEN5 (47). The possibility that FCRL6 expression increases as a function of ontogeny was also confirmed by comparing CD16$^+$ NK cells isolated from cord and adult blood samples. FCRL6 is expressed at significantly higher levels among circulating adult CD16$^+$ cells suggesting that it emerges later in ontogeny than CD16 and segregates NK cells that are more mature (45). Within the T cell compartment, FCRL6 is present on innate-like γδ T cells, but is not biased among Vδ1 or Vδ2 subsets. However, its expression by γδ T cells similarly correlates with perforin and is relatively more abundant on CD16^{hi} Vδ2 cells that have greater cytotoxic propensity (48). Among CD8$^+$ T cells, FCRL6 is primarily restricted to perforin-expressing effector (CD45RA$^+$CCR7$^-$ or CD28$^-$2B4$^+$) and effector memory (CD45RA$^-$CCR7$^-$ or CD28$^+$2B4$^+$) subpopulations, rather than central memory or naïve cells. Interestingly, a small (∼2%), but consistent population of FCRL6$^+$CD4$^+$ T cells that co-express perforin, CD57, and NKG2D, but lacks CCR7 is present in the blood of some donors (46). Such rare CD4$^+$ T cells possess cytolytic function (49). These data indicate that FCRL6 distinctly marks mature NK and T cell subpopulations with cytotoxic potential.

FCRL6 RECRUITS SHP-2 TO AN ITIM AND IS AN MHCII/HLA-DR LIGAND

The presence of two tyrosines in the FCRL6 cytoplasmic tail suggests that, like other FCRLs, it harbors regulatory function. One of these tyrosines (Y371) is positioned among amino acids that conform to a consensus ITIM, but the sequence surrounding both tyrosines (Y356, Y371) could represent a non-canonical ITAM. GST pull down assays of Y356F and Y371F mutants performed with Jurkat lysates uncovered recruitment of the SHIP1 inositol phosphatase as well as the GRB2 adapter protein to the Y356 residue and the SHP1/SHP2 tyrosine phosphatases to the Y371 site (50). Immunoprecipitation of FCRL6 from pervanadate treated NK or T cells validated its capacity for pY and interactions with multiple pY proteins [unpublished data and (46)], including SHP-2 to the Y371 residue (44). These findings imply an inhibitory role for FCRL6 in cytotoxic lymphocytes. However, an important question for understanding the fundamental biology of FCRL6 is the nature of its extracellular partner(s).

In flow cytometry-based studies, we were unable to detect Ig binding to FCRL6 by surface staining (46). To search for FCRL6 binding partners, we engineered a cell-based GFP reporter system that expressed a chimeric receptor comprised of the FCRL6 ectodomain in frame with the cytoplasmic tail of mouse CD3ζ (51). In co-culture assays with various cell types, the FCRL6-CD3ζ reporter line was activated by antigen presenting cells (APCs) including B lymphocytes and dendritic cells. This work led to identifying MHCII/HLA-DR as an FCRL6 ligand. Furthermore, interactions between FCRL6 and HLA-DR appeared to differ according to the nature of the β chain component of the heterodimer. This observation suggests that binding affinities between FCRL6 and MHCII may differ according to HLA-DR haplotype. Within the context of this finding FCRL6 is not unique. Several other surface immunoreceptors have also been found to bind MHCII (see **Figure 1**). Intriguingly, the LAG-3 immunoreceptor, a CD4 relative also expressed by T cells, is upregulated by exhausted cells in chronic immune conditions including malignancies, and exhibits inhibitory effects through interactions with MHCII/HLA-class II (52, 53). Notably, LAG3 has become an attractive immunotherapeutic target and at least three LAG3-specific ICI mAbs are in development (54). However, recent work has identified additional non-MHCII ligands for LAG3 (55). Furthermore, a third MHCII receptor expressed by NK cells was recently identified. The natural cytotoxicity receptor NKp44, which has different isoforms as well as expression outside the NK lineage (6), was found to bind subsets of MHCII/HLA-DP molecules (56). These findings collectively indicate the existence of multiple immunoreceptors that may serve to modulate relationships between cytotoxic lymphocytes and MHCII-expressing cells in different settings [recently reviewed by (57)].

FCRL6-MHCII INTERACTIONS REPRESS EFFECTOR FUNCTIONS BY CYTOTOXIC LYMPHOCYTES

Efforts to investigate the functional properties of FCRL6 were initially unrevealing. While the genetic regulation of *FCRL6* has not yet been explored in detail, modulation experiments showed that the receptor is down-regulated from the NK cell surface when exposed to activating cytokines such as IL-2, IL-12, or IL-15 and by CD8$^+$ T cells upon anti-CD3 activation [(44) and our unpublished data]. This analysis suggests that FCRL6 is sensitive to cellular activation. Beyond its induction, re-directed killing assays with FCRL6-expressing NK-92 transfectants or freshly isolated NK or CD8$^+$ T cells were used to target receptor-specific mAb-coated P815 cells for cytolysis. Work by our group and the Colonna laboratory found no effect for FCRL6 on NK cell degranulation (surface LAMP1 detection), cytoplasmic IFNγ production, or the anterograde cytolysis efficiency of ^{51}Cr-labeled P815 target cells (44). Furthermore, FCRL6 did not influence activation receptor (CD16)-mediated killing. A potential regulatory role for FCRL6 on cytokine production was also underwhelming. Cultured CD56$^+$ NK cells cross-linked with FCRL6 mAbs demonstrated only slight increases in IFNγ and TNFα production when IL-2 was present, but no impact was

found for IL-4, IL-5, or IL-10 (44). Furthermore, no differences in cytokine production were observed in similar studies with $CD8^+$ T cells +/– anti-CD3 or IL-2. Thus, FCRL6 does not appear markedly influence cytokine generation by these cytotoxic lymphocytes *in vitro*.

In recent studies that identified the upregulation of FCRL6 and LAG3 in the microenvironment of HLA-DR^+ solid tumors [detailed below and (7)], we revisited FCRL6 function with respect to its MHCII ligand. The regulation of NK cell cytotoxicity by MHC class I molecules has been well-characterized, and serves as the basis for the "missing-self" hypothesis (58), but evidence also exists that MHC class II expression can protect target cells from NK cell-mediated killing. Early work demonstrated that enforced expression of HLA-DR by K562 cells, a classic human erythroleukemic MHCII–negative target cell line, could inhibit lysis by freshly isolated human NK cells (59). Furthermore, transplantation of HLA-DR^+ K562 cells into NOD/SCID mice provided protection of tumors from elimination by adoptively transferred human blood NK cells (60). We thus generated NK-92 FCRL6 transductants and used them for cytotoxicity assays by employing HLA-DR^+ K562 target cells. These experiments demonstrated that HLA-DR expression by K562 cells inhibited the cytotoxicity of FCRL6-expressing NK cells (7). Additional support for this inhibitory axis was found for $CD8^+$ T cell responses. By employing an FCRL6 mAb that disrupts HLA-DR binding to FCRL6-CD3ζ reporter cells and in cell staining assays (51), we investigated the effect of FCRL6 blockade during pathogen-specific peptide stimulation *in vitro*. The addition of FCRL6 or PD-L1 blocking mAbs to healthy donor mononuclear cells co-cultured in MHC class I–restricted peptides from CMV, EBV, and influenza virus epitopes, resulted in enhanced frequencies of IFNγ and TNFα cytokines upon restimulation (7). These studies indicate that FCRL6 is a potentially novel ICI target capable of suppressing effector cell activity following engagement with HLA-class II molecules.

FCRL6$^+$ NK AND T LYMPHOCYTES EXPAND IN CHRONIC IMMUNE DISORDERS

The significance of FCRL6 in immune-related disorders was first shown by Wilson et al. who found significantly expanded $FCRL6^+$ effector and effector memory $CD8^+$ T cell frequencies in HIV-1 infected individuals (44). This expression pattern did not seem to correlate with viral titers or $CD4^+$ counts. An increase in circulating $FCRL6^+CD4^+$ cells, which are typically rare among healthy individuals, was also detected in HIV^+ donor samples. Initial evidence for a role in tumor immunology came from studies in CLL. Unlike the other FCRL molecules that are expressed by CLL B cells (34), FCRL6 expression by the B cell clone was undetectable. Instead, increased frequencies of $FCRL6^+$ NK and T lymphocytes were evident in the circulation of CLL patients (46). While blood $CD8^+$ T cells are generally expanded in CLL, T cells derived from these patients are also known to have abnormal function (61, 62). An analysis of CLL donors from our cohort demonstrated that, in addition to a global increase in CD8 T cells, the frequencies of effector and effector memory cell populations were elevated compared to healthy control samples (46). The frequency of $FCRL6^+$ cells among these $CD8^+$ subsets was also greater in CLL patients, as were FCRL6-expressing NK cells and cytotoxic $CD4^+$ cells. These findings suggest that the expansion of $FCRL6^+$ cytotoxic T and NK cells in different disease states could reflect the influence of chronic immune activation on the terminal differentiation of effector cells and contribute to their dysfunction. Furthermore, the increased numbers of cytotoxic cells marked by FCRL6 could reflect a blunted capacity for clearance of the inciting disease process by taking advantage of its potential inhibitory properties. This could infer a role for cytokines or some other systemic influence on the expansion of $FCRL6^+$ cells, but the mechanistic basis for this remains undefined.

FCRL6 EXPRESSION IS UPREGULATED IN SOLID TUMORS EXPRESSING HLA CLASS II

Evidence that an inhibitory receptor restricted to cytotoxic lymphocytes interacts with MHCII/HLA-DR suggests that FCRL6 might have roles in tolerance through its interactions with APCs as well as other non-traditional MHCII-expressing cells including malignancies (see **Figure 1**). The endogenous expression of MHCII/HLA-DR molecules by tumor cells has been observed in many cancers including 40–50% of melanoma cases (63, 64). Importantly, MHCII expression correlates with favorable clinical responses to anti-PD-1 ICI in melanoma, classical Hodgkin's disease, breast cancer, and ovarian cancer (64–67). In breast cancer, PD-1 inhibition is more efficacious in the triple negative subtype (TNBC) (68), but responses vary by PD-1/PD- L1 expression and TIL frequencies (69). Accordingly, MHCII is expressed by ∼30% of TNBC cases (70) and portends increased therapeutic responses and TIL recruitment (71, 72). Despite the clinical favorability of $MHCII^+$ status, chronic ICI therapy typically leads to tumor resistance by adaptation and the delivery of immunosuppressive signals through alternative checkpoint pathways (4).

To investigate these evasion mechanisms, in collaboration with Johnson and Balko, we recently performed transcriptome profiling and tissue staining of patients who developed resistance to PD-1 immunotherapy in melanoma, non-small cell lung cancer (NSCLC), and TNBC (18). This study included melanoma and NSCLC samples ($n = 58$) before and after targeted PD-1 ICI. $MHCII^+$ tumors, confirmed by dual RNA-*in situ* and immunohistochemistry analysis, demonstrated an adaptive immune signature including the upregulation of genes encoding *CD4*, *CD8a*, and ICI receptors. Chiefly among these was LAG3, which was exclusively expressed by infiltrating T cells with a bias toward $CD8^+$ rather than $CD4^+$ cells. A comparison of melanoma samples derived from patients pre and post anti-PD-1 treatment revealed increased frequencies of $LAG3^+$ TILs as a function of developing adaptive resistance in paired specimens. High levels of $LAG3^+$ TILs were also found in $MHCII^+$ TNBC ($n = 112$) and were associated with $CD4^+$ infiltrates.

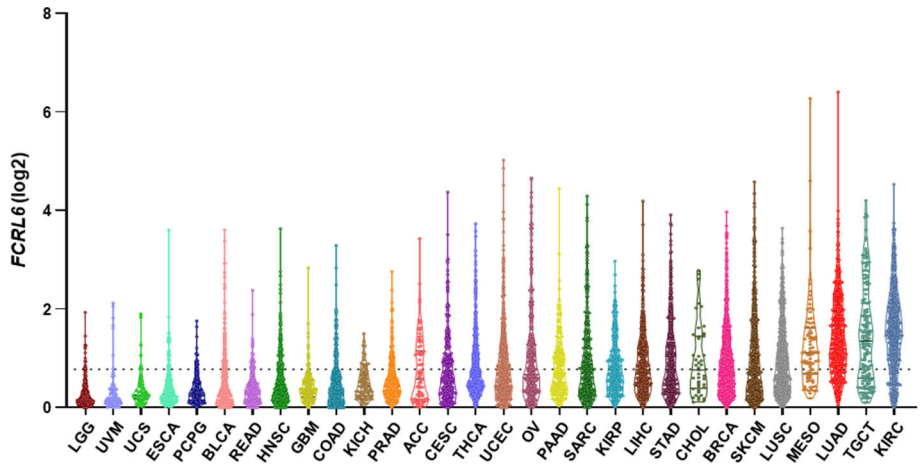

FIGURE 2 | *FCRL6* expression among various cancers. A violin plot demonstrating the expression (log2) of *FCRL6* (ENSG00000181036) in non-hematopoietic cancers ($n = 30$) from The Cancer Genome Atlas (TCGA) (73). LGG, lower grade glioma ($n = 529$); UVM, uveal melanoma ($n = 80$); UCS, uterine carcinosarcoma ($n = 56$); ESCA, esophageal carcinoma ($n = 173$); PCPG, pheochromocytoma and paraganglioma ($n = 186$); BLCA, bladder carcinoma ($n = 427$); READ, rectum adenocarcinoma ($n = 177$); HNSC, head and neck squamous cell carcinoma ($n = 546$); GBM, glioblastoma ($n = 174$); COAD, colon adenocarcinoma ($n = 499$); KICH, kidney chromophobe ($n = 89$); PRAD, prostate adenocarcinoma ($n = 548$); ACC, adrenocortical carcinoma ($n = 79$); CESC, cervical squamous carcinoma ($n = 309$); THCA, thyroid carcinoma ($n = 568$); UCEC, uterine corpus endometrial carcinoma ($n = 579$); OV, ovarian serous cystadenocarcinoma ($n = 379$); PAAD, pancreatic adenocarcinoma ($n = 182$); SARC, sarcoma ($n = 265$); KIRP, kidney renal papillary cell carcinoma ($n = 320$); LIHC, liver hepatocellular carcinoma ($n = 424$); STAD, stomach adenocarcinoma ($n = 407$); CHOL, cholangiocarcinoma ($n = 45$); BRCA, breast carcinoma ($n = 1,205$); SKCM, skin cutaneous melanoma ($n = 472$); LUSC, lung squamous cell carcinoma ($n = 551$); MESO, mesothelioma ($n = 86$); LUAD, lung adenocarcinoma ($n = 573$); TGCT, testicular germ cell tumor ($n = 156$); and KIRC, kidney renal clear cell carcinoma ($n = 599$). The median and quartiles are demarcated (black lines) for samples in the plot of each cancer subtype. RPKM transcript data were downloaded from the R2: Genomics Analysis and Visualization Platform (http://r2.amc.nl), plotted using Prism software, and ordered by median values of expression. The dotted black line indicates the mean expression value (*FCRL6* log2 = 0.78) of the 30 cancer subtypes. Note that THCA and cancers to the right on the plot exceed the mean.

Given the known interaction between LAG3 and MHCII (52, 53), these findings implied that tumors may exploit MHCII expression to blunt eradication by TILs. This hypothesis was further supported by studies in an *in vivo* MMTV-neu breast cancer mouse model. Enforced MHCII expression generally promoted tumor rejection and CD4 recruitment, but in mice that formed refractory tumors, there was evidence of adaptive resistance including the upregulation of chemokines that foster T cell recruitment as well as the *Pdcd1* (Pd-1) and *Lag3* inhibitory receptor genes. Importantly, anti-tumor immunity was enhanced by treatment with a combination of anti-PD-1 and LAG3 ICI.

With clinical and mechanistic evidence that MHCII$^+$ tumors may actively suppress effector cell cytotoxicity, we turned to the possibility that FCRL6 may operate similarly in this process. As detailed above, FCRL6 suppressed NK cell cytotoxicity of HLA-DR expressing target cells and enhanced effector T cell cytokine production following Ab-mediated blockade. Like LAG3, *FCRL6* was more highly expressed by MHCII$^+$ melanomas and NSCLCs. While a similar trend was evident for *FCRL3*, it did not reach significance. A linear relationship was also evident for *LAG3* and *FCRL6* with the degree of HLA-DR$^+$ tumor cells. Similarly, both *FCRL6* transcript and protein expression was elevated in melanoma samples from patients who experienced relapse after progression on anti-PD-1 ICI therapy. Consequently, FCRL6$^+$ infiltrates also correlated with LAG3 and HLA-DR status in TNBC. Staining of TNBC specimens showed that TIL co-expression of FCRL6 and LAG3 was strongly correlated with elevated tumor-specific HLA-DR expression. Finally, in these breast tumors, an inverse correlation was found for FCRL6 and LAG3 reactivity with the fraction of granzyme B$^+$ cytotoxic CD8$^+$ cells present. This disclosed a potential suppressive role for these ICI receptors in the tumor microenvironment. These findings collectively implicate a novel inhibitory role for FCRL6 in cell-mediated responses to MHCII$^+$ tumors and its potential as a new ICI target that influences adaptive resistance mechanisms to anti-PD-1 therapy.

FCRL6 UPREGULATION BY MALIGNANCIES HAS PROGNOSTIC SIGNIFICANCE

Given its discrete expression by cytotoxic T and NK lymphocytes and newfound role in tumor immunity, we explored the possibility that detection of *FCRL6* in the tumor microenvironment could have prognostic clinical significance. To pursue this hypothesis, we analyzed *FCRL6* transcript expression from RNA-sequencing data performed on 30 non-hematopoietic cancer types (10,683 samples) from TCGA (73) (**Figure 2**). *FCRL6* expression (log2) was heterogeneous among these cancer types but, in accord with our recent findings (7), lung adenocarcinomas (LUAD), cutaneous melanomas (SKCM), and breast carcinomas (BRCA) were among the tumors with higher median expression levels. We next assessed survival in these cancer types according to *FCRL6* expression. By

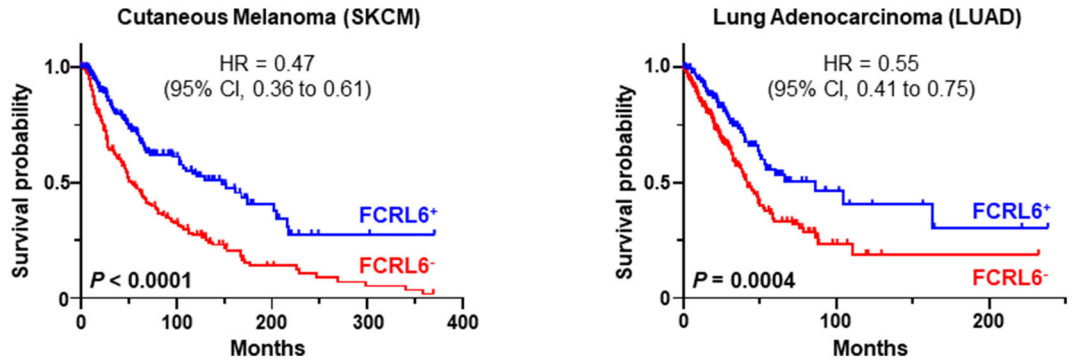

FIGURE 3 | *FCRL6* overexpression predicts favorable overall survival (OS) in cutaneous melanoma and lung adenocarcinoma. Kaplan-Meier plots demonstrating the relationship between *FCRL6* gene expression and patient clinical outcomes by OS. TCGA (reads per kilobase million—RPKM) transcript data for SKCM ($n = 458$) and LUAD ($n = 497$) were downloaded from the publicly available cBioPortal (https://www.cbioportal.org/) database (74) for analysis with the R2: Genomics Analysis and Visualization Platform (http://r2.amc.nl). Optimal threshold cut-off values for determining high or low *FCRL6* expression as a continuous variable were compared using Cox Regression analysis and the R2 Genomics platform. Comparisons of OS curves and *P*-values were made using the Log-rank test. Hazard ratio (HR) and 95% confidence interval (CI) for comparisons between the groups are indicated. Kaplan-Meier plots were generated using Prism software.

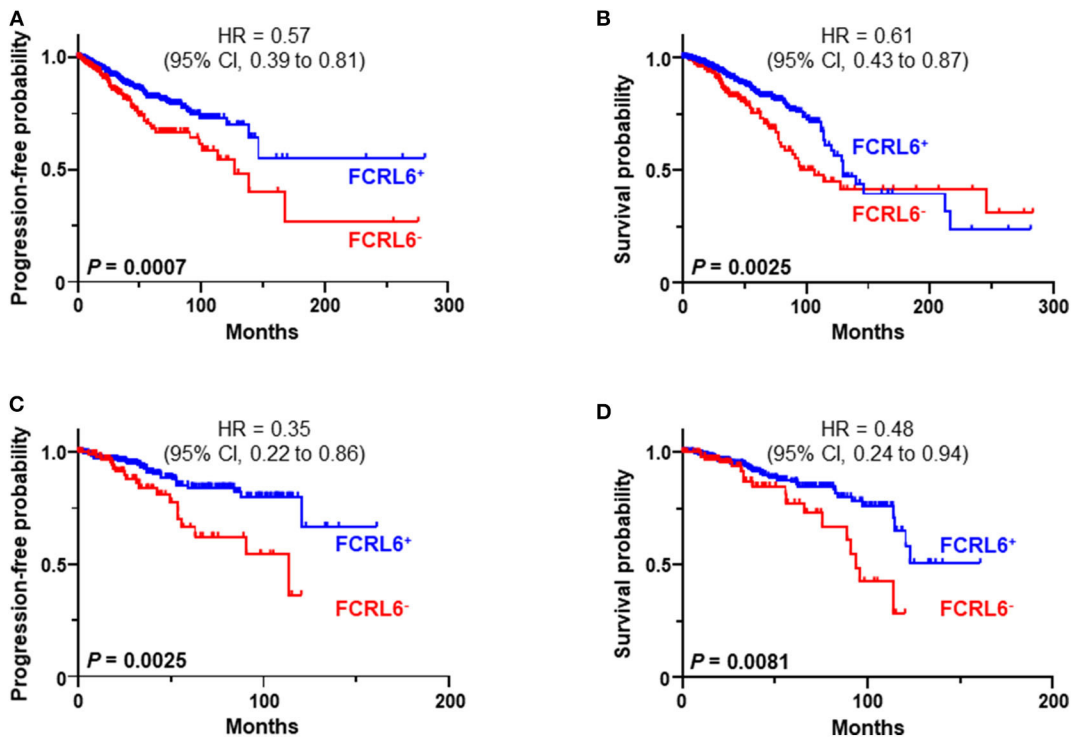

FIGURE 4 | *FCRL6* overexpression predicts favorable progression free (PFS) and overall survival (OS) in breast carcinoma. Kaplan-Meier plots demonstrating the relationship between *FCRL6* gene expression and patient clinical outcomes by PFS and OS for **(A,B)** all breast carcinomas (BRCA, $n = 1,067$) and **(C,D)** Her2 negative samples ($n = 550$). TCGA (reads per kilobase million—RPKM) transcript data for BRCA were downloaded from the publically available cBioPortal (https://www.cbioportal.org/) database (74) for analysis with the R2: Genomics Analysis and Visualization Platform (http://r2.amc.nl). Optimal threshold cut-off values for determining high or low *FCRL6* expression as a continuous variable were compared using Cox Regression analysis and the R2 Genomics platform. Comparisons of PFS and OS curves and *P*-values were made using the Log-rank test. HR and 95% CI for comparisons between the groups are indicated. Kaplan-Meier plots were generated using Prism software.

employing Cox Regression analysis along with the R2: Genomics Analysis and Visualization Platform (http://r2.amc.nl), we defined optimized cut-off values to segregate samples according to *FCRL6* expression. Kaplan-Meier plots demonstrated that higher *FCRL6* expression predicted increased overall survival (OS) in SKMM (n = 458) and LUAD ($n = 497$) TCGA samples

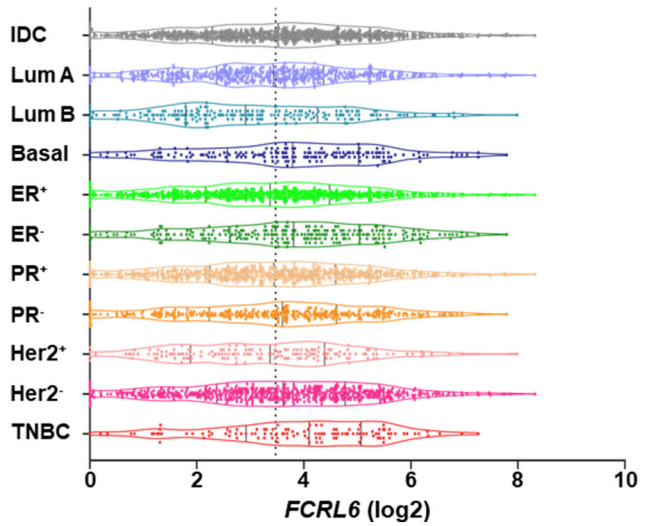

FIGURE 5 | Among breast cancer subtypes *FCRL6* transcript expression is highest in TNBC. A violin plot demonstrating the mean expression (log2) of *FCRL6* (ENSG00000181036) among TCGA BRCA tumor subtypes downloaded from the publicly available cBioPortal (https://www.cbioportal.org/) database (74). Intraductal carcinoma (IDC, $n = 976$), Luminal A (Lum A, $n = 499$), Luminal B (Lum B, $n = 197$), Basal ($n = 171$), estrogen receptor positive (ER^+, $n = 795$), ER negative (ER^-, $n = 237$), progesterone receptor positive (PR^+, $n = 687$), PR negative (PR^-, $n = 342$), Her2 receptor positive ($Her2^+$, $n = 160$) Her2 receptor negative ($Her2^-$, $n = 557$), and triple negative breast cancer (TNBC, $n = 115$). The median and quartiles are demarcated (black lines) for samples in the plot of each subtype. Mean (*x*) *FCRL6* expression ± SEM: TNBC (3.905 ± 0.1455), ER^- (3.76 ± 0.1104), Basal (3.733 ± 0.1296), $Her2^-$ (3.543 ± 0.07162), IDC (3.466 ± 0.05328), PR^- (3.449 ± 0.09192), PR^+ 3.396 ± 0.06334), Lum A (3.384 ± 0.07137), ER^+ (3.316 ± 0.05859), $Her2^+$ (3.263 ± 0.1262), and Lum B (3.022 ± 0.1196). Note the dotted black line indicates the mean value (*FCRL6* log2 = 3.47) of the 11 breast cancer subtypes.

(**Figure 3**). In SKMM, median OS was 2.7-fold higher for patients with elevated *FCRL6* expression. Patients with *FCRL6*-positive tumors had a median OS of 148.2 months vs. 54.4 months for samples with low *FCRL6* transcripts (HR = 0.47, CI = 0.36–0.61, $P < 0.0001$). In LUAD, elevated *FCRL6* predicted a 2.1-fold higher median OS. $FCRL6^+$ tumors exhibited a median OS of 86.0 months vs. 41.7 months for $FCRL6^-$ samples (HR = 0.55, CI = 0.41–0.75, $P = 0.0004$). Consistent with the known responsiveness of these tumors to ICI therapy and the TIL concentrations in the tumor microenvironment (75–82), these findings indicate that elevated *FCRL6* expression confers a generally favorable prognosis for the OS of patients with these tumors.

We next investigated *FCRL6* expression among BRCA ($n = 1{,}067$) TCGA samples (**Figure 4**). *FCRL6* was able to predict progression free survival (PFS) among all BRCA samples with elevated transcript expression again correlating with a favorable outcome (**Figure 4A**). For *FCRL6*-high cases the median PFS was not reached for this TCGA BRCA cohort, while the median PFS for *FCRL6*-low cases was 113.8 months (HR = 0.44, CI = 0.22–0.86, $P = 0.0025$). Interestingly, analysis of OS indicated an advantage for patients with tumors possessing high *FCRL6* transcripts (**Figure 4B**). Median OS was 129.7 months for *FCRL6*-high cases and 107.2 months for patient samples with *FCRL6*-low expression (HR = 0.61, CI = 0.43–0.97, $P = 0.0025$). This benefit across this entire series of TCGA BRCA tumors appeared evident for up to 12 years after diagnosis, but for patients with *FCRL6*-high samples that lived beyond this time period ($n = 10/19$), this factor became detrimental. Notably, this is a minority of patients from a heterogeneous cohort of samples and mortality at later time points beyond diagnosis and treatment could be multifactorial for this group. With regard to the disease status of these 10 individuals, six were tumor-free at death, two died with positive tumor status, and data was not available for two cases. We additionally assessed TCGA BRCA samples from patients with Her2 negative status ($n = 550$) (**Figures 4C,D**). Elevated *FCRL6* expression in patients with Her2 negative tumors was prognostically advantageous for both PFS and OS. Median PFS for patients with *FCRL6* high Her2 negative tumors was not reached while for low expressors it was 113.8 months (HR = 0.44, CI = 0.22–0.86, $P = 0.0025$). Median OS for *FCRL6*-high Her2 negative BRCA tumors was also not reached and for *FCRL6*-low expression was 93.8 months (HR = 0.48, CI = 0.25–0.94, $P = 0.0081$). Elevated FCRL6 expression also portended significantly higher PFS and OS in patients with intraductal breast carcinoma ($n = 765$) and estrogen positive ($n = 782$) tumor status (data not shown). To better understand the distribution of $FCRL6^+$ TILs within the context of BRCA heterogeneity, we analyzed the mean expression levels of *FCRL6* among 11 different BRCA subtypes. The highest *FCRL6* transcripts were found in TNBC, followed by ER^- > Basal > $Her2^-$ tumor samples (**Figure 5**). These findings parallel the known elevated frequency of cytotoxic lymphocytes and NK cell TILs in TNBC that are associated with an improved prognosis as well as the sensitivity of these tumors to ICI and neoadjuvant chemotherapy (69, 72, 83–85). While analysis of FCRL6 protein expression by primary samples would be helpful for validation, given its restricted expression by cytotoxic lymphocytes, these findings at the transcript level support the potential utility of *FCRL6* as a prognostic marker and ICI target.

CONCLUDING REMARKS

In summary, members of the FCRL family are preferentially expressed by B cells and generally exert inhibitory tyrosine-based regulation on BCR signaling. Given their expression by B cells there is a growing appreciation of their roles in lymphoproliferative disorders and potential as immunotherapeutic targets. In contrast to FCRL1–5, FCRL6 has a distinct expression pattern outside the B lineage among cytotoxic T and NK lymphocytes. Furthermore, its elevated expression in the tumor microenvironment, including NSCLC, melanoma, and breast cancer, significantly correlates with improved PFS and OS. However, its ITIM-based repressive function in these cells becomes operative upon engagement with its partner MHCII/HLA-DR. This newfound axis has growing

significance in tumor immunology as endogenous HLA class II expression by cancer cells has been found to correlate with increased TIL numbers, responsiveness to anti PD-1 directed ICI, and a more favorable prognosis. However, some tumors that develop resistance to ICI appear to upregulate HLA class II to blunt recognition by cytotoxic cells expressing FCRL6 as well as other MHCII-binding molecules (e.g., LAG3 and NKp44). Thus, FCRL6 may serve as a novel ICI target. Future studies that model its *in vivo* regulation are required to investigate this possibility, but are hampered by the interspecies diversity of this FCRL representative in mice and humans. Additionally, the distinct MHCII allotypes that FCRL6 interacts with, and how these relationships impact cytotoxic cells during homeostasis in tolerance with APCs vs. disease states, are important topics for future study.

AUTHOR CONTRIBUTIONS

RSD wrote and edited the manuscript.

FUNDING

This work was supported in part by the V Foundation for Cancer Research, Breast Cancer Research Foundation of Alabama, and the UAB Cancer Immunobiology Program.

ACKNOWLEDGMENTS

The author thanks Dr. Yufeng Li for statistical advice and Peter D. Burrows and Robert S. Welner for critically reading the manuscript.

REFERENCES

1. Balar AV, Weber JS. PD-1 and PD-L1 antibodies in cancer: current status and future directions. *Cancer Immunol Immunother.* (2017) 66:551–64. doi: 10.1007/s00262-017-1954-6
2. Postow MA, Callahan MK, Wolchok JD. Immune checkpoint blockade in cancer therapy. *J Clin Oncol.* (2015) 33:1974–82. doi: 10.1200/JCO.2014.59.4358
3. Haslam A, Prasad V. Estimation of the percentage of US patients with cancer who are eligible for and respond to checkpoint inhibitor immunotherapy drugs. *JAMA Netw Open.* (2019) 2:e192535. doi: 10.1001/jamanetworkopen.2019.2535
4. Koyama S, Akbay EA, Li YY, Herter-Sprie GS, Buczkowski KA, Richards WG, et al. Adaptive resistance to therapeutic PD-1 blockade is associated with upregulation of alternative immune checkpoints. *Nat Commun.* (2016) 7:10501. doi: 10.1038/ncomms10501
5. Wang DY, Eroglu Z, Ozgun A, Leger PD, Zhao S, Ye F, et al. Clinical features of acquired resistance to anti-pd-1 therapy in advanced melanoma. *Cancer Immunol Res.* (2017) 5:357–62. doi: 10.1158/2326-6066.CIR-16-0287
6. Cantoni C, Bottino C, Vitale M, Pessino A, Augugliaro R, Malaspina A, et al. NKp44, a triggering receptor involved in tumor cell lysis by activated human natural killer cells, is a novel member of the immunoglobulin superfamily. *J Exp Med.* (1999) 189:787–96. doi: 10.1084/jem.189.5.787
7. Johnson DB, Nixon MJ, Wang Y, Wang DY, Castellanos E, Estrada MV, et al. Tumor-specific MHC-II expression drives a unique pattern of resistance to immunotherapy via LAG-3/FCRL6 engagement. *JCI insight.* (2018) 3:e120360. doi: 10.1172/jci.insight.120360
8. Davis RS. Fc receptor-like molecules. *Annu Rev Immunol.* (2007) 25:525–60. doi: 10.1146/annurev.immunol.25.022106.141541
9. Li FJ, Won WJ, Becker EJ Jr, Easlick JL, Tabengwa EM, Li R, et al. Emerging roles for the FCRL family members in lymphocyte biology and disease. *Curr Top Microbiol Immunol.* (2014) 382:29–50. doi: 10.1007/978-3-319-07911-0_2
10. Bulian P, Shanafelt TD, Fegan C, Zucchetto A, Cro L, Nuckel H, et al. CD49d is the strongest flow cytometry-based predictor of overall survival in chronic lymphocytic leukemia. *J Clin Oncol.* (2014) 32:897–904. doi: 10.1200/JCO.2013.50.8515
11. Polson AG, Zheng B, Elkins K, Chang W, Du C, Dowd P, et al. Expression pattern of the human FcRH/IRTA receptors in normal tissue and in B-chronic lymphocytic leukemia. *Int Immunol.* (2006) 18:1363–73. doi: 10.1093/intimm/dxl069
12. Nagata S, Ise T, Pastan I. Fc receptor-like 3 protein expressed on IL-2 nonresponsive subset of human regulatory T cells. *J Immunol.* (2009) 182:7518–26. doi: 10.4049/jimmunol.0802230
13. Swainson LA, Mold JE, Bajpai UD, McCune JM. Expression of the autoimmune susceptibility gene FcRL3 on human regulatory T cells is associated with dysfunction and high levels of programmed cell death-1. *J Immunol.* (2010) 184:3639–47. doi: 10.4049/jimmunol.0903943
14. Leu CM, Davis RS, Gartland LA, Fine WD, Cooper MD. FcRH1: an activation coreceptor on human B cells. *Blood.* (2005) 105:1121–6. doi: 10.1182/blood-2004-06-2344
15. Zhao X, Xie H, Zhao M, Ahsan A, Li X, Wang F, et al. Fc receptor-like 1 intrinsically recruits c-Abl to enhance B cell activation and function. *Sci Adv.* (2019) 5:eaaw0315. doi: 10.1126/sciadv.aaw0315
16. Davis RS, Stephan RP, Chen CC, Dennis G Jr, Cooper MD. Differential B cell expression of mouse Fc receptor homologs. *Int Immunol.* (2004) 16:1343–53. doi: 10.1093/intimm/dxh137
17. Ehrhardt GR, Davis RS, Hsu JT, Leu CM, Ehrhardt A, Cooper MD. The inhibitory potential of Fc receptor homolog 4 on memory B cells. *Proc Natl Acad Sci USA.* (2003) 100:13489–94. doi: 10.1073/pnas.1935944100
18. Haga CL, Ehrhardt GR, Boohaker RJ, Davis RS, Cooper MD. Fc receptor-like 5 inhibits B cell activation via SHP-1 tyrosine phosphatase recruitment. *Proc Natl Acad Sci USA.* (2007) 104:9770–5. doi: 10.1073/pnas.0703354104
19. Jackson TA, Haga CL, Ehrhardt GR, Davis RS, Cooper MD. FcR-like 2 Inhibition of B cell receptor-mediated activation of B cells. *J Immunol.* (2010) 185:7405–12. doi: 10.4049/jimmunol.1002305
20. Kochi Y, Myouzen K, Yamada R, Suzuki A, Kurosaki T, Nakamura Y, et al. FCRL3, an autoimmune susceptibility gene, has inhibitory potential on B-cell receptor-mediated signaling. *J Immunol.* (2009) 183:5502–10. doi: 10.4049/jimmunol.0901982
21. Zhu Z, Li R, Li H, Zhou T, Davis RS. FCRL5 exerts binary and compartment-specific influence on innate-like B-cell receptor signaling. *Proc Natl Acad Sci USA.* (2013) 110:E1282–90. doi: 10.1073/pnas.1215156110
22. Won WJ, Foote JB, Odom MR, Pan J, Kearney JF, Davis RS. Fc receptor homolog 3 is a novel immunoregulatory marker of marginal zone and B1 B cells. *J Immunol.* (2006) 177:6815–23. doi: 10.4049/jimmunol.177.10.6815
23. Nimmerjahn F, Ravetch JV. Fcgamma receptors: old friends and new family members. *Immunity.* (2006) 24:19–28. doi: 10.1016/j.immuni.2005.11.010
24. Sohn HW, Krueger PD, Davis RS, Pierce SK. FcRL4 acts as an adaptive to innate molecular switch dampening BCR signaling and enhancing TLR signaling. *Blood.* (2011) 118:6332–41. doi: 10.1182/blood-2011-05-353102
25. Li FJ, Schreeder DM, Li R, Wu J, Davis RS. FCRL3 promotes TLR9-induced B-cell activation and suppresses plasma cell differentiation. *Eur J Immunol.* (2013) 43:2980–92. doi: 10.1002/eji.201243068
26. Liu Y, Bezverbnaya K, Zhao T, Parsons MJ, Shi M, Treanor B, et al. Involvement of the HCK and FGR src-family kinases in FCRL4-mediated immune regulation. *J Immunol.* (2015) 194:5851–60. doi: 10.4049/jimmunol.1401533
27. Wilson TJ, Fuchs A, Colonna M. Cutting edge: human FcRL4 and FcRL5 are receptors for IgA and IgG. *J Immunol.* (2012) 188:4741–5. doi: 10.4049/jimmunol.1102651
28. Hatzivassiliou G, Miller I, Takizawa J, Palanisamy N, Rao PH, Iida S, et al. IRTA1 and IRTA2, novel immunoglobulin superfamily receptors expressed in B cells and involved in chromosome 1q21 abnormalities in B cell malignancy. *Immunity.* (2001) 14:277–89. doi: 10.1016/S1074-7613(01)00109-1

29. Franco A, Damdinsuren B, Ise T, Dement-Brown J, Li H, Nagata S, et al. Human Fc receptor-like 5 binds intact IgG via mechanisms distinct from those of Fc receptors. *J Immunol.* (2013) 190:5739–46. doi: 10.4049/jimmunol.1202860
30. Agarwal S, Kraus Z, Dement-Brown J, Alabi O, Starost K, Tolnay M. Human Fc receptor-like 3 inhibits regulatory T cell function and binds secretory IgA. *Cell Rep.* (2020) 30:1292–9.e3. doi: 10.1016/j.celrep.2019.12.099
31. Miller I, Hatzivassiliou G, Cattoretti G, Mendelsohn C, Dalla-Favera R. IRTAs: a new family of immunoglobulinlike receptors differentially expressed in B cells. *Blood.* (2002) 99:2662–9. doi: 10.1182/blood.V99.8.2662
32. Alizadeh AA, Eisen MB, Davis RE, Ma C, Lossos IS, Rosenwald A, et al. Distinct types of diffuse large B-cell lymphoma identified by gene expression profiling. *Nature.* (2000) 403:503–11. doi: 10.1038/35000501
33. Ise T, Nagata S, Kreitman RJ, Wilson WH, Wayne AS, Stetler-Stevenson M, et al. Elevation of soluble CD307 (IRTA2/FcRH5) protein in the blood and expression on malignant cells of patients with multiple myeloma, chronic lymphocytic leukemia, and mantle cell lymphoma. *Leukemia.* (2007) 21:169–74. doi: 10.1038/sj.leu.2404445
34. Li FJ, Ding S, Pan J, Shakhmatov MA, Kashentseva E, Wu J, et al. FCRL2 expression predicts IGHV mutation status and clinical progression in chronic lymphocytic leukemia. *Blood.* (2008) 112:179–87. doi: 10.1182/blood-2008-01-131359
35. Shea LK, Honjo K, Redden DT, Tabengwa E, Li R, Li FJ, et al. Fc receptor-like 2 (FCRL2) is a novel marker of low-risk CLL and refines prognostication based on IGHV mutation status. *Blood Cancer J.* (2019) 9:47. doi: 10.1038/s41408-019-0207-7
36. Damle RN, Wasil T, Fais F, Ghiotto F, Valetto A, Allen SL, et al. Ig V gene mutation status and CD38 expression as novel prognostic indicators in chronic lymphocytic leukemia. *Blood.* (1999) 94:1840–7. doi: 10.1182/blood.V94.6.1840
37. Hamblin TJ, Orchard JA, Ibbotson RE, Davis Z, Thomas PW, Stevenson FK, et al. CD38 expression and immunoglobulin variable region mutations are independent prognostic variables in chronic lymphocytic leukemia, but CD38 expression may vary during the course of the disease. *Blood.* (2002) 99:1023–9. doi: 10.1182/blood.V99.3.1023
38. Elkins K, Zheng B, Go M, Slaga D, Du C, Scales SJ, et al. FcRL5 as a target of antibody-drug conjugates for the treatment of multiple myeloma. *Mol Cancer Ther.* (2012) 11:2222–32. doi: 10.1158/1535-7163.MCT-12-0087
39. Stewart AK, Krishnan AY, Singhal S, Boccia RV, Patel MR, Niesvizky R, et al. Phase I study of the anti-FcRH5 antibody-drug conjugate DFRF4539A in relapsed or refractory multiple myeloma. *Blood Cancer J.* (2019) 9:17. doi: 10.1038/s41408-019-0178-8
40. Li J, Stagg NJ, Johnston J, Harris MJ, Menzies SA, DiCara D, et al. Membrane-proximal epitope facilitates efficient T cell synapse formation by anti-FcRH5/CD3 and is a requirement for myeloma cell killing. *Cancer Cell.* (2017) 31:383–95. doi: 10.1016/j.ccell.2017.02.001
41. Imboden JB, Eriksson EC, McCutcheon M, Reynolds CW, Seaman WE. Identification and characterization of a cell-surface molecule that is selectively induced on rat lymphokine-activated killer cells. *J Immunol.* (1989) 143:3100–3.
42. Guselnikov SV, Ershova SA, Mechetina LV, Najakshin AM, Volkova OY, Alabyev BY, et al. A family of highly diverse human and mouse genes structurally links leukocyte FcR, gp42 and PECAM-1. *Immunogenetics.* (2002) 54:87–95. doi: 10.1007/s00251-002-0436-x
43. Davis RS, Dennis G Jr., Odom MR, Gibson AW, Kimberly RP, et al. Fc receptor homologs: newest members of a remarkably diverse Fc receptor gene family. *Immunol Rev.* (2002) 190:123–36. doi: 10.1034/j.1600-065X.2002.19009.x
44. Wilson TJ, Presti RM, Tassi I, Overton ET, Cella M, Colonna M. FcRL6, a new ITIM-bearing receptor on cytolytic cells, is broadly expressed by lymphocytes following HIV-1 infection. *Blood.* (2007) 109:3786–93. doi: 10.1182/blood-2006-06-030023
45. Honjo K, Won WJ, King RG, Ianov L, Crossman DK, Easlick JL, et al. Fc Receptor-Like 6 (FCRL6) discloses progenitor B cell heterogeneity that correlates with pre-BCR dependent and independent pathways of natural antibody selection. *Front Immunol.* (2020) 11:82. doi: 10.3389/fimmu.2020.00082
46. Schreeder DM, Pan J, Li FJ, Vivier E, Davis RS. FCRL6 distinguishes mature cytotoxic lymphocytes and is upregulated in patients with B-cell chronic lymphocytic leukemia. *Eur J Immunol.* (2008) 38:3159–66. doi: 10.1002/eji.200838516
47. Vivier E, Sorrell JM, Ackerly M, Robertson MJ, Rasmussen RA, Levine H, et al. Developmental regulation of a mucinlike glycoprotein selectively expressed on natural killer cells. *J Exp Med.* (1993) 178:2023–33. doi: 10.1084/jem.178.6.2023
48. Angelini DF, Borsellino G, Poupot M, Diamantini A, Poupot R, Bernardi G, et al. FcgammaRIII discriminates between 2 subsets of Vgamma9Vdelta2 effector cells with different responses and activation pathways. *Blood.* (2004) 104:1801–7. doi: 10.1182/blood-2004-01-0331
49. Appay V, Zaunders JJ, Papagno L, Sutton J, Jaramillo A, Waters A, et al. Characterization of CD4(+) CTLs *ex vivo*. *J Immunol.* (2002) 168:5954–8. doi: 10.4049/jimmunol.168.11.5954
50. Kulemzin SV, Zamoshnikova AY, Yurchenko MY, Vitak NY, Najakshin AM, Fayngerts SA, et al. FCRL6 receptor: expression and associated proteins. *Immunol Lett.* (2011) 134:174–82. doi: 10.1016/j.imlet.2010.09.023
51. Schreeder DM, Cannon JP, Wu J, Li R, Shakhmatov MA, Davis RS. Cutting edge: FcR-like 6 is an MHC class II receptor. *J Immunol.* (2010) 185:23–7. doi: 10.4049/jimmunol.1000832
52. Baixeras E, Huard B, Miossec C, Jitsukawa S, Martin M, Hercend T, et al. Characterization of the lymphocyte activation gene 3-encoded protein. A new ligand for human leukocyte antigen class II antigens. *J Exp Med.* (1992) 176:327–37. doi: 10.1084/jem.176.2.327
53. Huard B, Prigent P, Pages F, Bruniquel D, Triebel F. T cell major histocompatibility complex class II molecules down-regulate CD4+ T cell clone responses following LAG-3 binding. *Eur J Immunol.* (1996) 26:1180–6. doi: 10.1002/eji.1830260533
54. Andrews LP, Marciscano AE, Drake CG, Vignali DA. LAG3 (CD223) as a cancer immunotherapy target. *Immunol Rev.* (2017) 276:80–96. doi: 10.1111/imr.12519
55. Wang J, Sanmamed MF, Datar I, Su TT, Ji L, Sun J, et al. Fibrinogen-like protein 1 Is a major immune inhibitory ligand of LAG-3. *Cell.* (2019) 176:334–47.e12. doi: 10.1016/j.cell.2018.11.010
56. Niehrs A, Garcia-Beltran WF, Norman PJ, Watson GM, Holzemer A, Chapel A, et al. A subset of HLA-DP molecules serve as ligands for the natural cytotoxicity receptor NKp44. *Nat Immunol.* (2019) 20:1129–37. doi: 10.1038/s41590-019-0448-4
57. Niehrs A, Altfeld M. Regulation of NK-cell function by HLA Class II. *Front Cell Infect Microbiol.* (2020) 10:55. doi: 10.3389/fcimb.2020.00055
58. Ljunggren HG, Karre K. In search of the 'missing self': MHC molecules and NK cell recognition. *Immunol Today.* (1990) 11:237–44. doi: 10.1016/0167-5699(90)90097-S
59. Jiang YZ, Couriel D, Mavroudis DA, Lewalle P, Malkovska V, Hensel NF, et al. Interaction of natural killer cells with MHC class II: reversal of HLA-DR1-mediated protection of K562 transfectant from natural killer cell-mediated cytolysis by brefeldin-A. *Immunology.* (1996) 87:481–6. doi: 10.1046/j.1365-2567.1996.483556.x
60. Weichold FF, Jiang YZ, Dunn DE, Bloom M, Malkovska V, Hensel NF, et al. Regulation of a graft-versus-leukemia effect by major histocompatibility complex class II molecules on leukemia cells: HLA-DR1 expression renders K562 cell tumors resistant to adoptively transferred lymphocytes in severe combined immunodeficiency mice/nonobese diabetic mice. *Blood.* (1997) 90:4553–8. doi: 10.1182/blood.V90.11.4553
61. Scrivener S, Goddard RV, Kaminski ER, Prentice AG. Abnormal T-cell function in B-cell chronic lymphocytic leukaemia. *Leuk Lymphoma.* (2003) 44:383–9. doi: 10.1080/1042819021000029993
62. Gorgun G, Holderried TA, Zahrieh D, Neuberg D, Gribben JG. Chronic lymphocytic leukemia cells induce changes in gene expression of CD4 and CD8 T cells. *J Clin Invest.* (2005) 115:1797–805. doi: 10.1172/JCI24176
63. Axelrod ML, Cook RS, Johnson DB, Balko JM. Biological consequences of MHC-II expression by tumor cells in cancer. *Clin Cancer Res.* (2019) 25:2392–402. doi: 10.1158/1078-0432.CCR-18-3200
64. Johnson DB, Estrada MV, Salgado R, Sanchez V, Doxie DB, Opalenik SR, et al. Melanoma-specific MHC-II expression represents a tumour-autonomous phenotype and predicts response to anti-PD-1/PD-L1 therapy. *Nat Commun.* (2016) 7:10582. doi: 10.1038/ncomms10582
65. Roemer MGM, Redd RA, Cader FZ, Pak CJ, Abdelrahman S, Ouyang J, et al. Major histocompatibility complex class ii and programmed

death ligand 1 expression predict outcome after programmed death 1 blockade in classic hodgkin lymphoma. *J Clin Oncol.* (2018) 36:942–50. doi: 10.1200/JCO.2017.77.3994

66. Rodig SJ, Gusenleitner D, Jackson DG, Gjini E, Giobbie-Hurder A, Jin C, et al. MHC proteins confer differential sensitivity to CTLA-4 and PD-1 blockade in untreated metastatic melanoma. *Sci Transl Med.* (2018) 10:aar3342. doi: 10.1126/scitranslmed.aar3342
67. Callahan MJ, Nagymanyoki Z, Bonome T, Johnson ME, Litkouhi B, Sullivan EH, et al. Increased HLA-DMB expression in the tumor epithelium is associated with increased CTL infiltration and improved prognosis in advanced-stage serous ovarian cancer. *Clin Cancer Res.* (2008) 14:7667–73. doi: 10.1158/1078-0432.CCR-08-0479
68. Santa-Maria CA, Nanda R. Immune checkpoint inhibitor therapy in breast cancer. *J Natl Compr Canc Netw.* (2018) 16:1259–68. doi: 10.6004/jnccn.2018.7046
69. Nanda R, Chow LQ, Dees EC, Berger R, Gupta S, Geva R, et al. Pembrolizumab in patients with advanced triple-negative breast cancer: phase Ib keynote-012 study. *J Clin Oncol.* (2016) 34:2460–7. doi: 10.1200/JCO.2015.64.8931
70. Park IA, Hwang SH, Song IH, Heo SH, Kim YA, Bang WS, et al. Expression of the MHC class II in triple-negative breast cancer is associated with tumor-infiltrating lymphocytes and interferon signaling. *PLoS ONE.* (2017) 12:e0182786. doi: 10.1371/journal.pone.0182786
71. Forero A, Li Y, Chen D, Grizzle WE, Updike KL, Merz ND, et al. Expression of the MHC class II pathway in triple-negative breast cancer tumor cells is associated with a good prognosis and infiltrating lymphocytes. *Cancer Immunol Res.* (2016) 4:390–9. doi: 10.1158/2326-6066.CIR-15-0243
72. Loi S, Dushyanthen S, Beavis PA, Salgado R, Denkert C, Savas P, et al. RAS/MAPK activation is associated with reduced tumor-infiltrating lymphocytes in triple-negative breast cancer: therapeutic cooperation between MEK and PD-1/PD-L1 immune checkpoint inhibitors. *Clin Cancer Res.* (2016) 22:1499–509. doi: 10.1158/1078-0432.CCR-15-1125
73. Cancer Genome Atlas Research N, Weinstein JN, Collisson EA, Mills GB, Shaw KR, Ozenberger BA, et al. The cancer genome atlas pan-cancer analysis project. *Nat Genet.* (2013) 45:1113–20. doi: 10.1038/ng.2764
74. Cerami E, Gao J, Dogrusoz U, Gross BE, Sumer SO, Aksoy BA, et al. The cBio cancer genomics portal: an open platform for exploring multidimensional cancer genomics data. *Cancer Discov.* (2012) 2:401–4. doi: 10.1158/2159-8290.CD-12-0095
75. Dieu-Nosjean MC, Antoine M, Danel C, Heudes D, Wislez M, Poulot V, et al. Long-term survival for patients with non-small-cell lung cancer with intratumoral lymphoid structures. *J Clin Oncol.* (2008) 26:4410–7. doi: 10.1200/JCO.2007.15.0284
76. Herbst RS, Soria JC, Kowanetz M, Fine GD, Hamid O, Gordon MS, et al. Predictive correlates of response to the anti-PD-L1 antibody MPDL3280A in cancer patients. *Nature.* (2014) 515:563–7. doi: 10.1038/nature14011
77. Tumeh PC, Harview CL, Yearley JH, Shintaku IP, Taylor EJ, Robert L, et al. PD-1 blockade induces responses by inhibiting adaptive immune resistance. *Nature.* (2014) 515:568–71. doi: 10.1038/nature13954
78. Remark R, Lupo A, Alifano M, Biton J, Ouakrim H, Stefani A, et al. Immune contexture and histological response after neoadjuvant chemotherapy predict clinical outcome of lung cancer patients. *Oncoimmunology.* (2016) 5:e1255394. doi: 10.1080/2162402X.2016.1255394
79. Robert C, Schachter J, Long GV, Arance A, Grob JJ, Mortier L, et al. Pembrolizumab versus ipilimumab in advanced melanoma. *N Engl J Med.* (2015) 372:2521–32. doi: 10.1056/NEJMoa1503093
80. Robert C, Long GV, Brady B, Dutriaux C, Maio M, Mortier L, et al. Nivolumab in previously untreated melanoma without BRAF mutation. *N Engl J Med.* (2015) 372:320–30. doi: 10.1056/NEJMoa1412082
81. Garon EB, Rizvi NA, Hui R, Leighl N, Balmanoukian AS, Eder JP, et al. Pembrolizumab for the treatment of non-small-cell lung cancer. *N Engl J Med.* (2015) 372:2018–28. doi: 10.1056/NEJMoa1501824
82. Rizvi NA, Mazieres J, Planchard D, Stinchcombe TE, Dy GK, Antonia SJ, et al. Activity and safety of nivolumab, an anti-PD-1 immune checkpoint inhibitor, for patients with advanced, refractory squamous non-small-cell lung cancer (CheckMate 063): a phase 2, single-arm trial. *Lancet Oncol.* (2015) 16:257–65. doi: 10.1016/S1470-2045(15)70054-9
83. Adams S, Gray RJ, Demaria S, Goldstein L, Perez EA, Shulman LN, et al. Prognostic value of tumor-infiltrating lymphocytes in triple-negative breast cancers from two phase III randomized adjuvant breast cancer trials: ECOG 2197 and ECOG 1199. *J Clin Oncol.* (2014) 32:2959–66. doi: 10.1200/JCO.2013.55.0491
84. Denkert C, von Minckwitz G, Darb-Esfahani S, Lederer B, Heppner BI, Weber KE, et al. Tumour-infiltrating lymphocytes and prognosis in different subtypes of breast cancer: a pooled analysis of 3771 patients treated with neoadjuvant therapy. *Lancet Oncol.* (2018) 19:40–50. doi: 10.1016/S1470-2045(17)30904-X
85. Emens LA, Cruz C, Eder JP, Braiteh F, Chung C, Tolaney SM, et al. Long-term clinical outcomes and biomarker analyses of atezolizumab therapy for patients with metastatic triple-negative breast cancer: a phase 1 study. *JAMA Oncol.* (2019) 5:74–82. doi: 10.1001/jamaoncol.2018.4224

Conflict of Interest: RSD has filed a patent on FCRL6-specific antibodies and their use in immunotherapy.

frontiers in Immunology

ORIGINAL RESEARCH
published: 21 October 2020
doi: 10.3389/fimmu.2020.592329

Inhibitory Receptor Trap: A Platform for Discovery of Inhibitory Receptors That Utilize Inositol Lipid and Phosphotyrosine Phosphatase Effectors

Bergren W. Crute[1], *Rachel Sheraden*[1], *Vanessa L. Ott*[2], *Isaac T. W. Harley*[1,3], *Andrew Getahun*[1,2] *and John C. Cambier*[1,2*]

[1] Department of Immunology and Microbiology, University of Colorado School of Medicine, Aurora, CO, United States, [2] Department of Biomedical Sciences, National Jewish Health, Denver, CO, United States, [3] Division of Rheumatology, Department of Medicine, University of Colorado School of Medicine, Aurora, CO, United States

OPEN ACCESS

Edited by:
Renato C. Monteiro, Université de Paris, France

Reviewed by:
Diane Lidke, University of New Mexico, United States
Zong Sheng Guo, University of Pittsburgh, United States

***Correspondence:**
John C. Cambier
john.cambier@cuanschutz.edu

Specialty section:
This article was submitted to Cancer Immunity and Immunotherapy, a section of the journal Frontiers in Immunology

Received: *06 August 2020*
Accepted: *29 September 2020*
Published: *21 October 2020*

Citation:
Crute BW, Sheraden R, Ott VL, Harley ITW, Getahun A and Cambier JC (2020) Inhibitory Receptor Trap: A Platform for Discovery of Inhibitory Receptors That Utilize Inositol Lipid and Phosphotyrosine Phosphatase Effectors. Front. Immunol. 11:592329. doi: 10.3389/fimmu.2020.592329

Among the areas of most impactful recent progress in immunology is the discovery of inhibitory receptors and the subsequent translation of this knowledge to the clinic. Although the original and canonical member of this family is FcγRIIB, more recent studies defined PD1 as an inhibitory receptor that constrains T cell immunity to tumors. These studies led to development of "checkpoint blockade" immunotherapies (CBT) for cancers in which PD1 interactions with its ligand are blocked. Unfortunately, although very effective in some patients, only a small proportion respond to this therapy. This suggests that additional as yet undescribed inhibitory receptors exist, which could be exploited. Here, we describe a new platform, termed inhibitory receptor trap (IRT), for discovery of members of this family. The approach takes advantage of the fact that many of the known inhibitory receptors mediate signaling by phospho-immunoreceptor tyrosine-based inhibition motif (ITIM) mediated recruitment of Src Homology 2 (SH2) domain-containing phosphatases including the SH2 domain-containing inositol phosphatase SHIP1 encoded by the INPP5D gene and the SH2 domain-containing phosphotyrosine phosphatases SHP1 and SHP2 encoded by the PTPN6 and PTPN11 genes respectively. Here, we describe the IRT discovery platform in which the SH2 domains of inhibitory phosphatases are used for affinity-based isolation and subsequent identification of candidate effectors *via* immunoblotting and high sensitivity liquid chromatography–mass spectrometry. These receptors may represent alternative targets that can be exploited for improved CBT. Salient observations from these studies include the following: SH2 domains derived from the respective phosphatases bind distinct sets of candidates from different cell types. Thus, cells of different identity and different activation states express partially distinct repertoires of up and downstream phosphatase effectors. Phosphorylated PD1 binds not only SHP2 but also SHIP1, thus the latter may be important in its inhibitory function. B cell antigen receptor signaling leads predominantly to CD79 mono-phosphorylation as indicated by much greater binding to

LynSH2 than Syk$(SH2)_2$. This balance of ITAM mono- versus bi-phosphorylation likely tunes signaling by varying activation of inhibitory (Lyn) and stimulatory (Syk) pathways.

Keywords: inhibitory receptor, SH2, ITIM, PD1, FcγRIIB, SHIP1, SHP1, SHP2

INTRODUCTION

Inhibitory receptors serve as key regulators of the immune system, terminating the immune response as appropriate, thus preventing the development of autoimmunity. Importantly, these controllers can be exploited therapeutically to enhance immunity to tumors and chronic infection (1, 2). While this so-called checkpoint blockade therapy (CBT) is very effective in some patients, only 15–20% benefit from the approach (3). While multiple factors play into the poor response rate, it may indicate that responses are limited by additional as yet undiscovered inhibitory receptors that have not yielded to discovery approaches employed to date. Elucidation of these may lead to more effective therapies. The work described herein seeks to define novel inhibitory receptors using an approach that identifies candidates based on their ability to engage inhibitory phosphatases that serve as the proximal downstream effectors of this receptor class.

The earliest described member of the immunoreceptor tyrosine-based Inhibition motif (ITIM)-containing inhibitory family is the low affinity IgG receptor FcγRIIB, which was initially shown by Phillips and Parker in 1984 to inhibit B cell antigen receptor signaling leading to blastogenesis (4, 5). Subsequent studies ascribed the point of B cell receptor (BCR) signal disruption as at or prior to phosphoinositide hydrolysis and calcium mobilization (6, 7). This inhibition occurred only when the two were co-aggregated. Later studies revealed that a 13 amino acid sequence in the cytoplasmic tail of the receptor contains all structural information required for engagement of inhibitory signaling machinery (8). With subsequent appreciation of other members of the inhibitory receptor family, a conserved sequence motif now known as the ITIM was recognized that occurs in most members of the family including in the 13aa FcγRIIB tail sequence (9, 10). The ITIM consensus motif consists of a tyrosine residue preceded by a -2 position hydrophobic amino acid and succeeded by a +3 position hydrophobic amino acid, therefore is I/VxYxxL. During signaling the conserved tyrosine is phosphorylated by Src family kinases. FcγRIIB ITIM tyrosine phosphorylation is mediated by Lyn that has been activated by BCR co-aggregation (11, 12). This relationship may explain the general requirement that to be activated most receptors in this family, e.g., PD1 and TIGIT, must be co-aggregated with a Src family kinase activating receptor such as BCR, T cell receptor (TCR), or FcγR1/2a/III/IV (13).

Inhibitory ITIM receptors described to date mediate signaling by recruitment of cytosolic inositol lipid and/or protein tyrosine phosphatases (10, 14, 15). This recruitment is mediated by phosphatase Src Homology 2 (SH2) domain binding to tyrosine phosphorylated ITIMs. The primary effector of FcγRIIB is the SH2-containing inositol lipid 5-phosphatase SHIP1 that contains a single SH2 that binds the pITIM (14, 16). SHIP1 would be expected to mediate inhibition of phosphoinositide breakdown by hydrolyzing PtdIns(3,4,5)P3 required for PLCγ translocation to the plasma membrane (17). Higher order BCR-FcγRIIB co-aggregation of these receptors can lead to recruitment of $(SH2)_2$ -containing phosphotyrosine phosphatase SHP1 (18, 19). Indeed, most members of the inhibitory ITIM-containing receptor family signal by engaging SHP1 *via* dual pITIM binding to tandem SH2 domains (20). The best known exception is PD1, which preferentially binds SHP2 *via* the receptor's pITIM and pITSM "switch" motif (15, 21). It appears that under some circumstances phosphorylated ITAMs (pITAMs) that normally transduce activating signals can recruit SHP1, at which point they have inhibitory function referred to as ITAMi (20, 22).

Activation of the tyrosine phosphatases is triggered by derepression resulting from tandem SH2 binding to dual pITIMs (21, 23–25). Interestingly, SHIP1 activation is triggered by phosphatase phosphorylation and interaction with partners such as DOK proteins (26). The consequence of these unique modes of activation is that SHP1 can only act locally on substrates within reach, while activated SHIP1 can inhibit responses to remotely stimulated receptors whose signaling requires generation and function of phosphatidylinositol 3,4,5 trisphosphate, the substrate of SHIP1 (27, 28). This occurs because SHIP1 can broadly reduce PtdIns3,4,5 levels globally, inhibiting signaling in trans.

Recruitment of SH2 containing phosphatases to membrane receptors is a shared inhibitory signaling mechanism among most immune system inhibitory receptors. While generally mediated by phosphorylated ITIMs, it appears that under appropriate conditions ITAMs and ITSMs can be inhibitory by use of this modality. It is known that both non-conserved sequences of the ITIM or ITAM and SH2 domains confer specificity in their interaction (29). In the example of SH2: ITAM interactions, the amino acids flanking the conserved tyrosines in the ITAM specify interactions with substrate, including phosphatases (29, 30). This specificity presumably underlies the non-redundant function of different ITIMs and ITAMs. We hypothesized that analysis of phosphatase SH2 domain binding specificity might be useful in resolving these relationships and identification of novel inhibitory receptors.

In this publication, we describe a method termed inhibitory receptor trap (IRT) for the isolation and identification of tyrosine phosphorylated surface receptors based on their binding to SH2 domains of specific downstream effector kinases and phosphatases. We have confirmed specific known inhibitory receptor—phosphatase interactions such as FcγRIIB : SHIP1SH2 and PD1:SHP2$(SH2)_2$ using IRT. We also have

identified CD79a association with the SH2 domains of inhibitory phosphatases which has been previous described. ITAMis are ITAMs that usually have embedded in them a sequence that shares great similarity to an ITIM allowing the recruitment of both activating and inhibitory signaling molecules (31). The significance of ITAMi containing receptors has been left largely uncharacterized and this approach may allow for identification and understanding of these molecules. We also demonstrate IRT capture of phosphorylated receptor proteins from cells stimulated *via* antigen receptor crosslinking. Utilizing cell surface biotinylation, IRT, and liquid chromatography–mass spectrometry (LC-MS/MS) in combination allows high throughput and sensitive probing of tyrosine phosphorylated receptor interactions with their cognate SH2-containing effectors.

MATERIAL AND METHODS

Mice

In all cases, 8–10-week-old female C57BL6/J mice purchased from Jackson Laboratories were used to obtain indicated immune cell populations. Mice were housed in the Animal Research Facilities at the University of Colorado Anschutz Medical Campus. All experiments were performed in accordance with the regulations and approval of University of Colorado Institutional Animal Care and Use Committee.

Cell Purification

Spleens were dissociated in complete medium [IMDM (HyClone), 5% FBS (Sigma), 1 mM sodium pyruvate (HyClone), 2 mM L-glutamine (Corning), 50 μM β-mercaptoethanol (Sigma), 50 μg/mL of Gentamicin (Gibco), and 100 U/mL of penicillin/streptomycin (Gibco)], and red blood cells removed using ammonium-chloride-potassium (ACK) lysis. Naive splenic B cells were isolated using negative selection with anti-CD43 (Ly-48) MicroBeads (Miltenyi Biotec 130-049-801). $CD3^+$ splenic T cells were purified by negative selection using the Pan T cell Isolation Kit II (Miltenyi Biotec 130-095-130).

Cell Culture and Activation

A20 cells were cultured in RPMI (Corning) containing 10% FBS, 1mM sodium pyruvate, 2mM L-glutamine, 50 μM β-mercaptoethanol, 50 μg/mL of Gentamycin, and 100 U/mL of penicillin/streptomycin. RBL-2H3 cells were cultured in MEM (Corning) containing 10% FBS, 2mM L-glutamine, and 100 U/mL of penicillin/streptomycin. RAW264.7 cells were cultured in DMEM high glucose (Corning) containing 10% FBS 1 mM sodium pyruvate, 2 mM L-glutamine, and 100 U/mL of penicillin/streptomycin. CD3+ T cells were either used directly *ex vivo* (naïve) or cultured at 1E6/mL in complete medium on plates pre-coated with 5 μg/mL of anti-CD3 (clone 145-2C11, BioLegend) and supplemented with soluble 0.5 μg/mL of anti-CD28 (clone 37.51, BioLegend) and 12.5 U/mL of IL-2 (Roche 11271164001) for 72 h to induce PD1 expression. PD1 expression was confirmed *via* flow cytometry staining (**Supplementary Figure 1**) with anti-PD1 PE (clone J43, eBioscience) anti-CD4 FITC (clone GK1.5, BD Biosciences), and anti-CD8 APC (clone 53-6.7, BD Biosciences).

Acute Cell Stimulation

In all cases, cells were acutely stimulated in serum free complete medium. 10E6 Purified B and T cells at 20E6 cells/ml were stimulated with 100 μM pervanadate (PV) for 5 min at 37°C. Anti-mouse IgG H+L (Zymed 61-6500) or $F(ab')_2$ anti-mouse IgG H+L (Jackson ImmunoResearch 315-006-003) were used at a final concentration of 10 μg/mL or 6.4 μg/mL to stimulate B cells for 5 min at 37°C. When indicated cells were surface biotinylated using EZ-Link™ Sulfo-NHS-LC-Biotin (Thermo Scientific A39257) as per manufacturers protocol. After stimulation cells were pelleted by centrifugation at 6000rpm for 30 seconds in a tabletop centrifuge. Supernatant was aspirated and cells were lysed by resuspension in cold lysis buffer composed of 25 mM Tris-HCl (pH 7.4), 150 mM NaCl, 1% NP-40, 1 mM EDTA, 1 mM DTT, and 5% glycerol supplemented with protease and phosphatase inhibitors (100 μg/mL aprotinin, 100 μg/mL α-1-antitrypsin, 100 μg/mL leupeptin, 1 mM PMSF, 10 mM NaF, 2 mM $NaVO_3$, and 10 mM tetrasodium pyrophosphate). Lysates were incubated on ice for at least 30min then cleared of particulate debris by centrifugation at ≥16,000g for 10min at 4°C. Cleared lysates were stored at -80°C.

Recombinant SH2 Domain Production and Purification

In brief, cDNAs encoding LynSH2, SHIP1SH2, SHP1$(SH2)_2$, and SHP2$(SH2)_2$ domain(s) were prepared from mouse B cells using PCR previously described (25, 32). Mouse cDNA sequences for Syk ENSMUST00000120135.7 were obtained from Ensembl. SH2 domains were defined according to UniProt entry P48025. SYK$(SH2)_2$ (1–831 bp) gBlock was purchased from IDT with engineered sites for restriction cloning. SHIP1SH2, SHP1$(SH2)_2$, and SHP2$(SH2)_2$ were cloned into the pGEX-5x-1 vector (GE Healthcare) for expressing recombinant GST fusion proteins. LynSH2 and SYK$(SH2)_2$ were cloned into the pGEX-6P-1 vector (GE Healthcare) for expressing recombinant GST fusion proteins. DH5α *Escherichia coli* were transformed with pGEX vectors containing SH2 domains for plasmid production. Rosetta II *E. coli* were transformed with SH2 domain-containing pGEX vectors for robust production of recombinant proteins. Cultures were inoculated with a single colony of Rosetta II *E. coli* containing SH2 domain pGEX vectors and grown overnight (16 h) at 37°C. 10mL of overnight culture was used to seed 1L of LB broth and allowed to grow for 3–4 h at 37°C reaching an OD600 ~0.6. Protein production was induced by addition of 0.25 mM IPTG for 3 h at 37°C. Bacteria were harvested by centrifugation at 4,000g for 10 min and lysed using previously established protocols for SH2-GST fusion protein production (25). Fusion proteins were isolated by GSH-Sepharose chromatography (GE Healthcare) and subsequently cleaved either on column or in solution using Factor Xa (NEB) or HRV3C (Pierce) proteases. Cleaved protein preparations were

depleted of GST by 3x adsorption using a GSH column. Purity was assessed using SDS-PAGE with Coomassie staining.

Recombinant SH2 Domain Conjugation to Sepharose Beads

In brief, CNBr-activated Sepharose 4B beads (GE Healthcare) were washed with 1 mM HCl for 10 min to achieve activation for coupling. Purified SH2 domains that had been dialyzed into 0.1 M $NaHCO_3$ (pH 8.3) containing 0.5 M NaCl were added to the activated Sepharose beads. Beads were conjugated with excess protein (1 mg protein/0.04g of CNBr Sepharose) overnight at 4°C while rotating. Beads were then incubated with 100 mM Tris HCl (pH 8.0) for 2 h at room temperature to quench unreacted groups. Conjugated beads were washed with 3 cycles of alternating pH buffers [each cycle consists of 100 mM sodium acetate (pH 4.0) containing 0.5 M NaCl and then 0.1 mM Tris-HCl (pH 8.5) containing 0.5 M NaCl]. Finally, conjugated beads were washed and stored in PBS + 0.02% sodium azide at 4°C.

Immunoprecipitation and SH2 Domain Enrichment (IRT)

Immunoprecipitation was performed with anti-PD1 clone J43 (eBioscience) and anti-FcγRIIB, clone 2.4G2. In brief, 0.5 μg of antibody/1E6 cells/100 μL was added and incubated for 1 h while rotating. Protein G beads (Life Technologies) that had been washed 3x in lysis buffer were added to lysates (500 μL of lysates/30-μL beads) and incubated for 2 h. Protein G beads were then washed 3x in lysis buffer and adsorbed protein eluted by boiling in reducing Laemmli SDS-PAGE sample buffer for 10 min. SH2 domain-conjugated Sepharose beads were washed 3x in lysis buffer before being added to cell lysates (500 μL of lysate/35-μL beads) and rotated at 4°C for 2 h. Beads were then washed 3x with lysis buffer and eluted by boiling in reducing Laemmli SDS-PAGE sample buffer for 10 min. 2-step enrichment was performed using SH2 domains as described before and eluting them 3x with 100 μL of 100 mM glycine (pH 2.5) for 5 min each. Low pH glycine eluates were combined and immediately neutralized by addition to 30 μL of 1 M TrisHCl (pH 8.5). 30 μL of streptavidin agarose (Thermo Scientific 20347) was then washed with PBS and added to each sample and rotated for 2 h at 4°C. Streptavidin agarose was washed 3x with lysis buffer and eluted by addition of reducing Laemmli SDS-PAGE sample buffer and boiled for 10 min.

Immunoblotting

Whole Cell lysates, immunoprecipitates or SH2 binding proteins were fractionated by SDS-PAGE and transferred to PVDF using semi-dry blotting conditions. PVDF was then blocked using either 3% BSA TBST [10 mM Tris-HCl (pH 8.0), 150 mM NaCl, and 0.05% Tween] or 5% non-fat dry milk TBST. Antibodies used to blot included: anti-pTyr clone 4G10, anti-PD1 (R&D Systems AF1021), anti-pCD79a Y182 (Cell Signaling Technology 5173S), anti-pFcγRIIB Y292 (Abcam EP926Y), and anti-β-actin (clone C4, Santa Cruz). In addition, we used rabbit polyclonal anti-FcγRIIB cytoplasmic tail, anti-CD22 cytoplasmic tail, and anti-CD79a raised in our laboratory as described previously (26, 32). Secondary antibodies used included anti-mouse IgG Trueblot HRP (clone eB144, Rockland), anti-rabbit IgG Trueblot HRP (clone eB182, eBioscience), anti-rabbit IgG HRP (Cell Signaling Technology 7074S), and anti-goat IgG HRP (R&D Systems HAF109). Blots were incubated in Pierce SuperSignal West Pico PLUS HRP (Thermo Scientific) substrate and visualized on a G:BOX by Syngene. Subsequent immunoblot images were quantified using Image Studio Lite ver 5.2 (LI-COR).

RESULTS

Design of the Inhibitory Receptor Trap (IRT) Platform

The goal of these experiments was to develop a novel approach for isolation of inhibitory receptors based on their ability to bind the SH2 domains of the inhibitory phosphatases. This method could be used for identification of new therapeutic targets for CBT and for characterization of the receptome of immune cell populations.

These phosphatases, the SH2-containing inositol 5-phospatase SHIP1, the SH2-containing protein phosphotyrosine phosphatase SHP-1, and SH2-containing protein phosphotyrosine phosphatase SHP-2, have been shown previously to function as the proximal effectors of ITIM-containing receptors. As shown in **Figure 1**, the approach taken for development of IRT involves initial stimulation of cells under conditions that induce tyrosine phosphorylation of ITIMs. These can include conditions that induce phosphorylation of substrates nonspecifically by inhibiting the phosphotyrosine phosphatases that normally balance their phosphorylation or conditions in which phosphorylation is stimulated by specific ligands. For the former, we utilized pervanadate stimulation. For the latter, we utilized antibodies against antigen receptors. Stimulation was followed by detergent lysis using NP40. As indicated, SH2 domain-conjugated Sepharose beads were added to cleared whole cell lysates to capture tyrosine phosphorylated binding partners. After washing, the beads were treated with reducing Laemmli buffer to elute SH2 bound proteins. Eluates were fractionated by SDS PAGE and 1) transferred electrophoretically to PVDF membrane that was then immunoblotted to define candidates, or 2) Comassie stained bands were excised from gels for analysis by LC-MS/MS. The latter approach provides for the unsupervised identification of interacting proteins. In this publication we have forgone presentation of LC-MS/MS analysis and focus on proving the effectiveness of our approach to identify known SH2 interactions.

Distinct SH2 Domain Adsorbents Capture Distinct Phosphorylated Proteins

Cells of the immune system utilize distinct inhibitory receptor–phosphatase effector pairs to control cellular activation and function. The specificity of these interactions of receptor effector pairs is determined by SH2 domain unique recognition of phosphotyrosine in the context of ITIM sequence (x) flanking conserved residues in the I/VxYxxL ITIM. We first wanted to

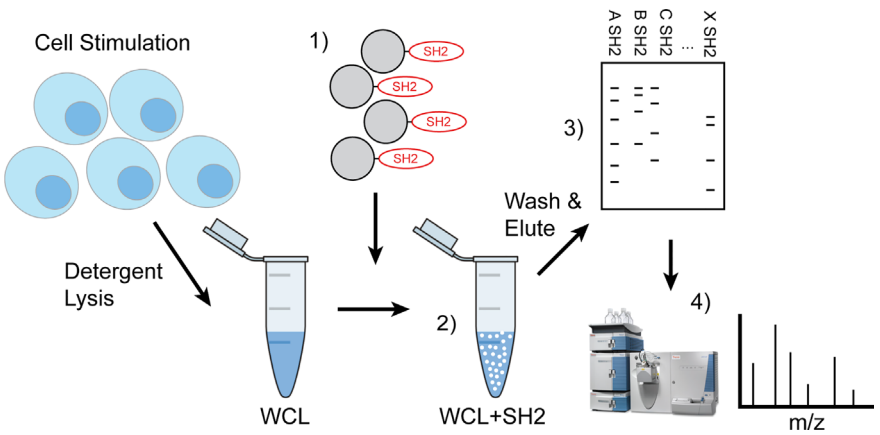

FIGURE 1 | Workflow of IRT (Inhibitory Receptor Trap). Cells were stimulated to induce phosphorylation of inhibitory receptors *via* chemical inhibition or antigen receptor cross linking and detergent lysates made. 1) Pre-washed SH2 domain conjugated beads were added to cleared cellular lysates 2) to capture phosphorylated proteins then washed to remove nonspecific interacting proteins and eluted using reducing Laemmli buffer. 3) Eluted phosphoproteins were subjected to SDS-PAGE electrophoresis and then transferred to PVDF for western blotting to define candidates or 4) stained bands were excised for analysis by LC-MS/MS.

determine if SH2 domains derived from different effector phosphatases and kinases bind distinct phosphoproteins. To address specificity, we developed SH2 domain probes from the activating tyrosine kinases Lyn and Syk and inhibitory phosphatases SHIP1, SHP1 and SHP2 and subjected pervanadate stimulated lysates from different cell types to IRT enrichment. Since the tandem SH2 domains found in Syk, SHP1, and SHP2 may bind cooperatively, the probes derived from these proteins contained both SH2 domains. We employed the single SH2 domains found in Lyn and SHIP1.

As seen in **Figures 2A–C**, SH2 domain adsorbents bind only a small proportion of tyrosine phosphorylated proteins detected in whole cell lysates, indicating some level of selectivity. Further, kinase SH2 adsorbents and phosphatase SH2 adsorbents bound largely distinct sets of tyrosine phosphoproteins in lysates of naïve B cells and naïve T cells. Interestingly, findings suggest that Lyn and Syk may have some interactions in common, and the three phosphatases may have some common interactions distinct from the kinases. These results demonstrate that different SH2 domains, whether singular or tandem, have unique specificity. Furthermore, as shown in **Figure 2C** wherein binding of B cell and T cell phosphoproteins was compared directly, these cells have partially distinct repertoires of phosphoproteins that bind to each of Lyn, SHIP1, Syk and SHP1. Finally, shown in **Figure 2D** is a comparison of IRT enrichment of SHIP1SH2 binding phosphoproteins from three different cell lines representing basophils (RBL-2H3), B cells (A20), and macrophages (RAW264.7). Anti-phosphotyrosine blotting of enriched proteins revealed both distinct and shared interactions across cell types supporting the existence of cell type specific inhibitory interactomes.

To further explore the utility of IRT, we tested its ability to detect previously demonstrated interactions between receptors and specific phosphatases and kinases. As expected, FcγRIIB was bound by SHIP1 (**Figure 3A**) consistent with the dominant role of SHIP1 in inhibitory signaling by this receptor (14, 16). The SHIP1SH2 IRT sample was subjected to mass spectrometric analysis, which confirmed the presence of FcγRIIB (data not shown). As expected, SHIP1, SHP1, and SHP2 SH2 domains all bound CD22 (33). Interestingly, all SH2 domains tested bound CD79a (**Figure 3A**). This was expected of Lyn, Syk, and SHIP1 (34, 35) and heavily suggested for SHP1 (36), but interactions between CD79a and SHP2 have not been demonstrated previously.

We next explored the ability of IRT to detect the previously demonstrated interaction between SHP2 and PD1 (15). In this experiment we utilized splenic T cells that were first activated by culture for 72 h with anti-CD3 and anti-CD28 antibodies and then stimulated acutely with pervanadate before lysis. Lysates were subjected to enrichment using SH2 domain adsorbents. As shown in **Figure 3B**, PD1 was bound by the $(SH2)_2$ domain of SHP2. SHP2 $(SH2)_2$ and SHP1$(SH2)_2$ IRT samples were subsequently subjected to mass spectrometric analysis, which confirmed PD1 enrichment by SHP2$(SH2)_2$ and lack of enrichment by SHP1$(SH2)_2$ (data not shown). Surprisingly, PD1 was also bound by the SH2 of SHIP1. This may indicate that SHIP1 functions as an alternative PD1 effector, the existence of which has been suggested by studies showing that PD1 mediated inhibition is partially preserved in the absence of SHP2 expression (37).

Further confirmation of the identity of PD1 and FcγRIIB among proteins that engage SH2 domain adsorbent was generated by analysis of the core protein mass generated by PNGaseF treatment of adsorbates prior to SDS-PAGE, transfer and blotting. PNGaseF treatment resulted in a molecular weight shift of the presumptive FcγRIIB from ~60 kDa to weight of 37 kDa, consistent with core protein mass (**Figure 3C**). PNGaseF treatment of SHP-2 adsorbates of activated T cells yielded a molecular weight shift of presumptive PD1 from 55–60 kDa to the core molecular weight of 32 kDa as would be expected (**Figure 3D**). Observation of molecular shifts for FcγRIIB and PD1 increases our confidence in prior observations made by immunoblotting. In addition, this experiment demonstrates that

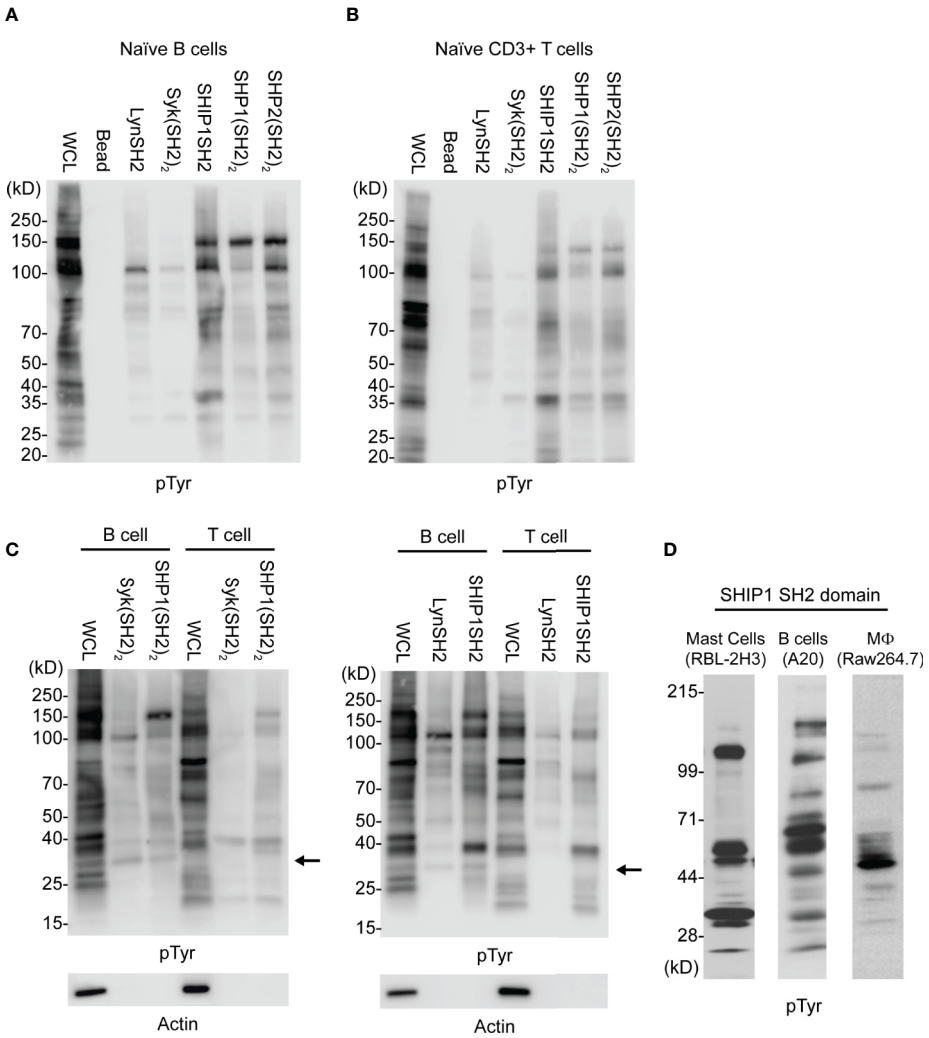

FIGURE 2 | Comparison of kinase and phosphatase SH2 binding proteins from PV stimulated cells. Cellular lysates derived from **(A)** splenic B cells and **(B)** splenic T cells enriched for phosphorylated tyrosine containing molecules using SH2 domain reagents derived from activating and inhibitory molecules. **(C)** Direct comparison between B and T cells using either tandem $(SH2)_2$ or single SH2 reagents. **(D)** Cellular lysates from indicated cell lines show differential enrichment for phosphoproteins when subjected to IRT using SHIP1SH2. Immunoblots are representative of $n = 3$ independent experiments.

N-glycanase treatment is useful in generation of more defined bands and core protein mass, and is therefore helpful in protein identification.

IRT Capture of Phosphatase Binding Partners Following Physiologic Phosphorylation

While pervanadate induced protein tyrosine phosphorylation is useful in defining SH2-phosphoprotein interactions that can occur in an unbridled situation in which phosphorylation is super-physiological, it is important to be able to detect interactions that occur upon specific receptor stimulation. Further, the latter allows analysis of requirement for co-aggregation to induce phosphorylation of sites required for phosphatase interactions.

Induction of FcγRIIB ITIM phosphorylation requires its co-ligation with antigen or activating IgG Fc receptors. To test physiologic requirements for induction of FcγRIIB competence to bind effector phosphatases detectably, we stimulated naïve B cells with equimolar amounts of affinity purified rabbit anti-IgG Heavy and Light chain antibodies to co-aggregate FcγRIIB and the BCR, or $F(ab')_2$ fragments of the same antibody to stimulate only BCR. Whole cell lysates were generated and blotted with tyrosine phosphospecific antibodies against FcγRIIB and CD79a. As shown in **Figure 4A**, stimulation with either antibody induced phosphorylation of CD79a detectable in whole cell lysates. As expected, phosphorylation of FcγRIIB was stimulation by anti-H+L but not $F(ab')_2$ anti-H+L. Phosphorylation of FcγRIIB by anti-H+L stimulation led to abundant FcγRIIB enrichment *via* SHIP1SH2 reagent (**Figure 4B**). The specificity of the SHIP1SH2 reagent for phosphorylated FcγRIIB was indicated by absence of FcγRIIB enrichment in unstimulated and $F(ab')_2$ anti-H+L conditions. We then determined the ability of IRT to capture

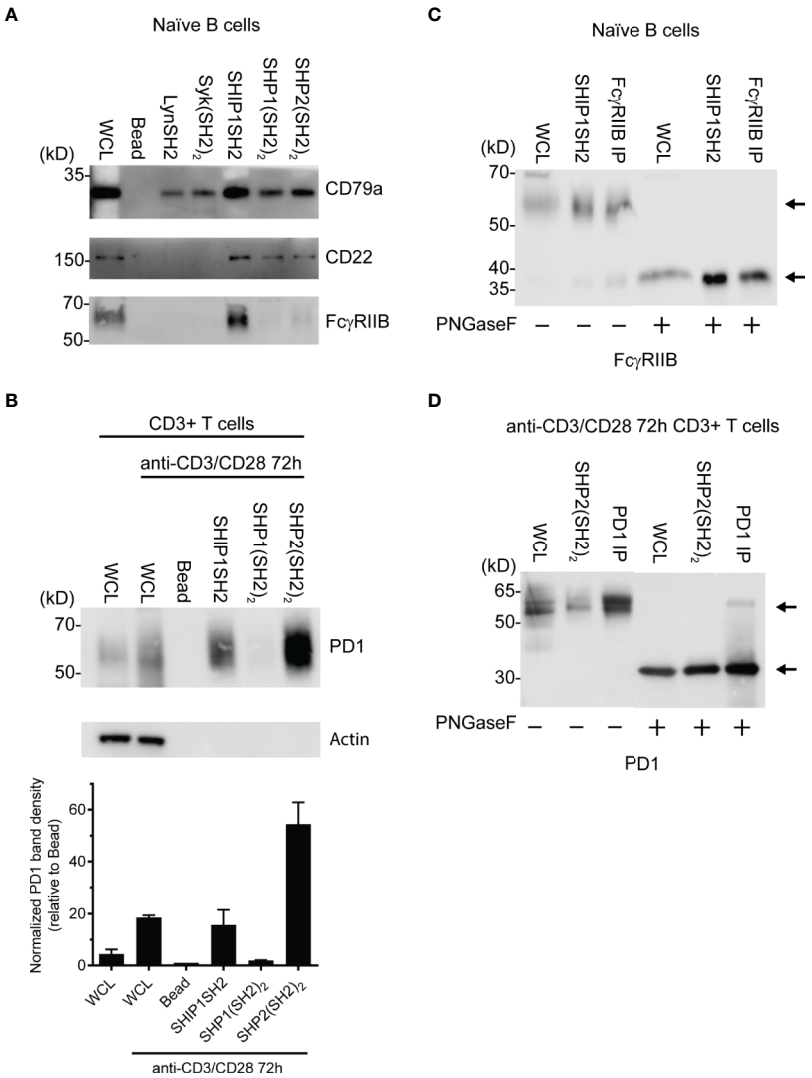

FIGURE 3 | Identification of specific SH2 substrates in PV stimulated cells **(A)** CD79a, CD22, and FcγRIIB are known tyrosine phosphorylated receptors that recruit SH2 domains. **(B)** (Top) Lysates of splenic T cells activated for 72 h with anti-CD3/CD28 were probed with SH2 domains from indicated molecules. PD1 is enriched specifically by the SHP2(SH2)$_2$ and SHIPSH2. (Bottom) Quantification of PD1 staining normalized to the bead control. Data is plotted from 3 independent experiments. **(C, D)** Cells were stimulated with PV prior to treatment with N-glycanase. FcγRIIB and PD1 have observed molecular weight shifts post N-glycanase treatment in WCL, SH2 reagent, and immunoprecipitation lanes. Bars in **(B)** represent ± SEM; immunoblots are representative of $n = 3$ independent experiments.

FcγRIIB and CD79a whose phosphorylation was stimulated by these ligands (**Figure 4C**). Receptor co-stimulation with IgG anti-H+L led to efficient capture of pFcγRIIB by SHIP1SH2 reagent. Interestingly, although to a lesser degree, pFcγRIIB was also captured by SHP1 and SHP2(SH2)$_2$ adsorbents, consistent with the function of these phosphatases in inhibitory pFcγRIIB signaling (10). When FcγRIIB was not co-engaged with BCR, in the case of F(ab')$_2$ anti-H+L stimulation, only basal pFcγRIIB could be detected in SHIP1SH2 adsorbents. Reminiscent of findings in **Figure 3**, all adsorbents captured phosphorylated CD79a, albeit with differing efficiency. It is curious that the Syk (SH2)$_2$ bound less pCD79a than the LynSH2. It is known that Syk binding to CD79 requires phosphorylation of both ITAM tyrosine residues, while Lyn binding does not (38, 39). This result may indicate that anti-BCR stimulates primarily monophosphorylation of CD79 ITAMs. We conclude from these experiments that SH2 domain adsorbents are able to capture receptors phosphorylated upon B cell antigen receptor crosslinking.

Refinement of IRT to Identify Cell Surface Binding Partners

As utilized to this point, phosphoproteins identified by IRT could be localized on the cell surface or may be intracellular. To focus the IRT only on identification of cell surface binding partners, we utilized cell surface biotinylation as an additional filter.

In this proof of concept experiment, naïve splenic B cells were cell surface biotinylated prior to pervanadate stimulation and

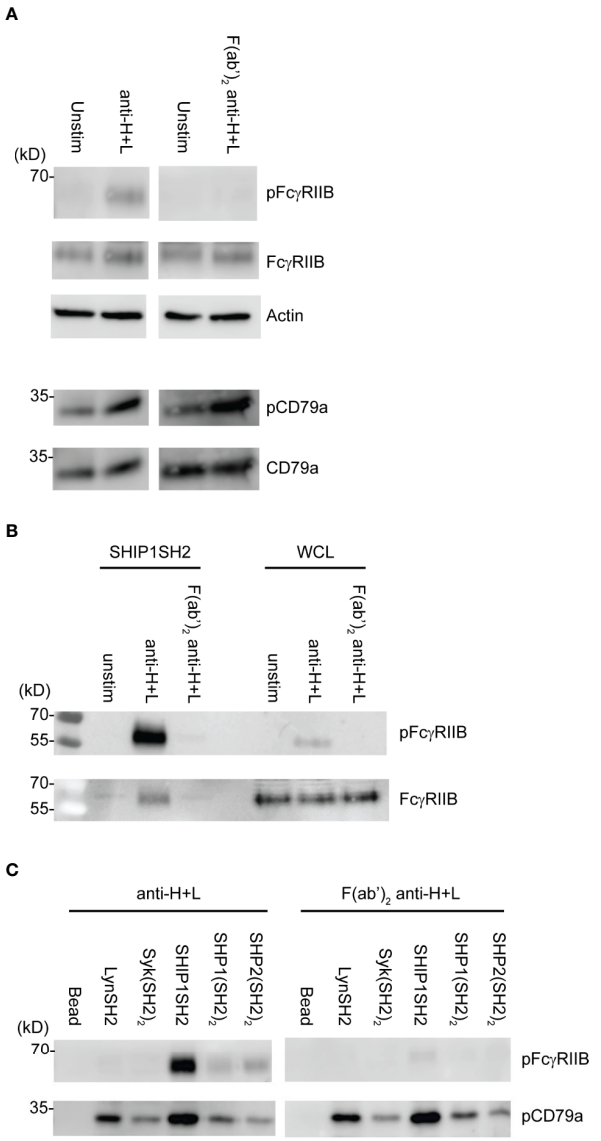

FIGURE 4 | Physiologic stimuli induce phosphorylation of physiologic targets which bind specific SH2 domains. *Ex vivo* splenic B cells were stimulated with either 10 μg/mL of anti-IgG H+L or 6.4 μg/mL F(ab')$_2$ anti-IgG H+L per condition. **(A)** 5E5 cell equivalents of WCL from unstim and anti-IgG H+L or F(ab')$_2$ anti-H+L were loaded and run by SDS-PAGE and blotted for pFcγRIIB, FcγRIIB, pCD79a, CD79a, and Actin. **(B)** 10E6 cells were left unstimulated, stimulated with anti-IgG H+L, or F(ab')$_2$ anti H+L, lysates were subjected to pull down using SHIP1SH2 reagent. Eluted proteins were run with 2E6 cell equivalents of WCL per condition and blotted for pFcγRIIB and total FcγRIIB. **(C)** 10E6 cells were stimulated with anti-IgG H+L and F(ab')$_2$ anti-H+L and subjected to pull down using SH2 domain reagents. Adsorbed proteins were eluted, run on SDS-PAGE and blotted for pFcγRIIB and pCD79a. Immunoblots are representative of $n = 3$ independent experiments.

SH2 domain adsorbent affinity purification. In this two-step enrichment protocol, binding partners were first enriched using SH2 domain adsorbents, with elution using low pH glycine buffer. Surface proteins were then isolated by adsorption to streptavidin agarose beads. Eluates were fractionated by SDS-PAGE and transferred to PVDF and analyzed by sequential blotting with anti-phosphotyrosine and streptavidin. Comparison of the SH2 domain affinity purified and 2-step enrichment by anti-pTyr blotting shows clearly that only a subset of binding partners are biotinylated cell surface proteins. Furthermore, reblotting with streptavidin reveals a similar repertoire although relative signal intensity of specific bands differs between pTyr and avidin blots. This may reflect the greater biotinylation of proteins that have larger extracellular domains, e.g. the 140Dda band relative to the ~60 kDa band (**Figure 5A**). Analysis of the relative capture of pCD79a, pFcγRIIB, and CD22 using the two protocols is consistent with this interpretation (**Figure 5B**). FcγRIIB which contains two linearly arranged extracellular Ig-like domains is sufficiently biotinylated to be captured by the avidin adsorbent. However, CD79a, containing only a single Ig-like domain, and its disulfide bonded partner CD79b also containing a single Ig-like domain, are not captured by avidin. This suggests that extension from the cell surface is a determinant of the utility of this approach. Specifically, 2-step enrichment may only be useful in identifying phosphatase binding partners that have large extracellular domains. The 2-step enrichment again confirms the selective purification of SH2 domain reagents and validity of this protocol to capture specific inhibitory receptors. Utilizing cell surface biotinylation and the 2-step enrichment described above allows for the purification of cell surface proteins for analysis *via* immunoblotting. The two-step approach is likely to be the most informative when combined with LC-MS/MS to define the SH2 domain-cell surface receptor interactome in an unsupervised manner.

DISCUSSION

The highly variable response of individuals to CBT in malignant disease underscores the importance of better understanding the inhibitory receptor landscape of immune system cells. However, identification of inhibitory receptors to be used as CBT therapeutic targets has historically been a challenge. Many known inhibitory immune receptors mediate their activity through the recruitment of inhibitory phosphatases *via* SH2 interactions with phosphorylated tyrosines in the receptor cytoplasmic tails. The approach taken here to identify novel inhibitory receptors was predicated on the assumption that additional as yet undefined inhibitory receptors exist, which utilizes this mechanism.

In this work we sought to develop a method, which we have termed IRT for Inhibitory Receptor Trap, to isolate and identify novel receptors that signal by engagement of the SH2 domains of inhibitory phosphatases (**Figure 1**). By targeting additional receptors, it should be possible to improve the efficacy of CBT. Our results indicate that SH2 domains of inhibitory phosphatases SHIP1, SHP1, and SHP2 can be used to effectively capture phosphorylated inhibitory receptors. We have shown that cell lines derived from different immune cell lineages (T cell, B cell, and myeloid) express unique repertoires of phosphatase SH2 domain binding receptors (**Figure 2D**). Utilizing *ex vivo* mouse splenic B cells and T cells, we showed that SH2 domain reagents from activating kinases bind common sets of proteins that are distinct from those of inhibitory phosphatases (**Figures 2A, B**). Differences

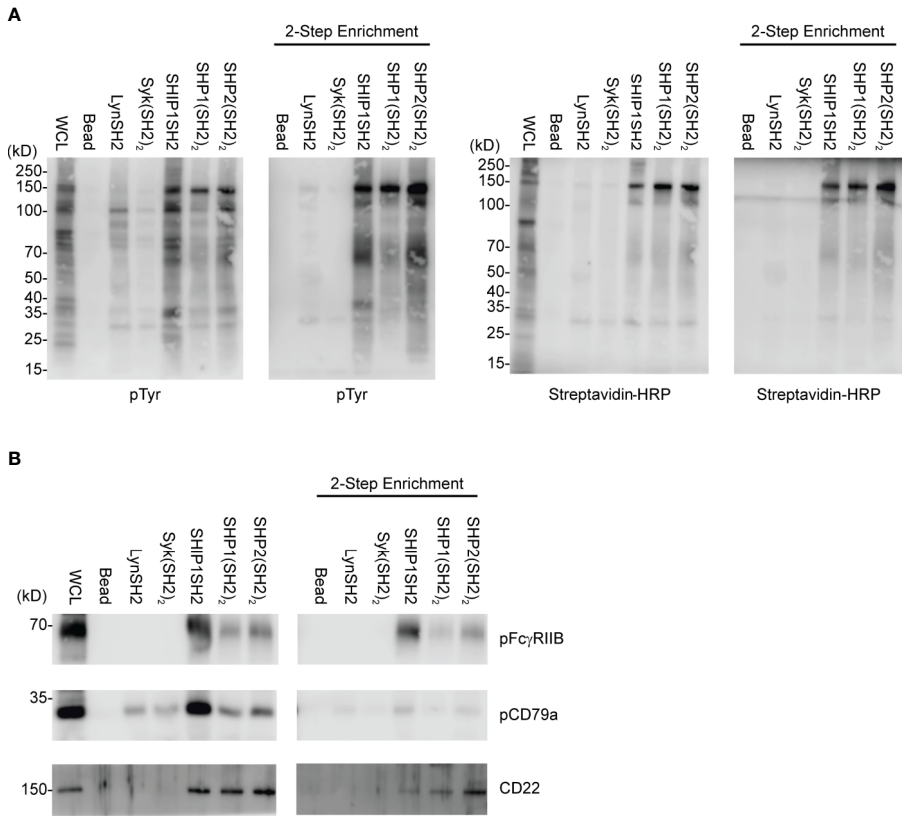

FIGURE 5 | IRT Refinement with cell surface biotinylation. Splenic B cells were cell surface biotinylated, PV stimulated, and subjected to either an SH2 domain pulldown or SH2 domain pulldown plus avidin enrichment. **(A)** Using this two-step method we can purify specific SH2 binding receptors. **(B)** pFcγRIIB, pCD79a, and CD22 were examined as specific SH2 domain substrates for their presence in two-step enrichment. Immunoblots are representative of $n = 3$ independent experiments.

are also seen in phosphoprotein sets bound by different phosphatases (**Figure 2D**). Furthermore, we observed binding of phosphatases to predicted partners including CD79a, FcγRIIB, CD22, and PD1 (**Figures 3A, B**). Our interest in defining receptor proteins led to the use of N-glycanase treatment in conjunction with immunoblotting as a tool to improve resolution of IRT (**Figure 3**). We demonstrated IRT effectiveness for capture of proteins, e.g., FcγRIIB and CD79a, phosphorylated as a consequence of specific receptor stimulation. Co-stimulation of these receptors using anti-IgG H+L induced sufficient phosphorylation to enable IRT capture of pFcγRIIB. However, stimulation by anti-H+L or $F(ab')_2$ anti-H+L led to capture of phosphorylated CD79a but not FcγRIIB (**Figure 4**). Finally, our experiments showed that cell surface biotinylation can be used in a 2-step purification approach to narrow IRT to reveal only surface receptors (**Figure 5**).

Interestingly, we noticed that in some cases multiple SH2 domain adsorbents bound apparently common phosphotyrosine-containing species in the same cell type and, in some cases, across cell types (**Figures 2A–D**). While we speculate based on size that these shared bands are the same proteins, without use of specific immunoblotting antibodies, we cannot make definitive conclusions. As shown in **Figure 2C**, when comparing B cells to T cells we noticed a band between the 25 and 40 kDa molecular weight markers (indicated by arrows) which is present in B but not T cell WCL and bound by multiple SH2 domains. The apparent identity of this band as CD79a was verified by anti-CD79a blot in **Figure 3A**.

The PD1 enrichment by SHIP1SH2 domains in pervanadate stimulated *ex vivo* splenic T cells was unexpected (**Figure 2E**). SHIP1 association with PD1 has not been reported by other groups who have explore PD1 binding partners (40). Interestingly a recent publication reported the dispensability of SHP2 in T cell exhaustion, it is possible that SHP2 and SHIP1 may play redundant roles in inhibitory PD1 signaling (37). In this context, it may be significant that the SHP2 (and SHP1) must be bound to their receptors to derepress phosphatase activity, while SHIP1 does not. In PD1 signaling, SHP2 would be expected to function locally dephosphorylating phosphotyrosines in reach, while SHIP1 may work broadly to reduce PtdIns3,4,5 levels globally inhibiting signaling in trans (23, 24, 27, 41).

Upon anti-H+L aggregation of antigen receptors on *ex vivo* splenic B cells, we observed predominant binding of phosphorylated FcγRIIB to SHIP1SH2 domain. There was significant, though lower, pFcγRIIB binding to the tandem SH2 domains of SHP1/2. This result is consistent with previous reports of SHP1 function in FcγRIIB signaling (**Figure 4C**)

(10, 19, 42). We would speculate that SHP1/2 binding to FcγRIIB ITIM occurs when antigen receptors are highly crosslinked resulting in higher levels of FcγRIIB phosphorylation, as suggested by the pITIM binding experiments of Lesourne and Daeron (19).

Mono- versus bi-phosphorylation of conserved ITAM tyrosines serves as a molecular switch. Monophosphorylation leading to recruitment of Lyn which acts in both activating and inhibitory signaling, and bi-phosphorylation which enables Syk binding and activation (29, 38, 43). Y182 of CD79a is the predominantly phosphorylated of the two tyrosines in the ITAM motif (39) suggesting that Lyn, *via* its single SH2 domain, may bind CD79a at greater quantity than Syk during BCR signaling. It has been previously observed that Y193F mutation of CD79a has a minor effect on BCR induced phosphorylayion,while Y182F mutation nearly completely abrogates receptor induced phosphorylation (39). The greater pCD79a enrichment in IRT by LynSH2 compared to $Syk(SH2)_2$ supports the notion that upon BCR stimulation CD79a is predominantly monophosphorylated, and this occurs on Y182.

Complementation of IRT with a filter that allows detection of only cell surface proteins yielded interesting and useful information. Avidin or phophosphotyrosine blotting of IRT enriched cell surface biotinylated pervanadate stimulated splenic B cells revealed a very bright band at ~150kD in both the SH2 domain and 2-step enrichment. This protein is likely CD22, and the strength of this signal probably relates to its large extracellular domain, mouse CD22 has a 681 amino acid extracellular domain, allowing greater biotinylation than small membrane proteins. For example, a lack of CD79a enrichment as seen in the 2-step enrichment when blotting for pTyr, avidin-HRP, and pCD79a (**Figures 5A, B**). This is presumably due to the smaller extracellular domain of CD79, of 109 amino acids, leading to reduced biotinylation. Furthermore, it is possible that associated immunoglobulin may mask some CD79 surfaces from biotinylation. Our data also shows 2-step enrichment clearly identifying pFcγRIIB which has a 181 amino acid extracellular domain and is not known to be constitutively associated with any other surface receptors (**Figure 5B**).

The fact that cell surface biotinylation may not enrich for receptors that have small extracellular domains or are closely associated with other receptors at the time of surface biotinylation should be a consideration in application of IRT.

In conclusion, our findings describe and justify the use of IRT for enrichment and identification of inhibitory receptors, which engage inhibitory phosphatases *via* phosphorylated ITIMs. We have developed IRT for use in an unsupervised manner with LC-MS/MS for the interrogation of cellular "inhibisomes" to better understand cellular inhibitory programming. We hope our method can be applied to CBT where there is an unmet need to identify new and novel inhibitory receptors to better tailor treatment of those suffering from malignant diseases.

DATA AVAILABILITY STATEMENT

The raw data supporting the conclusions of this article will be made available by the authors, without undue reservation.

ETHICS STATEMENT

The animal study was reviewed and approved by University of Colorado Institutional Animal Care and Use Committee.

AUTHOR CONTRIBUTIONS

BC, RS, and VO performed the experiments. BC and VO analyzed the data. BC, IH, AG, and JC designed the experiments and wrote the paper. All authors contributed to the article and approved the submitted version.

FUNDING

This work was supported by National Institutes of Health grants R01AI077597 (JCC), R01AI24487(JCC), R21AI149019 (AG) and by the Arthritis National Research Foundation (AG). IH was supported by NIAMS-5T32AR007534-32

ACKNOWLEDGMENTS

The authors acknowledge National Jewish Health and the University of Colorado School of Medicine for provision of an environment optimal for the conduct of research. We also thank the CU Department of Immunology and Microbiology flow facility and the Cambier laboratory manager Soojin Kim for their support.

SUPPLEMENTARY MATERIAL

The Supplementary Material for this article can be found online at: https://www.frontiersin.org/articles/10.3389/fimmu.2020.592329/full#supplementary-material

REFERENCES

1. Wykes MN, Lewin SR. Immune checkpoint blockade in infectious diseases. *Nat Rev Immunol* (2018) 18:91–104. doi: 10.1038/nri.2017.112
2. Odorizzi PM, Wherry EJ. Inhibitory Receptors on Lymphocytes: Insights from Infections. *J Immunol* (2012) 188:2957–65. doi: 10.4049/jimmunol.1100038
3. Darvin P, Toor SM, Sasidharan Nair V, Elkord E. Immune checkpoint inhibitors: recent progress and potential biomarkers. *Exp Mol Med* (2018) 50:1–11. doi: 10.1038/s12276-018-0191-1
4. Phillips NE, Parker DC. Fc-dependent inhibition of mouse B cell activation by whole anti-mu antibodies. *J Immunol* (1983) 130:602–6.

5. Phillips NE, Parker DC. Cross-linking of B lymphocyte Fc gamma receptors and membrane immunoglobulin inhibits anti-immunoglobulin-induced blastogenesis. *J Immunol* (1984) 132:627–32.
6. Choquet D, Partiseti M, Amigorena S, Bonnerot C, Fridman WH, Korn H. Cross-linking of IgG receptors inhibits membrane immunoglobulin-stimulated calcium influx in B lymphocytes. *J Cell Biol* (1993) 121:355–63. doi: 10.1083/jcb.121.2.355
7. Bijsterbosch MK, Klaus GG. Crosslinking of surface immunoglobulin and Fc receptors on B lymphocytes inhibits stimulation of inositol phospholipid breakdown via the antigen receptors. *J Exp Med* (1985) 162:1825–36. doi: 10.1084/jem.162.6.1825
8. Muta T, Kurosaki T, Misulovin Z, Sanchez M, Nussenzweig MC, Ravetch JV. A 13-amino acid motif in the cytoplamic domain of FcγRIIb modulates B cell receptor signaling. *Nature* (1994) 368:70–3. doi: 10.1038/368070a0
9. Daëron M, Latour S, Malbec O, Espinosa E, Pina P, Pasmans S, et al. The same tyrosine-based inhibition motif, in the intra-cytoplasmic domain of FcγRIIB, regulates negatively BCR-, TCR-, and FcR-dependent cell activation. *Immunity* (1995) 3:635–46. doi: 10.1016/1074-7613(95)90134-5
10. D'Ambrosio D, Hippen K, Minskoff S, Mellman I, Pani G, Siminovitch K, et al. Recruitment and activation of PTP1C in negative regulation of antigen receptor signaling by Fc gamma RIIB1. *Sci (80-)* (1995) 268:293–7. doi: 10.1126/science.7716523
11. Chan VWF, Meng F, Soriano P, DeFranco AL, Lowell CA. Characterization of the B Lymphocyte Populations in Lyn-Deficient Mice and the Role of Lyn in Signal Initiation and Down-Regulation. *Immunity* (1997) 7:69–81. doi: 10.1016/S1074-7613(00)80511-7
12. Malbec O, Fong DC, Turner M, Tybulewicz VLJ, Cambier JC, Fridman WH, et al. Fc ϵ Receptor I-Associated Lyn-dependent phosphorylation of FcgReceptor IIB during negative regulation of mast cell activation. *J Immunol* (1998) 160:1647–58.
13. Thaventhiran T. T Cell Co-inhibitory Receptors-Functions and Signalling Mechanisms. *J Clin Cell Immunol* (2013) S12:4. doi: 10.4172/2155-9899.S12-004
14. Ono M, Bolland S, Tempst P, Ravetch JV. Role of the inositol phosphatase SHIP in negative regulation of the immune system by the receptor Fc(gamma) RIIB. *Nature* (1996) 383:263–6. doi: 10.1038/383263a0
15. Okazaki T, Maeda A, Nishimura H, Kurosaki T, Honjo T. PD-1 immunoreceptor inhibits B cell receptor-mediated signaling by recruiting src homology 2-domain-containing tyrosine phosphatase 2 to phosphotyrosine. *Proc Natl Acad Sci* (2001) 98:13866–71. doi: 10.1073/pnas.231486598
16. D'Ambrosio D, Fong DC, Cambier JC. The SHIP phosphatase becomes associated with FcγRIIB1 and is tyrosine phosphorylated during "negative" signaling. *Immunol Lett* (1996) 54:77–82. doi: 10.1016/S0165-2478(96)02653-3
17. Wang XJ, Liao HJ, Chattopadhyay A, Carpenter G. EGF-dependent translocation of green fluorescent protein-tagged PLC-γ1 to the plasma membrane and endosomes. *Exp Cell Res* (2001) 267:28–36. doi: 10.1006/excr.2001.5241
18. Sato K, Ochi A. Superclustering of B cell receptor and Fc gamma RIIB1 activates Src homology 2-containing protein tyrosine phosphatase-1. *J Immunol* (1998) 161:2716–22.
19. Lesourne R, Bruhns P, Fridman WH, Daëron M. Insufficient Phosphorylation Prevents FcγRIIB from Recruiting the SH2 Domain-containing Protein-tyrosine Phosphatase SHP-1. *J Biol Chem* (2001) 276:6327–36. doi: 10.1074/jbc.M006537200
20. Getahun A, Cambier JC. Of ITIMs, ITAMs, and ITAMis: Revisiting immunoglobulin Fc receptor signaling. *Immunol Rev* (2015) 268:66–73. doi: 10.1111/imr.12336
21. Marasco M, Berteotti A, Weyershaeuser J, Thorausch N, Sikorska J, Krausze J, et al. Molecular mechanism of SHP2 activation by PD-1 stimulation. *Sci Adv* (2020) 6:eaay4458. doi: 10.1126/sciadv.aay4458
22. Mkaddem SB, Benhamou M, Monteiro RC. Understanding Fc receptor involvement in inflammatory diseases: From mechanisms to new therapeutic tools. *Front Immunol* (2019) 10:811:811. doi: 10.3389/fimmu.2019.00811
23. Yang J, Liu L, He D, Song X, Liang X, Zhao ZJ, et al. Crystal structure of human protein-tyrosine phosphatase SHP-1. *J Biol Chem* (2003) 278:6516–20. doi: 10.1074/jbc.M210430200
24. Wang W, Liu L, Song X, Mo Y, Komma C, Henry D, et al. Crystal Structure of Human Protein Tyrosine Phosphatase SHP-1 in the Open Conformation. *J Cell Biochem* (2011) 112:2062–71. doi: 10.1002/jcb.23125
25. Famiglietti SJ, Nakamura K, Cambier JC. Unique features of SHIP, SHP-1 and SHP-2 binding to FcgammaRIIb revealed by surface plasmon resonance analysis. *Immunol Lett* (1999) 68:35–40. doi: 10.1016/S0165-2478(99)00027-9
26. Tamir I, Stolpa JC, Helgason CD, Nakamura K, Bruhns P, Daeron M, et al. The RasGAP-binding protein p62(dok) is a mediator of inhibitory FcγRIIB signals in B cells. *Immunity* (2000) 12:347–58. doi: 10.1016/S1074-7613(00)80187-9
27. Bléry M, Delon J, Trautmann A, Cambiaggi A, Olcese L, Biassoni R, et al. Reconstituted killer cell inhibitory receptors for major histocompatibility complex class I molecules control mast cell activation induced via immunoreceptor tyrosine-based activation motifs. *J Biol Chem* (1997) 272:8989–96. doi: 10.1074/jbc.272.14.8989
28. Brauweiler A, Merrell K, Gauld SB, Cambier JC. Cutting Edge: Acute and Chronic Exposure of Immature B Cells to Antigen Leads to Impaired Homing and SHIP1-Dependent Reduction in Stromal Cell-Derived Factor-1 Responsiveness. *J Immunol* (2007) 178:3353–7. doi: 10.4049/jimmunol.178.6.3353
29. Johnson SA, Pleiman CM, Pao L, Schneringer J, Hippen K, Cambier JC. Phosphorylated immunoreceptor signaling motifs (ITAMs) exhibit unique abilities to bind and activate Lyn and Syk tyrosine kinases. *J Immunol* (1995) 155:4596–603.
30. Liu BA, Jablonowski K, Shah EE, Engelmann BW, Jones RB, Nash PD. SH2 domains recognize contextual peptide sequence information to determine selectivity. *Mol Cell Proteomics* (2010) 9:2391–404. doi: 10.1074/mcp.M110.001586
31. Barrow AD, Trowsdale J. You say ITAM and I say ITIM, let's call the whole thing off: the ambiguity of immunoreceptor signalling. *Eur J Immunol* (2006) 36:1646–53. doi: 10.1002/eji.200636195
32. O'Neill SK, Getahun A, Gauld SB, Merrell KT, Tamir I, Smith MJ, et al. Monophosphorylation of CD79a and CD79b ITAM Motifs Initiates a SHIP-1 Phosphatase-Mediated Inhibitory Signaling Cascade Required for B Cell Anergy. *Immunity* (2011) 35:746–56. doi: 10.1016/j.immuni.2011.10.011
33. Nitschke L. The role of CD22 and other inhibitory co-receptors in B-cell activation. *Curr Opin Immunol* (2005) 17:290–7. doi: 10.1016/j.coi.2005.03.005
34. Pao LI, Cambier JC. Syk, but not Lyn, Recruitment to B Cell Antigen Receptor and Activation Following Stimulation of CD45- B Cells. *J Immunol* (1997) 158:2663–9.
35. Manno B, Oellerich T, Schnyder T, Corso J, Lösing M, Neumann K, et al. The Dok-3/Grb2 adaptor module promotes inducible association of the lipid phosphatase SHIP with the BCR in a coreceptor-independent manner. *Eur J Immunol* (2016) 46:2520–30. doi: 10.1002/eji.201646431
36. Mkaddem SB, Murua A, Flament H, Titeca-Beauport D, Bounaix C, Danelli L, et al. Lyn and Fyn function as molecular switches that control immunoreceptors to direct homeostasis or inflammation. *Nat Commun* (2017) 8:246. doi: 10.1038/s41467-017-00294-0
37. Rota G, Niogret C, Dang AT, Barros CR, Fonta NP, Alfei F, et al. Shp-2 Is Dispensable for Establishing T Cell Exhaustion and for PD-1 Signaling In Vivo. *Cell Rep* (2018) 23:39–49. doi: 10.1016/j.celrep.2018.03.026
38. Kurosaki T, Johnson SA, Pao L, Sada K, Yamamura H, Cambier JC. Role of the Syk autophosphorylation site and SH2 domains in B cell antigen receptor signaling. *J Exp Med* (1995) 182:1815–23. doi: 10.1084/jem.182.6.1815
39. Pao LI, Famiglietti SJ, Cambier JC. Asymmetrical phosphorylation and function of immunoreceptor tyrosine-based activation motif tyrosines in B cell antigen receptor signal transduction. *J Immunol* (1998) 160:3305–14.
40. Riley JL. PD-1 signaling in primary T cells. *Immunol Rev* (2009) 229:114–25. doi: 10.1111/j.1600-065X.2009.00767.x
41. Chacko GW, Tridandapani S, Damen JE, Liu L, Krysral G, Coggeshall KM. Negative Signaling in B Lymphocytes Induces Tyrosine Phosphorylation of the 145-kDa Inositol Polyphosphate 5-Phosphatase, SHIP. *J Immunol* (1996) 157:2234–8.
42. Ono M, Okada H, Bolland S, Yanagi S, Kurosaki T, Ravetch JV. Deletion of SHIP or SHP-1 Reveals Two Distinct Pathways for Inhibitory Signaling. *Cell* (1997) 90:293–301. doi: 10.1016/S0092-8674(00)80337-2

43. DeFranco AL, Chan VWF, Lowell CA. Positive and negative roles of the tyrosine kinase Lyn in B cell function. *Semin Immunol* (1998) 10:299–307. doi: 10.1006/smim.1998.0122

Conflict of Interest: The authors declare that the research was conducted in the absence of any commercial or financial relationships that could be construed as a potential conflict of interest.

frontiers in Immunology

REVIEW
published: 12 November 2020
doi: 10.3389/fimmu.2020.575609

Targeting NK Cell Inhibitory Receptors for Precision Multiple Myeloma Immunotherapy

Helmi Alfarra[1], *Jackson Weir*[1], *Stacy Grieve*[1] *and Tony Reiman*[1,2,3]*

[1] Department of Biology, University of New Brunswick, Saint John, NB, Canada, [2] Department of Oncology, Saint John Regional Hospital, Saint John, NB, Canada, [3] Department of Medicine, Dalhousie University, Saint John, NB, Canada

Innate immune surveillance of cancer involves multiple types of immune cells including the innate lymphoid cells (ILCs). Natural killer (NK) cells are considered the most active ILC subset for tumor elimination because of their ability to target infected and malignant cells without prior sensitization. NK cells are equipped with an array of activating and inhibitory receptors (IRs); hence NK cell activity is controlled by balanced signals between the activating and IRs. Multiple myeloma (MM) is a hematological malignancy that is known for its altered immune landscape. Despite improvements in therapeutic options for MM, this disease remains incurable. An emerging trend to improve clinical outcomes in MM involves harnessing the inherent ability of NK cells to kill malignant cells by recruiting NK cells and enhancing their cytotoxicity toward the malignant MM cells. Following the clinical success of blocking T cell IRs in multiple cancers, targeting NK cell IRs is drawing increasing attention. Relevant NK cell IRs that are attractive candidates for checkpoint blockades include KIRs, NKG2A, LAG-3, TIGIT, PD-1, and TIM-3 receptors. Investigating these NK cell IRs as pathogenic agents and therapeutic targets could lead to promising applications in MM therapy. This review describes the critical role of enhancing NK cell activity in MM and discusses the potential of blocking NK cell IRs as a future MM therapy.

Keywords: natural killer cell, immune checkpoint inhibitor, inhibitory receptors of lymphocytes, multiple myeloma, immunotherapy, precision medicine, chimeric antigen receptor NK, monoclonal antibody therapy

OPEN ACCESS

Edited by:
Ali A. Zarrin,
TRex Bio, United States

Reviewed by:
Camille Guillerey,
University of Queensland, Australia
Rafael Solana,
University of Cordoba, Spain

****Correspondence:***
Tony Reiman
anthony.reiman@horizonnb.ca

Specialty section:
This article was submitted to Cancer Immunity and Immunotherapy, a section of the journal Frontiers in Immunology

Received: *23 June 2020*
Accepted: *19 October 2020*
Published: *12 November 2020*

Citation:
Alfarra H, Weir J, Grieve S and Reiman T (2020) Targeting NK Cell Inhibitory Receptors for Precision Multiple Myeloma Immunotherapy. Front. Immunol. 11:575609. doi: 10.3389/fimmu.2020.575609

INTRODUCTION

Multiple myeloma (MM) is characterized by the accumulation of malignant plasma cells (PCs), resulting in increased monoclonal protein in the blood and urine (1). MM represents 1% of cancers and 13% of hematological malignancies, with a higher prevalence in aging populations (2, 3). In 2019, approximately 3,300 Canadians were newly diagnosed with MM, and 1,550 Canadians died from this disease (4). MM is a progressive disease that begins as an asymptomatic precursor called monoclonal gammopathy of undetermined significance (MGUS), before developing into smoldering MM (SMM), and ultimately, fully active symptomatic MM.

In recent years, there have been several notable therapeutic advancements for MM. Hematopoietic stem cell transplantation (HSCT) (5), proteasome inhibitors (PIs), immunomodulatory drugs (IMiDs) (6), histone deacetylase inhibitors (HDACi) (7), and novel

combinations therapies (8, 9) have significantly improved the control of MM and extended overall survival (OS) (2, 5, 7, 10, 11). However, MM remains incurable as most patients eventually relapse due to the development of resistance to these conventional treatments (12). Inherent intra- and inter-patient heterogeneity contributes to the lack of curative success for this disease. Additionally, MM is considered a disease of the immune system. Gradual immune dysregulation and impairment of NK cells, T cells, B cells, and dendritic cells (DCs) allow malignant plasma cells to escape immunosurveillance (2). A better understanding of the immune environment of MM may lead to alternative therapeutic strategies that re-engage the immune system to inhibit MM growth.

Natural killer (NK) cells are an intriguing immune cell type in MM given the recent development of monoclonal antibodies (mAbs), elotuzumab (anti-SLAMF7), and daratumumab (anti-CD38) that enhance NK cell-mediated tumour cell toxicity by activating the antibody dependent cellular cytotoxicity (ADCC) mechanism (13–15). Although these mAbs have improved the clinical outcomes of both newly diagnosed and relapsed or refractory MM (RRMM) patients, only a subgroup of patients responds to these mAbs, highlighting the complexity of MM. CAR-NK cell therapies and combinations of existing treatments also work to restore the innate killing capacity of NK cells in MM.

Given the success of blocking T cell IRs in multiple cancer types, blocking the IRs on NK cells offers another possibility to enhance anti-myeloma cell immunity. This review discusses NK cell IRs (**Figure 1**) and their potential as novel NK cell-based MM immunotherapies to complement current treatment options. This line of investigation has the potential to maximize clinical benefit, thereby leading to efficient and safe immunotherapy options for MM patients.

NK CELL BIOLOGY

NK cells are a cytotoxic subset of innate lymphoid cells (ILCs). They are the first responders against malignant and infected cells and are functionally classified by their innate capacity to eliminate cells without prior sensitization or recognition of presented antigens (16, 17). NK cells also produce cytokines and chemokines that stimulate other branches of the immune response including DCs and T cells (18, 19). Consequently, NK cells can limit cancer cell progression (20).

NK cells comprise 5% to 15% of peripheral blood lymphocytes (21, 22). Generally, they are defined as $CD56^{+ve}CD3^{-ve}$ and classified into two major populations—$CD56^{dim}$ and $CD56^{bright}$. The $CD56^{dim}$ cells are considered the cytotoxic population and express more immunoglobulin-like receptors to detect stressed cells and induce cell death. $CD56^{bright}$ cells are known as the pro-inflammatory cytokine releasers and specialize in promoting other components of the immune system through IFN-γ and TNF-α production (23–26). Notably, $CD56^{bright}$ NK cells have been shown to display cytotoxic activity when primed with IL-15 (27).

When an NK cell encounters a cell, it does not necessarily induce cell lysis. Instead, cytotoxicity is dependent on expression of AR and IRs on the NK cells that are engaged by specific ligands expressed on target cells (28). For example, inhibitory receptors expressed on the surface of a NK cell bind inhibitory ligands on a healthy cell (29). Without any activating ligands on the healthy cell's surface, the inhibitory signal predominates and there is no cell lysis (**Figure 2A**). The inhibitory ligands human leukocyte antigen class I (HLA-I) are expressed on most healthy cells, preventing NK-mediated cell lysis. The first-described mechanism of NK cell function the "missing-self hypothesis" showed that when target cells lacked expression of this "self" ligand, HLA-I, the effector NK cells were free to become

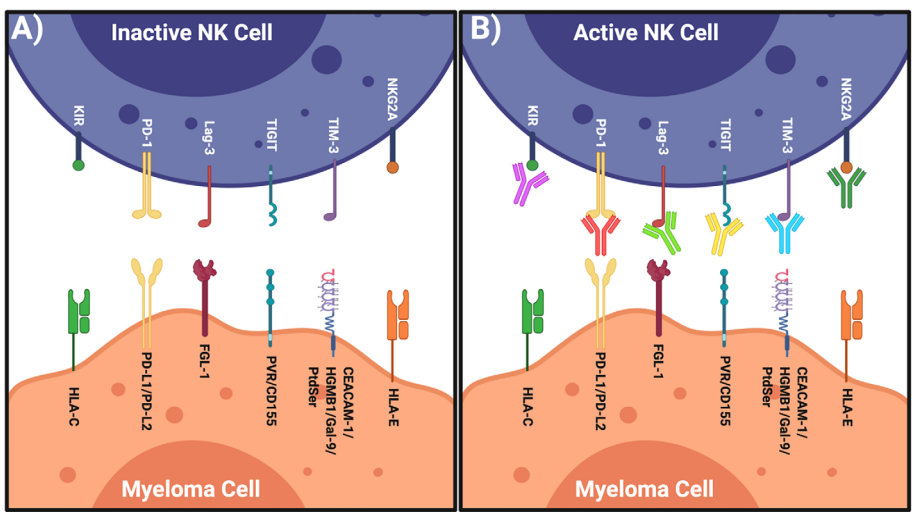

FIGURE 1 | Restoring NK Cells by Targeting Their IRs. **(A)** Left: inactive NK cell has inhibitory receptors and complimentary ligands on the myeloma cell. **(B)** Right: NK cell activated when inhibitory axis is blocked *via* specific blocking mAbs. Figure created with BioRender.com.

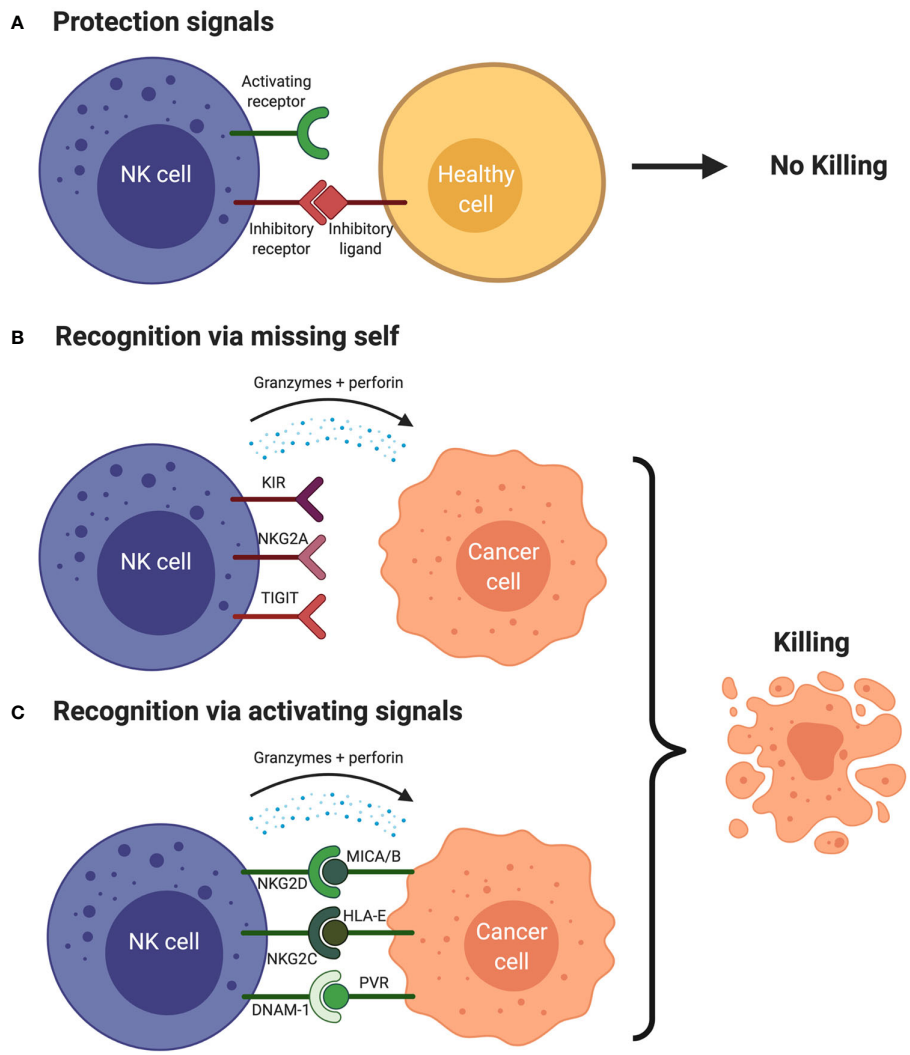

FIGURE 2 | NK cell Surveillance of Cancer Cell **(A)** The presence of inhibitory signals and lack of activating signals prevents the activation of the NK cells which avoids the lysis of the healthy cells. **(B)** NK cell recognizes the cancer cell due to the lack of human leukocyte antigens (HLAs) and/or other inhibitory ligands on cancer cell ("missing-self hypothesis"), which results in production of cytokines, granzyme B and perforins that leads to the cancer cell killing. This scenario is simplified. Activation signals are still necessary to induce activation as the absence of inhibitory signals alone is usually insufficient. **(C)** NK cell is activated *via* the activating signals and the engagement with the activating ligands on the cancer cell in the lack of inhibitory signals, which leads to the production of perforins and granzyme B and cytokines, which ultimately yields cancer cell killing. Figure created with BioRender.com.

activated and remove the target cells (17) (**Figure 2B**). Interestingly, cancer cells often downregulate HLA-I (30), but we now know the story is much more complex and includes many additional IRs and ligands (**Figure 1**).

While the "missing self" mechanism of cell death works primarily through the lack of inhibitory signals, NK cells can also kill cancer cells with adequate activation signals (**Figure 2C**). For example, natural killer group 2D (NKG2D) is an activating receptor which recognizes HLA-I polypeptide-related sequence A/B (MICA/B), and UL16 binding proteins 1–6 (ULBP1-6) activating ligands. NKG2D ligands (NKG2DL) are often upregulated on malignantly transformed cells for NK cell detection (28, 31). NK cells express other ARs and a detailed review of their function can be found elsewhere (32, 33).

When an NK cell comes in contact with a stressed cell, different patterns of inhibitory and activating ligand expression are detected through the NK cell's IRs and ARs and the balance of these ligands and receptors dictates NK cell function. Activated NK cells can send suicide or self-destruction signals to the target cell and induce cell lysis through direct exocytosis of granzyme and perforin (34–36). Stimulated NK cells have also been shown to kill cancer cells *via* apoptotic pathways (i.e., Fas or TRAIL) and cytokine production (i.e., TNF-α and IFN-γ) that are important for both innate and adaptive immune responses (36).

NK cells are integral members of anti-cancer immunity. While the cytotoxic mechanisms presented above represent ideal scenarios, the complex cancer immune microenvironment is marked by NK cell dysfunction and impairment. Deciphering how NK cell dysfunction contributes to tumorigenesis is essential to improve patient outcomes.

NK CELL SURVEILLANCE OF MALIGNANT CELLS

Several studies have reported the importance of NK cells in the immunosurveillance of tumor growth. An epidemiological study described that low activity of NK cells increased the risk of cancer specifically stomach, lung, and intestine (37). Other studies in mice models and humans associated tumor relapse and metastasis with decreased NK cell immunosurveillance (38–41). Preclinical studies are consistent with clinical data demonstrating that an NK cell-mediated immune response affects tumor formation and metastases (40, 42, 43). It has also been reported that the infiltration of NK cells into some solid tumors affects tumorigenesis in these cancer types (44–49) and can serve as a positive prognostic factor (48, 50).

NK Cells in Hematological Cancers

NK cell numbers and functions have been linked to the prognosis of different blood cancers (41, 51–55). For example, the presence of NK cells in the bone marrow (BM) of Acute Lymphoblastic Leukemia (ALL) at diagnosis correlated with improved response to chemotherapy combinations treatments and increased tumor remission rates (55). Additionally, the predominance of activated NK cells expressing NKp46, FasL and KIR2DL5A in ALL patients was associated with better leukemia control after treatment with methotrexate, cytarabine, and hydrocortisone (54). Similarly, IFN-γ release by NK cells, an indication of their active state, was a favorable prognostic marker in chronic myeloid leukemia (CML) (56). Finally, a lower percentage of NK cells in the peripheral blood have been associated with a poorer prognosis of pediatric non-Hodgkin's lymphomas (NHL), adult chronic lymphocytic leukemia (CLL), diffuse large B-cell lymphoma (DLBCL) (41, 51, 52), and high-risk myelodysplastic syndrome (MDS) (57). Despite these studies supporting an impact of NK cells on disease progression, the relationship between NK cells and outcome in the setting of some cancers is still controversial. It remains to be confirmed whether the increase in NK cell number and activity is a result of tumor progression or an indication of antitumor immune response.

Likewise, the correlation between NK cells and the progression of MM is controversial (58–65). Some studies have shown a decrease in NK cell number in the peripheral blood of myeloma patients when compared to healthy controls (58–60), while other studies demonstrated an increase or no difference (61–63). A recent study using single-cell RNA sequencing showed enrichment of NK cell populations during MGUS, and phenotypic shifts later in MM progression that potentially point to a compromised immune system (66). Discrepancy is also observed in terms of NK cell functionality where either reduced NK cell function (65) or high NK cell function (59, 67) are linked with advanced clinical stage, high-risk disease and reduced survival.

Due to the complexity, heterogeneity, and plasticity of NK cells in cancer patients, the discrepancies are difficult to distill into a single explanation (67). One likely explanation seems to relate back to which NK cell subpopulations are being measured. For example, it was reported that MM patients with a high $CD56^{+ve}CD3^{-ve}$ subset had a poorer prognosis. By contrast, patients with high of $CD57^{+ve}CD8^{-ve}$ subset of NK cells had a better prognosis (59). This suggests that there are essential distinctions to be made between these two populations, and that the existence of mature NK cells ($CD57^{+ve}$) in early stage patients, but not the immature subset, forecasts good outcomes (59). Secondly, the production of NK cell stimulatory cytokines (e.g., IL-7 and IL-12) by myeloma cells in some patients could also explain differences in NK cell activity or number observed in different patient subsets since some patients' immune system may be trying to control the disease (59, 68).

Finally, heterogeneity in ligand and receptor expressions within patient subsets may account for variability in research studies. For example, some patients may have reduced levels of activating ligands such as MICA/B that normally send signals to the activating receptor of the NK cell, NKG2D (**Figure 3A**). This reduction in MICA/B levels on the myeloma cells leads to loss of NK cell activation through NKG2D receptor, allowing MM cells to evade NK cell surveillance (69, 70). Alternatively, HLA-I ligand upregulation on MM cells may also block NK cell activity (67, 71). Interestingly, myeloma cells harvested from MM patients from the BM early in disease progression expressed a relatively low level of HLA Class I ligands and were subsequently responsive to the NK cell mediated cytotoxicity. As disease progressed into fully active myeloma, the tumorigenic MM cells displayed higher HLA-I ligands expression, rendering them more resistant to NK cell-mediated cell death (72). Another mechanism that may also be responsible for altered NK cell function in MM includes upregulation of IRs such as PD-1 on NK cells found in the peripheral blood or BM of MM, which may lead to decreased NK cell function due to its engagement with its ligands PD-L1/2 on MM cells (71, 73, 74) (**Figure 3A**).

These studies not only provide a possible explanation for a discrepancy regarding the role of NK cells in MM, but also point to how an imbalance in ARs and IRs could lead to NK cell dysfunction in MM (64, 75) (**Figure 3A**). Upregulation of various IRs on the surface of NK cells combined with the overexpression of their cognate ligands on the cancer cells can be a dynamic escape tactic used by cancer cells to hinder NK cell activity (**Figure 3A**). A better understanding of the interplay between MM cells and NK cells may lead to the rational development of novel NK cell-based therapies.

RESTORING NK CELLS FOR MM THERAPY

NK cells play an integral role in tumor surveillance, but are thought to be dysfunctional in MM patients. Immunosuppressive cells and

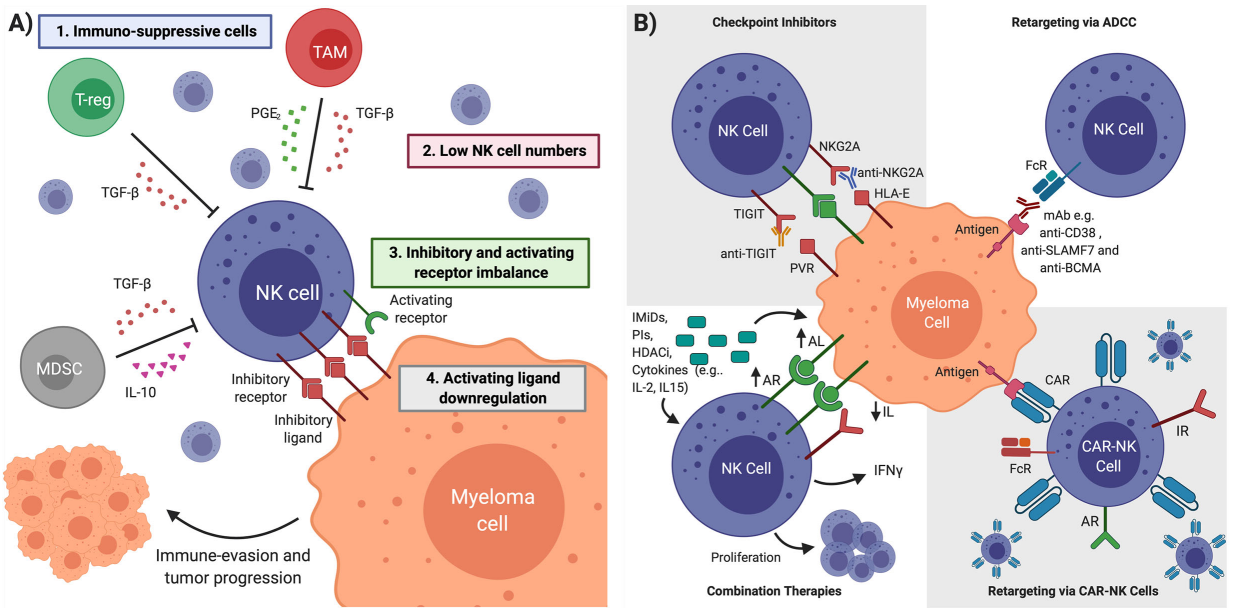

FIGURE 3 | NK Cell Restoration Approaches for Multiple Myeloma Immunotherapy. **(A)** NK cell impairment in MM is characterized by (1) immunosuppressive cells and cytokines (2) low NK cell numbers (3) inhibitory and activating receptor imbalance in favor of NK cell inhibition (4) downregulation of activating ligands on cancer cell. Multiple myeloma cells in an impaired NK cell environment evade detection and continue proliferation. **(B)** Several therapeutic interventions can overcome NK cell impairment. Checkpoint inhibitors block inhibitory receptors to unleash NK cell cytotoxicity. Antibody-dependent cellular cytotoxicity (ADCC) uses mAbs designed to bind tumor-specific antigens and mediate anti-myeloma NK cell killing. Immunomodulatory drugs (IMiDs), proteosome inhibitors (PIs), histone deacetylase inhibitors (HADCi) and cytokines can upregulate activating ligands (ALs) and downregulate inhibitory ligands (ILs) on cancerous cells, upregulate activating receptors (ARs) and IFN-γ in NK cells, as well as promote NK cell proliferation. CAR-NK cells are engineered to target tumor-specific antigens and kill cancerous cells upon introduction to patient. TGFβ is Transforming growth factor beta, PGE2 is Prostaglandin E. Figure created with BioRender.com.

cytokines, low NK cell numbers, IR and AR imbalance, and AR downregulation all lead to NK cell impairment and their inability to kill MM cells (**Figure 3A**). Given this suppressive environment, several therapeutic interventions have been established to restore anti-myeloma NK cell function. While this review focuses primarily on targeting NK IRs, there are several other clinically relevant treatment strategies that can re-engage NK cells to mediate an anti-MM phenotype.

mAbs ADCC

The mAb-ADCC approach recruits NK cells to myeloma cells that may otherwise be unrecognizable as stressed cells due to low activating ligand expression and IR/AR imbalance. As $CD56^{bright}$ NK cells mature to $CD56^{dim}$ cells, they express the Fcγ receptor III (also called CD16) that is important for ADCC against mAb-coated cancer cells (23–26). Patients treated with mAbs that bind tumor specific antigens on MM cells allow NK cells to recognize the Fc region and induce ADCC toward the MM cell (76) (**Figure 3B**).

Currently approved mAbs targeting MM cells include elotuzumab and daratumumab, targeting SLAMF7 and CD38 respectively. Both mAbs enhance NK cell cytotoxicity *via* ADCC (77, 78). Elotuzumab has also been shown to enhance NK cells through a secondary, indirect mechanism (79). The success of these antibody-based therapies may reflect the dynamic expression of their receptor targets. For example, after initial treatment, expression of these receptors was found to be decreased (80, 81). Alternatively, since CD38 is broadly expressed on NK cells, treatment with anti-CD38 mAbs may lead to a substantial depletion of the NK cell population (74). As a whole, mAbs have been successful in treating a subset of MM patients.

CAR-NK Cell Therapy

Adoptive NK cell therapy aims to restore patient innate immune surveillance and control cancer progression by supplementing with new NK cells. This approach has shown promise against MM and other hematological malignancies including leukemia (82). Chimeric antigen receptor NK (CAR-NK) cells are a type of adoptive transfer therapy that uses genetically manipulated NK cells to specifically target tumor antigens. CAR-NK cell development builds on the recent success of CAR-T cells in cancer therapy. The significant clinical outcomes of anti-CD19 CAR-T cells in MM justified the creation of CAR-T cells targeting other antigens expressed on myeloma cells, including CD38 (83), CD138 (84), SLAMF7 (85), SLAMF3 (86), CD56 (87), NKG2D (88), and most successfully BCMA (89). However, despite their early success, CAR-T cells are not exempt from limitations such as Graft-versus-Host disease (GvHD), cytokine release syndrome, neurotoxicity and off-tumor/on target toxicity (90, 91) that threaten patient safety. CAR-NK cells were developed to overcome some of the limitations of CAR-T cells.

Compared to CAR-T cells, CAR-NK cells have shorter half-lives which may reduce some of the toxic side effects such as the induction of GvHD and the production of cytokines (92, 93). In addition, NK cells inherently express a range of ARs that prime them for activation (**Figure 3B**). NK cells also express Fc receptors that can enhance NK cell ADCC, suggesting that combination CAR-NK therapy with mAb therapy may be relevant therapeutic avenue to explore. Importantly, unlike CAR-T cells, CAR-NK cells are not HLA restricted; therefore, sources of CAR-NKs could include primary NK cells, NK cell lines (e.g., NK-92), umbilical cord blood or induced pluripotent stem cells (iPSCs) (94, 95). Taken together, these properties suggest CAR-NK cells could be a favourable alternative to CAR-T cells. Interestingly, NK cell lines make great candidates for NK genetic engineering allowing for the production of an "off-the-shelf therapeutic". CAR-NK cells targeting several different antigens, including CD138, SLAMF7, CD19, CD20, CD33 and CD123, using both primary NK cells and NK cell lines, are currently being investigated in pre-clinical studies of both solid and hematological malignancies (96, 97). In hematological malignancies, anti-CD19 CAR-NK-92 cells improved cytotoxicity against leukemia cells and non-Hodgkin's lymphoma or chronic lymphocytic leukemia (CLL) expressing CD19 (98, 99). In MM, preclinical results have shown efficacy of CAR-NK cells targeting CD138 (100). CAR-NK cells targeting BCMA, NKG2D (101), or SLAMF7 (102) are also being explored within a MM context.

Early clinical trials using anti-CD33 CAR-NK-92 cells showed no major adverse effects in relapsed/refractory acute myeloid leukemia (AML) patients, supporting the notion that CAR-NK cells could be a safe alternative to CAR-T cells in hematological malignancies (103). The first CAR-NK cell clinical trial in MM (NCT03940833) plans to use anti-BCMA CAR-NK cells to treat 20 patients with relapsed and refractory MM. Although still in the early stages, CAR-NK cells are becoming a promising NK cell-based therapy for overcoming the immunosuppressive environment of MM.

Combination Therapies

IMiDs have become a staple of MM treatment in the last two decades. Although their canonical mechanism of action is not often thought to include NK cells, IMiDs can act to restore NK cell activity. IMiDs reduce the NK cell activation threshold (104), increase NK cell proliferation and enhance NK cell mediated cytotoxicity (105). Multiple studies also show lenalidomide or the chemotherapeutic melphalan increases activating ligand expression on MM cells (106, 107). Furthermore, *in-vitro* and *in-vivo* studies have shown that the combination of elutuzumab and lenalidomide enhanced anti-proliferative effects more than any single agent and was associated with increase NK cell activation as demonstrated by the stimulation of activating cytokine production and induction of MM cell death in *in vitro* co-culture assays. Interestingly, in *in-vivo* established MM xenografts, although NK cells recruitment to tumor sites was not associated with lenalidomide, this recruitment could be enhanced by the addition of elotuzumab, likely through an ADCC-mediated mechanism (108). Another *in-vitro* study on BM mononuclear cells from MM patients have been shown that combination of daratumumab-IPH2102 anti-killer cell immunoglobulin-like receptors (anti-KIR) with lenalidomide have improved the NK cell ADCC activity and myeloma cell lysis (108, 109) (**Figure 3B**).

Proteosome inhibitors, such as bortezomib, also enhance anti-MM NK cell killing by downregulating HLA-I (110), upregulating NKG2D and DNAM-1 ligands (106), and increasing tumor cell susceptibility to NK cell activity *via* upregulation of the TRAIL and FasL apoptotic pathways (111). Bortezomib in combination with elozuzumab and daratumumab have proven effective (112, 113). Histone deacetylase (HDAC) inhibitors might also upregulate activating ligand MICA and improve the anti-MM NK cell response (114).

Expectedly, certain cytokines have been shown to augment NK cell function in MM and other hematological cancers. These cytokines include IL-2 and TNF-α (114), IL-15 and IL-21 (115, 116). However, given the ability of different cytokines to upregulate other parts of the immune system at a considerably high level, there are significant risks associated with their use. Although IL-2, for example, has been approved for metastatic renal cell carcinoma and metastatic melanoma, it is not a standard treatment in monotherapy due to severe side effects in high doses (117). Moving forward, incorporating lose dose cytokines in combination with other treatments should be the focus.

NK CELL IRS

Targeting NK IRs may unleash the breaks preventing NK cells from detecting and killing myeloma cells. Common IRs include KIRs, NK group 2 member A (NKG2A), T-cell immunoglobulin and mucin-domain containing-3 (TIM-3), T-cell Ig and ITIM domain (TIGIT), V-domain Ig-containing suppressor of T cell activation (VISTA), programmed death-1 (PD-1), cytotoxic T-lymphocyte-associated protein 4 (CTLA4) and lymphocytic-activation gene 3 (LAG-3) (**Figure 1**). In order to overcome IR/AR imbalance and the altered activation threshold following AR downregulation, the use of immune checkpoint inhibitors to block IRs on NK cells will reduce the inhibitory signal thereby enhancing NK cell activation (**Figure 1**).

KIRs are a group of inhibitory and activating type I transmembrane glycoproteins expressed on most NK cells and some T-cell subsets (118, 119). Belonging to the immunoglobulin superfamily, KIRs have a transmembrane domain, a cytoplasmic tail, and two or three Ig-domains. Generally, short cytoplasmic domains (KIR2DS/KIR3DS), transduce activating signals to the lymphocyte while long cytoplasmic domains (KIR2DL/KIR3DL) inhibit lymphocyte-mediated cytotoxicity (120).

The significant ligands of the KIR family include the HLA-I molecules. The most well-characterized inhibitory ligand is HLA-C where KIR2DL1 binds the C2 allele of HLA-C, and KIR2DL2 binds the C1 allele (121, 122), although activating KIRs have also been shown to interact with HLA-C (123). Inhibitory KIRs also interact with HLA-B (124), HLA-A (125), and HLA-F (126). Although KIR expression on NK cells was initially thought

to vary stochastically, it is now understood that NK cells undergo an educational process as they mature, altering the expression of specific KIRs to maximize the balance between self-tolerance and effective defense (127). Additionally, a study evaluating hematopoietic stem cell transplantation in leukemia patients showed that NK cells expressing KIR2DL2/3 inhibitory receptors were still able to kill HLA-C expressing cancer cells if KIR2DS1 activating receptor was co-expressed (128), suggesting that KIR activating receptor profiles of patients should also be considered when targeting the KIR-HLA-I blockade.

In non-transplantation settings, blocking the KIR-ligand axis may improve tumor immunity, similar to other checkpoint inhibitors (129). Thus, several researchers have started developing anti-KIR antibodies to effectively create missing-self tumor cells and to lower the NK cell activation threshold. Pre-clinical studies showed that the anti-KIR mAb 1-7F9 (also called IPH2101) blocked inhibitory receptors KIR2DL1/2/3 and activated antitumor NK cytotoxicity against HLA-C expressing AML cells (130). In MM, combining lenalidomide with IPH2101 in mouse models augmented the anti-myeloma NK cell response and increased tumor clearance (131).

Despite this pre-clinical success, heterogeneity in KIR expression can make mAbs targeting of these KIRs difficult in a clinical setting (132). A phase I trial (NCT00552396) (n=32) investigated IPH2101 as monotherapy in MM patients and found increased NK cell cytotoxicity against MM cells *ex-vivo*. IPH2101 appeared safe and tolerable at the dose that achieved full inhibitory KIR saturation (133). Another phase I trial (NCT01217203) (n=15) by the same research group this time they investigated the IPH2101-Len combination. Several patients experience severe adverse events, and five reported objective responses (134).

A phase II clinical trial treating MM patients with anti-KIR2D mAb (IPH2101) showed a surprising decrease in NK cell activity and KIR2D expression (129) that is thought to be driven by monocyte trogocytosis, a process of surface protein exchange at the immunological synapse. The same group ran another phase II trial (NCT01248455) (n=9) studying IPH2101 as monotherapy in SMM patients. They postulated treating SMM rather than later stage MM could be the ideal time point for NK cell-based therapy to prevent the more aggressive MM cells from mediating an anti-immune response. IPH2101 was well tolerated with no grade 3 or 4 toxicities, however the study was discontinued due to a lack of patients meeting the defined primary objective (50% decline in M-protein) (135). Due to limited success in these early clinical studies, targeting KIRs may be more effective in combination with other therapies that augment KIR immunogenetics and education of NK cells (136, 137). So far, seven anti-KIR mAb clinical trials in MM are in progress (**Table 1**). One of the ongoing trials is evaluating anti-KIR mAbs in combination with anti-PD1 therapies, anti-CTLA-4 or daratumumab in myeloma and lymphoma patients (NCT01592370). Several anti-KIR combination therapy clinical trials are also in the recruitment stages. Combinations with other drugs or interventions such as CAR-T cell therapy, CAR-NK cell therapy, or in the setting of adoptive cellular transfer therapy may also improve the response. Trials with greater patient enrollment and the ability to characterize individual patient NK cell profiles would offer value and help identify patients profiles that respond best to this intervention.

NKG2A is an inhibitory receptor that belongs to the C-type lectins. It is a type II membrane receptor that forms a heterodimer with CD94 (138). NKG2A/CD94 is primarily expressed on NK cells and some T cells (139). Nearly half of the circulating NK cells express NKG2A/CD94. While its expression corresponds with a lack of KIR expression (140), other IRs including PD-1 and LIR-1 can be co-expressed with NKG2A/CD94 (139–141). NKG2A/CD94 recognizes the HLA-E ligand, a non-classical HLA class I molecule. Typically, HLA-E is expressed by healthy cells. Therefore, its interaction with NKG2A/CD94 represses activation signals and reduces cytokine secretion and NK cell cytotoxicity (142–146). NKG2A competes with the activating receptors NKG2C and NKG2E for the binding to HLA-E (17, 147, 148).

Both ligand and receptor are highly expressed in patient samples across tumor types (149–153). Even though intra-tumoral NKG2A^{+ve} NK cells are seen in the tumor microenvironment, the upregulation of HLA-E by cancer cells implies that these NK cells are functionally exhausted. In this way, high expression of HLA-E or exhausted NKG2A^{+ve} NK cells are associated with poor prognosis in different cancers (143, 144, 154–158). These observations suggest that inhibiting NKG2A/CD94 is a possible strategy that will release NK cell activity through checkpoint blockade therapy.

As proof-of-principle that NKG2A is important for NK cell activity and that it might serve as a relevant therapeutic target, NKG2A protein expression was knocked out in a human retroviral NK cell model to generate NKG2A-null NK cells. When NKG2A expression was lost, these cells showed higher cytotoxicity toward HLA-E positive cancer cells (159). Hence, reducing NKG2A expression or inhibiting it may provide an effective treatment strategy alone or in and combination therapy (150).

Accordingly, monalizumab, a novel IgG4 humanized antibody developed to block CD94/NKG2A, was shown to cause cancer cell death (139). Although not studied in MM, preclinical and clinical investigations in different cancer settings provide evidence that blocking CD94/NKG2A is a viable therapeutic option. For example, *in-vitro* pre-clinical investigations using NK cells from chronic lymphoid leukemia (CLL) patients showed that monalizumab restored their cytotoxicity (143). Similarly, using cells from previously treated patients with head and neck squamous cell carcinoma, it was shown that monalizumab boosted NK ADCC as well as unleashed CD8+ T cells. Monalizumab also synergized with anti-PD-1/PD-L1 blockade and cetuximab mAb combined therapy in *in-vitro* assays (139). Further *in-vivo* mouse studies revealed that the anti-NKG2A antibody could kill engrafted primary human leukemia through an NK cell-mediated mechanism (158).

Although there is limited knowledge regarding the role of NKG2A in MM, *in-vitro* experiments showed that the level of

TABLE 1 | Selected clinical trials evaluating the safety, tolerability and efficacy of potential NK IRs for Multiple Myeloma NK cell-based immunotherapy (access date: August 10, 2020).

Receptor	Trial	Disease	Drugs	Phase	Participants	Results	Last Update Posted
KIR	NCT01217203	Relapsed multiple myeloma	IPH2101, Lenalidomide	I	15	Complete; Objective response in 5 patients; Severe adverse events in 5 patients; No autoimmunity	February 28, 2014
	NCT01222286	Smoldering multiple myeloma	IPH2101	II	30	Complete; No objective response; Adverse events in all patients	May 9, 2014
	NCT00999830	Multiple myeloma	IPH2101	II	27	Completed; Primary response in one patient (based on M-protein); Adverse events in 25 of 27 patients	March 24, 2016
	NCT00552396	Multiple myeloma	Anti-KIR (1-7F9)	I	32	Complete; No dose-limiting toxicity; Severe adverse event in 1 patient; Increased patient NK cell cytotoxicity against MM *ex vivo*	March 31, 2016
	NCT02252263	Multiple myeloma	Elotuzumab, Lirilumab, Urelumab	I	44	Complete; No results	November 1, 2017
	NCT01592370	Non-Hodgkin's lymphoma, Hodgkin lymphoma, multiple myeloma	Nivolumab, Ipilimumab, Lirilumab, Daratumumab, Pomalidomide, Dexamethasone	I/II	375	Ongoing	May 18, 2020
	NCT01248455	Multiple myeloma, smoldering multiple myeloma	Anti-KIR	II	9	Terminated; Lack of patients meeting primary objective (50% decline in M-protein)	November 19, 2019
NKG2A	NCT02921685	Hematologic malignancies	Monalizumab	I	18	Ongoing	September 19, 2018
LAG-3/TIGIT	NCT04150965	Relapsed refractory multiple myeloma	Elotuzumab, Pomalidomide, Dexamethasone, Anti-LAG-3, Anti-TIGIT	I/II	104	Ongoing	July 7, 2020
PD1	NCT02903381	Smoldering multiple myeloma	Nivolumab, Lenalidomide, Dexamethasone	II	41	Suspended; Safety concerns	July 21, 2020
	NCT02636010	Multiple myeloma	Pembrolizumab	II	20	Complete; No results	April 29, 2020
	NCT02331368	Multiple myeloma	Autologous Stem Cell Transplant, Melphalan, Lenalidomide, MK-3475	II	32	Terminated; Complete response in 7 of 23 evaluable patients; Severe adverse events in 14 of 32 total patients	July 27, 2018
	NCT03848845	Multiple myeloma	GSK2857916, Pembrolizumab	II	40	Ongoing	August 5, 2020
	NCT03605719	Recurrent plasma cell myeloma	Carfilzomib, Dexamethasone, Nivolumab, Pelareorep	I	62	Ongoing	November 25, 2019
	NCT03530683	Lymphoma, multiple myeloma	TTI-622, Rituximab, PD-1 Inhibitor, Proteasome-inhibitors	I	156	Ongoing	September 12, 2019
	NCT03111992	Multiple myeloma	PDR001, CJM112, LCL161	I	26	Complete; No results	April 21, 2020
	NCT03357952	Multiple myeloma	Daratumumab, JNJ-63723283	II/III	10	Ongoing; All patients with treatment emergent adverse events; No dose limiting toxicity so far	January 3, 2020
	NCT03221634	Multiple myeloma	Pembrolizumab, Daratumumab	II	0	Withdrawn; Business reasons	March 25, 2019
	NCT03292263	Multiple myeloma	Melphalan, Nivolumab, Autologous Stem Cell Transplantation	I/II	30	Ongoing	March 17, 2020
	NCT02906332	Multiple myeloma	Pembrolizumab, Lenalidomide, Dexamethasone	II	16	Ongoing; Combination is well tolerated; Preliminary data show potential efficacy	January 31, 2020
	NCT02807454	Multiple myeloma	Daratumumab, Durvalumab, Pomalidomide, Dexamethasone	II	37	Ongoing	July 2, 2020
	NCT02685826	Multiple myeloma	Durvalumab, Lenalidomide, Dexamethasone	I/II	56	Ongoing; Majority of patients with adverse events; Dose-limiting toxicity in 2 patients	April 27, 2020
	NCT02616640	Multiple myeloma	Durvalumab, Pomalidomide, Dexamethasone	I	114	Ongoing	April 17, 2020
	NCT02576977	Multiple myeloma	Pembrolizumab, Pomalidomide, Dexamethasone	III	251	Terminated; Anti-PD1 treatment combination had unfavourable benefit-risk profile in relapsed refractory multiple myeloma	July 31, 2020

(Continued)

TABLE 1 | Continued

Receptor	Trial	Disease	Drugs	Phase	Participants	Results	Last Update Posted
	NCT02579863	Multiple myeloma	Pembrolizumab, Lenalidomide, Dexamethasone	III	310	Terminated; Anti-PD1 treatment combination had unfavourable benefit-risk profile in newly diagnosed multiple myeloma	August 3, 2020
	NCT02289222	Multiple myeloma	MK-3475, Pomalidomide, Dexamethasone	I/II	48	Terminated; Due to inclusion of an IMiD in combination with pembrolizumab	November 5, 2019
	NCT02077959	Multiple myeloma	Lenalidomide, Pidilizumab	I/II	20	Complete; No results	May 30, 2019
	NCT02036502	Multiple myeloma	Pembrolizumab, Lenalidomide, Dexamethasone, Carfilzomib	I	77	Complete; Tolerable safety profile; Notable anti-tumor activity	July 13, 2020
	NCT02726581	Multiple myeloma	Nivolumab, Elotuzumab, Pomalidomide, Dexamethasone	III	348	Ongoing	August 10, 2020

HLA-E on the myeloma cells could potentiate the inhibition of NKG2A (67). This suggests that anti-NKG2A may be beneficial for patients that have functional levels of HLA-E (67, 148), although studies proving this hypothesis are still ongoing. This preliminary evidence, combined with positive preclinical studies in other malignancies (149, 156), points to the therapeutic potential of blocking NKG2A in MM. An ongoing phase I clinical trial (NCT02921685) is investigating monalizumab as monotherapy in patients with hematologic malignancies that were previously treated with an allogeneic HSCT (**Table 1**).

TIM-3 is an IR expressed on functional and mature NK cells and other lymphocytes. TIM-3 interacts with specific ligands that include HMGB1 (high mobility group protein B1 proteins), CEACAM-1 (carcinoembryonic antigen cell adhesion molecule 1), PtdSer (phosphatidylserine), and galectin-9 (160–162). Engagement of TIM-3 with its ligands decreases cytokine production and NK cell toxicity, which eventually leads to tumor immunity and disease progression (163–165).

Like other IRs, expression of TIM-3 was also observed in circulating NK cells from cancers including lung adenocarcinoma (164), gastric cancer (166), advanced melanoma (167), bladder cancer (168), and follicular B-cell NHL. Upregulation of TIM-3 is linked to lymphocyte exhaustion and dysfunction (162, 169) and consequently can lead to poorer survival and tumor progression in several cancers (170).

Preclinical studies harvesting NK cells from patients with solid tumors have shown that blocking TIM-3 with anti-TIM-3 antibodies unleashed NK cell activity and induced IFN-γ production in NK cells (164, 171). Additional studies demonstrated that blocking TIM-3 reduced tumor growth in mouse models (169) or increased NK cell cytotoxicity against K562 leukemic cells (172).

It is important to note that there is still debate in the literature with contradictory assumptions about TIM-3 interaction with its ligands (173). For example, one study showed that binding of TIM-3 with Gal-9 stimulated IFN-γ release by NK cells, although this did not enhance NK cell-mediated toxicity (174). In another study, an anti-Gal-9 antibody that blocks its interaction with TIM-3 reduced IFN-γ production from NK cells from healthy donors when cocultured with primary AML blasts (160). Further, blocking of TIM-3 on IL15-stimulated NK cells showed little or no significant lysis of human pancreatic cancer cell lines (175). Similarly, and counter-intuitively, higher TIM-3 expression has been associated with increased tumor progression (166, 168, 171). Indeed, in a severe aplastic anemia mouse model, it was observed that the activity of the TIM-3^{-ve} NK cell population was higher than the TIM-3^{+ve} NK cell population (176). These results suggest that effect of TIM-3 blockade on NK cells may be tumor-specific and reflect the complex expression profiles of immune markers in both a cancer-specific and patient-specific manner.

TIM-3 blocking mAbs are under clinical investigation either alone or in combination with anti-PD-1/PD-L1 mAbs. Initial results of TIM-3 blocking in solid tumors reported a manageable safety profile and revealed early signs of activity even in patients previously treated with PD-1 or PD-L1 mAb (177, 178). Recent data from a current clinical trial on high-risk myelodysplastic

syndrome (HR-MDS) and AML patients demonstrated that the combined treatment of the TIM-3 mAb MBG453 with decitabine was safe and well-tolerated and confirmed anti-tumor activity (179).

Overall, preliminary data suggests TIM-3 is a promising therapeutic target in several cancer types and supports the further clinical development of anti-TIM-3 inhibitors. No studies have specifically explored the role of TIM-3 in MM.

TIGIT is another inhibitory receptor expressed by both NK and T cells (180, 181). Several cancer types showed a high level of TIGIT on the tumor-infiltrating lymphocytes (TILs) (182). TIGIT recognizes the poliovirus receptor (PVR), also known as CD155 or Necl5, as well as the Nectin-2 (CD112), or Nectin-3 ligands that are overexpressed on multiple cancer types (183–185) and linked to unfavorable prognosis in several cancers (186, 187).

The majority of studies evaluating the role of TIGIT on tumor progression have focused on T cells and shown that TIGIT suppresses activity of T cells. In MM, refractory MM patients treated with DARA-pomalidomide combined therapy showed an increase in the exhausted T cells expressing $CD28^{-ve}LAG3^{+ve}TIGIT^{+ve}$ (188, 189). Although NK cells were not evaluated, given that TIGIT is also expressed on NK cells, it is plausible that NK cells may also be inhibited.

When focusing on NK cells, TIGIT has been shown to both contribute to and inhibit tumor progression. In one study, Jia et al. (190) found that, although the number of $TIGIT^{+ve}$ NK cells in AML patients were significantly lower in comparison to the healthy controls, these $TIGIT^{+ve}$ NK cells also express high levels of ARs CD16 and CD160. Importantly, functional experiments showed an elevated expression of granzyme B and increased IFN-γ and TNF-α production by $TIGIT^{+ve}$ NK cells compared with $TIGIT^{-ve}$ NK cells. Therefore, the authors suggest that TIGIT expression on NK cells could be associated with activated and functional status of NK cell in AML and may impede tumor progression (190). The role of TIGIT is also complicated by the duality of the TIGIT ligand PVR. PVR is also a ligand recognized by the AR DNAM-1 that is expressed on NK cells. DNAM-1 has been shown to play a prominent role in NK cell-mediated anti-MM response (191). While TIGIT expression is increased in MM patients, DNAM-1 expression is decreased (192).

Given the dynamic nature of TIGIT expression on both NK cells and T cells as well as the dual role of TIGIT ligand PVR, particularly in MM, understanding how TIGIT affects NK cell function is critical. The complexity of this immune environment highlights the necessity to profile patients for expression of key IRs and ARs in order to better understand how to specifically harness NK cells to mediate an anti-tumor response in MM. $CD8^{+ve}$T cells in the BM of newly diagnosed and relapsed MM patients expressed higher levels of TIGIT compared with those in the healthy group. In this cohort, the investigators observed moderate levels of TIGIT on the NK cells from newly diagnosed or relapsed patients (186). The same study investigated the anti-TIGIT mAb in an *in-vivo* model and showed that the anti-TIGIT mAb decreased myeloma disease burden in the BM and prolonged survival compared with control-Ig, or anti-PD-1 mAb-treated mice (186). This suggests that TIGIT expression is more dominant than PD-1 in the immunosuppressive function in MM, although the precise role of NK cells in this model was not examined.

The high expression of TIGIT on NK cells suggests that a blockade of TIGIT as a monotherapy or in combination with other therapies may reverse NK cell exhaustion and enhance their activation (181). There are numerous pre-clinical studies evaluating this hypothesis and examining how blocking TIGIT affects an anti-tumor immune response. In an *in-vivo* study, it was observed that $TIGIT^{-ve}$ NK cells prevented colon tumor progression in mice. Similarly, the TIGIT blocking mAb overturned the exhaustion of antitumor NK cells, reactivating them and subsequently decreasing tumor growth (181). Importantly, it was observed that the absence of NK cells reduced the therapeutic effects of this TIGIT blocking mAb, suggesting that the presence of NK cells and the level of TIGIT expression on these NK cells may be critical for the clinical outcome of TIGIT blocking immunotherapy.

Blocking TIGIT in combination with other therapies has also shown pre-clinical success. Combined treatments with anti-TIGIT and anti-PD-1 antibodies in a mouse models showed significant growth reductions in lymphoma (193) and other tumors (194, 195) compared to monotherapies. Furthermore, co-expression of TIGIT with either PD-1 or TIM-3 has been correlated with a dysfunctional phenotype in TILs (195). Additional studies have shown that PVR expression can be induced by chemotherapy (192) or by IL-8 signaling through the CXCR1/CXCR2 axis (191), suggesting that a combination of anti-TIGIT mAbs with chemotherapy may be beneficial when patients' immune cells have TIGIT expression.

Anti-TIGIT mAbs are now in phase I/II clinical trials as monotherapy or in combination with anti-PD-1 in solid tumors. Preliminary data from one trial (NCT02964013) showed a manageable safety profile and positive clinical response. Functional studies assessing how anti-TIGIT mAbs affect NK cells activity through cytokine production and NK cell degranulation in preclinical and clinical MM models may lead to an improved understanding of how to utilize NK cells in MM therapy.

PD-1 is a surface receptor initially marked for its inhibitory function in T lymphocytes but is expressed on both T and NK cells (196). In healthy tissue, PD-1 regulates T cell activation and maintains self-tolerance (197, 198). PD-1 has two ligands (PD-Ls): PD-L1 and PD-L2 (199). When bound to either of these ligands, PD-1 inactivates its cognate NK or T cells. Since its discovery as an IR, PD-1 has become a central point of study for understanding negative immune cell regulation. Although the receptor plays a crucial role in protective immunity, PD-1 is of particular interest for its implications in tumor immune evasion. While PD-1 may protect healthy cells from immune cytotoxicity, some cancers harness PD-L1 as an evasion approach to bypass immune surveillance (200). While PD-L1 is lowly expressed in healthy human tissue, expression has been shown to be abundant across several different cancer types from different lineages (201).

Expectedly, PD-L1 expression is upregulated in relapsed and refractory MM patients (202–205), although some studies report low expression of PD-L1 in MM (206, 207).

Recent work using mouse models argues PD-1 also plays a robust inhibitory role in NK cells, elucidating the responsiveness of anti-PD-1 treated patients with low tumor HLA expression who would not be expected to show high T cell activity (208). Therefore, studying PD-1 expression and function on NK cells may also be of therapeutic value.

While some studies show that PD-1 is only lowly expressed on activated NK cells (209) and that depletion of NK cells did not significantly affect therapeutic efficacy of the anti-PD-L1 therapy (210), some recent studies support the role of NK cells in the PD-1/PD-L1 inhibitory pathways (211). Some peripheral blood subpopulations display high levels of PD-1 expression and the interruption of the PD-1/PD-L1 axis could partially restore antitumor function of these NK cells in an ovarian cancer model (212). In MM, early preclinical studies of the interplay between PD-1 and PD-L1 in the NK cell showed that blocking PD-1 enhanced NK cell-mediated MM killing while preserving healthy cells (213). Additionally, recent findings showed that in MM patients samples, only NK cells that were positive for myeloma cell markers stained for PD-1, suggesting that PD-1 on NK cells was acquired from MM cells (214). As before, the discrepancy in research findings points to the complexity of the immune landscape and the need for a better understanding of the relationship between immune cell players and the expression of specific receptors and their ligands across patient datasets.

Despite success in solid tumors, anti PD-1/PD-L1 mAbs failed as monotherapy in MM (215) (**Table 1**). Failure as monotherapy has driven clinical testing of these antibodies in combination therapies. Data from phase I and phase II trials – NCT02289222 (n= 48) and NCT02036502 (n=62) – reported a very good response and acceptable safety profile for the combination of Pembrolizumab (Pem) with Lenalidomide (Len) or Pomalidomide (Pom) and Dexamethasone (Dex) in MM patients (216, 217). Another phase II trial (NCT02331368) (n=32) Pem in the early post-ASCT period was considered safe, and Pem with low Len dose was able to maintain and extend post-ASCT responses in a subgroup of patients (218). However, the immune-related adverse events and related toxicity of anti-PD-1-IMiDs combinations were unpredictable in RRMM trials, leading to patient mortality. The FDA determined that the benefit/risk ratio of the combination in RRMM is not worth the continuation of anti-PD-1-IMiDs trials.

Other combination regimens, such as anti-PD-1-radiation therapy, anti-PD-1-tumor vaccination, or combinations with other IR blockades may enhance the prognosis of refractory MM patients. Currently, blocking PD-1 with CARs has attracted the interest of investigators, with a new phase II trial (NCT04162119) recruiting patients to explore the safety and efficacy of BCMA-PD1-CAR-T cells in RRMM. BCMA-PD-1-CAR-T cell therapy works by administering T cells modified to target BCMA and secrete a PD-1Fc fusion protein capable of blocking the PD-L1/PD-1 inhibitory axis.

Given that low numbers of anti-MM T cells are a commonality amongst relapsed patients while NK cell-mediated MM cytotoxicity can be enhanced by anti-PD-1 therapy (219), the potential to harness anti-PD-1 therapy through NK cells to complement T cell-based therapies is still of interest. Therefore, a focus on combination therapies specifically enhancing the NK cell MM response may be of value.

LAG-3 is a transmembrane protein expressed on activated T cells, NK cells, B cells, and dendritic cells (220–224). Best known for its diverse function in T cells, LAG-3 acts to control T cell activation and proliferation, while inhibiting T-reg function (221, 225). LAG-3 negatively regulates T cells by competing with CD4 in the binding of human leukocyte antigen class II (HLA-II) (226). LAG-3 can further inhibit T cell activation through binding FGL-1 independent of HLA-II. Targeting the LAG3-FGL-1 axis in murine models with mAbs promotes the antitumor T cell response (227–229)

While PD-1 and CTLA-4 were the focus of initial immune checkpoint therapies, LAG-3 is part of the next wave of IRs being clinically investigated (230). Studies demonstrated strong co-expression of PD-1 and LAG-3 on antitumor T cells (231). Combination treatment with mAbs against both negative receptors significantly reduced tumor growth in mouse models that were unresponsive to monotherapy mAb treatment, which indicates synergy between the PD-1 and LAG-3 inhibitory pathways (232). Other mouse studies revealed that anti-LAG-3 mAbs enhanced anti-PD-1 therapies and increased the secretion of activating cytokines released by tumor-infiltrating T cells (233).

In MM, one study looked at immune checkpoint expression in the pathological shift from smoldering MM to symptomatic MM and demonstrated that LAG-3 expression on T cells increased with disease progression, suggesting LAG-3 as a potential target for immunotherapy (234). Investigating biological markers on T cells after autologous stem cell transplants of MM patients, high LAG-3 expression on peripheral blood T cells post-transplant was associated with a lower event-free survival (235). This observation is supported by another study that also showed high T cell LAG-3 expression post-transplant was linked to poor prognosis of MM patients (236). The role of LAG-3 on NK cells in MM is an area of ongoing investigation.

Although LAG-3 is expressed on NK cells, it should not be considered a canonical immune checkpoint because of its low or absent expression in healthy patients (230, 237, 238). Much of the role of LAG-3 in NK cells is still unknown; however one study showed that LAG-3 expression on NK cell contributes to the effectiveness of anti-LAG-3 mAbs (238).

A more recent analysis of the status of LAG-3 on the NK cell surface following exposure to IFN-α demonstrated an increased expression of LAG3 (239). This paper proposes more studies on the impact of other cytokines on these IRs, and questions whether a single cytokine or a group of them cooperate and upregulate the IR, and/or one cytokine triggers one or array of other chemokines.

Further characterization showed that LAG3 was expressed in the NK cells populations that show high expression of activation and maturation markers. Additionally, *in-vitro* LAG3 blocking on NK cells using mAb led to an increase in the production of cytokines IFN-γ, TNF-α, MIP-1α and MIP-1β, without affecting the cytotoxic activity, which suggests that LAG3 is a negative regulator of cytokine production by mature NK cells (239).

An anti-LAG-3 mAb is currently under clinical investigation in hematological malignancies (**Table 1**).

PERSPECTIVES

Targeting IRs with mAbs has shown preliminary success in early clinical trials with positive response rates for some cancers. Emerging evidence also suggests that targeting IRs expressed on NK cells in MM remains a viable option and requires further exploration with particular attention paid to understanding the heterogeneity in ligand expression both within and across MM patients, the interplay between NK and T cells in response to IR blockade therapy, and how NK-targeted therapy can be combined with existing therapeutic options in MM patients.

In this review, we have highlighted the preclinical evidence that IRs on the NK cell such as KIRs, NKG2A, TIGIT, TIM-3, PD-1, and LAG-3 may impact MM biology and response to treatments. KIRs remain the most promising target. Not only were anti-KIR antibodies shown to be well tolerated, but they were also shown to enhance NK cell function (133, 134). As monotherapy, a phase I clinical trials showed that targeting KIRs in monotherapy increased NK cell cytotoxicity against MM cells *ex-vivo* (NCT00552396). Another phase I clinical trial of anti-KIR in combination with lenalidomide demonstrated positive objective responses in a subset of patients (NCT01217203). Although some of the phase II trials did not report significant patient responses, we argue that a lack of understanding regarding the expression of KIRs limits our ability to predict positive responses in clinical trials.

Many of the IRs such as TIGIT, LAG-3, PD-1, and VISTA are expressed not only on NK cells, but also on T cells. Theoretically, blocking an IR expressed on both NK cells and T cells should enhance the anti-cancer effects of both immune cell types. However, the bulk of research on these IRs, particularly in the case of PD-1 and VISTA, has only elucidated their role on T cells, while neglecting to explore the role of NK cells. This is the case within the MM field as well as within the broader cancer community, highlighting the need for a more comprehensive understanding of how each immune cell type independently and collectively contributes to an anti-cancer effect. Specifically, the importance of NK cells has been shown in a study where the presence of NK cells affects the efficacy of a TIGIT-blocking mAb (181). NK cells serve as an important mediator of the immune response that have several advantages over T cells. For example, T cell activation requires both antigen recognition *via* the TCR using restricted receptors produced by gene rearrangement followed by a second activating, costimulatory signal. NK cells, on the other hand, are equipped with a repertoire of receptors to initiate activating signals that lead to NK cell-mediated cytotoxic cell lysis and cytokine production (29, 240), making them a more attractive target than T cells. The activation mechanism for NK cells relies simply on the balanced expression of ARs and IRs where the use of IR-targeted therapies can shift this balance in favour of an anti-tumour response. Additionally, as part of the innate immune system, NK cells are the first responders and are not only able to initiate an immune response much faster than T cells but are also responsible for recruiting T cells (241). By incorporating analysis of NK cell biology along with T cell assessment in both preclinical and clinical trials, the precise role of NK cells in MM development can be better understood. There may also be NK cell IRs playing a role in MM that have yet to be elucidated. Although there is little support for their role in healthy NK cells, preliminary evidence suggests VISTA and CTLA-4 IRs may affect NK function within a diseased microenvironment.

Tailoring treatment to patient-specific expression of receptors is widely adopted within the solid tumor community, but its use in MM is still relatively new. To ensure success of IR blockade therapy in MM, it is essential to estimate the patient's expression of NK specific inhibitory ligands on malignant MM cells as well as the expression and functionality of targetable IRs on NK cells or T cells. Similarly, assessing the NK cells' percentage, viability and functionality prior to the initiation of therapy may predict response to therapy. Previous trials proposed that the intra-tumoral level of IRs such as PD-1 on TILs were significant determinants of success for IR mAb therapies (242). However, there is not only heterogeneity in the percentage and activity of NK cells within a MM patient population (59, 65, 67), but also in the expression of specific IRs or ligands. Such differential expression can affect activity of NK cell functionality.

With this knowledge, prescription of specific IRs mAb relevant to individual expression patterns will more likely augment the immune cells to eradicate the cancer cells by hampering their evasion strategies in a precision-focused manner.

Early failure in clinical trials blocking these IRs is likely a complicated story reflecting not only intra- and inter-patient heterogeneity discussed above, but may also reflect the impaired immune landscape that is also temporally dynamic. A better understanding of how NK cell proliferation, function, and expression of receptors or their ligands changes during disease progression as well as in response to specific chemotherapeutics will improve our ability to effectively target NK cells to enhance their anti-tumor response. Specifically, studies have shown that expression of ligands such as PVR, PD-L1 can be enhanced by chemotherapy and/or IFN-γ (191, 192, 243). Similarly, NK cell contact with malignant MM cells was shown to enhance expression of PD-1 and CD94 by a process called trogocytosis (67, 214) and LAG-3 due to the exposure to the IFN-α (239). Recent studies also show a shift in NK cell populations during MM disease progression from MGUS to active MM (66, 67). Combined with knowledge regarding receptor or ligand expression, understanding these temporal dynamics will improve targeted IR therapy and the ability to treat the right patients at the right time.

Additionally, given the complex immune landscape in which NK cells reside, blocking a single NK cell IR may be insufficient in overcoming NK cell impairment in patients with severely

compromised immune systems. Combination therapies further restoring immune and NK cell function may enhance NK cell IR therapies and elicit better patient outcomes. For example, a trial assessing both TIGIT and LAG-3 targeting in combination with anti-PD-1 is ongoing (NCT04150965). Similarly, IR-targeted therapy not only has implications for the intrinsic cytotoxic capabilities of NK cells, but can also be used within an ADCC and CAR-NK cell context. Considering the unique characteristic of the NK cells, which mediating ADCC, combining mAb against specific antigens expressed on myeloma cells with mAb targeting specific NK IRs according to their functional level and their cognate ligands on myeloma cells could enhance the NK cells killing. The combination of PD-1 blockade with mAbs daratumumab or elotuzumab are intriguing possibilities currently under investigation (219). Similarly, concomitantly using CAR-NK cells or genetically engineered NK cell/NK cell lines for adoptive cellular therapy with NK IRs blockade may also enhance the NK-mediated immune response and offer an interesting strategy to treat MM patients. Despite failure of some combination strategies with PD-1/PD-L1 checkpoint blockade in MM due to significant toxicity (217), the careful selection of patient-specific combination strategies may yield more promising results.

To conclude, we can say that there is a body of knowledge supporting the role of NK cells, IRs and cancer progression, although the evidence characterizing NK cells and their subpopulations in myeloma patients or the myeloma-NK cell interaction is still lacking. Therefore, we envision some key steps and factors to be considered in order to build on the foundation of myeloma-NK cell biology:

1. Profile NK cell receptors and subpopulations, NK cell activity and abundance, and NK cell function in myeloma.
2. Profile the expression of NK cell receptor cognate ligands in myeloma.
3. The immunosuppressive nature of myeloma poses a general challenge to immunotherapies in myeloma including those involving NK cells, and understanding and overcoming this challenge is critical to success.
4. Investigate the mechanisms that control specific ligands on the surface of myeloma.
5. Study ligand expression at the transcriptional and protein levels.
6. Evaluate the role of chemokines and soluble factors released in the microenvironment and if they positively or negatively mediate NK receptors and/or their ligands.
7. Explore the integration of NK cell-based therapies with traditional myeloma therapies pre-clinically to optimize clinical trial design.
8. Pursue the promise of CAR-NK cells in clinical trials.
9. *In vitro* and *in vivo* models should be used to study:

-Myeloma–NK cell interaction

-Impact of NK cell receptor targeting on the effectiveness of mAb therapy for myeloma

-Personalizing approaches to NK cell-based therapies using knowledge of NK cell function and myeloma-NK cell ligand expression heterogeneity.

-Approaches to building CAR-NK cells as myeloma therapeutics (autologous, allogeneic, "off the shelf")

Mobilizing NKs in MM is particularly attractive due to their natural capacity to distinguish damaged cells from healthy cells, allowing them to specifically eliminate only the damaged cells. Utilizing NK-based immunotherapy in MM remains an interesting and understudied area of research. This review highlights the important role that NK IRs may play in MM. With more research, we propose the development of a patient-specific strategy that incorporates precise IR blocking that can be adjusted according to patient-specific responses and changes due to different treatments regiments. This will involve more investigation into NK cell characteristics, their related ligands and NK cells subpopulations in MM patients as well as the MM microenvironment throughout disease stages. With this understanding comes the potential for novel IR-blockade immunotherapies regimen that could improve disease control and thus increase survival outcomes.

AUTHOR CONTRIBUTIONS

All authors contributed to the article and approved the submitted version. HA and TR conceptualized and designed the manuscript. JW and HA designed and created the figures and generated the clinical trial table. SG critically edited the manuscript.

FUNDING

This work is supported by a grant from The Canadian Institutes of Health Research (CIHR)-The New Brunswick Health Research Foundation (NBHRF) iCT SPOR grant SMC-151513, Canadian Cancer Society (CCS) 706194 and The Terry Fox Research Institute (TFRI) 1067.

REFERENCES

1. Kyle RA, Rajkumar SV. Multiple myeloma. *Blood* (2008) 111(6):2962–72. doi: 10.1182/blood-2007-10-078022
2. Pinto V, Bergantim R, Caires HR, Seca H, Guimarães JE, Vasconcelos MH. Multiple Myeloma: Available Therapies and Causes of Drug Resistance. *Cancers (Basel)* (2020) 12(2):407. doi: 10.3390/cancers12020407
3. Lozano E, Díaz T, Mena M-P, Suñe G, Calvo X, Calderón M, et al. Loss of the Immune Checkpoint CD85j/LILRB1 on Malignant Plasma Cells Contributes to Immune Escape in Multiple Myeloma. *J Immunol* (2018) 200(8):2581–91. doi: 10.4049/jimmunol.1701622
4. Committee CCSA. *Canadian Cancer Statistics 2019*. Toronto, ON: Canadian Cancer Society (2019).
5. Rajkumar SV. Multiple myeloma: Every year a new standard? *Hematol Oncol* (2019) 37(S1):62–5. doi: 10.1002/hon.2586
6. Rajkumar SV. Multiple myeloma: 2018 update on diagnosis, risk-stratification, and management. *Am J Hematol* (2018) 93(8):981–1114. doi: 10.1002/ajh.25117

7. Giuliani N, Accardi F, Marchica V, Dalla Palma B, Storti P, Toscani D, et al. Novel targets for the treatment of relapsing multiple myeloma. *Expert Rev Hematol* (2019) 12(7):481–96. doi: 10.1080/17474086.2019.1624158
8. Boudreault JS, Touzeau C, Moreau P. Triplet combinations in relapsed/refractory myeloma: update on recent phase 3 trials. *Expert Rev Hematol* (2017) 10(3):207–15. doi: 10.1080/17474086.2017.1285694
9. Lonial S, Nooka AK. Novel combination approaches for myeloma. *Hematology Am Soc Hematol Educ Program* (2015) 2015(1):286–93. doi: 10.1182/asheducation-2015.1.286
10. Palumbo A, Anderson K. Multiple Myeloma. *New Engl J Med* (2011) 364 (11):1046–60. doi: 10.1056/NEJMra1011442
11. Kumar SK, Rajkumar V, Kyle RA, van Duin M, Sonneveld P, Mateos MV, et al. Multiple myeloma. *Nat Rev Dis Primers* (2017) 3:17046. doi: 10.1038/nrdp.2017.46
12. Kumar SK, Lee JH, Lahuerta JJ, Morgan G, Richardson PG, Crowley J, et al. Risk of progression and survival in multiple myeloma relapsing after therapy with IMiDs and bortezomib: a multicenter international myeloma working group study. *Leukemia* (2012) 26(1):149–57. doi: 10.1038/leu.2011.196
13. Afram G, Gran C, Borg Bruchfeld J, Wagner AK, Hussain A, Alici E, et al. Impact of performance status on overall survival in patients relapsed and/or refractory Multiple Myeloma: real-life outcomes of Daratumumab treatment. *Eur J Haematol* (2020) 105(2):196–202. doi: 10.1111/ejh.13426
14. Laubach JP, Paba Prada CE, Richardson PG, Longo DL. Daratumumab, Elotuzumab, and the Development of Therapeutic Monoclonal Antibodies in Multiple Myeloma. *Clin Pharmacol Ther* (2017) 101(1):81–8. doi: 10.1002/cpt.550
15. van de Donk NW, Moreau P, Plesner T, Palumbo A, Gay F, Laubach JP, et al. Clinical efficacy and management of monoclonal antibodies targeting CD38 and SLAMF7 in multiple myeloma. *Blood* (2016) 127(6):681–95. doi: 10.1182/blood-2015-10-646810
16. Kiessling R, Klein E, Pross H, Wigzell H. "Natural" killer cells in the mouse. II. Cytotoxic cells with specificity for mouse Moloney leukemia cells. Characteristics of the killer cell. *Eur J Immunol* (1975) 5(2):117–21. doi: 10.1002/eji.1830050209
17. Vivier E, Tomasello E, Baratin M, Walzer T, Ugolini S. Functions of natural killer cells. *Nat Immunol* (2008) 9(5):503–10. doi: 10.1038/ni1582
18. Chiossone L, Dumas P-Y, Vienne M, Vivier E. Natural killer cells and other innate lymphoid cells in cancer. *Nat Rev Immunol* (2018) 18(11):671–88. doi: 10.1038/s41577-018-0061-z
19. Pallmer K, Oxenius A. Recognition and Regulation of T Cells by NK Cells. *Front Immunol* (2016) 7:251:251. doi: 10.3389/fimmu.2016.00251
20. Herberman RB, Nunn ME, Lavrin DH. Natural cytotoxic reactivity of mouse lymphoid cells against syngeneic acid allogeneic tumors. I. Distribution of reactivity and specificity. *Int J Cancer* (1975) 16(2):216–29. doi: 10.1002/ijc.2910160204
21. Campbell KS, Hasegawa J. Natural killer cell biology: an update and future directions. *J Allergy Clin Immunol* (2013) 132(3):536–44. doi: 10.1016/j.jaci.2013.07.006
22. Adib Rad H, Basirat Z, Mostafazadeh A, Faramarzi M, Bijani A, Nouri HR, et al. Evaluation of peripheral blood NK cell subsets and cytokines in unexplained recurrent miscarriage. *J Chin Med Assoc* (2018) 81(12):1065–70. doi: 10.1016/j.jcma.2018.05.005
23. Cooper MA, Fehniger TA, Caligiuri MA. The biology of human natural killer-cell subsets. *Trends Immunol* (2001) 22(11):633–40. doi: 10.1016/S1471-4906(01)02060-9
24. Fu B, Tian Z, Wei H. Subsets of human natural killer cells and their regulatory effects. *Immunology* (2014) 141(4):483–9. doi: 10.1111/imm.12224
25. Freud AG, Mundy-Bosse BL, Yu J, Caligiuri MA. The Broad Spectrum of Human Natural Killer Cell Diversity. *Immunity* (2017) 47(5):820–33. doi: 10.1016/j.immuni.2017.10.008
26. Wang W, Erbe AK, Hank JA, Morris ZS, Sondel PM. NK Cell-Mediated Antibody-Dependent Cellular Cytotoxicity in Cancer Immunotherapy. *Front Immunol* (2015) 6:368:368. doi: 10.3389/fimmu.2015.00368
27. Wagner JA, Rosario M, Romee R, Berrien-Elliott MM, Schneider SE, Leong JW, et al. CD56bright NK cells exhibit potent antitumor responses following IL-15 priming. *J Clin Invest* (2017) 127(11):4042–58. doi: 10.1172/jci90387
28. Moretta A, Bottino C, Vitale M, Pende D, Cantoni C, Mingari MC, et al. Activating receptors and coreceptors involved in human natural killer cell-mediated cytolysis. *Annu Rev Immunol* (2001) 19:197–223. doi: 10.1146/annurev.immunol.19.1.197
29. Lanier LL. Up on the tightrope: natural killer cell activation and inhibition. *Nat Immunol* (2008) 9(5):495–502. doi: 10.1038/ni1581
30. Ljunggren HG, Kärre K. In search of the 'missing self': MHC molecules and NK cell recognition. *Immunol Today* (1990) 11(7):237–44. doi: 10.1016/0167-5699(90)90097-s
31. Lopez-Soto A, Huergo-Zapico L, Acebes-Huerta A, Villa-Alvarez M, Gonzalez S. NKG2D signaling in cancer immunosurveillance. *Int J Cancer* (2015) 136(8):1741–50. doi: 10.1002/ijc.28775
32. Kruse PH, Matta J, Ugolini S, Vivier E. Natural cytotoxicity receptors and their ligands. *Immunol Cell Biol* (2014) 92(3):221–9. doi: 10.1038/icb.2013.98
33. Moretta L, Montaldo E, Vacca P, Del Zotto G, Moretta F, Merli P, et al. Human natural killer cells: origin, receptors, function, and clinical applications. *Int Arch Allergy Immunol* (2014) 164(4):253–64. doi: 10.1159/000365632
34. Sun JC, Lanier LL. NK cell development, homeostasis and function: parallels with CD8(+) T cells. *Nat Rev Immunol* (2011) 11(10):645–57. doi: 10.1038/nri3044
35. Voskoboinik I, Whisstock JC, Trapani JA. Perforin and granzymes: function, dysfunction and human pathology. *Nat Rev Immunol* (2015) 15(6):388–400. doi: 10.1038/nri3839
36. Takeda K, Hayakawa Y, Smyth MJ, Kayagaki N, Yamaguchi N, Kakuta S, et al. Involvement of tumor necrosis factor-related apoptosis-inducing ligand in surveillance of tumor metastasis by liver natural killer cells. *Nat Med* (2001) 7(1):94–100. doi: 10.1038/83416
37. Imai K, Matsuyama S, Miyake S, Suga K, Nakachi K. Natural cytotoxic activity of peripheral-blood lymphocytes and cancer incidence: an 11-year follow-up study of a general population. *Lancet* (2000) 356(9244):1795–9. doi: 10.1016/s0140-6736(00)03231-1
38. Kim S, Iizuka K, Aguila HL, Weissman IL, Yokoyama WM. In vivo natural killer cell activities revealed by natural killer cell-deficient mice. *Proc Natl Acad Sci U S A* (2000) 97(6):2731–6. doi: 10.1073/pnas.050588297
39. Street SE, Cretney E, Smyth MJ. Perforin and interferon-gamma activities independently control tumor initiation, growth, and metastasis. *Blood* (2001) 97(1):192–7. doi: 10.1182/blood.v97.1.192
40. Vela M, Corral D, Carrasco P, Fernandez L, Valentin J, Gonzalez B, et al. Haploidentical IL-15/41BBL activated and expanded natural killer cell infusion therapy after salvage chemotherapy in children with relapsed and refractory leukemia. *Cancer Lett* (2018) 422:107–17. doi: 10.1016/j.canlet.2018.02.033
41. Plonquet A, Haioun C, Jais J, Debard A, Salles G, Bene M, et al. Peripheral blood natural killer cell count is associated with clinical outcome in patients with aaIPI 2–3 diffuse large B-cell lymphoma. *Ann Oncol* (2007) 18(7):1209–15. doi: 10.1093/annonc/mdm110
42. Lee DA, Denman CJ, Rondon G, Woodworth G, Chen J, Fisher T, et al. Haploidentical Natural Killer Cells Infused before Allogeneic Stem Cell Transplantation for Myeloid Malignancies: A Phase I Trial. *Biol Blood Marrow Transplant* (2016) 22(7):1290–8. doi: 10.1016/j.bbmt.2016.04.009
43. Lorenzo-Herrero S, Lopez-Soto A, Sordo-Bahamonde C, Gonzalez-Rodriguez AP, Vitale M, Gonzalez S. NK Cell-Based Immunotherapy in Cancer Metastasis. *Cancers (Basel)* (2018) 11(1):29–51. doi: 10.3390/cancers11010029
44. Villegas FR, Coca S, Villarrubia VG, Jiménez R, Chillón M, Jareño J, et al. Prognostic significance of tumor infiltrating natural killer cells subset CD57 in patients with squamous cell lung cancer. *Lung Cancer* (2002) 35(1):23–8. doi: 10.1016/S0169-5002(01)00292-6
45. Coca S, Perez-Piqueras J, Martinez D, Colmenarejo A, Saez MA, Vallejo MA, et al. The prognostic significance of intratumoral natural killer cells in patients with colorectal carcinoma. *Cancer* (1997) 79(12):2320–8. doi: 10.1002/(sici)1097-0142(19970615)79:12<2320::aid-cncr5>3.0.co;2-p
46. Min B-W, Kim W-B, Kim K-R, Um J-W, Moon H-Y. The Prognostic Significance of Intratumoral Natural Killer Cells in Colorectal Cancer. *Ann Surg Treat Res* (2003) 65(4):316–21.
47. Eckl J, Buchner A, Prinz PU, Riesenberg R, Siegert SI, Kammerer R, et al. Transcript signature predicts tissue NK cell content and defines renal cell carcinoma subgroups independent of TNM staging. *J Mol Med* (2012) 90 (1):55–66. doi: 10.1007/s00109-011-0806-7

48. Pasero C, Gravis G, Granjeaud S, Guerin M, Thomassin-Piana J, Rocchi P, et al. Highly effective NK cells are associated with good prognosis in patients with metastatic prostate cancer. *Oncotarget* (2015) 6(16):14360. doi: 10.18632/oncotarget.3965
49. Türkseven MR, Oygür T. Evaluation of natural killer cell defense in oral squamous cell carcinoma. *Oral Oncol* (2010) 46(5):e34–e7. doi: 10.1016/j.oraloncology.2010.02.019
50. Habif G, Crinier A, Andre P, Vivier E, Narni-Mancinelli E. Targeting natural killer cells in solid tumors. *Cell Mol Immunol* (2019) 16(5):415–22. doi: 10.1038/s41423-019-0224-2
51. Apostolopoulos A, Symeonidis A, Zoumbos N. Prognostic significance of immune function parameters in patients with chronic lymphocytic leukaemia. *Eur J Haematol* (1990) 44(1):39–44. doi: 10.1111/j.1600-0609.1990.tb00345.x
52. Palmer S, Hanson CA, Zent CS, Porrata LF, LaPlant B, Geyer SM, et al. Prognostic importance of T and NK-cells in a consecutive series of newly diagnosed patients with chronic lymphocytic leukaemia. *Br J Haematol* (2008) 141(5):607–14. doi: 10.1111/j.1365-2141.2008.07070.x
53. Messaoudene M, Fregni G, Fourmentraux-Neves E, Chanal J, Maubec E, Mazouz-Dorval S, et al. Mature cytotoxic CD56bright/CD16+ natural killer cells can infiltrate lymph nodes adjacent to metastatic melanoma. *Cancer Res* (2014) 74(1):81–92. doi: 10.1158/0008-5472.CAN-13-1303
54. Sullivan EM, Jeha S, Kang G, Cheng C, Rooney B, Holladay M, et al. NK cell genotype and phenotype at diagnosis of acute lymphoblastic leukemia correlate with postinduction residual disease. *Clin Cancer Res* (2014) 20 (23):5986–94. doi: 10.1158/1078-0432.CCR-14-0479
55. Mizia-Malarz A, Sobol-Milejska G. NK Cells as Possible Prognostic Factor in Childhood Acute Lymphoblastic Leukemia. *Dis Markers* (2019) 2019:1–4. doi: 10.1155/2019/3596983
56. B Blom, V van Hoeven and MD Hazenberg eds. ILCs in hematologic malignancies: Tumor cell killers and tissue healers. In: *Seminars in immunology*. United States: Elsevier. doi: 10.1016/j.smim.2019.06.002
57. Epling-Burnette PK, Bai F, Painter JS, Rollison DE, Salih HR, Krusch M, et al. Reduced natural killer (NK) function associated with high-risk myelodysplastic syndrome (MDS) and reduced expression of activating NK receptors. *Blood J Am Soc Hematol* (2007) 109(11):4816–24. doi: 10.1182/blood-2006-07-035519
58. Famularo G, D'Ambrosio A, Quintieri F, Di SG, Parzanese I, Pizzuto F, et al. Natural killer cell frequency and function in patients with monoclonal gammopathies. *J Clin Lab Immunol* (1992) 37(3):99–109.
59. Garcia-Sanz R, Gonzalez M, Orfao A, Moro MJ, Hernandez J, Borrego D, et al. Analysis of natural killer-associated antigens in peripheral blood and bone marrow of multiple myeloma patients and prognostic implications. *Br J Haematol* (1996) 93(1):81–8. doi: 10.1046/j.1365-2141.1996.4651006.x
60. Schütt P, Brandhorst D, Stellberg W, Poser M, Ebeling P, Müller S, et al. Immune parameters in multiple myeloma patients: influence of treatment and correlation with opportunistic infections. *Leukemia Lymphoma* (2006) 47(8):1570–82. doi: 10.1080/10428190500472503
61. De Rossi G, De Sanctis G, Bottari V, Tribalto M, Lopez M, Petrucci MT, et al. Surface markers and cytotoxic activities of lymphocytes in monoclonal gammopathy of undetermined significance and untreated multiple myeloma. *Cancer Immunol Immunother* (1987) 25(2):133–6. doi: 10.1007/BF00199953
62. Omede P, Boccadoro M, Gallone G, Frieri R, Battaglio S, Redoglia V, et al. Multiple myeloma: increased circulating lymphocytes carrying plasma cell-associated antigens as an indicator of poor survival. *Blood* (1990) 76 (7):1375–9. doi: 10.1182/blood.V76.7.1375.bloodjournal7671375
63. Tienhaara A, Pelliniemi TT. Peripheral blood lymphocyte subsets in multiple myeloma and monoclonal gammopathy of undetermined significance. *Clin Lab Haematol* (1994) 16(3):213–23. doi: 10.1111/j.1365-2257.1994.tb00414.x
64. Fauriat C, Mallet F, Olive D. Impaired activating receptor expression pattern in natural killer cells from patients with multiple myeloma. *Leukemia* (2006) 20(4):732–3. doi: 10.1038/sj.leu.2404096
65. Jurisic V, Srdic T, Konjevic G, Markovic O, Colovic M. Clinical stage-depending decrease of NK cell activity in multiple myeloma patients. *Med Oncol* (2007) 24(3):312–7. doi: 10.1007/s12032-007-0007-y
66. Zavidij O, Haradhvala NJ, Mouhieddine TH, Sklavenitis-Pistofidis R, Cai S, Reidy M, et al. Single-cell RNA sequencing reveals compromised immune microenvironment in precursor stages of multiple myeloma. *Nat Cancer* (2020) 1:493–506. doi: 10.1038/s43018-020-0053-3
67. Barberi C, De Pasquale C, Allegra A, Sidoti Migliore G, Oliveri D, Loiacono F, et al. Myeloma cells induce the accumulation of activated CD94low NK cells by cell-to-cell contacts involving CD56 molecules. *Blood Adv* (2020) 4 (10):2297–307. doi: 10.1182/bloodadvances.2019000953
68. Naume B, Gately M, Espevik T. A comparative study of IL-12 (cytotoxic lymphocyte maturation factor)-, IL-2-, and IL-7-induced effects on immunomagnetically purified CD56+ NK cells. *J Immunol (Baltimore Md 1950)* (1992) 148(8):2429–36.
69. Jinushi M, Vanneman M, Munshi NC, Tai Y-T, Prabhala RH , Ritz J, et al. MHC class I chain-related protein A antibodies and shedding are associated with the progression of multiple myeloma. *Proc Natl Acad Sci* (2008) 105 (4):1285–90. doi: 10.1073/pnas.0711293105
70. Raulet DH. Roles of the NKG2D immunoreceptor and its ligands. *Nat Rev Immunol* (2003) 3(10):781–90. doi: 10.1038/nri1199
71. Gao M, Gao L, Yang G, Tao Y, Hou J, Xu H, et al. Myeloma cells resistance to NK cell lysis mainly involves an HLA class I-dependent mechanism. *Acta Biochim Biophys Sin* (2014) 46(7):597–604. doi: 10.1093/abbs/gmu041
72. Carbone E, Neri P, Mesuraca M, Fulciniti MT, Otsuki T, Pende D, et al. NKG2D, and natural cytotoxicity receptors regulate multiple myeloma cell recognition by natural killer cells. *Blood* (2005) 105(1):251–8. doi: 10.1182/blood-2004-04-1422
73. Frohn C, Höppner M, Schlenke P, Kirchner H, Koritke P, Luhm J. Anti-myeloma activity of natural killer lymphocytes. *Br J Haematol* (2002) 119 (3):660–4. doi: 10.1046/j.1365-2141.2002.03879.x
74. Stocker N, Gaugler B, Ricard L, de Vassoigne F, Marjanovic Z, Mohty M, et al. Daratumumab prevents programmed death ligand-1 expression on antigen-presenting cells in de novo multiple myeloma. *Cancer Med* (2020) 9 (6):2077–84. doi: 10.1002/cam4.2827
75. Costello RT, Boehrer A, Sanchez C, Mercier D, Baier C, Le Treut T, et al. Differential expression of natural killer cell activating receptors in blood versus bone marrow in patients with monoclonal gammopathy. *Immunology* (2013) 139(3):338–41. doi: 10.1111/imm.12082
76. Scott AM, Allison JP, Wolchok JD. Monoclonal antibodies in cancer therapy. *Cancer Immun* (2012) 12:14–21.
77. Hsi ED, Steinle R, Balasa B, Szmania S, Draksharapu A, Shum BP, et al. CS1, a Potential New Therapeutic Antibody Target for the Treatment of Multiple Myeloma. *Clin Cancer Res* (2008) 14(9):2775–84. doi: 10.1158/1078-0432.CCR-07-4246
78. Nijhof IS, Bueren J, Kessel Bv, Andre P, Morel Y, Lokhorst HM, et al. Daratumumab-mediated lysis of primary multiple myeloma cells is enhanced in combination with the human anti-KIR antibody IPH2102 and lenalidomide. *Haematologica* (2015) 100(2):263–8. doi: 10.3324/haematol.2014.117531
79. Collins SM, Bakan CE, Swartzel GD, Hofmeister CC, Efebera YA, Kwon H, et al. Elotuzumab directly enhances NK cell cytotoxicity against myeloma via CS1 ligation: evidence for augmented NK cell function complementing ADCC. *Cancer Immunol Immunother* (2013) 62(12):1841–9. doi: 10.1007/s00262-013-1493-8
80. Hu Y, Liu H, Fang C, Li C, Xhyliu F, Dysert H, et al. Targeting of CD38 by the tumor suppressor miR-26a serves as a novel potential therapeutic agent in multiple myeloma. *Cancer Res* (2020) 80:2031–44. doi: 10.1158/0008-5472.Can-19-1077
81. Nijhof IS, Casneuf T, van Velzen J, van Kessel B, Axel AE, Syed K, et al. CD38 expression and complement inhibitors affect response and resistance to daratumumab therapy in myeloma. *Blood* (2016) 128(7):959–70. doi: 10.1182/blood-2016-03-703439
82. Cheng M, Chen Y, Xiao W, Sun R, Tian Z. NK cell-based immunotherapy for malignant diseases. *Cell Mol Immunol* (2013) 10(3):230–52. doi: 10.1038/cmi.2013.10
83. Drent E, Themeli M, Poels R, de Jong-Korlaar R, Yuan H, de Bruijn J, et al. A Rational Strategy for Reducing On-Target Off-Tumor Effects of CD38-Chimeric Antigen Receptors by Affinity Optimization. *Mol Ther* (2017) 25 (8):1946–58. doi: 10.1016/j.ymthe.2017.04.024
84. Sun C, Mahendravada A, Ballard B, Kale B, Ramos C, West J, et al. Safety and efficacy of targeting CD138 with a chimeric antigen receptor for the

treatment of multiple myeloma. *Oncotarget* (2019) 10(24):2369–83. doi: 10.18632/oncotarget.26792
85. Chu J, He S, Deng Y, Zhang J, Peng Y, Hughes T, et al. Genetic modification of T cells redirected toward CS1 enhances eradication of myeloma cells. *Clin Cancer Res* (2014) 20(15):3989–4000. doi: 10.1158/1078-0432.Ccr-13-2510
86. Venniyil Radhakrishnan S, Luetkens T, Yousef S, Bhardwaj N, Steinbach MN, Weidner J, et al. Chimeric Antigen Receptor (CAR) T Cells Specific for CD229: A Potentially Curative Approach for Multiple Myeloma. *Blood* (2017) 130 (Supplement 1):3142–. doi: 10.1182/blood.V130.Suppl_1.3142.3142
87. Benjamin R, Condomines M, Gunset G, Sadelain M. Abstract 3499: CD56 targeted chimeric antigen receptors for immunotherapy of multiple myeloma. *Cancer Res* (2012) 72(8 Supplement):3499. doi: 10.1158/1538-7445.AM2012-3499
88. Murad JM, Baumeister SH, Werner L, Daley H, Trébéden-Negre H, Reder J, et al. Manufacturing development and clinical production of NKG2D chimeric antigen receptor-expressing T cells for autologous adoptive cell therapy. *Cytotherapy* (2018) 20(7):952–63. doi: 10.1016/j.jcyt.2018.05.001
89. Ali SA, Shi V, Maric I, Wang M, Stroncek DF, Rose JJ, et al. T cells expressing an anti-B-cell maturation antigen chimeric antigen receptor cause remissions of multiple myeloma. *Blood* (2016) 128(13):1688–700. doi: 10.1182/blood-2016-04-711903
90. Casucci M, Hawkins RE, Dotti G, Bondanza A. Overcoming the toxicity hurdles of genetically targeted T cells. *Cancer Immunol Immunother* (2015) 64(1):123–30. doi: 10.1007/s00262-014-1641-9
91. Grywalska E, Sosnowska-Pasiarska B, Smok-Kalwat J, Pasiarski M, Niedźwiedzka-Rystwej P, Roliński J. Paving the Way toward Successful Multiple Myeloma Treatment: Chimeric Antigen Receptor T-Cell Therapy. *Cells* (2020) 9(4):983. doi: 10.3390/cells9040983
92. Glienke W, Esser R, Priesner C, Suerth JD, Schambach A, Wels WS, et al. Advantages and applications of CAR-expressing natural killer cells. *Front Pharmacol* (2015) 6:21. doi: 10.3389/fphar.2015.00021
93. Hermanson DL, Kaufman DS. Utilizing chimeric antigen receptors to direct natural killer cell activity. *Front Immunol* (2015) 6:195. doi: 10.3389/fimmu.2015.00195
94. Rezvani K. Adoptive cell therapy using engineered natural killer cells. *Bone Marrow Transplant* (2019) 54(2):785–8. doi: 10.1038/s41409-019-0601-6
95. Suck G, Odendahl M, Nowakowska P, Seidl C, Wels WS, Klingemann HG, et al. NK-92: an 'off-the-shelf therapeutic' for adoptive natural killer cell-based cancer immunotherapy. *Cancer Immunol Immunother* (2016) 65 (4):485–92. doi: 10.1007/s00262-015-1761-x
96. Kloess S, Kretschmer A, Stahl L, Fricke S, Koehl U. CAR-Expressing Natural Killer Cells for Cancer Retargeting. *Transfusion Med Hemother* (2019) 46 (1):4–13. doi: 10.1159/000495771
97. Liu E, Tong Y, Dotti G, Shaim H, Savoldo B, Mukherjee M, et al. Cord blood NK cells engineered to express IL-15 and a CD19-targeted CAR show long-term persistence and potent antitumor activity. *Leukemia* (2018) 32(2):520–31. doi: 10.1038/leu.2017.226
98. Romanski A, Uherek C, Bug G, Seifried E, Klingemann H, Wels WS, et al. CD19-CAR engineered NK-92 cells are sufficient to overcome NK cell resistance in B-cell malignancies. *J Cell Mol Med* (2016) 20(7):1287–94. doi: 10.1111/jcmm.12810
99. Liu E, Marin D, Banerjee P, Macapinlac HA, Thompson P, Basar R, et al. Use of CAR-Transduced Natural Killer Cells in CD19-Positive Lymphoid Tumors. *New Engl J Med* (2020) 382(6):545–53. doi: 10.1056/NEJMoa1910607
100. Jiang H, Zhang W, Shang P, Zhang H, Fu W, Ye F, et al. Transfection of chimeric anti-CD138 gene enhances natural killer cell activation and killing of multiple myeloma cells. *Mol Oncol* (2014) 8(2):297–310. doi: 10.1016/j.molonc.2013.12.001
101. Maroto-Martín E, Encinas J, García-Ortiz A, Alonso R, Leivas A, Paciello ML, et al. PS1209 NKG2D and BCMA-CAR NK Cells Efficiently Eeliminate Multiple Myeloma Cells. A Comprehensive Comparison Between Two Clinically Relevant CARs. *HemaSphere* (2019) 3(S1):550–1. doi: 10.1097/01.HS9.0000563120.66927.63
102. Chu J, Deng Y, Benson DM, He S, Hughes T, Zhang J, et al. CS1-specific chimeric antigen receptor (CAR)-engineered natural killer cells enhance in vitro and in vivo antitumor activity against human multiple myeloma. *Leukemia* (2014) 28(4):917–27. doi: 10.1038/leu.2013.279
103. Tang X, Yang L, Li Z, Nalin AP, Dai H, Xu T, et al. First-in-man clinical trial of CAR NK-92 cells: safety test of CD33-CAR NK-92 cells in patients with relapsed and refractory acute myeloid leukemia. *Am J Cancer Res* (2018) 8 (6):1083–9.
104. Lagrue K, Carisey A, Morgan DJ, Chopra R, Davis DM. Lenalidomide augments actin remodeling and lowers NK-cell activation thresholds. *Blood* (2015) 126(1):50–60. doi: 10.1182/blood-2015-01-625004
105. Davies FE, Raje N, Hideshima T, Lentzsch S, Young G, Tai YT, et al. Thalidomide and immunomodulatory derivatives augment natural killer cell cytotoxicity in multiple myeloma. *Blood* (2001) 98(1):210–6. doi: 10.1182/blood.v98.1.210
106. Soriani A, Zingoni A, Cerboni C, Iannitto ML, Ricciardi MR, Di Gialleonardo V, et al. ATM-ATR-dependent up-regulation of DNAM-1 and NKG2D ligands on multiple myeloma cells by therapeutic agents results in enhanced NK-cell susceptibility and is associated with a senescent phenotype. *Blood* (2009) 113(15):3503–11. doi: 10.1182/blood-2008-08-173914
107. Mohyuddin GR, Qazilbash MH. The therapeutic role of natural killer cells in multiple myeloma. *Adv Cell Gene Ther* (2019) 2(2):1–9. doi: 10.1002/acg2.49
108. Balasa B, Yun R, Belmar NA, Fox M, Chao DT, Robbins MD, et al. Elotuzumab enhances natural killer cell activation and myeloma cell killing through interleukin-2 and TNF-α pathways. *Cancer Immunol Immunother* (2015) 64(1):61–73. doi: 10.1007/s00262-014-1610-3
109. Nijhof IS, Lammerts van Bueren JJ, van Kessel B, Andre P, Morel Y, Lokhorst HM, et al. Daratumumab-mediated lysis of primary multiple myeloma cells is enhanced in combination with the human anti-KIR antibody IPH2102 and lenalidomide. *Haematologica* (2015) 100(2):263–8. doi: 10.3324/haematol.2014.117531
110. Shi J, Tricot GJ, Garg TK, Malaviarachchi PA, Szmania SM, Kellum RE, et al. Bortezomib down-regulates the cell-surface expression of HLA class I and enhances natural killer cell-mediated lysis of myeloma. *Blood* (2008) 111 (3):1309–17. doi: 10.1182/blood-2007-03-078535
111. Hallett WH, Ames E, Motarjemi M, Barao I, Shanker A, Tamang DL, et al. Sensitization of tumor cells to NK cell-mediated killing by proteasome inhibition. *J Immunol* (2008) 180(1):163–70. doi: 10.4049/jimmunol.180.1.163
112. Palumbo A, Chanan-Khan A, Weisel K, Nooka AK, Masszi T, Beksac M, et al. Daratumumab, Bortezomib, and Dexamethasone for Multiple Myeloma. *New Engl J Med* (2016) 375(8):754–66. doi: 10.1056/NEJMoa1606038
113. Wang Y, Sanchez L, Siegel DS, Wang ML. Elotuzumab for the treatment of multiple myeloma. *J Hematol Oncol* (2016) 9(1):55–. doi: 10.1186/s13045-016-0284-z
114. Nwangwu CA, Weiher H, Schmidt-Wolf IGH. Increase of CIK cell efficacy by upregulating cell surface MICA and inhibition of NKG2D ligand shedding in multiple myeloma. *Hematol Oncol* (2017) 35(4):719–25. doi: 10.1002/hon.2326
115. Wagner J, Pfannenstiel V, Waldmann A, Bergs JWJ, Brill B, Huenecke S, et al. A Two-Phase Expansion Protocol Combining Interleukin (IL)-15 and IL-21 Improves Natural Killer Cell Proliferation and Cytotoxicity against Rhabdomyosarcoma. *Front Immunol* (2017) 8:676(676):1–16. doi: 10.3389/fimmu.2017.00676
116. Park JY, Lee SH, Yoon SR, Park YJ, Jung H, Kim TD, et al. IL-15-induced IL-10 increases the cytolytic activity of human natural killer cells. *Mol Cells* (2011) 32(3):265–7. doi: 10.1007/s10059-011-1057-8
117. Jiang T, Zhou C, Ren S. Role of IL-2 in cancer immunotherapy. *Oncoimmunology* (2016) 5(6):e1163462. doi: 10.1080/2162402X.2016.1163462
118. Varbanova V, Naumova E, Mihaylova A. Killer-cell immunoglobulin-like receptor genes and ligands and their role in hematologic malignancies. *Cancer Immunol Immunother* (2016) 65(4):427–40. doi: 10.1007/s00262-016-1806-9
119. Leone P, De Re V, Vacca A, Dammacco F, Racanelli V. Cancer treatment and the KIR–HLA system: an overview. *Clin Exp Med* (2017) 17(4):419–29. doi: 10.1007/s10238-017-0455-4
120. Robinson J, Mistry K, McWilliam H, Lopez R, Marsh SGE. IPD—the Immuno Polymorphism Database. *Nucleic Acids Res* (2010) 38(Database issue):D863–D9. doi: 10.1093/nar/gkp879

121. Colonna M, Brooks EG, Falco M, Ferrara GB, Strominger JL. Generation of allospecific natural killer cells by stimulation across a polymorphism of HLA-C. *Science* (1993) 260(5111):1121–4. doi: 10.1126/science.8493555
122. Falco M, Moretta L, Moretta A, Bottino C. KIR and KIR ligand polymorphism: a new area for clinical applications? *Tissue Antigens* (2013) 82(6):363–73. doi: 10.1111/tan.12262
123. Stewart CA, Laugier-Anfossi F, Vély F, Saulquin X, Riedmuller J, Tisserant A, et al. Recognition of peptide-MHC class I complexes by activating killer immunoglobulin-like receptors. *Proc Natl Acad Sci U S A* (2005) 102 (37):13224–9. doi: 10.1073/pnas.0503594102
124. Peruzzi M, Wagtmann N. Long EO. A p70 killer cell inhibitory receptor specific for several HLA-B allotypes discriminates among peptides bound to HLA-B*2705. *J Exp Med* (1996) 184(4):1585–90. doi: 10.1084/jem.184.4.1585
125. Döhring C, Scheidegger D, Samaridis J, Cella M, Colonna M. A human killer inhibitory receptor specific for HLA-A1,2. *J Immunol* (1996) 156(9):3098–101.
126. Goodridge JP, Burian A, Lee N, Geraghty DE. HLA-F and MHC class I open conformers are ligands for NK cell Ig-like receptors. *J Immunol* (2013) 191 (7):3553–62. doi: 10.4049/jimmunol.1300081
127. Andersson S, Fauriat C, Malmberg J-A, Ljunggren H-G, Malmberg K-J. KIR acquisition probabilities are independent of self-HLA class I ligands and increase with cellular KIR expression. *Blood* (2009) 114(1):95–104. doi: 10.1182/blood-2008-10-184549
128. Pende D, Marcenaro S, Falco M, Martini S, Bernardo ME, Montagna D, et al. Anti-leukemia activity of alloreactive NK cells in KIR ligand-mismatched haploidentical HSCT for pediatric patients: evaluation of the functional role of activating KIR and redefinition of inhibitory KIR specificity. *Blood* (2009) 113(13):3119–29. doi: 10.1182/blood-2008-06-164103
129. Carlsten M, Korde N, Kotecha R, Reger R, Bor S, Kazandjian D, et al. Checkpoint Inhibition of KIR2D with the Monoclonal Antibody IPH2101 Induces Contraction and Hyporesponsiveness of NK Cells in Patients with Myeloma. *Clin Cancer Res* (2016) 22:5211–22. doi: 10.1158/1078-0432.CCR-16-1108
130. Romagné F, André P, Spee P, Zahn S, Anfossi N, Gauthier L, et al. Preclinical characterization of 1-7F9, a novel human anti-KIR receptor therapeutic antibody that augments natural killer-mediated killing of tumor cells. *Blood* (2009) 114(13):2667–77. doi: 10.1182/blood-2009-02-206532
131. Benson DM, Bakan CE, Zhang S, Collins SM, Liang J, Srivastava S, et al. IPH2101, a novel anti-inhibitory KIR antibody, and lenalidomide combine to enhance the natural killer cell versus multiple myeloma effect. *Blood* (2011) 118(24):6387–91. doi: 10.1182/blood-2011-06-360255
132. Tognarelli S, Wirsching S, von Metzler I, Rais B, Jacobs B, Serve H, et al. Enhancing the Activation and Releasing the Brakes: A Double Hit Strategy to Improve NK Cell Cytotoxicity Against Multiple Myeloma. *Front Immunol* (2018) 9:2743:1–15. doi: 10.3389/fimmu.2018.02743
133. Benson DM Jr, Hofmeister CC, Padmanabhan S, Suvannasankha A, Jagannath S, Abonour R, et al. A phase 1 trial of the anti-KIR antibody IPH2101 in patients with relapsed/refractory multiple myeloma. *Blood* (2012) 120(22):4324–33. doi: 10.1182/blood-2012-06-438028
134. Benson DM Jr, Cohen AD, Jagannath S, Munshi NC, Spitzer G, Hofmeister CC, et al. A Phase I Trial of the Anti-KIR Antibody IPH2101 and Lenalidomide in Patients with Relapsed/Refractory Multiple Myeloma. *Clin Cancer Res an Off J Am Assoc Cancer Res* (2015) 21(18):4055–61. doi: 10.1158/1078-0432.ccr-15-0304
135. Korde N, Carlsten M, Lee M-J, Minter A, Tan E, Kwok M, et al. A phase II trial of pan-KIR2D blockade with IPH2101 in smoldering multiple myeloma. *Haematologica* (2014) 99(6):e81–e3. doi: 10.3324/haematol.2013.103085
136. Cooley S, Parham P, Miller JS. Strategies to activate NK cells to prevent relapse and induce remission following hematopoietic stem cell transplantation. *Blood* (2018) 131(10):1053–62. doi: 10.1182/blood-2017-08-752170
137. Mahaweni NM, Ehlers FAI, Bos GMJ, Wieten L. Tuning Natural Killer Cell Anti-multiple Myeloma Reactivity by Targeting Inhibitory Signaling via KIR and NKG2A. *Front Immunol* (2018) 9:2848:1–8. doi: 10.3389/fimmu.2018.02848
138. Lee N, Llano M, Carretero M, Ishitani A, Navarro F, López-Botet M, et al. HLA-E is a major ligand for the natural killer inhibitory receptor CD94/NKG2A. *Proc Natl Acad Sci U S A* (1998) 95(9):5199–204. doi: 10.1073/pnas.95.9.5199
139. André P, Denis C, Soulas C, Bourbon-Caillet C, Lopez J, Arnoux T, et al. Anti-NKG2A mAb Is a Checkpoint Inhibitor that Promotes Anti-tumor Immunity by Unleashing Both T and NK Cells. *Cell* (2018) 175(7):1731–43.e13. doi: 10.1016/j.cell.2018.10.014
140. Godal R, Bachanova V, Gleason M, McCullar V, Yun GH, Cooley S, et al. Natural Killer Cell Killing of Acute Myelogenous Leukemia and Acute Lymphoblastic Leukemia Blasts by Killer Cell Immunoglobulin-Like Receptor–Negative Natural Killer Cells after NKG2A and LIR-1 Blockade. *Biol Blood Marrow Transplant* (2010) 16(5):612–21. doi: 10.1016/j.bbmt.2010.01.019
141. Soulas C, Remark R, Brezar V, Lopez J, Bonnet E, Caraguel F, et al. Abstract 2714: Combination of monalizumab and durvalumab as a potent immunotherapy treatment for solid human cancers. *Cancer Res* (2018) 78 (13 Supplement):2714–. doi: 10.1158/1538-7445.Am2018-2714
142. Braud VM, Allan DS, O'Callaghan CA, Söderström K, D'Andrea A, Ogg GS, et al. HLA-E binds to natural killer cell receptors CD94/NKG2A, B and C. *Nature* (1998) 391(6669):795–9. doi: 10.1038/35869
143. McWilliams EM, Mele JM, Cheney C, Timmerman EA, Fiazuddin F, Strattan EJ, et al. Therapeutic CD94/NKG2A blockade improves natural killer cell dysfunction in chronic lymphocytic leukemia. *Oncoimmunology* (2016) 5 (10):e1226720. doi: 10.1080/2162402X.2016.1226720
144. Nguyen S, Beziat V, Dhedin N, Kuentz M, Vernant J, Debre P, et al. HLA-E upregulation on IFN-γ-activated AML blasts impairs CD94/NKG2A-dependent NK cytolysis after haplo-mismatched hematopoietic SCT. *Bone marrow Transplant* (2009) 43(9):693–9. doi: 10.1038/bmt.2008.380
145. Borrego F, Masilamani M, Kabat J, Sanni TB, Coligan JE. The cell biology of the human natural killer cell CD94/NKG2A inhibitory receptor. *Mol Immunol* (2005) 42(4):485–8. doi: 10.1016/j.molimm.2004.07.031
146. Borrego F, Kabat J, Kim D-K, Lieto L, Maasho K, Peña J, et al. Structure and function of major histocompatibility complex (MHC) class I specific receptors expressed on human natural killer (NK) cells. *Mol Immunol* (2002) 38(9):637–60. doi: 10.1016/S0161-5890(01)00107-9
147. Houchins JP, Lanier LL, Niemi EC, Phillips JH, Ryan JC. Natural killer cell cytolytic activity is inhibited by NKG2-A and activated by NKG2-C. *J Immunol* (1997) 158(8):3603–9.
148. Wieten L, Mahaweni NM, Voorter CEM, Bos GMJ, Tilanus MGJ. Clinical and immunological significance of HLA-E in stem cell transplantation and cancer. *Tissue Antigens* (2014) 84(6):523–35. doi: 10.1111/tan.12478
149. Tinker AV, Hirte HW, Provencher D, Butler M, Ritter H, Tu D, et al. Dose-Ranging and Cohort-Expansion Study of Monalizumab (IPH2201) in Patients with Advanced Gynecologic Malignancies: A Trial of the Canadian Cancer Trials Group (CCTG): IND221. *Clin Cancer Res* (2019) 25(20):6052–60. doi: 10.1158/1078-0432.Ccr-19-0298
150. Gillard-Bocquet M, Caer C, Cagnard N, Crozet L, Perez M, Fridman WH, et al. Lung Tumor Microenvironment Induces Specific Gene Expression Signature in Intratumoral NK Cells. *Front Immunol* (2013) 4:19(19):1–6. doi: 10.3389/fimmu.2013.00019
151. Sun C, Xu J, Huang Q, Huang M, Wen H, Zhang C, et al. High NKG2A expression contributes to NK cell exhaustion and predicts a poor prognosis of patients with liver cancer. *Oncoimmunology* (2017) 6(1):e1264562. doi: 10.1080/2162402X.2016.1264562
152. Stringaris K, Sekine T, Khoder A, Alsuliman A, Razzaghi B, Sargeant R, et al. Leukemia-induced phenotypic and functional defects in natural killer cells predict failure to achieve remission in acute myeloid leukemia. *Haematologica* (2014) 99(5):836–47. doi: 10.3324/haematol.2013.087536
153. Sun H, Sun C. The Rise of NK Cell Checkpoints as Promising Therapeutic Targets in Cancer Immunotherapy. *Front Immunol* (2019) 10:2354. doi: 10.3389/fimmu.2019.02354
154. Demaria O, Cornen S, Daeron M, Morel Y, Medzhitov R, Vivier E. Harnessing innate immunity in cancer therapy. *Nature* (2019) 574 (7776):45–56. doi: 10.1038/s41586-019-1593-5
155. Marín R, Ruiz-Cabello F, Pedrinaci S, Méndez R, Jiménez P, Geraghty DE, et al. Analysis of HLA-E expression in human tumors. *Immunogenetics* (2003) 54(11):767–75. doi: 10.1007/s00251-002-0526-9
156. Palmisano GL, Contardi E, Morabito A, Gargaglione V, Ferrara GB, Pistillo MP. HLA-E surface expression is independent of the availability of HLA class I signal sequence-derived peptides in human tumor cell lines. *Hum Immunol* (2005) 66(1):1–12. doi: 10.1016/j.humimm.2004.10.006

157. Sarkar S, van Gelder M, Noort W, Xu Y, Rouschop KM, Groen R, et al. Optimal selection of natural killer cells to kill myeloma: the role of HLA-E and NKG2A. *Cancer Immunol Immunother* (2015) 64(8):951–63. doi: 10.1007/s00262-015-1694-4
158. Ruggeri L, Urbani E, Andre P, Mancusi A, Tosti A, Topini F, et al. Effects of anti-NKG2A antibody administration on leukemia and normal hematopoietic cells. *Haematologica* (2016) 101(5):626–33. doi: 10.3324/haematol.2015.135301
159. Kamiya T, Seow SV, Wong D, Robinson M, Campana D. Blocking expression of inhibitory receptor NKG2A overcomes tumor resistance to NK cells. *J Clin Invest* (2019) 129(5):2094–106. doi: 10.1172/JCI123955
160. Folgiero V, Cifaldi L, Li Pira G, Goffredo BM, Vinti L, Locatelli F. TIM-3/Gal-9 interaction induces IFNgamma-dependent IDO1 expression in acute myeloid leukemia blast cells. *J Hematol Oncol* (2015) 8:36. doi: 10.1186/s13045-015-0134-4
161. Gao X, Zhu Y, Li G, Huang H, Zhang G, Wang F, et al. TIM-3 expression characterizes regulatory T cells in tumor tissues and is associated with lung cancer progression. *PloS One* (2012) 7(2):e30676. doi: 10.1371/journal.pone.0030676
162. Das M, Zhu C, Kuchroo VK. Tim-3 and its role in regulating anti-tumor immunity. *Immunol Rev* (2017) 276(1):97–111. doi: 10.1111/imr.12520
163. Golden-Mason L, McMahan RH, Strong M, Reisdorph R, Mahaffey S, Palmer BE, et al. Galectin-9 Functionally Impairs Natural Killer Cells in Humans and Mice. *J Virol* (2013) 87(9):4835–45. doi: 10.1128/jvi.01085-12
164. Xu L, Huang Y, Tan L, Yu W, Chen D, Lu C, et al. Increased Tim-3 expression in peripheral NK cells predicts a poorer prognosis and Tim-3 blockade improves NK cell-mediated cytotoxicity in human lung adenocarcinoma. *Int Immunopharmacol* (2015) 29(2):635–41. doi: 10.1016/j.intimp.2015.09.017
165. Ngiow SF, von Scheidt B, Akiba H, Yagita H, Teng MW, Smyth MJ. Anti-TIM3 antibody promotes T cell IFN-gamma-mediated antitumor immunity and suppresses established tumors. *Cancer Res* (2011) 71(10):3540–51. doi: 10.1158/0008-5472.Can-11-0096
166. Wang Z, Zhu J, Gu H, Yuan Y, Zhang B, Zhu D, et al. The Clinical Significance of Abnormal Tim-3 Expression on NK Cells from Patients with Gastric Cancer. *Immunol Invest* (2015) 44(6):578–89. doi: 10.3109/08820139.2015.1052145
167. da Silva IP, Gallois A, Jimenez-Baranda S, Khan S, Anderson AC, Kuchroo VK, et al. Reversal of NK-cell exhaustion in advanced melanoma by Tim-3 blockade. *Cancer Immunol Res* (2014) 2(5):410–22. doi: 10.1158/2326-6066.Cir-13-0171
168. Farkas AM, Audenet F, Anastos H, Galsky M, Sfakianos J, Bhardwaj N. Tim-3 and TIGIT mark Natural Killer cells susceptible to effector dysfunction in human bladder cancer. *J Immunol* (2018) 200(1 Supplement):124.14–.14. doi: 10.1158/1538-7445.AM2018-4745
169. Sakuishi K, Apetoh L, Sullivan JM, Blazar BR, Kuchroo VK, Anderson AC. Targeting Tim-3 and PD-1 pathways to reverse T cell exhaustion and restore anti-tumor immunity. *J Exp Med* (2010) 207(10):2187–94. doi: 10.1084/jem.20100643
170. Pu F, Chen F, Zhang Z, Qing X, Lin H, Zhao L, et al. TIM-3 expression and its association with overall survival in primary osteosarcoma. *Oncol Lett* (2019) 18(5):5294–300. doi: 10.3892/ol.2019.10855
171. Gallois A, Silva I, Osman I, Bhardwaj N. Reversal of natural killer cell exhaustion by TIM-3 blockade. *Oncoimmunology* (2015) 3(12):e946365–e. doi: 10.4161/21624011.2014.946365
172. Hou H, Liu W, Wu S, Lu Y, Peng J, Zhu Y, et al. Tim-3 negatively mediates natural killer cell function in LPS-induced endotoxic shock. *PloS One* (2014) 9(10):e110585. doi: 10.1371/journal.pone.0110585
173. Han G, Chen G, Shen B, Li Y. Tim-3: an activation marker and activation limiter of innate immune cells. *Front Immunol* (2013) 4:449. doi: 10.3389/fimmu.2013.00449
174. Gleason MK, Lenvik TR, McCullar V, Felices M, O'Brien MS, Cooley SA, et al. Tim-3 is an inducible human natural killer cell receptor that enhances interferon gamma production in response to galectin-9. *Blood* (2012) 119 (13):3064–72. doi: 10.1182/blood-2011-06-360321
175. Van Audenaerde JRM, De Waele J, Marcq E, Van Loenhout J, Lion E, Van den Bergh JMJ, et al. Interleukin-15 stimulates natural killer cell-mediated killing of both human pancreatic cancer and stellate cells. *Oncotarget* (2017) 8(34):56968–79. doi: 10.18632/oncotarget.18185
176. Fu RJr., Ding S, Liu C, Liu B, Liu H, Zhaoyun L, et al. The Role of Decreased TIM-3 Expression of Natural Killer Cells in the Immune Pathogenesis of Severe Aplastic Anemia. *Blood* (2019) 134(Supplement_1):3747–. doi: 10.1182/blood-2019-127769
177. Fourcade J, Sun Z, Benallaoua M, Guillaume P, Luescher IF, Sander C, et al. Upregulation of Tim-3 and PD-1 expression is associated with tumor antigen-specific CD8+ T cell dysfunction in melanoma patients. *J Exp Med* (2010) 207(10):2175–86. doi: 10.1084/jem.20100637
178. Liu F, Zeng G, Zhou S, He X, Sun N, Zhu X, et al. Blocking Tim-3 or/and PD-1 reverses dysfunction of tumor-infiltrating lymphocytes in HBV-related hepatocellular carcinoma. *Bull Cancer* (2018) 105(5):493–501. doi: 10.1016/j.bulcan.2018.01.018
179. Borate U, Esteve J, Porkka K, Knapper S, Vey N, Scholl S, et al. Phase Ib Study of the Anti-TIM-3 Antibody MBG453 in Combination with Decitabine in Patients with High-Risk Myelodysplastic Syndrome (MDS) and Acute Myeloid Leukemia (AML). *Blood* (2019) 134 (Supplement_1):570–. doi: 10.1182/blood-2019-128178
180. Stanietsky N, Simic H, Arapovic J, Toporik A, Levy O, Novik A, et al. The interaction of TIGIT with PVR and PVRL2 inhibits human NK cell cytotoxicity. *Proc Natl Acad Sci USA* (2009) 106(42):17858–63. doi: 10.1073/pnas.0903474106
181. Zhang Q, Bi J, Zheng X, Chen Y, Wang H, Wu W, et al. Blockade of the checkpoint receptor TIGIT prevents NK cell exhaustion and elicits potent anti-tumor immunity. *Nat Immunol* (2018) 19(7):723–32. doi: 10.1038/s41590-018-0132-0
182. Hung AL, Maxwell R, Theodros D, Belcaid Z, Mathios D, Luksik AS, et al. TIGIT and PD-1 dual checkpoint blockade enhances antitumor immunity and survival in GBM. *Oncoimmunology* (2018) 7(8):e1466769–e. doi: 10.1080/2162402X.2018.1466769
183. Iguchi-Manaka A, Kai H, Yamashita Y, Shibata K, Tahara-Hanaoka S, Honda S, et al. Accelerated tumor growth in mice deficient in DNAM-1 receptor. *J Exp Med* (2008) 205(13):2959–64. doi: 10.1084/jem.20081611
184. Chan CJ, Andrews DM, McLaughlin NM, Yagita H, Gilfillan S, Colonna M, et al. DNAM-1/CD155 interactions promote cytokine and NK cell-mediated suppression of poorly immunogenic melanoma metastases. *J Immunol* (2010) 184(2):902–11. doi: 10.4049/jimmunol.0903225
185. Stein N, Tsukerman P, Mandelboim O. The paired receptors TIGIT and DNAM-1 as targets for therapeutic antibodies. *Hum Antibodies* (2017) 25(3-4):111–9. doi: 10.3233/hab-160307
186. Guillerey C, Harjunpää H, Carrié N, Kassem S, Teo T, Miles K, et al. TIGIT immune checkpoint blockade restores CD8+ T-cell immunity against multiple myeloma. *Blood* (2018) 132(16):1689–94. doi: 10.1182/blood-2018-01-825265
187. Molfetta R, Zitti B, Lecce M, Milito ND, Stabile H, Fionda C, et al. CD155: A Multi-Functional Molecule in Tumor Progression. *Int J Mol Sci* (2020) 21 (3):922–36. doi: 10.3390/ijms21030922
188. Neri P, Maity R, Tagoug I, McCulloch S, Duggan P, Jimenez-Zepeda V, et al. Immunome Single Cell Profiling Reveals T Cell Exhaustion with Upregulation of Checkpoint Inhibitors LAG3 and Tigit on Marrow Infiltrating T Lymphocytes in Daratumumab and IMiDs Resistant Patients. *Blood* (2018) 132(Supplement 1):242–. doi: 10.1182/blood-2018-99-117531
189. Minnie SA, Kuns RD, Gartlan KH, Zhang P, Wilkinson AN, Samson L, et al. Myeloma escape after stem cell transplantation is a consequence of T-cell exhaustion and is prevented by TIGIT blockade. *Blood* (2018) 132(16):1675–88. doi: 10.1182/blood-2018-01-825240
190. Jia B, Zhao C, Claxton DF, Ehmann WC, Rybka WB, Mineishi S, et al. TIGIT Expression Positively Associates with NK Cell Function in AML Patients. *Blood* (2018) 132(Supplement 1):5250–. doi: 10.1182/blood-2018-99-113578
191. Mekhloufi A, Kosta A, Stabile H, Molfetta R, Zingoni A, Soriani A, et al. Bone Marrow Stromal Cell-Derived IL-8 Upregulates PVR Expression on Multiple Myeloma Cells via NF-kB Transcription Factor. *Cancers (Basel)* (2020) 12 (2):440–62. doi: 10.3390/cancers12020440
192. Niu C, Jin H, Li M, Zhu S, Zhou L, Jin F, et al. Low-dose bortezomib increases the expression of NKG2D and DNAM-1 ligands and enhances induced NK

and γδ T cell-mediated lysis in multiple myeloma. *Oncotarget* (2017) 8 (4):5954–64. doi: 10.18632/oncotarget.13979
193. Sunseri N, Chen X, Wald N, Preillon J, Smith SM, Driessens G, et al. Beyond PD-1: Investigating the Therapeutic Potential of TIGIT Blockade in DLBCL. *Blood* (2019) 134(Supplement_1):391–. doi: 10.1182/blood-2019-131493
194. Johnston RJ, Comps-Agrar L, Hackney J, Yu X, Huseni M, Yang Y, et al. The immunoreceptor TIGIT regulates antitumor and antiviral CD8(+) T cell effector function. *Cancer Cell* (2014) 26(6):923–37. doi: 10.1016/j.ccell.2014.10.018
195. Kurtulus S, Sakuishi K, Ngiow SF, Joller N, Tan DJ, Teng MW, et al. TIGIT predominantly regulates the immune response via regulatory T cells. *J Clin Invest* (2015) 125(11):4053–62. doi: 10.1172/jci81187
196. Fife BT, Pauken KE. The role of the PD-1 pathway in autoimmunity and peripheral tolerance. *Ann N Y Acad Sci* (2011) 1217:45–59. doi: 10.1111/j.1749-6632.2010.05919.x
197. Keir ME, Butte MJ, Freeman GJ, Sharpe AH. PD-1 and its ligands in tolerance and immunity. *Annu Rev Immunol* (2008) 26:677–704. doi: 10.1146/annurev.immunol.26.021607.090331
198. Sharpe AH, Pauken KE. The diverse functions of the PD1 inhibitory pathway. *Nat Rev Immunol* (2018) 18(3):153–67. doi: 10.1038/nri.2017.108
199. Dong Y, Sun Q, Zhang X. PD-1 and its ligands are important immune checkpoints in cancer. *Oncotarget* (2017) 8(2):2171–86. doi: 10.18632/oncotarget.13895
200. Kleffel S, Posch C, Barthel SR, Mueller H, Schlapbach C, Guenova E, et al. Melanoma Cell-Intrinsic PD-1 Receptor Functions Promote Tumor Growth. *Cell* (2015) 162(6):1242–56. doi: 10.1016/j.cell.2015.08.052
201. Dong H, Strome SE, Salomao DR, Tamura H, Hirano F, Flies DB, et al. Tumor-associated B7-H1 promotes T-cell apoptosis: a potential mechanism of immune evasion. *Nat Med* (2002) 8(8):793–800. doi: 10.1038/nm730
202. Katsuya Y, Fujita Y, Horinouchi H, Ohe Y, Watanabe S, Tsuta K. Immunohistochemical status of PD-L1 in thymoma and thymic carcinoma. *Lung Cancer* (2015) 88(2):154–9. doi: 10.1016/j.lungcan.2015.03.003
203. Nomi T, Sho M, Akahori T, Hamada K, Kubo A, Kanehiro H, et al. Clinical significance and therapeutic potential of the programmed death-1 ligand/programmed death-1 pathway in human pancreatic cancer. *Clin Cancer Res* (2007) 13(7):2151–7. doi: 10.1158/1078-0432.Ccr-06-2746
204. Wilmotte R, Burkhardt K, Kindler V, Belkouch MC, Dussex G, Tribolet N, et al. B7-homolog 1 expression by human glioma: a new mechanism of immune evasion. *Neuroreport* (2005) 16(10):1081–5. doi: 10.1097/00001756-200507130-00010
205. Tamura H, Ishibashi M, Yamashita T, Tanosaki S, Okuyama N, Kondo A, et al. Marrow stromal cells induce B7-H1 expression on myeloma cells, generating aggressive characteristics in multiple myeloma. *Leukemia* (2013) 27(2):464–72. doi: 10.1038/leu.2012.213
206. Tremblay-LeMay R, Rastgoo N, Chang H. Modulating PD-L1 expression in multiple myeloma: an alternative strategy to target the PD-1/PD-L1 pathway. *J Hematol Oncol* (2018) 11(1):46. doi: 10.1186/s13045-018-0589-1
207. Jelinek T, Paiva B, Hajek R. Update on PD-1/PD-L1 Inhibitors in Multiple Myeloma. *Front Immunol* (2018) 9:2431. doi: 10.3389/fimmu.2018.02431
208. Hsu J, Hodgins JJ, Marathe M, Nicolai CJ, Bourgeois-Daigneault M-C, Trevino TN, et al. Contribution of NK cells to immunotherapy mediated by PD-1/PD-L1 blockade. *J Clin Invest* (2018) 128(10):4654–68. doi: 10.1172/JCI99317
209. Judge SJ, Dunai C, Sturgill I, Stoffel K, Darrow M, Canter R, et al. PD-1 is not expressed on highly activated Natural Killer cells in human and murine models. *J Immunol* (2019) 202(1 Supplement):126.27–27. doi: 10.1172/JCI133353
210. Kearl TJ, Jing W, Gershan JA, Johnson BD. Programmed Death Receptor-1/Programmed Death Receptor Ligand-1 Blockade after Transient Lymphodepletion To Treat Myeloma. *J Immunol* (2013) 190(11):5620–8. doi: 10.4049/jimmunol.1202005
211. Gordon SR, Maute RL, Dulken BW, Hutter G, George BM, McCracken MN, et al. PD-1 expression by tumour-associated macrophages inhibits phagocytosis and tumour immunity. *Nature* (2017) 545(7655):495–9. doi: 10.1038/nature22396
212. Pesce S, Greppi M, Grossi F, Del Zotto G, Moretta L, Sivori S, et al. PD/1-PD-Ls Checkpoint: Insight on the Potential Role of NK Cells. *Front Immunol* (2019) 10:1242. doi: 10.3389/fimmu.2019.01242
213. Benson DMJr, Bakan CE, Mishra A, Hofmeister CC, Efebera Y, Becknell B, et al. The PD-1/PD-L1 axis modulates the natural killer cell versus multiple myeloma effect: a therapeutic target for CT-011, a novel monoclonal anti–PD-1 antibody. *Blood* (2010) 116(13):2286–94. doi: 10.1182/blood-2010-02-271874
214. Hasim MS, Vulpis E, Sciumè G, Shih HY, Scheer A, MacMillan O, et al. NK cells acquire PD-1 from the membrane of tumor cells. *bioRxiv* (2020). doi: 10.1101/2020.06.26.174342 2020.06.26.174342.
215. Jelinek T, Paiva B, Hajek R. Update on PD-1/PD-L1 Inhibitors in Multiple Myeloma. *Front Immunol* (2018) 9:2431:1–13. doi: 10.3389/fimmu.2018.02431
216. Badros AZ, Ma N, Rapoport AP, Lederer E, Lesokhin AM. Long-term remissions after stopping pembrolizumab for relapsed or refractory multiple myeloma. *Blood Adv* (2019) 3(11):1658–60. doi: 10.1182/bloodadvances.2019000191
217. Mateos M-V, Orlowski RZ, Ocio EM, Rodríguez-Otero P, Reece D, Moreau P, et al. Pembrolizumab combined with lenalidomide and low-dose dexamethasone for relapsed or refractory multiple myeloma: phase I KEYNOTE-023 study. *Br J Haematol* (2019) 186(5):e117–e21. doi: 10.1111/bjh.15946
218. D'Souza A, Hari P, Pasquini M, Braun T, Johnson B, Lundy S, et al. A Phase 2 Study of Pembrolizumab during Lymphodepletion after Autologous Hematopoietic Cell Transplantation for Multiple Myeloma. *Biol Blood marrow Transplant J Am Soc Blood Marrow Transplant* (2019) 25 (8):1492–7. doi: 10.1016/j.bbmt.2019.04.005
219. Lesokhin AM, Bal S, Badros AZ. Lessons Learned from Checkpoint Blockade Targeting PD-1 in Multiple Myeloma. *Cancer Immunol Res* (2019) 7 (8):1224–9. doi: 10.1158/2326-6066.Cir-19-0148
220. Triebel F, Jitsukawa S, Baixeras E, Roman-Roman S, Genevee C, Viegas-Pequignot E, et al. LAG-3, a novel lymphocyte activation gene closely related to CD4. *J Exp Med* (1990) 171(5):1393–405. doi: 10.1084/jem.171.5.1393
221. Huard B, Tournier M, Hercend T, Triebel F, Faure F. Lymphocyte-activation gene 3/major histocompatibility complex class II interaction modulates the antigenic response of CD4+ T lymphocytes. *Eur J Immunol* (1994) 24 (12):3216–21. doi: 10.1002/eji.1830241246
222. Huard B, Gaulard P, Faure F, Hercend T, Triebel F. Cellular expression and tissue distribution of the human LAG-3-encoded protein, an MHC class II ligand. *Immunogenetics* (1994) 39(3):213–7. doi: 10.1007/bf00241263
223. Kisielow M, Kisielow J, Capoferri-Sollami G, Karjalainen K. Expression of lymphocyte activation gene 3 (LAG-3) on B cells is induced by T cells. *Eur J Immunol* (2005) 35(7):2081–8. doi: 10.1002/eji.200526090
224. Workman CJ, Wang Y, El Kasmi KC, Pardoll DM, Murray PJ, Drake CG, et al. LAG-3 regulates plasmacytoid dendritic cell homeostasis. *J Immunol* (2009) 182(4):1885–91. doi: 10.4049/jimmunol.0800185
225. Huang C-T, Workman CJ, Flies D, Pan X, Marson AL, Zhou G, et al. Role of LAG-3 in regulatory T cells. *Immunity* (2004) 21(4):503–13. doi: 10.1016/j.immuni.2004.08.010
226. Wu X, Gu Z, Chen Y, Chen B, Chen W, Weng L, et al. Application of PD-1 Blockade in Cancer Immunotherapy. *Comput Struct Biotechnol J* (2019) 17:661–74. doi: 10.1016/j.csbj.2019.03.006
227. Wang J, Sanmamed MF, Datar I, Su TT, Ji L, Sun J, et al. Fibrinogen-like Protein 1 Is a Major Immune Inhibitory Ligand of LAG-3. *Cell* (2019) 176(1-2):334–47.e12. doi: 10.1016/j.cell.2018.11.010
228. Xu F, Liu J, Liu D, Liu B, Wang M, Hu Z, et al. LSECtin expressed on melanoma cells promotes tumor progression by inhibiting antitumor T-cell responses. *Cancer Res* (2014) 74(13):3418–28. doi: 10.1158/0008-5472.CAN-13-2690
229. Kouo T, Huang L, Pucsek AB, Cao M, Solt S, Armstrong T, et al. Galectin-3 Shapes Antitumor Immune Responses by Suppressing CD8+ T Cells via LAG-3 and Inhibiting Expansion of Plasmacytoid Dendritic Cells. *Cancer Immunol Res* (2015) 3(4):412–23. doi: 10.1158/2326-6066.CIR-14-0150
230. Anderson AC, Joller N, Kuchroo VK. Lag-3, Tim-3, and TIGIT: Co-inhibitory Receptors with Specialized Functions in Immune Regulation. *Immunity* (2016) 44(5):989–1004. doi: 10.1016/j.immuni.2016.05.001
231. Blackburn SD, Shin H, Haining WN, Zou T, Workman CJ, Polley A, et al. Coregulation of CD8+ T cell exhaustion by multiple inhibitory receptors during chronic viral infection. *Nat Immunol* (2009) 10(1):29–37. doi: 10.1038/ni.1679
232. Woo S-R, Turnis ME, Goldberg MV, Bankoti J, Selby M, Nirschl CJ, et al. Immune inhibitory molecules LAG-3 and PD-1 synergistically regulate T-cell function to promote tumoral immune escape. *Cancer Res* (2012) 72 (4):917–27. doi: 10.1158/0008-5472.CAN-11-1620

233. Burova E, Hermann A, Dai J, Ullman E, Halasz G, Potocky T, et al. Preclinical Development of the Anti-LAG-3 Antibody REGN3767: Characterization and Activity in Combination with the Anti-PD-1 Antibody Cemiplimab in Human PD-1xLAG-3-Knockin Mice. *Mol Cancer Ther* (2019) 18(11):2051–62. doi: 10.1158/1535-7163.Mct-18-1376
234. Mussetti A, Pellegrinelli A, Cieri N, Garzone G, Dominoni F, Cabras A, et al. PD-L1, LAG3, and HLA-DR are increasingly expressed during smoldering myeloma progression. *Ann Hematol* (2019) 98(7):1713–20. doi: 10.1007/s00277-019-03648-4
235. Fabienne L, Pennell M, Benson DM, Efebera Y, Chaudhry M, Woyach JA, et al. Exploring LAG-3 Expression in Multiple Myeloma Patients Following Autologous Stem Cell Transplant. *Blood* (2018) 132(Supplement 1):3434–. doi: 10.1182/blood-2018-99-119577
236. Lucas F, Pennell M, Huang Y, Benson DM, Efebera YA, Chaudhry M, et al. T Cell Transcriptional Profiling and Immunophenotyping Uncover LAG3 as a Potential Significant Target of Immune Modulation in Multiple Myeloma. *Biol Blood Marrow Transplant* (2020) 26(1):7–15. doi: 10.1016/j.bbmt.2019.08.009
237. Sivori S, Vacca P, Del Zotto G, Munari E, Mingari MC, Moretta L. Human NK cells: surface receptors, inhibitory checkpoints, and translational applications. *Cell Mol Immunol* (2019) 16(5):430–41. doi: 10.1038/s41423-019-0206-4
238. Lanuza PM, Pesini C, Arias MA, Calvo C, Ramirez-Labrada A, Pardo J. Recalling the Biological Significance of Immune Checkpoints on NK Cells: A Chance to Overcome LAG3, PD1, and CTLA4 Inhibitory Pathways by Adoptive NK Cell Transfer? *Front Immunol* (2020) 10:3010:1–11. doi: 10.3389/fimmu.2019.03010
239. Narayanan S, Ahl PJ, Bijin VA, Kaliaperumal N, Lim SG, Wang C-I, et al. LAG3 is a Central Regulator of NK Cell Cytokine Production. *bioRxiv* (2020) 2020.01.31.928200. doi: 10.1101/2020.01.31.928200
240. Lanier LL. NK cell receptors. *Annu Rev Immunol* (1998) 16(1):359–93. doi: 10.1146/annurev.immunol.16.1.359
241. Rosenberg J, Huang J. CD8(+) T Cells and NK Cells: Parallel and Complementary Soldiers of Immunotherapy. *Curr Opin Chem Eng* (2018) 19:9–20. doi: 10.1016/j.coche.2017.11.006
242. Barrueto L, Caminero F, Cash L, Makris C, Lamichhane P, Deshmukh RR. Resistance to Checkpoint Inhibition in Cancer Immunotherapy. *Transl Oncol* (2020) 13(3):100738–. doi: 10.1016/j.tranon.2019.12.010
243. Iwasa M, Harada T, Oda A, Bat-Erdene A, Teramachi J, Tenshin H, et al. PD-L1 upregulation in myeloma cells by panobinostat in combination with interferon-γ. *Oncotarget* (2019) 10(20):1903–17. doi: 10.18632/oncotarget.26726

Conflict of Interest: The authors declare that the research was conducted in the absence of any commercial or financial relationships that could be construed as a potential conflict of interest.

frontiers in Immunology

ORIGINAL RESEARCH
published: 17 November 2020
doi: 10.3389/fimmu.2020.558757

Molecular and Clinical Characterization of PD-1 in Breast Cancer Using Large-Scale Transcriptome Data

Qiang Liu[†], *Ran Cheng*[†], *Xiangyi Kong*[†], *Zhongzhao Wang*[*], *Yi Fang*[*] *and Jing Wang*[*]

Department of Breast Surgical Oncology, National Cancer Center/National Clinical Research Center for Cancer/Cancer Hospital, Chinese Academy of Medical Sciences and Peking Union Medical College, Beijing, China

OPEN ACCESS

Edited by:
Ali A. Zarrin,
TRex Bio, United States

Reviewed by:
Ye Li,
University of Texas MD Anderson Cancer Center, United States
Bipulendu Jena,
Independent Researcher, San Diego, CA, United States

***Correspondence:**
Jing Wang
wangjing@cicams.ac.cn
Yi Fang
fangyi@cicams.ac.cn
Zhongzhao Wang
wangzhongzhao@cicams.ac.cn

[†]*These authors have contributed equally to this work*

Specialty section:
This article was submitted to Cancer Immunity and Immunotherapy, a section of the journal Frontiers in Immunology

Received: *04 May 2020*
Accepted: *16 October 2020*
Published: *17 November 2020*

Citation:
Liu Q, Cheng R, Kong X, Wang Z, Fang Y and Wang J (2020) Molecular and Clinical Characterization of PD-1 in Breast Cancer Using Large-Scale Transcriptome Data. Front. Immunol. 11:558757. doi: 10.3389/fimmu.2020.558757

Despite the impressive impact of PD-1 (programmed cell death protein 1)-targeted cancer immunotherapy, a great part of patients with cancer fail to respond. PD-1 impact on immune cells in addition to T cells, and the synergistic role of PD-1 with other immune modulators remain largely unknown. To fill this gap, we systematically investigated PD-1-related transcriptome data and relevant clinical information derived from TCGA (The Cancer Genome Atlas) and METABRIC (Molecular Taxonomy of Breast Cancer International Consortium), which involved a total of 2,994 breast cancer patients. Our results revealed the relationship among PD-1 and major molecular and clinical characteristics in breast cancer. More importantly, we depicted the association landscape between PD-1 and other immune cell populations. Gene ontology analyses and gene set variation analysis (GSVA) of genes correlated with PD-1 revealed that PD-1 was mainly involved in immune responses and inflammatory activities. We also elucidated the association of PD-1 with other immune modulators in pan-cancer level, especially the potential synergistic relationship between PD-1 and other immune checkpoints members in breast cancer. In short, the expression level of PD-1 was bound up with breast cancer malignancy, which could be used as a potential biomarker; PD-1 might manipulate the anti-tumor immune response by impacting not just T cells, and this might vary among different tumor types. Furthermore, PD-1 might synergize with other immune checkpoint members to modulate the immune microenvironment in breast cancer.

Keywords: breast cancer, cancer immunotherapy, PD-1, immune response, inflammatory activity

INTRODUCTION

Breast cancer is the most frequently diagnosed women cancer all over the world (1). As development of comprehensive treatments, including resection by surgery, chemotherapy, radiotherapy, endocrine therapy, and targeted therapy, many early stage breast cancers can be effectively controlled (2). However, for advanced breast cancers, the existing standard treatments have limited effectiveness because of the aggressiveness of tumors, resistance to treatments, recurrence, and metastasis during or after treatments (3). In the past decade, researches suggested that tumor

cells' immunologic escape of and aberrant human immune surveillance play essential roles in the carcinogenesis, progression, and metastasis of cancers (4), and studies focused on anticancer immune responses have achieved marked success of many malignant tumors in preclinical and clinical trials (5–9), the PD-1 (programmed cell death protein 1) and PD-L1 (programmed cell death-ligand 1) axis has been identified as one of the most encouraging findings in cancer immunotherapy (10).

PD-1 is a receptor that is expressed on the surface of activated T cells, and the PD-L1 and PD-L2 are ligands of PD-1 that are expressed on the surface of antigen-presenting cells (11). The PD-1 and PD-L1 interaction can result in T cells inactivation and ensure that the immune system can be activated at the appropriate time, thus minimize the possibility of chronic autoimmune inflammation. However, tumor cells or non-transformed cells in the tumor microenvironment overexpressing PD-L1, leading to generate an adaptive immune resistance in response to endogenous immune anti-tumor activity (12). The antibody of PD-1/PD-L1 can block the immune escape mediated by PD-1 and PD-L1 interaction and has been approved by the FDA in a fast speed (13). In the first clinical trials of breast cancer, the inhibitors of PD-1/PD-L1 showed promising activity (14, 15). However, many problems still need to be resolved, including the lack of clearly available data in breast cancer, notably regarding PD-1 expression and its prognostic value, and the application of PD-1/PD-L1 inhibitors in combination with other immune checkpoint inhibitors.

Despite the impressive impact of PD-1/PD-L1-targeted cancer immunotherapy, a large proportion of cancer patients fail to respond (16). Furthermore, although the combination of PD-1/PD-L1 blockade with complementary checkpoint inhibitors has achieved some success for some malignant tumors in the preclinical and clinical trials, the impact of PD-1 on immune cells in addition to T cells and the synergistic role of PD-1 with other immune modulators remain mostly unknown (17). In the present study, we systematically investigated the PD-1-related transcriptome profile and revealed its potential role in inducing immune responses and inflammatory activities as well as its potential relationship with immune modulators.

METHODS

Data Collection

Transcriptome data from TCGA (The Cancer Genome Atlas) were downloaded by GDCRNA tools (access date: February 01, 2020) (18). The edgeR (19) and limma packages (20) available from the Bioconductor project (21) offer a well-developed suite of statistical methods for dealing with this question for RNA-seq data. Raw count data were normalized using TMM implemented in edgeR, and then were transformed by voom in limma, only genes with cpm > 1 in more than half of the samples were kept. Sieved TCGA breast cancer clinical data were kindly provided by Dr. Hai Hu and Dr. Jianfang Liu (Chan Soon-Shiong Institute of Molecular Medicine, Windber). Human epidermal growth factor receptor 2 (HER2) status was recalled using DNA copy number for cases without immunohistochemistry or fluorescence *in situ* hybridization (FISH) status. Standardized survival data of TCGA cohort were downloaded from TCGA-CDR (TCGA Pan-Cancer Clinical Data Resource) (22). The METABRIC (Molecular Taxonomy of Breast Cancer International Consortium) dataset (23) containing 1904 tumor cases was downloaded from the cBioPortal database (http://www.cbioportal.org/) (access date: Feb 01, 2019). A total of 2,994 samples with full clinical characteristics and transcriptome data were used to perform the following data exploration. The detailed clinical characteristics of breast cancer patients from TCGA and METABRIC are listed in **Tables S1** and **S2**, respectively).

Bioinformatics Analysis

Gene ontology analyses of the genes that correlated with PD-1 were performed using clusterProfiler package (24). Immunologically related genes were collected from The ImmPort (Immunology Database and Analysis Portal) database (https://www.immport.org/home) (25). The absolute abundance of immune cell populations was estimated using Microenvironment Cell Populations-counter algorithm (26).

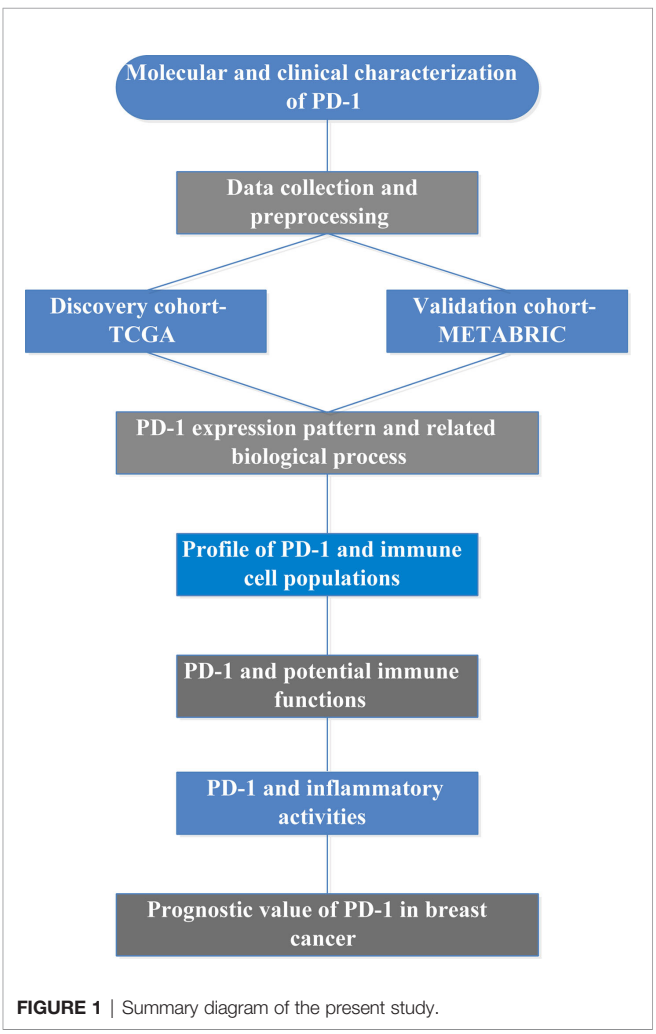

FIGURE 1 | Summary diagram of the present study.

GSVA (Gene Set Variation Analysis) (27) was used to calculate scores of gene sets that correlated with immune functions and inflammatory activities (28). Association of PD-1 and other immune modulators in pan-cancer were depicted through the database of TISIDB (29), which is an integrated repository portal for tumor-immune system interactions. The study summary diagram is shown in **Figure 1**.

Statistical Analysis

Spearman correlation method was used to estimate the correlations between continuous variables. Student t-test, one-way ANOVA, or Pearson's Chi-squared test were used to determine any differences in variables between groups. R language was used to perform all statistical tests. The prognostic value of PD-1 was evaluated through Cox proportional hazards model analysis. Several packages including ggplot2 pheatmap, pROC (30), circlize (31), and corrgram (32) were used to perform other statistical calculations and graphical work (33), and $P < 0.05$ was considered to have the statistically significant difference.

RESULTS

PD-1 Expression Pattern in Breast Cancer

To characterize the relationship between PD-1 expression and molecular and clinical features in breast cancer, individuals were dichotomized into high and low groups based on the expression of PD-1 using median cut. We found that PD-1 was asscociated with patient age, American Joint Committee on Cancer (AJCC) stage, tumor grade, estrogen receptor (ER) status, progesterone receptor (PR) status and HER2 status (**Tables 1** and **2**). Next, we further detected that the PD-1 expression was upregulated in tumor tissues, the ER-negative group (ER-) and PR-negative group (PR-) in both TCGA and METABRIC datasets, while upregulation of PD-1 in the

TABLE 1 | Association between PD-1 mRNA expression and clinicopathologic characteristics in TCGA cohort.

		Expression		
	Total (n = 1090)	**PD-1 high (n = 545)**	**PD-1 low (n = 545)**	**P-value**
Age (years)				
>=55	517 (47.4%)	277 (50.8%)	240 (44.0%)	0.025
<55	573 (52.6%)	268 (49.2%)	305 (56.0%)	
T stage				
T1	279 (25.6%)	130 (23.9%)	149 (27.3%)	0.028
T2	631 (57.9%)	330 (60.6%)	301 (55.2%)	
T3	137 (12.6%)	72 (13.2%)	65 (11.9%)	
T4	40 (3.7%)	13 (2.4%)	27 (5.0%)	
Unknown	3 (0.3%)	0 (0%)	3 (0.6%)	
N stage				
N0	514 (47.2%)	257 (47.2%)	257 (47.2%)	0.065
N1	360 (33.0%)	177 (32.5%)	183 (33.6%)	
N2	120 (11.0%)	57 (10.5%)	63 (11.6%)	
N3	76 (7.0%)	48 (8.8%)	28 (5.1%)	
Unknown	20 (1.8%)	6 (1.1%)	14 (2.6%)	
M stage				
M0	907 (83.2%)	452 (82.9%)	455 (83.5%)	0.061
M1	22 (2.0%)	6 (1.1%)	16 (2.9%)	
Unknown	161 (14.8%)	87 (16.0%)	74 (13.6%)	
AJCC stage				
I	181 (16.6%)	82 (15.0%)	99 (18.2%)	0.097
II	621 (57.0%)	319 (58.5%)	302 (55.4%)	
III	250 (22.9%)	131 (24.0%)	119 (21.8%)	
IV	20 (1.8%)	5 (0.9%)	15 (2.8%)	
Unknown	18 (1.7%)	8 (1.5%)	10 (1.8%)	
ER status				
Negative	236 (21.7%)	155 (28.4%)	81 (14.9%)	<0.001
Positive	803 (73.7%)	372 (68.3%)	431 (79.1%)	
Unknown	51 (4.7%)	18 (3.3%)	33 (6.1%)	
PR status				
Negative	343 (31.5%)	203 (37.2%)	140 (25.7%)	<0.001
Positive	694 (63.7%)	323 (59.3%)	371 (68.1%)	
Unknown	53 (4.9%)	19 (3.5%)	34 (6.2%)	
HER2 status				
Negative	895 (82.1%)	449 (82.4%)	446 (81.8%)	0.032
Positive	168 (15.4%)	89 (16.3%)	79 (14.5%)	
Unknown	27 (2.5%)	7 (1.3%)	20 (3.7%)	

TABLE 2 | Association between PD-1 mRNA expression and clinicopathologic characteristics in METABRIC cohort.

		Expression		
	Total (n = 1904)	**PD-1 high (n = 952)**	**PD-1 low (n = 952)**	**P-value**
Age (years)				
>=55	952 (50.0%)	522 (54.8%)	430 (45.2%)	<0.001
<55	952 (50.0%)	430 (45.2%)	522 (54.8%)	
Tumor size				
>=2cm	592 (31.1%)	293 (30.8%)	299 (31.4%)	0.079
<2cm	1292 (67.9%)	644 (67.6%)	648 (68.1%)	
Unknown	20 (1.1%)	15 (1.6%)	5 (0.5%)	
AJCC stage				
0	4 (0.2%)	3 (0.3%)	1 (0.1%)	0.039
I	475 (24.9%)	218 (22.9%)	257 (27.0%)	
II	800 (42.0%)	413 (43.4%)	387 (40.7%)	
III	115 (6.0%)	68 (7.1%)	47 (4.9%)	
IV	9 (0.5%)	2 (0.2%)	7 (0.7%)	
Unknown	501 (26.3%)	248 (26.1%)	253 (26.6%)	
Tumor grade				
I	165 (8.7%)	50 (5.3%)	115 (12.1%)	<0.001
II	740 (38.9%)	311 (32.7%)	429 (45.1%)	
III	927 (48.7%)	551 (57.9%)	376 (39.5%)	
Unknown	72 (3.8%)	40 (4.2%)	32 (3.4%)	
ER status				
Negative	445 (23.4%)	309 (32.5%)	136 (14.3%)	<0.001
Positive	1459 (76.6%)	643 (67.5%)	816 (85.7%)	
PR status				
Negative	895 (47.0%)	526 (55.3%)	369 (38.8%)	<0.001
Positive	1009 (53.0%)	426 (44.7%)	583 (61.2%)	
HER2 status				
Negative	1668 (87.6%)	800 (84.0%)	868 (91.2%)	<0.001
Positive	236 (12.4%)	152 (16.0%)	84 (8.8%)	

HER2-positive group was only observed in the METABRIC dataset (**Figures 2A–F**). Meanwhile, we observed that PD-1 expression was upregulated in the molecular subtypes such as basal-like and HER2-enriched when compared with luminal A, while no difference was found between luminal A and luminal B subtypes. While no claudin-low subtype was found in the TCGA cohort, the other four subtypes were consistently in both the TCGA and METABRIC cohorts (**Figures 2G, H**). Subsequently, we also found that PD-1 expression was enriched in higher grade tumors in the METABRIC dataset (**Figure 2I**). PD-1 overexpression was also oberved in the triple-negative breast cancer (TNBC) subtype and could be as a predictor for TNBC subtype in both TCGA (AUC = 0.671) and METABRIC (AUC = 0.672) databases (**Figures 3A–D**). One potential limitation of this result was that this was a primary result based on only one gene. Future studies focusing on investigating robust biomarkers for TNBC might consider combining PD-1 and other biomarkers together, and comparing the predictive capacity between each other. In summary, these findings suggest that PD-1 expression is enriched in higher malignant breast cancer and might be a potential biomaker in TNBC.

PD-1 Was Bound Up With Immune Functions in Breast Cancer

To further explore PD-1 related biological processes in breast cancer, a total of 1008 genes and 449 genes, seived from TCGA and METABRIC datasets, respectively, have strongly correlation with PD-1 according to Spearman correlation analysis ($|R| > 0.4$ and $P < 0.05$). Subsequently, GO (gene ontology) enrichment analyses were performed to investigate PD-1's potential biological functions. We found that PD-1-related genes were mainly involved in immune-related pathways and inflamatory pathways (**Figure 4A**), including T cell regulation-related biological processes and leukocyte regulation-related pathways. Importantly, these results were also validated in METABRIC datasets (**Figure 4B**).

PD-1 Related Immune Response

To further investigate PD-1-related immune functions in breast cancer, 4723 immunologically related genes were retrieved from the ImmPort (25). Genes that were most correlated with PD-1 (Spearman $|R| > 0.4$, $P < 0.05$) were seived to depict the expression pattern of these immunologically related genes in breast cancer. Subsequently, we found that 508 and 248 immune-related genes in TCGA and METABRIC datasets, respectively, were correlated with PD-1 postively, while only 6 and no immunologically related genes, respectively, were correlated with PD-1 negatively (**Figures S1A, B**).

The Relationship Between PD-1 Expression and Immune Cell Populations

Previously, Tao Jiang et al. reported PD-1 is a positively correlated with T cells, monocytic lineage cells, and myeloid

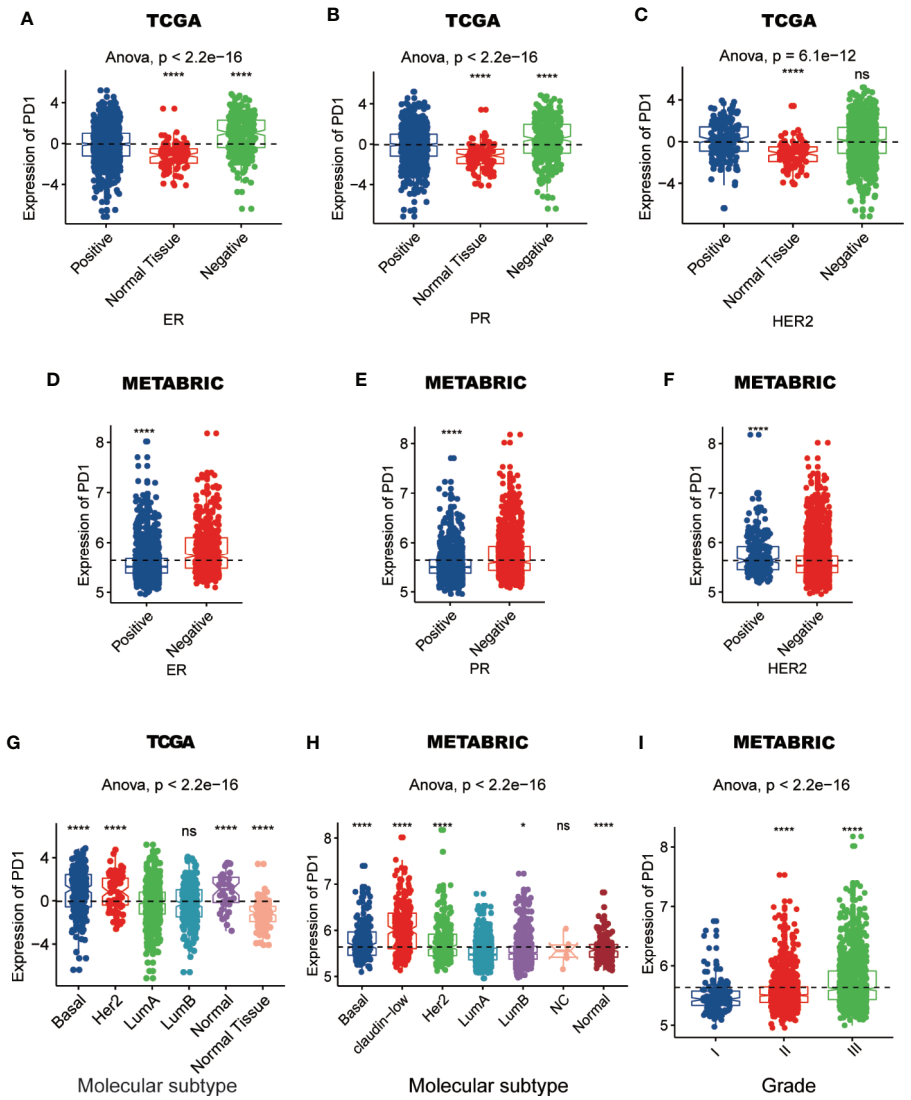

FIGURE 2 | The expression of PD-1 in different ER, PR, and HER2 status **(A–F)**, molecular subtypes **(G, H)**, and grades **(I)** in TCGA or METABRIC cohort. (*: P < 0.05, ****: P < 0.0001, ns: no significant difference).

dendritic cells, but not with cytotoxic lymphocytes, natural killer (NK) cells, or B lineage cells in diffuse glioma (34). In breast cancer, to further clarify the immune manipulative functions of PD-1, the Microenvironment Cell Populations-counter algorithm was used to calculate the absolute abundance of immune cell populations (26). The abundance pattern of these cell populations in breast cancer is depicted in **Figures 5A, B**. We observed that PD-1 expression was strongly correlated with immune cell population scores of T cells, CD8+ T cells, cytotoxic lymphocytes, NK cells, B lineage cells, monocytic lineage cells, and myeloid dendritic cells, but not neutrophils, endothelial cells, or fibroblasts (**Figures 5C, D**). These findings suggest that PD-1 may not just be involved in regualting T cell immunity, other immune cell immunity might also be involved. Furthermore, the immune regulatory pattern of PD-1 may be varied in different tumors.

Relationship of the Expression of PD-1 and Immune Modulators in Pan-Cancer

To explore the synergistic role of PD-1 and other immune modulators in pan-cancer, we systematically analyzed the correlations between PD-1 expression and three types of immune modulators described in the previous study conducted by Charoentong et al. (35). Interestingly, we found a similar correlation pattern between immune modulators and PD-1 across 30 tumor types in which the majority of immunoinhibitors and immunostimulators were correlated

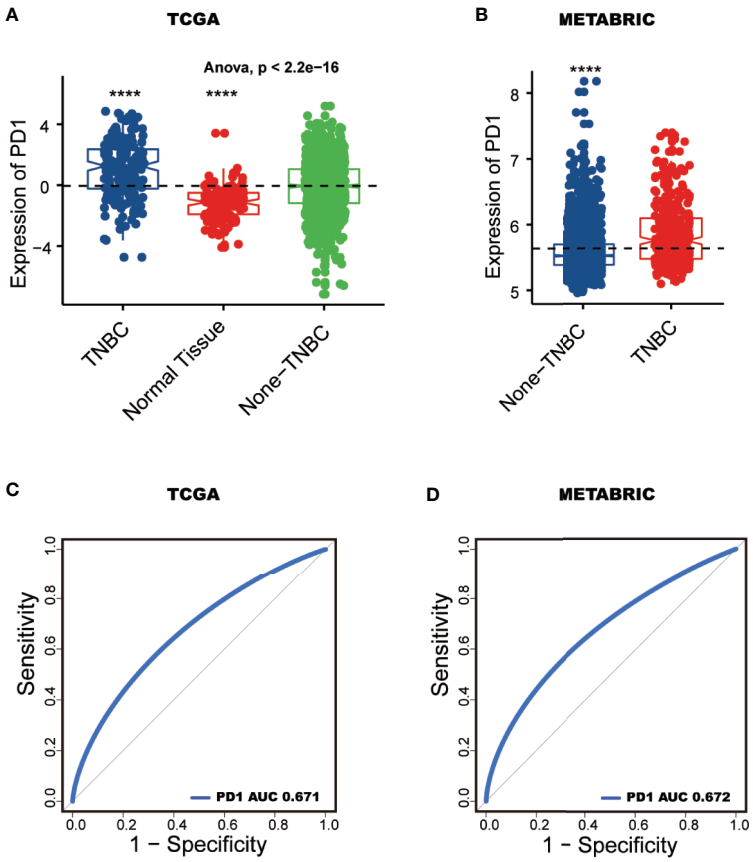

FIGURE 3 | PD-1 serves as a potential biomarker. PD-1 expression pattern between TNBC and none-TNBC tissues in TCGA and METABRIC **(A, B)**. ROC curves predict PD-1 as a biomarker of TNBC **(C, D)**. (****: P < 0.0001).

with PD-1 positively (**Figures S2** and **S3**), while only a small number of immunoinhibitors and immunostimulators were negatively correlated with PD-1. More interestingly, we observed that PD-1 was positively correlated with almost all MHC molecules across 30 tumor types (**Figure S4**). These results provide a landscape perspective regarding the correlation of PD-1 with immune modulators, and we could compare this correlation pattern of PD-1 with immune modulators in various tumors. The general PD-1 correlation pattern trends were similar in various tumors. These observations suggest that PD-1 might synergize with other immune modulators in manipulating the anti-tumor immune response.

PD-1 Is Synergistic With Other Immune Checkpoint Members in Breast Cancer-Induced Immune Response

We estimated the association of PD-1 with other immune checkpoint members to further explore the synergistic role of PD-1 in breast cancer-induced immune responses (**Figures 6A–D**). The detailed R and p-values of correlations between PD-1 and other checkpoint members are listed in **Tables S3**. Interestingly, we found that PD-1 was strongly correlated with similar checkpoint members including PD-L2, CD274 (PD-L1) CTLA4, IDO1, and LAG3, as well as other checkpoint members including BTLA, ICOS, CD27, CD40, and CD48. These findings revealed that PD-1 might manipulate anti-tumor immune responses through co-regulation with the above mentioned immune checkpoint molecules, thereby lending support to using combination cancer immunotherapy targeting these molecules in future studies.

Asscociation Between PD-1 and Specific Cell Immune Responses

The specific immune regulatory role of PD-1 in breast cancer remains largely unknown. To further explore the association between PD-1 and specific immune responses, GSVA of gene ontology biological pathways was performed. Consistent with the above results, we found that PD-1 was strongly correlated with both T and B cell immunity (**Figures 7A, B**). PD-1 was positively correlated with T cell proliferation, T cell differentiation, T cell activation and T cell receptor signaling pathways. Meanwhile, we also observed that PD-1 was positively correlated with B cell activation.

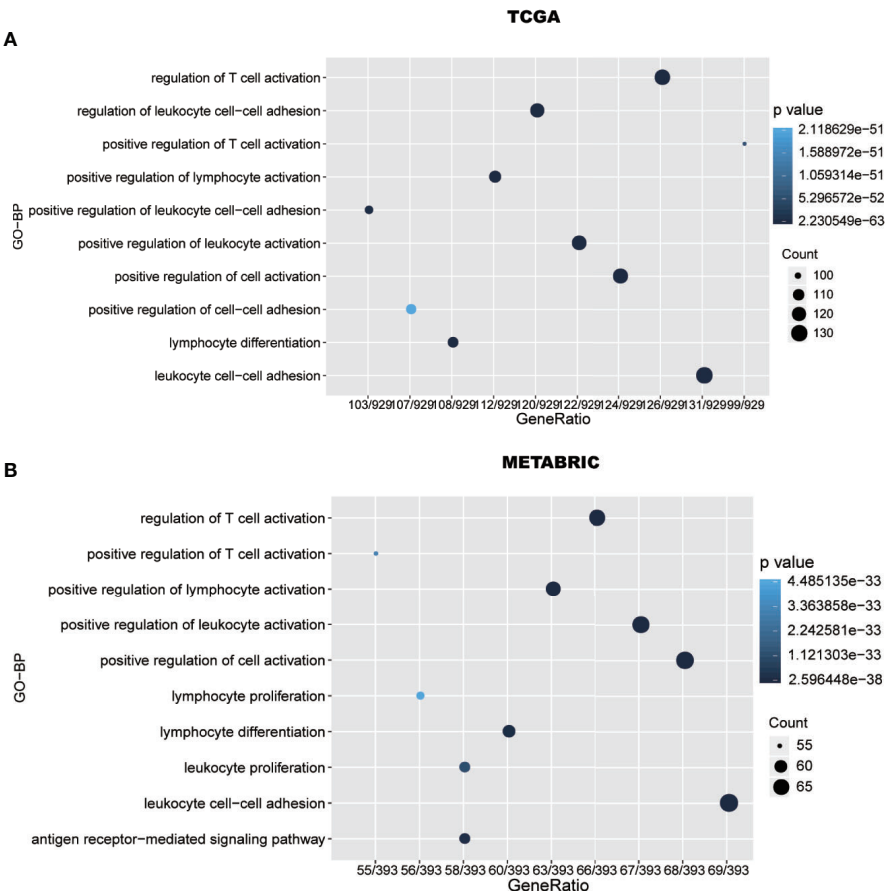

FIGURE 4 | PD-1 is closely related to immune functions in breast cancer. Gene ontology analysis shows that PD-1 is mainly involved in immune response and inflammatory response in TCGA and METABRIC databases **(A**, **B)**.

Relationship Between PD-1 and Inflammatory Activities

To further understand the role of PD-1 in mediating inflammatory activities, 104 genes were derived from seven clusters and defined as metagenes using the GSVA algorithm (28), implicating different types of inflammation and immune functions. Detailed information of these metagenes is shown in **Table S4**. We found that LAG3 was positively correlated with MHC-I, MHC-II, LCK, STAT1, HCK, and interferon, but not IgG (**Figures 7C, D**). Among these seven clusters, PD-1 showed the strongest correlation with MHC-II and LCK in both TCGA and METABRIC databases. These results further suggested that PD-1 not only correlated with T cell immunity but also with other immune cells. In summary, these findings indicated that PD-1 has important immune and inflammatory functions in breast cancer.

Prognostic Value of PD-1 in Breast Cancer

To explore the influence on breast cancer survival, we evaluated the prognostic value of PD-1 in both TCGA (n = 1090) and METABRIC (n = 1994) cohorts. Interestingly, our data indicated that PD-1 was an independent prognostic factor in breast cancer on the basis of TCGA cohort multivariate analysis after adjusting for patient age, AJCC stage, ER, PR, and HER2 status (**Figure 8A**). In the METABRIC cohort, the PD-1 expression level was also an independent prognostic indicator for breast cancer after adjusting for tumor grade, AJCC stage, ER, PR, and HER2 status (**Figure 8B**). Despite the fact that PD-1 was upregulated in higher malignant tumors, our results suggest that PD-1 is predictive of good prognosis in breast cancer patients.

DISCUSSION

The development of immune therapies for solid tumors have promoted clinical advances (36), PD-1/PD-L1 are critical biological suppressors of cytotoxic immune reactions, and the PD-L1 expression is one of the major immunologic escape mechanisms in tumors (37). However, despite the impressive impact of PD-1/PD-L1-targeted cancer immunotherapy, a large

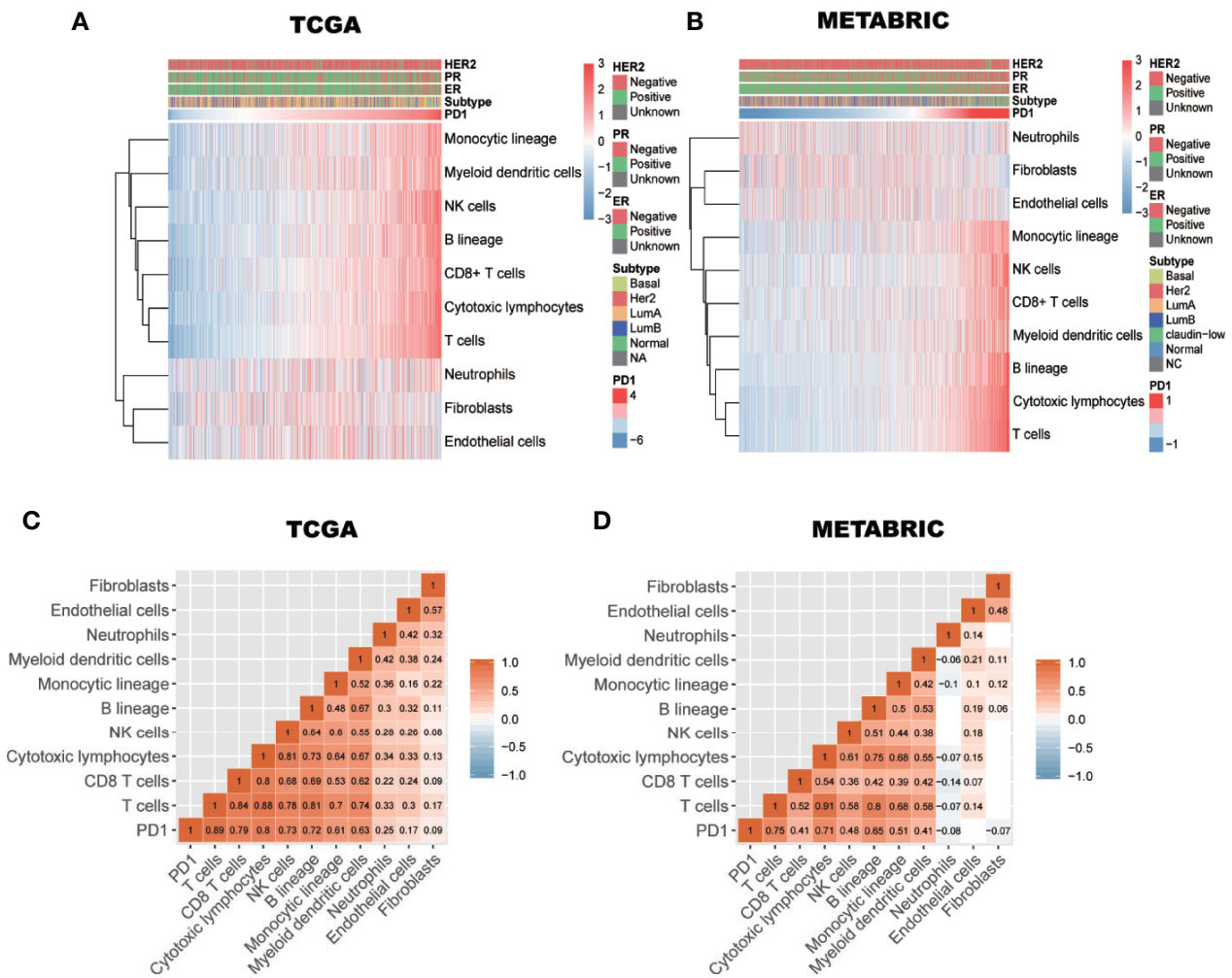

FIGURE 5 | The relationship between PD-1 expression and immune cell populations in TCGA and METABRIC databases **(A–D)**. Subtypes denotes breast cancer molecular subtypes including Basal, basal-like; Her2, Her2-enriched; LumA, luminal A; LumB, luminal B.

proportion of cancer patients fail to respond. To understand why this occurs, we need to have a better understanding of the molecular regulatory mechanisms of PD-1/PD-L1.

Whether PD-1/PL-L1 predicts prognosis in breast cancer patients is currently being debated, and large-scale investigations are still required to further confirm the specific relationship between PD-1/PD-L1 and prognosis of breast cancer (38). PD-1 was found to be significantly associated with better DFS and OS in Ren et al.'s study of only 195 TNBC patients (39). The present study used large-scale transcriptome data to provide additional strong evidence to support the correlation between high PD-1 expression and good prognosis in breast cancer patients. We estimated the association of PD-1 with other checkpoint proteins and found that PD-1 was strongly correlated with similar checkpoint members. Some of these results were consistent with previous studies, while some results have never been reported before. For instance, previous studies reported that LAG-3 and PD-1 were co-expressed on tumor-infiltrating lymphocytes, and blockade of both pathways had synergistic effects on anti-tumor CD8+ T cell stimulation and response (40, 41).

In the present study, one interesting finding was that the immune inhibitors and immune stimulators were positively and concomitantly correlated with PD-1 expression. For primary and secondary resistance to immunotherapy, the etiologies are multifaceted, tumor intrinsic factors, and the complex interplay between cancer and its microenvironment all should to be taken into consideration (42). One possible explanation for immunotherpy resistance might be that there are complex interactions between PD-1 expression, immune inhibitors, and immune stimulators. Hence, the result that immune inhibitors and immune stimulators are positively correlated at the same time in the same sets of patients is reflective of a complex tumor microenvironment. More importantly, these results also suggest

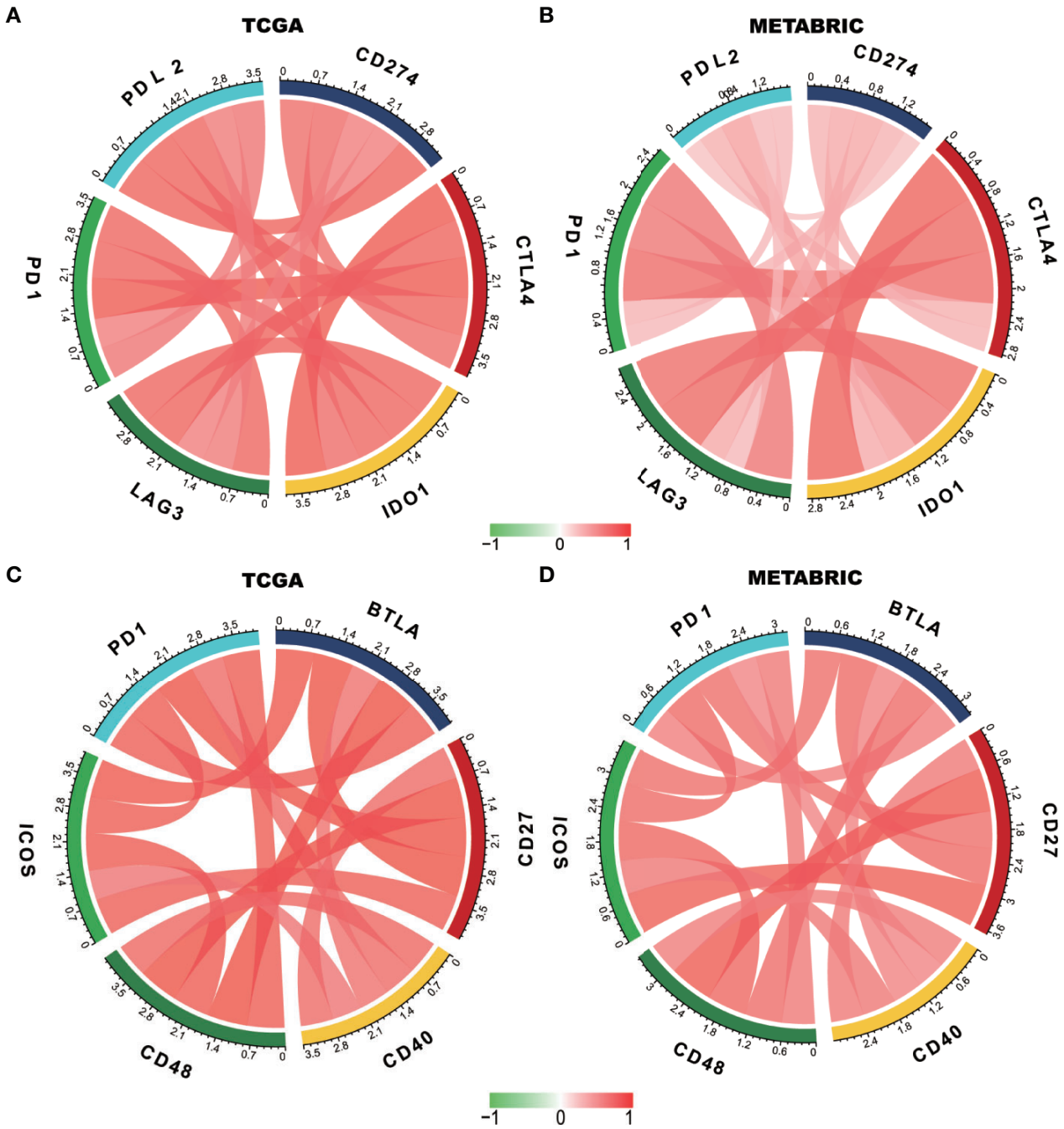

FIGURE 6 | PD-1 expression is correlated with immune checkpoint members in TCGA and METABRIC databases **(A–D)**.

that when using immunotherapy, both activation of stimulatory pathways and blockade of inhibitory checkpoints can occur and should therefore be taken into consideration.

It is generally agreed that PD-1 mainly inhibits the activation and immunologic function of T cells (43). We found that PD-1 was not only strongly correlated with T cell immunity, but also with B cell immunity. Tumor-infiltrating B cells with distinct phenotypes and functions, which might play specific roles in the anti-tumor responses (44). However, there is still a lack of direct evidence to support B cells have the immunosuppressive role in human cancers (45). Further study is needed to explore the possible manipulation by B cells-mediated immune suppression through the overexpression of PD-1. Moreover, analysis of the relationship between PD-1 and inflammatory activity, further

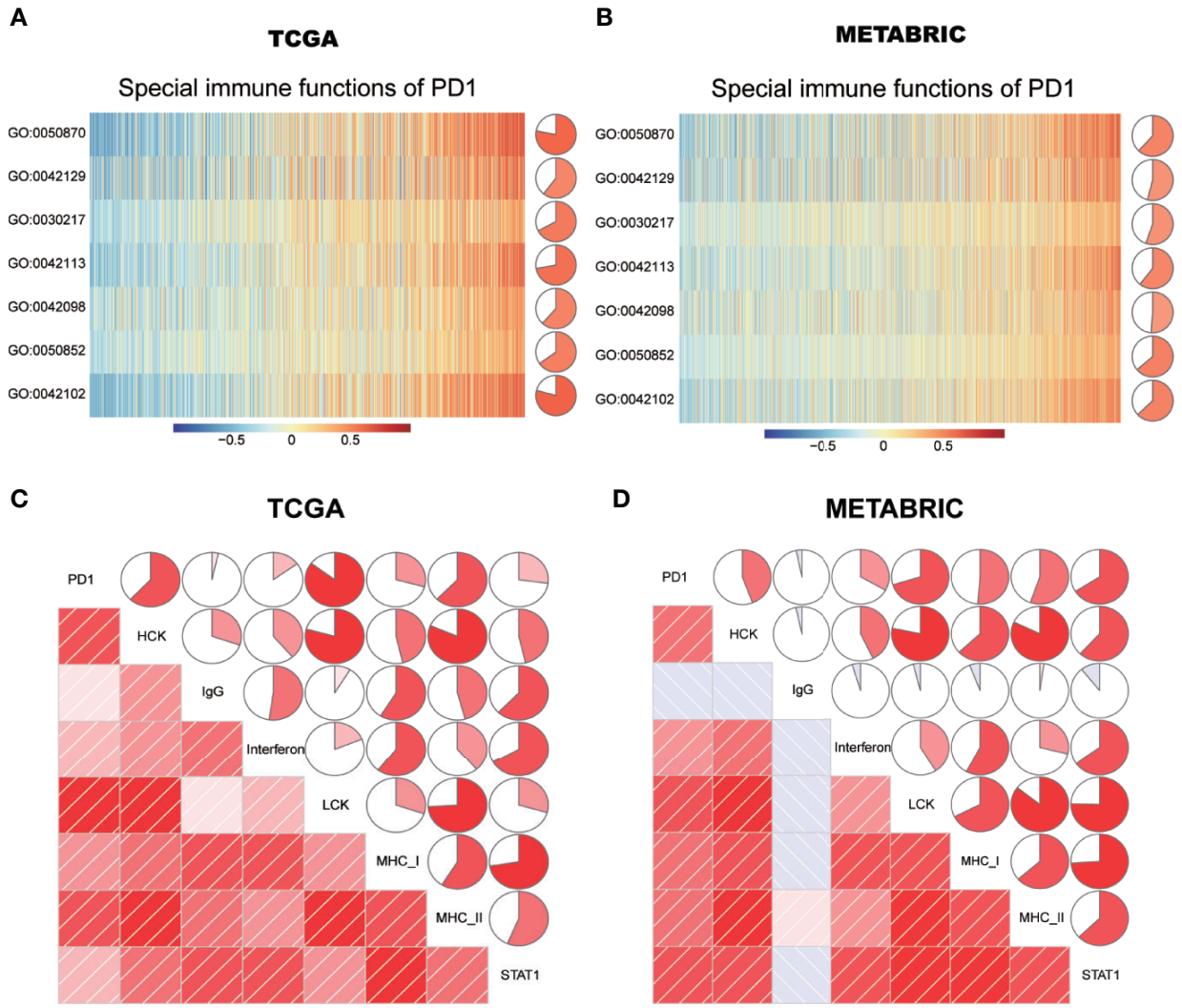

FIGURE 7 | PD-1-related cell immunity and inflammatory activities in breast cancer. The relationship between PD-1 and cell immunity in TCGA and METABRIC datasets **(A, B)**. The relationship between PD-1 and inflammatory activities in TCGA and METABRIC datasets **(C, D)**. GO:0030217: T cell differentiation; GO:0042098:T cell proliferation; GO:0042102: positive regulation of T cell proliferation; GO:0042113: B cell activation; GO:0042129: regulation of T cell proliferation; GO:0050852: T cell receptor signaling pathway; GO:0050870: positive regulation of T cell activation. The pie denotes the correlation coefficient of PD-1 and GO term.

suggested that PD-1 was not only correlated with T cell immunity but also with other immune cells. These findings indicated that PD-1 plays essential immune and inflammatory functions in breast cancer. In our study, we focused on characterizing the role of PD-1; however, future studies should address whether there is any concomitant over-expression of PD-L1 on tumors, on immune cell populations, or on any of these immune cells in parallel with overexpression of PD-1. This would be helpful in gaining a deeper understanding of the association of PD1/PDL1 with related immune cell populations.

In summary, the expression of PD-1 was closely associated with the malignancy and might be as a potential biomaker in breast cancer, especially for TNBC. PD-1 might manipulate the anti-tumor immune response by impacting multiple immune cells, and this could vary with different tumors. Furthermore, PD-1 might synergize with other immune checkpoint members to modulate the immune microenvironment in breast cancer, which could be applied in the development of new targeted drugs for immunotherapy.

This study had limitations. Because detailed treatment information was not available in the TCGA database, treatment effects were potential confounders that should be considered when available and adjusted for appropriately. In certain cases, a proxy for standard of care, such as age, treating hospital, and year of diagnosis can alleviate some of the bias when treatment is unknown. A future study using an alterative source of data should address this problem.

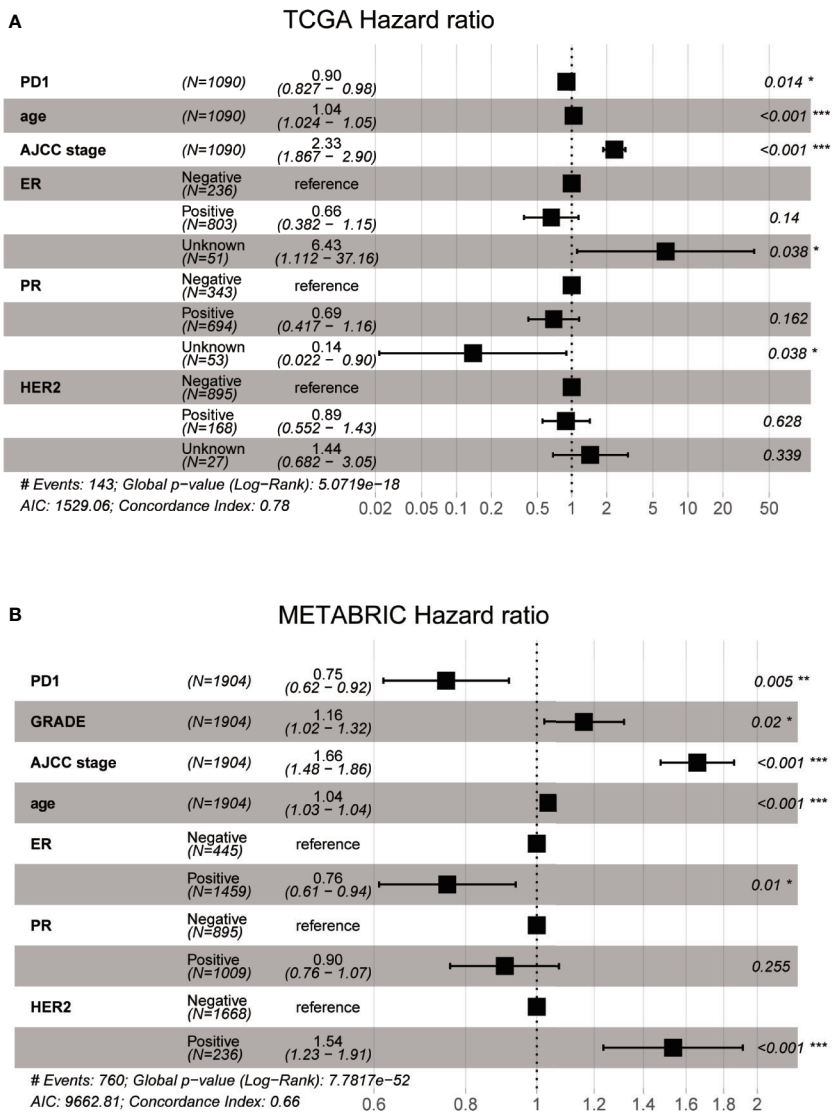

FIGURE 8 | Prognostic value of PD-1 in breast cancer using TCGA and METABRIC databases (**A** and **B**).

DATA AVAILABILITY STATEMENT

Publicly available datasets were analyzed in this study. This data can be found here—TCGA: https://portal.gdc.cancer.gov/; METABRIC: http://www.cbioportal.org.

AUTHOR CONTRIBUTIONS

JW: Conception and design and study supervision. YF and ZW: Acquisition of data and development of methodology. QL and RC: Analysis and interpretation of data and writing the original manuscript. XK: Verification and revision of the manuscript. All authors contributed to the article and approved the submitted version.

FUNDING

This work was supported by the Natural Science Foundation of China (No. 81872160); the Beijing Municipal Natural Science Foundation (Key Project) (No. 7191009); the Beijing Municipal Natural Science Foundation (No. 7204293); the Special Research Fund for Central Universities, Peking Union Medical College (No. 3332019053); the Beijing Hope Run Special Fund of Cancer Foundation of China (No. LC2019B03); the Beijing Hope Run Special Fund of Cancer Foundation of China (No. LC2019L07); the Golden Bridge Project Seed Fund of Beijing Association for Science and Technology; the PhD. Innovation Fund of Cancer Hospital, Chinese Academy of Medical Sciences (No. C2019-1051-09).

ACKNOWLEDGMENTS

The authors would like to thank Professor Hai Hu and Doctor Jianfang Liu for their kindly help providing us high-quality TCGA breast cancer clinical data. We wish to thank TCGA project organizers as well as all study participants. The first author is particularly indebted to Ping He for help during the study.

SUPPLEMENTARY MATERIAL

The Supplementary Material for this article can be found online at: https://www.frontiersin.org/articles/10.3389/fimmu.2020.558757/full#supplementary-material

SUPPLEMENTARY FIGURE 1 | PD-1-related immune responses. Most of immune-related genes are positively correlated with PD-1 expression in TCGA and METABRIC databases, while a small number of genes are negatively associated (A and B), Subtypes denotes breast cancer molecular subtypes including Basal, basal-like; Her2, Her2-enriched; LumA, luminal A; LumB, luminal B.

SUPPLEMENTARY FIGURE 2 | PD-1 expression is correlated with immunoinhibitors in pan-cancer.

SUPPLEMENTARY FIGURE 3 | PD-1 expression is correlated with immunostimulators in pan-cancer.

SUPPLEMENTARY FIGURE 4 | PD-1 expression is correlated with MHC molecules in pan-cancer.

REFERENCES

1. DeSantis CE, Ma J, Gaudet MM, Newman LA, Miller KD, Goding Sauer A, et al. Breast cancer statistics, 2019. *CA Cancer J Clin* (2019) 69:438–51. doi: 10.3322/caac.21583
2. Moo TA, Sanford R, Dang C, Morrow M. Overview of Breast Cancer Therapy. *PET Clin* (2018) 13:339–54. doi: 10.1016/j.cpet.2018.02.006
3. Gerber B, Freund M, Reimer T. Recurrent breast cancer: treatment strategies for maintaining and prolonging good quality of life. *Dtsch Arztebl Int* (2010) 107:85–91. doi: 10.3238/arztebl.2010.0085
4. Ghahremanloo A, Soltani A, Modaresi SMS, Hashemy SI. Recent advances in the clinical development of immune checkpoint blockade therapy. *Cell Oncol (Dordr)* (2019) 42:609–26. doi: 10.1007/s13402-019-00456-w
5. Wolchok JD, Chiarion-Sileni V, Gonzalez R, Rutkowski P, Grob JJ, Cowey CL, et al. Overall Survival with Combined Nivolumab and Ipilimumab in Advanced Melanoma. *N Engl J Med* (2017) 377:1345–56. doi: 10.1056/NEJMoa1709684
6. Reck M, Rodriguez-Abreu D, Robinson AG, Hui R, Csoszi T, Fulop A, et al. Pembrolizumab versus Chemotherapy for PD-L1-Positive Non-Small-Cell Lung Cancer. *N Engl J Med* (2016) 375:1823–33. doi: 10.1056/NEJMoa1606774
7. Ferris RL, Blumenschein G Jr., Fayette J, Guigay J, Colevas AD, Licitra L, et al. Nivolumab for Recurrent Squamous-Cell Carcinoma of the Head and Neck. *N Engl J Med* (2016) 375:1856–67. doi: 10.1056/NEJMoa1602252
8. Motzer RJ, Escudier B, McDermott DF, George S, Hammers HJ, Srinivas S, et al. Nivolumab versus Everolimus in Advanced Renal-Cell Carcinoma. *N Engl J Med* (2015) 373:1803–13. doi: 10.1056/NEJMoa1510665
9. Brahmer JR, Tykodi SS, Chow LQ, Hwu WJ, Topalian SL, Hwu P, et al. Safety and activity of anti-PD-L1 antibody in patients with advanced cancer. *N Engl J Med* (2012) 366:2455–65. doi: 10.1056/NEJMoa1200694
10. Yasunaga M. Antibody therapeutics and immunoregulation in cancer and autoimmune disease. *Semin Cancer Biol* (2020) 64:1–12. doi: 10.1016/j.semcancer.2019.06.001
11. Zhao Y, Harrison DL, Song Y, Ji J, Huang J, Hui E. Antigen-Presenting Cell-Intrinsic PD-1 Neutralizes PD-L1 in cis to Attenuate PD-1 Signaling in T Cells. *Cell Rep* (2018) 24:379–390 e6. doi: 10.1016/j.celrep.2018.06.054
12. Pardoll DM. The blockade of immune checkpoints in cancer immunotherapy. *Nat Rev Cancer* (2012) 12:252–64. doi: 10.1038/nrc3239
13. O'Donnell JS, Long GV, Scolyer RA, Teng MW, Smyth MJ. Resistance to PD1/PDL1 checkpoint inhibition. *Cancer Treat Rev* (2017) 52:71–81. doi: 10.1016/j.ctrv.2016.11.007
14. Bedognetti D, Maccalli C, Al Bader SB, Marincola FM, Seliger B. Checkpoint inhibitors and their application in breast cancer. *Breast Care* (2016) 11:108–15. doi: 10.1159/000445335
15. Hartkopf AD, Taran F-A, Wallwiener M, Walter CB, Krämer B, Grischke E-M, et al. PD-1 and PD-L1 immune checkpoint blockade to treat breast cancer. *Breast Care* (2016) 11:385–90. doi: 10.1159/000453569
16. Bersanelli M, Buti S. From targeting the tumor to targeting the immune system: Transversal challenges in oncology with the inhibition of the PD-1/PD-L1 axis. *World J Clin Oncol* (2017) 8:37–53. doi: 10.5306/wjco.v8.i1.37
17. Ott PA, Hodi FS, Kaufman HL, Wigginton JM, Wolchok JD. Combination immunotherapy: a road map. *J Immunother Cancer* (2017) 5:16. doi: 10.1186/s40425-017-0218-5
18. Li R, Qu H, Wang S, Wei J, Zhang L, Ma R, et al. GDCRNATools: an R/Bioconductor package for integrative analysis of lncRNA, miRNA and mRNA data in GDC. *Bioinf (Oxford England)* (2018) 34:2515–7. doi: 10.1093/bioinformatics/bty124
19. Robinson MD, McCarthy DJ, Smyth GK. edgeR: a Bioconductor package for differential expression analysis of digital gene expression data. *Bioinf (Oxford England)* (2010) 26:139–40. doi: 10.1093/bioinformatics/btp616
20. Ritchie ME, Phipson B, Wu D, Hu Y, Law CW, Shi W, et al. limma powers differential expression analyses for RNA-sequencing and microarray studies. *Nucleic Acids Res* (2015) 43:e47. doi: 10.1093/nar/gkv007
21. Huber W, Carey VJ, Gentleman R, Anders S, Carlson M, Carvalho BS, et al. Orchestrating high-throughput genomic analysis with Bioconductor. *Nat Methods* (2015) 12:115–21. doi: 10.1038/nmeth.3252
22. Liu J, Lichtenberg T, Hoadley KA, Poisson LM, Lazar AJ, Cherniack AD, et al. An integrated TCGA pan-cancer clinical data resource to drive high-quality survival outcome analytics. *Cell* (2018) 173:400–16.e11. doi: 10.1158/1538-7445.AM2018-3287
23. Curtis C, Shah SP, Chin S-F, Turashvili G, Rueda OM, Dunning MJ, et al. The genomic and transcriptomic architecture of 2,000 breast tumours reveals novel subgroups. *Nature* (2012) 486:346–52. doi: 10.1038/nature10983
24. Yu G, Wang L-G, Han Y, He Q-Y. clusterProfiler: an R package for comparing biological themes among gene clusters. *Omics: J Integr Biol* (2012) 16:284–7. doi: 10.1089/omi.2011.0118
25. Bhattacharya S, Andorf S, Gomes L, Dunn P, Schaefer H, Pontius J, et al. ImmPort: disseminating data to the public for the future of immunology. *Immunol Res* (2014) 58:234–9. doi: 10.1007/s12026-014-8516-1
26. Becht E, Giraldo NA, Lacroix L, Buttard B, Elarouci N, Petitprez F, et al. Estimating the population abundance of tissue-infiltrating immune and stromal cell populations using gene expression. *Genome Biol* (2016) 17:218. doi: 10.1186/s13059-016-1113-y
27. Hänzelmann S, Castelo R, Guinney J. GSVA: gene set variation analysis for microarray and RNA-seq data. *BMC Bioinf* (2013) 14:7. doi: 10.1186/1471-2105-14-7
28. Rody A, Holtrich U, Pusztai L, Liedtke C, Gaetje R, Ruckhaeberle E, et al. T-cell metagene predicts a favorable prognosis in estrogen receptor-negative and HER2-positive breast cancers. *Breast Cancer Res: BCR* (2009) 11:R15. doi: 10.1186/bcr2234
29. Ru B, Wong CN, Tong Y, Zhong JY, Zhong SSW, Wu WC, et al. TISIDB: an integrated repository portal for tumor–immune system interactions. *Bioinf (Oxford England)* (2019) 35:4200–2. doi: 10.1093/bioinformatics/btz210
30. Robin X, Turck N, Hainard A, Tiberti N, Lisacek F, Sanchez J-C, et al. pROC: an open-source package for R and S+ to analyze and compare ROC curves. *BMC Bioinf* (2011) 12:77. doi: 10.1186/1471-2105-12-77
31. Gu Z, Gu L, Eils R, Schlesner M, Brors B. circlize implements and enhances circular visualization in R. *Bioinf (Oxford England)* (2014) 30:2811–2. doi: 10.1093/bioinformatics/btu393
32. Friendly M. Corrgrams: Exploratory displays for correlation matrices. *Am Statistician* (2002) 56:316–24. doi: 10.1198/000313002533

33. Wickham H. *Wiley Interdiscip Rev Comput Stat*. (2011) 3:180–5. doi: 10.1002/wics.147
34. Liu S, Wang Z, Wang Y, Fan X, Zhang C, Ma W, et al. PD-1 related transcriptome profile and clinical outcome in diffuse gliomas. *Oncoimmunology* (2018) 7: e1382792. doi: 10.1080/2162402X.2017.1382792
35. Charoentong P, Finotello F, Angelova M, Mayer C, Efremova M, Rieder D, et al. Pan-cancer immunogenomic analyses reveal genotype-immunophenotype relationships and predictors of response to checkpoint blockade. *Cell Rep* (2017) 18:248–62. doi: 10.1016/j.celrep.2016.12.019
36. Zhang H, Chen J. Current status and future directions of cancer immunotherapy. *J Cancer* (2018) 9:1773–81. doi: 10.7150/jca.24577
37. Schutz F, Stefanovic S, Mayer L, von Au A, Domschke C, Sohn C. PD-1/PD-L1 Pathway in Breast Cancer. *Oncol Res Treat* (2017) 40:294–7. doi: 10.1159/000464353
38. Jiang C, Cao S, Li N, Jiang L, Sun T. PD-1 and PD-L1 correlated gene expression profiles and their association with clinical outcomes of breast cancer. *Cancer Cell Int* (2019) 19:233. doi: 10.1186/s12935-019-0955-2
39. Ren X, Wu H, Lu J, Zhang Y, Luo Y, Xu Q, et al. PD1 protein expression in tumor infiltrated lymphocytes rather than PDL1 in tumor cells predicts survival in triple-negative breast cancer. *Cancer Biol Ther* (2018) 19:373–80. doi: 10.1080/15384047.2018.1423919
40. Woo SR, Turnis ME, Goldberg MV, Bankoti J, Selby M, Nirschl CJ, et al. Immune inhibitory molecules LAG-3 and PD-1 synergistically regulate T-cell function to promote tumoral immune escape. *Cancer Res* (2012) 72:917–27. doi: 10.1158/0008-5472.CAN-11-1620
41. Lichtenegger FS, Rothe M, Schnorfeil FM, Deiser K, Krupka C, Augsberger C, et al. Targeting LAG-3 and PD-1 to Enhance T Cell Activation by Antigen-Presenting Cells. *Front Immunol* (2018) 9:385. doi: 10.3389/fimmu.2018.00385
42. Murciano-Goroff YR, Warner AB, Wolchok JD. The future of cancer immunotherapy: microenvironment-targeting combinations. *Cell Res* (2020) 30(6):507–19. doi: 10.1038/s41422-020-0337-2
43. Mizuno R, Sugiura D, Shimizu K, Maruhashi T, Watada M, Okazaki IM, et al. PD-1 Primarily Targets TCR Signal in the Inhibition of Functional T Cell Activation. *Front Immunol* (2019) 10:630. doi: 10.3389/fimmu.2019.00630
44. Zhang Y, Gallastegui N, Rosenblatt JD. Regulatory B cells in anti-tumor immunity. *Int Immunol* (2015) 27:521–30. doi: 10.1093/intimm/dxv034
45. Ren Z, Peng H, Fu YX. PD-1 Shapes B Cells as Evildoers in the Tumor Microenvironment. *Cancer Discovery* (2016) 6:477–8. doi: 10.1158/2159-8290.CD-16-0307

Conflict of Interest: The authors declare that the research was conducted in the absence of any commercial or financial relationships that could be construed as a potential conflict of interest.

Advantages of publishing in Frontiers

OPEN ACCESS
Articles are free to read for greatest visibility and readership

FAST PUBLICATION
Around 90 days from submission to decision

HIGH QUALITY PEER-REVIEW
Rigorous, collaborative, and constructive peer-review

TRANSPARENT PEER-REVIEW
Editors and reviewers acknowledged by name on published articles

Frontiers
Avenue du Tribunal-Fédéral 34
1005 Lausanne | Switzerland

Visit us: www.frontiersin.org
Contact us: frontiersin.org/about/contact

REPRODUCIBILITY OF RESEARCH
Support open data and methods to enhance research reproducibility

DIGITAL PUBLISHING
Articles designed for optimal readership across devices

FOLLOW US
@frontiersin

IMPACT METRICS
Advanced article metrics track visibility across digital media

EXTENSIVE PROMOTION
Marketing and promotion of impactful research

LOOP RESEARCH NETWORK
Our network increases your article's readership